Zooming-in on Chromosomes in Mouse Meiosis

DNA double-strand break repair proteins and meiotic chromosome dynamics

Fabrizia Carofiglio

ISBN: 978-90-5335-939-6

Layout and cover: Fabrizia Carofiglio; Ridderprint BV

Printing: Ridderprint BV, Ridderkerk, the Netherlands

The work described in this thesis was performed at the Department of Reproduction and Development at the Erasmus MC in Rotterdam, the Netherlands.

Printing of this thesis was financially supported by Erasmus University Rotterdam, and Department of Reproduction and Development, Erasmus MC.

Zooming-in on Chromosomes in Mouse Meiosis

DNA double-strand break repair proteins and meiotic chromosome dynamics

Inzoomen op chromosomen in de meiose bij muizen

Hersteleiwitten van DNA-dubbelstrengsbreuken
en dynamiek van de chromosomen

Thesis

to obtain the degree of Doctor from the Erasmus University Rotterdam
by command of the rector magnificus

Prof.dr. H.A.P. Pols

and in accordance with the decision of the Doctorate Board.

The public defense shall be held on
Tuesday 4 November 2014 at 15.30 hrs

by

Fabrizia Carofiglio
born in Bari, Italy

DOCTORAL COMMITTEE

Promotor:	Prof.dr. J.A. Grootegoed
Other members:	Prof.dr. A.B. Houtsmuller
	Prof.dr. C.P. Verrijzer
	Prof.dr. C.L. Wyman
Copromotor:	Dr.ir. W.M. Baarends

TABLE OF CONTENTS

1

Introduction and scope of the thesis

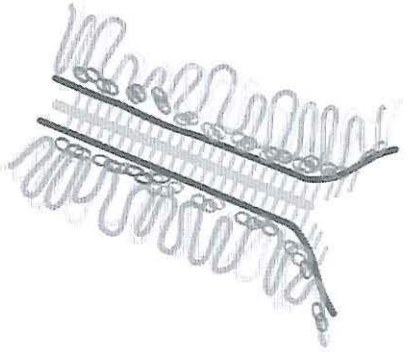

INTRODUCTION

In sexually reproducing species, generation of a new organism occurs by fusion of two specialized cells, named gametes, one of paternal and the other one of maternal origin. In most animal species, the cells that constitute the body are diploid, meaning that they carry two copies of each chromosome (2n). In order to generate diploid offspring, gametes need to carry a single chromosome set (haploid; 1n) that, combined with a haploid counterpart, will reconstitute a diploid genome. The haploid chromosome set consists of a single autosome from each pair. which may have been inherited either paternally or maternally. This choice occurs during the formation of both maternal and paternal gametes, meaning that many different combinations can be formed in the zygote, randomly. Moreover, recombination between chromosome pairs has taken place in meiosis in the father and the mother, so that each autosome carries a new combination of genes inherited from the grandparents. Together, this guarantees that new organisms will always be generated with a unique genome. This provides a very strong evolutionary advantage for sexually reproducing species, since it will dramatically increase genetic variation and thereby increase the probability of survival of the species in a changing environment (Coop and Przeworski, 2007).

Gametogenesis is the process that leads to the formation of gametes, cells that are specifically competent for reproduction, from a diploid germ cell precursor (Figure 1). Haploidization of the germ cell precursor occurs via meiosis, that consists of two subsequent cell divisions that follow a single DNA replication event and a lengthy meiotic prophase. The first of these two cell divisions, meiosis I, includes the meiotic prophase during which chromosomal rearrangements take place (see below), followed by a reductional division which results in separation of the homologs of each chromosome pair. This is immediately followed by meiosis II, which leads to separation of sister chromatids, comparable to what happens in a mitotic division (Figure 1).

1.1 MALE AND FEMALE GAMETOGENESIS

In all animal species with meiosis and sexual reproduction, gametogenesis differs between male and female individuals. Describing gametogenesis and meiosis, below, we will focus on mammalian species, in particular the mouse.

In male mammals, four mature gametes (spermatozoa) are obtained from a single spermatogonium via a long developmental process, named spermatogenesis (Clermont, 1972). Spermatogenesis occurs from puberty onwards and it consists of premeiotic, meiotic, and postmeiotic phases. Premeiotically, spermatogenic stem cells, which are the descendants of the embryonic primordial germ cells, give rise to new generations of mitotically active spermatogonia, throughout reproductive life (Gordon and Ruddle, 1981). After a last round of DNA replication, in premeiotic S phase, the cells enter meiotic prophase, becoming primary spermatocytes. After completion of meiosis I, secondary spermatocytes carry a haploid set of chromosomes in which each chromosome is composed of two sister chromatids. Upon completion of meiosis II, the sister chromatids have segregated to two daughter cells, the spermatids, so that each primary spermatocyte gives rise to four haploid spermatids. These round spermatids undergo the lengthy postmeiotic process of spermiogenesis, which includes chromatin and cellular changes resulting in the formation of mature spermatozoa (reviewed in (Rathke et al, 2014)).

Unlike male gametogenesis, oogenesis in females yields only one gamete per diploid precursor cell entering into meiosis, which serves an important biological function, to provide each oocyte with a large amount of resources (Borum, 1961). The mature oocyte is the primary source of biomolecules for the zygote. The cytoplasmic content of the gamete precursor is conveyed to only one of the four haploid cells, which becomes the oocyte that will be able to support the early stages of embryonic development.

Following the formation of primordial germ cells, which migrate into the undifferentiated gonads around embryonic day 8-10 in the mouse (Sasaki and Matsui, 2008), a hallmark of female gametogenesis is that meiosis starts already during fetal development (Crone et al, 1965; McClellan et al, 2003). However, the meiotic prophase is arrested shortly before its completion, at the diplotene stage, and this arrest is named the dictyate arrest (reviewed in (Sen and Caiazza, 2013)). In mouse female embryos, meiosis I is initiated around embryonic day 15 and progresses to dictyate arrest by embryonic day 19-20, approximately one day before the end of mouse pregnancy. Resumption of the process starts from puberty onwards, for a limited number of oocytes per time unit; only a small cohort is recruited for growth during a specific ovarian cycle, and only few oocytes survive up to ovulation. Completion of the first meiotic division takes place just prior to ovulation and results in

extrusion of the first polar body that carries a haploid chromosome set, and does not take part in further development. The other haploid chromosome set is found in the developing oocyte, in which meiosis II becomes arrested at the prometaphase stage. Fertilization triggers completion of the second meiotic cell division (Clift and Schuh, 2013; Donahue, 1972), leading to the extrusion of the second polar body and formation of the diploid zygote, which now contains both the male and female haploid genomes.

1.2 MEIOTIC PROPHASE I

The mitotic germ cells originate from somatic cells in the embryo, and they carry autosomes and sex chromosomes, in pairs. For each pair, one chromosome is paternally inherited and the other is maternally inherited. Although the maternally and paternally inherited chromosomes are themselves the result of recombination of the sets of genes in the previous generation, there is an overall sequence homology between the two autosomes of each pair. This homology is key to meiotic chromosome pairing and recombination. Recombination is triggered by the regulated induction of DNA double-strand breaks (DSBs) throughout the genome. Repair of these breaks is instrumental for several meiotic processes discussed below on which this thesis will focus.

In addition to the autosome pairs, most mammalian species have one pair of sex chromosomes, XX in female and XY in male. These sex chromosomes and their behavior in meiosis are described below. However, it is important to note, that, in male meiotic prophase, the largely heterologous X and Y chromosomes encounter difficulties in pairing and recombination (Handel and Hunt, 1992). In contrast, in female meiotic prophase, two X chromosomes can engage in pairing and recombination, not different from the autosomes. For the description of meiotic prophase in this paragraph, we focus on the autosomes, in mouse meiotic prophase.

After premeiotic S phase, the genome is replicated, as in a mitotic cell cycle. The replicated chromosomes consist of two sister chromatids, entirely identical and connected by cohesins, that form the ring-shaped multi-subunit cohesion complex at many sites along the length of the two sister chromatids (Nasmyth and Haering, 2005, 2009). In mitosis, chromosome condensation and sister-chromatid resolution would be the steps to follow DNA replication, towards metaphase and subsequent completion of the mitotic division. However, in meiotic prophase, we will be look-

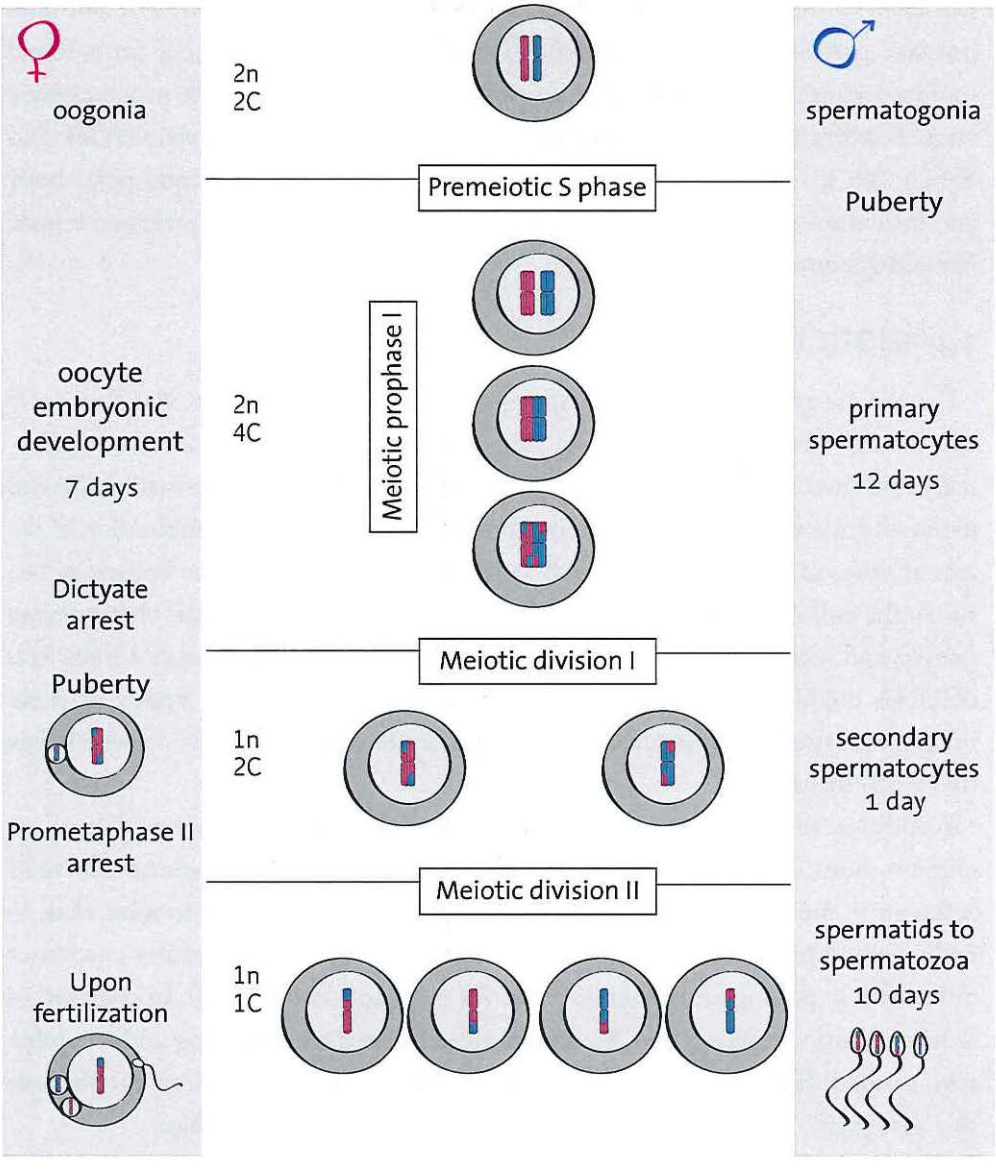
oogonia
2n
2C
spermatogonia
Premeiotic S phase
Puberty
oocyte
embryonic
development
7 days
2n
4C
Meiotic prophase I
primary
spermatocytes
12 days
Dictyate
arrest
Meiotic division I
Puberty
1n
2C
secondary
spermatocytes
1 day
Prometaphase II
arrest
Meiotic division II
spermatids to
spermatozoa
10 days
Upon
fertilization
1n
1C

◀ Figure 1: Gametogenesis in male and female mouse

Gametogenesis can be divided into three phases: premeiotic, meiotic and postmeiotic. During the premeiotic stage, diploid (2n) precursor germ cells, that carry a paternal (blue) and a maternal (pink) chromosome set, undergo mitotic cell divisions to generate a pool of oogonia (females) and spermatogonia (males) that will be entering meiosis. After a single DNA replication event (premeiotic S phase), diploid meiotic cells (2n, 4C) will undergo two sequential cell divisions. During the meiotic phase of gametogenesis, homologous chromosomes need to find each other, tightly interact, and be engaged in exchange of chromatid segments, which results in the formation of crossovers. At the end of meiotic prophase I, homologous chromosomes will be separated by Meiosis I, generating two haploid cells (1n, 2C), that carry a single homolog per pair. Due to crossovers, every homolog will consist of two non-identical sister chromatids. The second meiotic division will mediate separation of sister chromatids, similar to a mitotic division. It will lead to the formation of four cells, carrying a haploid genetic set (1n 1C). In males, spermatogonia keep replicating during the entire life of the individual. At puberty, some spermatogonia will be recruited to progress further in gametogenesis. Male gametogenesis (spermatogenesis) will, from puberty onwards, occur in synchronous waves. Spermatogonia that enter meiosis are called primary spermatocytes. Meiotic prophase I lasts approximately 12 days, then Meiotic division I generates two haploid secondary spermatocytes. Meiosis II interphase is extremely short (1day) and secondary spermatocytes rapidly undergo the second meiotic division that yields the generation of four round spermatids. At this point, several nuclear and cytoplasmic changes need to occur during spermiogenesis, to allow maturation of spermatids into spermatozoa. Four haploid spermatozoa are formed starting from a single diploid spermatogoinum. In females meiosis starts around embryonic day 14 (E14.5) and lasts about 7 days. Meiotic prophase will progress till a stage that precedes chromosome condensation. At this point, oocytes undergo the dictyate arrest. Resumption of gametogenesis occurs at puberty: before oocytes are ovulated, Meiotic division I takes place. This division is asymmetrical with respect to the cytoplasm of the oocyte, therefore one haploid chromosome set will be extruded as the so-called polar body. The oocyte that received the majority of the cytoplasm will arrest at prometaphase II. The second meiotic divison will occur upon fertilization of the oocyte by a spermatozoon. Meiotic division II is also asymmetrical and will lead to the extrusion of the second polar body, carrying one of the two haploid chromatid sets. Thus, female gametogenesis results in the generation of only one mature gamete competent for reproduction. n = ploidy number. C = DNA content.

ing at a much more complicated and exciting series of events.

1.2.1 Chromosome organization in meiosis

In meiotic prophase, the chromosomes are first organized in chromatin loops, at the base of which cohesin rings stabilize the intersister (IS) chromatid connections. The cohesin ring consists of two cohesin subunits, SMC1 and SMC3, which are members of the family of SMC proteins (for Structural Maintenance of Chromosomes), and it is closed by a kleisin subunit (RAD21) associated to an SA (stromal antigen) protein (STAG1/2) (Nasmyth and Haering, 2009). These proteins are called into action in mitotic as well as in meiotic cells. In addition, meiosis-specific paralogs of these proteins (SMC1□, REC8, STAG3, RAD21L) are expressed during meiosis (Bannister et al, 2004; Eijpe et al, 2003; Novak et al, 2008; Prieto et al, 2002; Prieto et al, 2001; Revenkova et al, 2001). Meiotic cohesins are required for several meiosis-specific processes. They participate in the assembly of the synaptonemal complex (see below) (Bannister et al, 2004; Eijpe et al, 2003; Herran et al, 2011; Llano et al, 2012; Prieto et al, 2001; Revenkova et al, 2001; Xu et al, 2005). It has been shown that the meiosis-specific cohesins STAG3 and SMC1□ mediate centromeric cohesion at anaphase I (Fukuda et al, 2014; Hopkins et al, 2014; Revenkova et al, 2004), ensuring that sister chromatid separation does not occur till the cell reaches anaphase II. In addition, recruitment of meiosis-specific cohesins is related to the role of cohesion in several steps of meiotic recombination (discussed below). The organization of chromosomes into two sister chromatids connected by cohesins now will develop towards a higher level of structural complexity, where each autosome searches and finds its homologous partner.

1.2.2 Homologous chromosome pairing

The autosome pairs will indeed pair, along their full length, in meiotic prophase. It is a fascinating question, how the homologous chromosomes are able to find and recognize each other. In various organisms, including yeast, it has been observed that rapid movement of chromosomes, led by the telomeric ends, helps in sorting chromosomes of identical length and global structure (Lee et al, 2012). For interphase mitotic cells, it has been shown that chromosomes occupy specific nuclear domains, defined as chromosome territories (CTs) (Cremer et al, 2008; Neusser et al, 2007; Parada et al, 2004; Parada et al, 2002). CTs are considered chromatin

domains in the nucleus, which are connected by a higher-order chromatin network (Albiez et al, 2006; Visser et al, 2000). A univocal model that describes the way these CTs are formed and how they are regulated has not yet been defined by compelling evidence. However, this nuclear organization has been described for different species, ranging from yeast (Bystricky et al, 2005; Molnar and Kleckner, 2008), to plants (Berr et al, 2006; Pecinka et al, 2004; Wang et al, 2002), mouse (Parada et al, 2004; Parada et al, 2002; Roix et al, 2003), primates and humans (Bolzer et al, 2005; Brianna Caddle et al, 2007; Cremer and Cremer, 2001; Khalil et al, 2007; Neusser et al, 2007). Based on the hypothesis that homologous chromosomes may be located close to each other upon completion of premeiotic S phase, the presence of premeiotic chromosome pairing has been investigated, and it was proposed that the meiosis-specific protein SPO11 plays a role in the achievement of transient homologous chromosome pairing before the onset of meiotic prophase, in mouse (Boateng et al, 2013). This would imply a second function for SPO11, independent of its DSB-inducing activity required for meiotic recombination (described below). The transitory homologous chromosome associations established at this stage are expected to be subsequently stabilized with the aid of meiotic recombination (Mahadevaiah et al, 2001), as explained in the following paragraphs. However, such premeiotic pairing is still under debate. A study performed in mouse models carrying mutations in meiosis-specific cohesin genes suggested that the meiosis-specific cohesin RAD21L mediates homologous chromosome pairing, even in the absence of SPO11. These authors observe chromosome pairing only in meiotic cells, increasing from meiosis onset to the pachytene stage (Ishiguro et al, 2014). This pairing is not maintained in the absence of proper meiotic recombination. Indeed, mouse meiocytes that lack SPO11 expression or SPO11 activity are characterized by severely impaired homologous chromosome pairing: spermatocytes show limited or absent interactions between homologous chromosomes, and heterologous pairing is observed (Baudat et al, 2000; Romanienko and Camerini-Otero, 2000). It appears clear that, next to a global and largely mechanical sorting of the autosome pairs, and to the potential mechanisms mediating a precise organization of the nuclear architechture, there need to be more precise mechanisms to detect and confirm homology. These mechanisms are interlinked, in time and place, with formation of the synaptonemal complex (SC).

1.2.3 The synaptonemal complex

The synaptonemal complex is a tripartite proteinaceous scaffold that mediates tight interactions, referred to as synapsis, between paired chromosomes, and keeps them together during the next steps of the meiotic prophase (Page and Hawley, 2004; Yang and Wang, 2009). At the onset of meiotic prophase, the axial element (AE) is assembled along the axis of each chromosome, which is made of cohesins, the synaptonemal complex proteins SYCP3 and SYCP2 (Di Carlo et al, 2000; Schalk et al, 1998; Yang et al, 2006; Yuan et al, 2000; Yuan et al, 1998), and the yeast Hop2 homologs HORMAD1 and HORMAD2 (Daniel et al, 2011; Fukuda et al, 2009; Wojtasz et al, 2009). When two homologs pair, the respective axial elements can interact with each other, thereby becoming lateral elements. At this point HORMADs are removed and the central element can assemble and zip the lateral elements together, resulting in synapsis formation. The central element consists of transverse filaments, made of SYCP1 (de Vries et al, 2005), and central element proteins, such as TEX12, SYCE1, SYCE2, SYCE3 (Bolcun-Filas et al, 2007; Bolcun-Filas et al, 2009; Costa et al, 2005; Hamer et al, 2006; Hamer et al, 2008; Schramm et al, 2011).

A major biological purpose of meiotic prophase is to achieve recombination between homologous chromosomes. To be able to recombine, it is essential that DNA double strand breaks are generated, early in meiotic prophase. This seemingly

Figure 2: The synaptonemal complex marks meiotic prophase I progression
The cartoon shows the DNA of a pair of homologous chromosomes after premeiotic S phase. The DNA (blue) is organized in chromatin loops at the basis of which cohesin rings (in grey) stabilize interactions between the sister chromatids. Each homolog consists of a pair of sister chromatids. Leptotene: along the axis of the homologs, the axial element (AE) starts to form by accumulation of synaptonemal complex proteins 2 and 3 (SYCP2 and SYCP3), depicted in red. Zygotene: when AEs of the two homologs are complete, they can interact with each other forming a platform for accumulation of another set of synaptonemal complex proteins. At this point, transverse filaments (TF), consisting of SYCP1, and the central element (CE) can be formed (green). The central element is composed of several proteins: SYCE1, SYCE2, SYCE3, TEX12. Pachytene: the assembly of the central element guarantees synapsis between the paired homologs along their entire length. Diplotene: the synaptonemal complex will be disassembled: first removing the TF/CE proteins, resulting in desynapsis of the chromosomes, then by disassembly of the AE/LE. The sister chromatids will still be kept together by sister chromatid cohesion. Underneath the schematic drawing of the synaptonemal complex throughout meiotic prophase I, representative images are shown of spread spermatocyte nuclei immunostained for the AE/LE component SYCP3 (red). The DNA of the same nuclei is counterstained with DAPI.

time
sister chromatid
sister chromatid
paternal homolog
AE/LE
dsDNA
TF/CE
cohesin
maternal homolog
SYCP3/SYCP1
DNA
Leptotene
Zygotene
Pachytene
Diplotene
SMC1αβ/REC8/RAD21/
RAD21L/SMC3/STAG3
SYCP2/SYCP3
SYCP1/TEX12/SYCE1/
SCYE2/SYCE3

self-destructive task is executed by SPO11, described below. Interestingly, these DSBs and their repair are also important for homologous chromosome pairing and SC formation (Baudat et al, 2000; Kauppi et al, 2013; Keeney et al, 1999; Keeney and Neale, 2006; Mahadevaiah et al, 2001). The series of events in pairing and recombination is highly integrated. Progress through meiotic prophase is interlinked with DSB repair, and checkpoint mechanisms are activated when a chromosome region might not be synapsed (Baarends et al, 2005; Turner, 2007; Turner et al, 2006; Turner et al, 2005). This synapsis checkpoint has been shown to be mediated by HORMAD proteins. HORMAD1/2 are indeed required for chromosome pairing and synapsis surveillance (Daniel et al, 2011; Fukuda et al, 2009; Wojtasz et al, 2012; Wojtasz et al, 2009). They are essential for recruitment of ATR to unsynapsed chromosomes, which can then mediate transcriptional silencing (Shin et al, 2007; Wojtasz et al, 2012).

The last S phase of gametogenesis, also referred to as the premeiotic S phase, takes place at the preleptotene stage of meiotic prophase. Then, based on the synapsis status of meiotic chromosomes, prophase I is divided into four stages: leptotene, zygotene, pachytene, and diplotene (Figure 2). At leptotene the proteins of the axial elements of the SC form small patches that will be joined together to build the chromosomal axes. When homologous chromosomes find each other and pair, they start to synapse in zygotene; at this timepoint, axial elements that interact with each other become lateral elements (LE). Synapsis is gradually achieved and completed for all chromosome pairs at pachytene. During this lengthy stage, we finally can also witness the most crucial event of meiotic prophase, when crossovers (COs) are formed which mediate the exchange of chromatid arms between homologous chromosomes. At least one crossover is needed per chromosome pair, to ensure proper orientation of the bivalents on the metaphase plate and segregation of the homologs at the first meiotic division. In mouse, 1-3 crossing overs are detected per chromosome pair (Anderson et al, 1999; Baudat and de Massy, 2007; de Boer et al, 2006; Hassold et al, 2000). At diplotene, the SC is disassembled and the chromosomes desynapse, so that they can segregate to the daughter cells, when the cohesion complex is removed only along the chromosome arms, at the methaphase to anaphase transition (Nasmyth and Haering, 2005; Watanabe, 2005). Note that the diplotene stage is the stage where oocyte development is halted, leading to the dictyate arrest (reviewed in (Sen and Caiazza, 2013)). In these arrested oocytes,

desynapsis is completed.

As a result of meiosis I, two daughter cells are generated. In spermatogenesis, these are the haploid secondary spermatocytes, which carry one set of chromosomes that are composed of two sister chromatids, still held together at the centromere by meiosis-specific cohesins. Following recombination, at least one sister chromatid per chromosome will have exchanged genetic material with the homolog, therefore in meiosis II the sister chromatids are no longer identical. However, the way they are separated in meiosis II is virtually identical to the mechanism of sister chromatid segregation in mitosis. At the end of meiosis II, the centromeric cohesion complexes will be removed, and the two sister chromatids will segregate to the daughter cells (Wassmann, 2013). In oogenesis, segregation of chromosomes will occur upon resumption of meiosis I after the dictyate arrest, leading to the generation of one oocyte and a polar body, both with a haploid chromosomal set, as described for secondary spermatocytes. Fertilization of the oocyte provides the trigger for the disassembly of cohesins at the centromeres and separation of the sister chromatids (Marangos and Carroll, 2004).

1.3 MEIOTIC RECOMBINATION

Crossovers are physical exchanges of DNA strands that results in recombination between homologous chromosomes. Evidently, this can only be achieved by controlled induction and repair of DNA double strand breaks (DSBs). Homologous recombination (HR) is a DNA double-strand break (DSB) repair process that requires the use of an intact template for repair (San Filippo et al, 2008) (Figure 3). In fact, it is used by mitotic cells for error-free repair of DSBs, which can occur at random sites by chance or by exposure to harsh environmental conditions. Possibly, homologous recombination repair is an ancient mechanisms which predates meiosis, in evolution. Exploring sexual reproduction, primitive unicellular organisms may have adopted mitotic HR repair as the basic mechanism to achieve meiotic homologous recombination. In meiotic prophase cells, two different templates are available: the sister chromatid and the chromatids of the homologous chromosome. This implies that there is a partner choice, for repair of every DSB. If all HR repair in meiotic prophase would occur using the DNA of the sister chromatid as a template, no recombination between paternally and maternally inherited chromosomes would take place. Hence, a mechanism has evolved which favours crossovers, where

the homologous chromosome is a preferred recombination partner. This mechanism is referred to as interhomolog bias (IH bias). It is a bias, meaning that intersister repair is not completely blocked. Schwacha and Kleckner (1994) developed an assay that allows discrimination between intersister and interhomolog recombination intermediates at budding yeast recombination hotspots (Schwacha and Kleckner, 1994)1994. DNA extracted from yeast cells undergoing meiotic recombination is extracted and digested with a restriction enzyme. After two-dimensional electrophoresis, a Southern blot is performed using parent-specific probes recognizing specific hotspots sites. Applying this assay, it has been established that the ratio between interhomolog and intersister interactions (both defined as joint molecules) is 10:1 (Kim et al, 2010). These joint molecules (JMs) can evolve into double Holliday Junctions (dHJs) (Bzymek et al, 2010) (discussed below) which will appear with an interhomolog bias of 5:1 (Hong et al, 2013; Schwacha and Kleckner, 1994). In budding yeast, several proteins have been identified that participate in repair template partner choice and have been shown to be required for establishment of interhomolog bias (Table I). Several of these proteins are components of, or associated with, the synaptonemal complex; others are involved in the mechanism of homologous recombination. Lack of any these proteins results in deviation from the 5:1 ratio interhomolog to intersister interactions.

In mouse, a similar analysis of recombination intermediates cannot be performed, so that no direct evidence has been obtained for the existence of an interhomolog bias mechanism in mammalian species. However, a regulatory mechanism for recombination partner choice can be expected to operate on meiotic DSBs also in mammals, although the key players involved in this process have not been identified.

1.3.1 SPO11

As a trigger to meiotic recombination, hundreds of DNA double-strand breaks (DSBs) are induced at the onset of meiotic prophase I by the meiosis-specific transesterase-like enzyme named SPO11 (Baudat et al, 2000; Keeney et al, 1999; Romanienko and Camerini-Otero, 2000). In budding yeast, several accessory proteins have been found to form a complex together with Spo11 to allow Spo11 dimerization and DNA binding (Rec102, Rec104, Ski8), but also to mediate Spo11 localization to the chromatin and its interaction with sites of DNA cleavage (Rec114, Mer2, Mei4) (Kumar et al, 2010; Panizza et al, 2011; Pittman et al, 1993; Tesse et

Table I - Factors involved in establishment of interhomolog bias in budding yeast

	gene name	mouse homolog	partner choice	mechanism in budding yeast	references
DSB repair	Rad51	*Rad51*	IS	In somatic cells	(Arbel et al, 1999; Hong et al, 2013)
			IH	• Catalytic-independent accessory role to Dmc1 activity • Repressed strand invasion activity	
	Dmc1	*Dmc1*	IH	Strand invasion	(Schwacha and Kleckner, 1994; Sheridan and Bishop, 2006),
	Rad54	*Rad54*	IS	Promotes Rad51 activity	(Niu et al, 2009)
	Mnd1/ Hop2	*Mnd1/ Hop2*	IH	Promotes Dmc1 activity	(Chen et al, 2004; Henry et al, 2006; Pezza et al, 2014)
Axis components	Hed1	-	IH	Binds to Rad51 to prevent its association with Rad54	(Busygina et al, 2008; Tsubouchi and Roeder, 2006)
	Rec8	*Rec8*	IS	Relieves inhibition of intersister recombination	(Hong et al, 2013; Kim et al, 2010)
	Red1	-	IH	Recruits Mek1 to DSBs	(Lai et al, 2011; Lin et al, 2010; Wan et al, 2004)
	Hop1	*Hormad1/2*	IH	Promotes Mek1 dimerization and autoactivation in its phosphorylated state	(Carballo et al, 2013; Niu et al, 2005; Wan et al, 2004; Wu et al, 2010)
Protein kinases	Mek1	-	IH	• Phosphorylates unknown target →prevents RAD51-mediated sister invasion • Phosphorylates RAD54→reduced affinity for RAD51→reduced RAD51 activity	(Niu et al, 2007; Wu et al, 2010)
	Mec1	*Atr*	IH	Phosphorylates Hop1	(Carballo et al, 2013)
	Pch2	*Trip13*	IH	Favours Hop1 phosphorylation	(Zanders et al, 2011)

al, 2003). In particular, it has been shown that designated sites of DSB formation are tethered to the SC via this pre-DSB recombinosome and subjected to Spo11 transesterase activity on the SC (Panizza et al, 2011). In mouse, only few homologs of the pre-DSB recombinosome components have been identified. Kumar et al. (2010) have shown that MEI4 (homolog of S. cerevisiae Mei4) localizes to the synaptonemal complex independent of SPO11, suggesting that, also in mouse meiotic prophase, DSB target sequences are first translocated to the chromosomal axes and then undergo DSB formation (Kumar et al, 2010). DSBs occur preferentially at specific genomic sites (hotspots) (Arnheim et al, 2007; Boulton et al, 1997; Gotoh et al, 1999; Khil et al, 2012; Smagulova et al, 2011) which are marked by chromatin modifications that render chromatin accessible for SPO11 activity. DSB hotspots appear to be subject to an interference mechanism, that is yet to be defined, which prevents the use of a hotspot for DSB induction, when a neighbouring hotspot has been already targeted (Billings et al, 2010). This hotspot interference may also contribute to the establishment of crossover interference, meaning that the frequency and spacing of crossing overs is not entirely random. The main known marker of hotspots is trimethylation of H3K4 (H3K4me3) (Borde et al, 2009; Buard et al, 2009) which appears to be deposited by the methyltransferase PRDM9 (Baker et al, 2014; Baudat et al, 2010; Grey et al, 2011). This protein, expressed during mouse meiosis, contains a zinc-finger array that binds to specific DNA motifs (Billings et al, 2013; Brick et al, 2012). Hypermutation of this region of the protein results in high variability of hotspots depending on the Prdm9 allele. When PRDM9 binds the genomic area of interest, the SET domain transfers methyl groups on H3K4 in the neighbouring nucleosomes (Hayashi et al, 2005; Wu et al, 2013), creating a favourable environment for DSB-induction. Also in yeast it has been shown that some regions of the genome are more frequently targeted for SPO11-mediated DSB formation, and are considered hotspots of recombination. Such genomic regions are enriched for H3K4me3 (Wu and Lichten, 1994) which is deposited by the methyltransferase Set1. This protein is part of the COMPASS complex, in which the component Spp1 mediates recognition of H3K4me3 residues and recruitment of the pre-DSB recombinosome via interaction with Mer2 (Acquaviva et al, 2013). A putative mouse homolog for Spp1 is thought to be CFP1.

1.3.1.1 SPO11 regulation

The number of SPO11-dependent DSBs has been quantified to range between 200 and 300 DSBs per nucleus. Yet it is highly important that the activity of SPO11 is well controlled, to prevent lethal destruction of the germ line genome at the very beginning of metotic prophase. The major feedback mechanism to limit SPO11 activity relies on ATM (ataxia telangiectasia mutated protein) (Lange et al, 2011), which is readily activated upon DSB induction, as a default DNA damage response (Rogakou et al, 1998). Activation of ATM results in its autophosphorylation which allows this protein to phosphorylate other targets, such as H2AX. It has been shown that a much higher number of DSBs is induced in meiotic cells from Atm knockout mice (Lange et al, 2011). In H2ax knockout mice, this has not been observed (Fernandez-Capetillo et al, 2003), indicating that phosphorylated H2AX is most likely not the mediator of SPO11 feedback mechanism. It has been proposed that ATM may phosphorylate SPO11 or its accessory proteins to limit their activity (Keeney and Neale, 2006; Lange et al, 2011; Neale et al, 2005). Indeed, a recent study in budding yeast reported Rec114 as a substrate of Atm, which undergoes conformational changes upon phosphorylation, thereby becoming unable to interact with Spo11 (Carballo et al, 2013). As mentioned above, repair of meiotic DSBs contributes to homologous chromosome pairing and thereby favours the establishment of synapsis. Indeed, in mouse expressing lower levels of SPO11, synapsis defects have been observed (Kauppi et al, 2013). Conversely, chromosome areas that are unsynapsed have been reported to accumulate further DSBs. These observations point to a role of synapsis achievement in the downregulation of SPO11 activity, suggesting that impaired homologous chromosome interactions can trigger additional SPO11-dependent DSB induction Repair of such additional DSBs specifically induced in unsynapsed chromosome regions is expected to help complete synapsis of those regions (Carballo et al, 2013). This hypothesis is supported by the analysis of meiosis in yeast strains carrying a mutation in Zip1 (the SC protein component responsible of mediating synapsis in budding yeast), which appear to experience more abundant DSB induction by SPO11 (Thacker et al, 2014).

1.3.2. DSB resection

Due to repression of the non-homologous end joining (NHEJ) pathway for DSB

repair (Goedecke et al, 1999), meiotic DSBs are forced in the HR-mediated repair, which requires a resection step at DSB ends to generate the single-stranded DNA (ssDNA) (Farah et al, 2009), that will be used for homology search. SPO11 acts as a homodimer, performing a transesterification on a 5' phosphate on either DNA strand, thereby establishing a covalent bond with the nucleotide (Keeney et al, 1997). To remove SPO11 and to expose the DSB, SPO11-bound oligos have to be released by endonucleolytic cleavage that requires the MRN complex and CtIP (Hartsuiker et al, 2009; Mimitou and Symington, 2009). MRN consists of three subunits: MRE11, which has endonucleolytic and mild exonucleolytic activity; RAD50 which associates with MRE11 forming two heterodimers that bridge the DSB ends; NBN (Nbs1) that interacts with ATM and participates to the triggering of H2AX phosphorylation as a DNA damage response (Lamarche et al, 2010). The MRE112RAD502NBN1 complex allows coordination of the two ends of a DSB to keep them in close proximity. The endonucleolytic cleavage of the SPO11-DNA complex releases so-called SPO11-oligos which can be around 25 or 40 nt long (Garcia et al, 2011). It has been speculated that the shorter SPO11-oligos separate immediately from the partner strand, whereas the longer ones stay annealed. Such a difference is thought to result in asymmetrical resection of the DSB ends, that implies two overhangs of different length and possibly differential recruitment of repair proteins such as DMC1 and RAD51 (see below) (Neale et al, 2005). When SPO11 oligos are released, both DSB ends are further resected in the 5'-3' direction by EXO1, which generates 3'-ssDNA overhangs (Schaetzlein et al, 2013; Zakharyevich et al, 2010). Resection can go up to 1kb, and a single-stranded DNA binding protein is therefore required to prevent formation of secondary structures in the 3'-overhangs. As in mitotic cells, replication protein A (RPA), a highly conserved ssDNA binding protein, composed of three subunits, rapidly coats the ssDNA generated at the sites of meiotic DSBs (Sakaguchi et al, 2009; Wang et al, 2005).

1.3.3 Joint molecules formation

RPA is rapidly replaced by recombinases, which are enzymes with ATP-ase dependent activity that perform strand exchange between two DNA molecules involved in homologous recombination (Bannister and Schimenti, 2004; Bishop, 1994; Moens et al, 1997; Plug et al, 1996; Sung et al, 2003; Tarsounas et al, 1999).

Recombinases are loaded and form a nucleoprotein filament with the ssDNA in the presynaptic step of homologous recombination (Masson et al, 1999; Sehorn et al, 2004; Zaitseva et al, 1999). The nucleoprotein filament scans the intact DNA searching possible homologous templates by coordinating the single-stranded resected DNA end and the dsDNA of the recombination partner (Bertucat et al, 2000; Cloud et al, 2012; De Vlaminck et al, 2012; Mazin and Kowalczykowski, 1998) which interact with two distinct domains of the protein. When a homologous template is found, one of the DNA strands is displaced, leading to the formation of a displacement loop (D-loop) (Petukhova et al, 2000; Sehorn et al, 2004). Annealing of the ssDNA in the nucleoprotein with the complementary strand of the template dsDNA (synaptic step) leads to the formation of a stable recombination intermediate (joint molecule) and provides a substrate for DNA synthesis. At this point, recombinases are removed, which renders the DNA molecule accessible for polymerase activity. After DNA synthesis is completed, homologous recombination can enter the post-synaptic stage. The newly synthetized strand can either dissociate from the D-loop and reanneal to the parental strand, or engage the other DSB end into second end capture. In the first case, the invading strand is displaced and relegate to the second resected DSB end, leading to reformation of the original DNA molecule. This process is termed synthesis dependent strand annealing (SDSA) (McMahill et al, 2007). When second end capture occurs, a double Holliday junction (dHJ) is formed. This is a dynamic junction between four single strands of DNA on two sides of the region involved in DSB repair or recombination (named after Robin Holliday, who described this in 1964) (Szostak et al, 1983). The double Holliday junction can result into a crossover (CO) or a non-crossover (NCO) event, depending on how they are resolved.

In mitotic cells, RAD51 is the protein responsible for the process of strand exchange. It is able to form a right-handed helical filament on ssDNA and mediate homology recognition of the intact repair template (Yu et al, 2001). Besides RAD51, a meiosis-specific homolog is present in mouse and in yeast: DMC1. This protein is also a recombinase, with 51% amino acid sequence identity to RAD51 in mouse (45% in budding yeast), and the two proteins are structurally very similar (Conway et al, 2004; Kinebuchi et al, 2004). Accumulation of both proteins at the sites of DSBs can be observed by immunofluorescence staining as foci, which colocalize almost completely at a resolution of around 300 nm, indicating that both

proteins participate in HR-mediated repair at every DSB. Expression of Rad51/RAD51 and Dmc1/DMC1 in meiotic prophase between yeast and mouse indicates that they are both essential for some highly conserved aspects of meiosis. In budding yeast, absence of Dmc1 results in complete lack of recombination intermediates, suggesting that Dmc1 is essential for the process (Hong et al, 2013). Similarly, it has been shown that mouse meiocytes (both male and female meiotic prophase cells) defective for DMC1 succeed in loading RAD51, but fail to complete recombination and are therefore depleted, resulting in infertility (Pittman et al, 1998; Yoshida et al, 1998). It is not known if RAD51 is essential for meiosis in mouse. Due to its somatic functions, mutational loss of RAD51 is a lethal condition. To study its role in meiotic prophase, this would require conditional knockout of the Rad51 gene. However, we anticipate, in view of the highly conserved expression of both RAD51 and DMC1 in meiotic prophase, and the many observations on localization of both proteins to sites of DSBs in meiotic prophase cells in species ranging from yeast to plants, and mammals, that it is warranted to investigate the possible respective roles of these two proteins in more detail.

► Figure 3: Homologous recombination during meiotic prophase I

(A) Meiotic nuclei carry two homologous chromosomes per pair, each consisting of the copies of the same dsDNA, the sister chromatids. (B) Meiotic recombination is initiated by the induction of DNA double strand breaks (DSBs) by the transesterase SPO11 (1). To perform DSB end resection, the covalently linked SPO11 homodimer needs to be removed. The MRN complex and CTIP perform an endonuclease cut in the DNA strands to which SPO11 is bound, thereby releasing SPO11-associated oligonucleotides. The exonuclease EXO1 will further resect the DNA strands in a 5'-3' direction, generating 3' single-stranded DNA (ssDNA) overhangs (2). Pre-synaptic phase of homologous recombination (HR): the ssDNA-binding protein RPA will coat the 3' overhangs to prevent formation of secondary structures in the ssDNA (3). Subsequently, the recombinases RAD51 and DMC1 will rapidly replace RPA on the resected ends, forming nucleoprotein filaments (4) to start homology search. Synaptic phase of HR: in meiotic cells an intact homologous template for repair can be found in the sister chromatid or in the homologous chromosome. RAD51/DMC1 nucleoprotein filaments can therefore perform intersister (IS) or interhomolog (IH) strand invasion (5). Recombinases are removed to allow DNA synthesis (dashed line), and the newly synthetized DNA strand can undergo synthesis dependent strand annealing (not shown) or second end capture, forming double Holliday junctions (dHJs) (6). At this stage RPA can be recruited again to ssDNA stretches. Post-synaptic phase: the newly synthetized DNA strand is religated to the opposite DSB end, and the complementary strand can be filled in. At this stage, dHJs generated upon IH strand invasion can be resolved either as crossovers or as non-crossovers. dHJs formed between sisters always yield non-crossover events (7). (C) Parallel to SPO11-mediated DSB induction, ATM signaling is activated, which results in phosphorylation of H2AX into γH2AX in the chromatin surrounding the DSB. The spreading of γH2AX is not linear and can occur in up to 3 Mb of DNA.

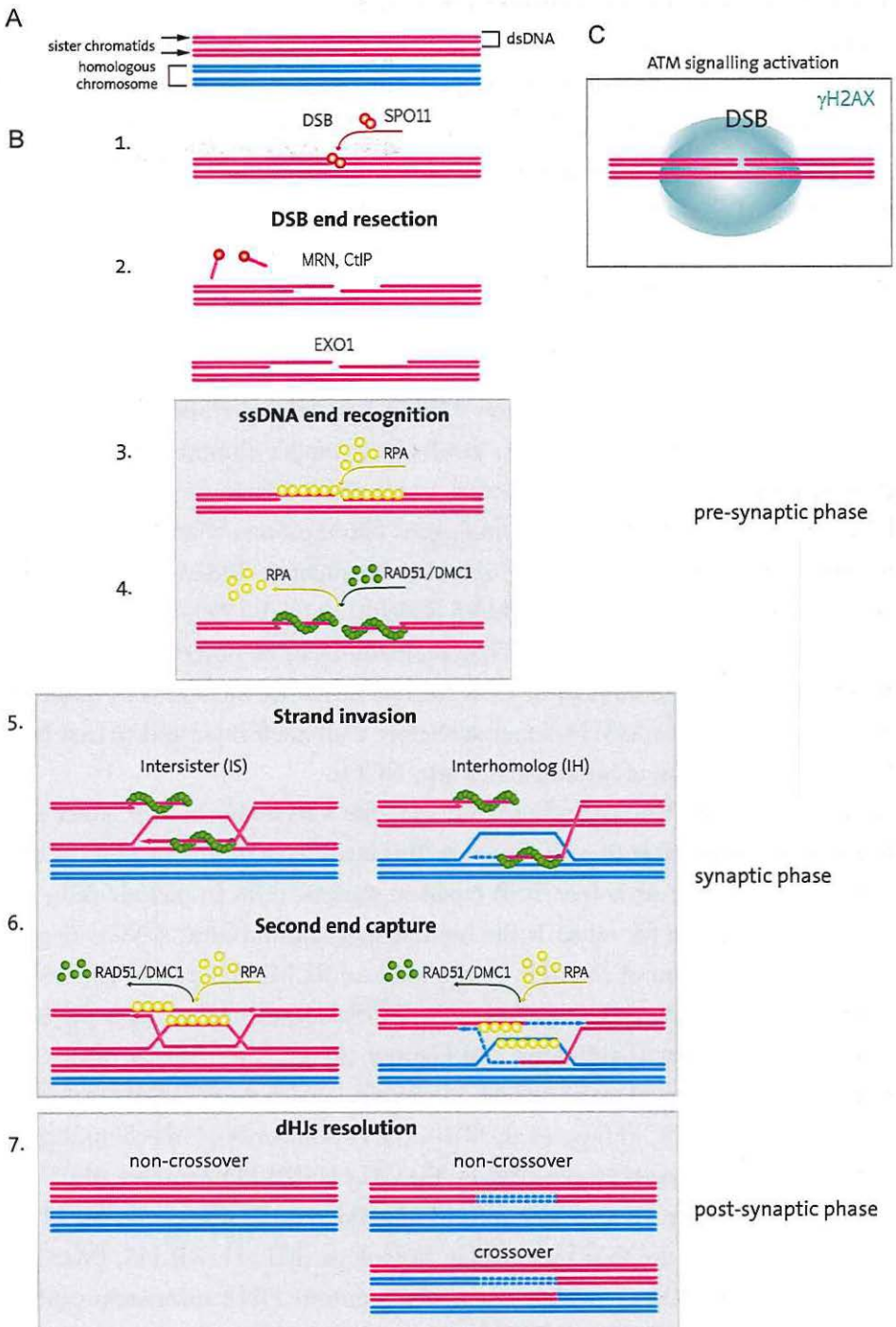
A
sister chromatids
homologous chromosome
dsDNA
B
1.
DSB
SPO11
DSB end resection
2.
MRN, CtIP
EXO1
ssDNA end recognition
3.
RPA
4.
RPA
RAD51/DMC1
pre-synaptic phase
5.
Strand invasion
Intersister (IS)
Interhomolog (IH)
synaptic phase
6.
Second end capture
RAD51/DMC1
RPA
RAD51/DMC1
RPA
7.
dHJs resolution
non-crossover
non-crossover
crossover
post-synaptic phase
C
ATM signalling activation
γH2AX
DSB

1.3.4 Joint molecules resolution

After recombinase recruitment to meiotic DSBs, another set of proteins appears to form foci associated with the SC and partially colocalizing with RAD51/DMC1 foci: the proteins that mediate postreplication mismatch repair (MMR) in somatic cells (Kolas et al, 2005). Two families are known to contribute to MMR, the MutS and the MutL(Kolodner and Marsischky, 1999). In yeast and in mouse, two proteins of the MutS family have been identified to participate in meiotic recombination: MSH4 and MSH5. These meiosis-specific proteins are known to interact with MutL proteins, forming a complex that mediates joint molecule resolution into CO events (Edelmann et al, 1999; Kneitz et al, 2000; Neyton et al, 2004; Rogacheva et al, 2014). However, it is not clear how MSH4/5 proteins perform their function in meiosis. Mutation of these proteins results in improper chromosome pairing and thereby inefficient DSB repair, pointing to a possible role in processing of recombination intermediates between homologous chromosomes that would contribute to stabilization of homologous chromosome interactions. Indeed, no COs are observed in meiotic cells lacking MSH4/5 (Edelmann et al, 1999; Kneitz et al, 2000; Wei et al, 2002). Notably, MSH4/5 accumulation can be observed at many more sites than the average number of COs formed in mouse meiotic cells (Cole et al, 2012), suggesting that MSH4/5 may act before COs are formed and/or may be also involved in resolution of intermediates into NCOs.

dHJs that involve the sister chromatid generate a recombination product that is genetically comprarable to a NCO event. This is the type of homologous recombination used also for error-free DSB repair in somatic cells. In meiotic cells, when the chosen template for repair is the homologous chromosome, a NCO is generated upon dissolution of the dHJ by the helicase BLM, that pushes the two HJs towards each other, and the topoisomerase TOPOIII, which separates the entangled DNA molecules (Symington and Gautier, 2011). Alternatively, dHJs can be resolved by symmetrical or asymmetrical cleavage, which may lead to formation of either a NCO or a CO (Heyer et al, 2010). The vast majority of interhomolog COs are obtained via resolution of a dHJ by the MLH1-MLH3 complex which leads to exchange between sister chromatids of homologous chromosomes. MLH1 and MLH3 are two of the four mammalian homologs (MLH1, MLH3, PMS1, and PMS2) of bacterial MutL, which play a role in mitotic DNA mismatch repair, and in meiosis (Hunter and Borts, 1997; Lipkin et al, 2002; Wang et al, 1999; Yao et al,

1999). NCOs genetically correspond to gene conversion events between the sisters (IS dHJs) or between the homologs (IH dHJs). Obviously, intersister gene conversion cannot be detected, because identical sequences will be exchanged. When occurring between homologs, they may contribute to genetic variation at a smaller scale, if the exchanged allelic sequences are not entirely identical. The exchanged tracts in gene conversion are much shorter than the chromosomal tracts recombined in a CO (Padhukasahasram and Rannala, 2013), which makes it unlikely to find a single nucleotide polymorphism (SNP) between them. This means that gene conversion events usually fall below the radar of genetic tests, and are very difficult to detect and quantify. Based on the fact that a NCO can be obtained through several mechanisms of JM resolution (SDSA, dHJ dissolution, and dHJ resolution), it is expected that gene conversions represent the vast majority of meiotic recombination outcomes. Indeed, COs have been quantified around an average of 25-28 per nucleus in mouse. Taking into consideration the much (about 10-fold) higher number of DSBs originally induced at the onset of meiosis, it can be deduced that gene conversions largely outnumber chromatid arm exchanges.

1.4 THE SEX CHROMOSOMES IN MEIOSIS

In mouse, as in virtually all placental mammals, the male is the heterogametic sex. This means that the males carry two different sex chromosomes, the X and the Y, and the females have two X chromosomes. The two sex chromosomes differ enormously, by size and gene content, and are largely heterologous (Sutton et al, 2011). The very small XY homologous region is located at the very end of the X and Y chromosomes, opposite from the telomeric ends, and is about 700 kilobase (kb) in length. This homologous region is named the pseudo-autosomal region (PAR), which is the only region where X and Y can pair in meiosis and where a CO can occur (Perry et al, 2001). In fact, this is an obligate CO, which occurs in every nucleus (Barchi et al, 2008). Outside the PARs, the heterologous regions of the X and Y chromosomes remain unsynapsed, in male meiotic prophase. In contrast, the two X chromosomes in meiotic prophase oocytes engage in complete synapsis. As a consequence of the extensive asynapsis of the X and Y chromosomes in primary spermatocytes, a silencing mechanism is triggered, which targets the unsynapsed regions of both X and Y. This global transcriptional silencing of the heterologous regions is named Meiotic Sex Chromosome Inactivation (MSCI) (Turner, 2007;

Turner et al, 2006; Turner et al, 2005). MSCI involves major chromatin modifications, so that the silenced XY pair becomes microscopically visible, from pachytene onwards, forming the heterochromatic sex body (or XY body). It has been shown that unpaired autosomal regions also undergo a similar chromatin modification resulting in silencing (Baarends and Grootegoed, 2003; Baarends et al, 2005; Schoenmakers et al, 2008; Shiu and Metzenberg, 2002; Shiu et al, 2001; Turner et al, 2005), which in fact also occurs in female meiotic prophase (Kouznetsova et al, 2009; Shin et al, 2013), and it is thought that MSCI is related to a more general and evolutionary ancient process of transcriptional inactivation that targets unsynapsed chromosome in meiotic cells, referred to as Meiotic Silencing of Unsynapsed Chromatin (MSUC). Meiotic silencing is mediated by several protein factors that belong to different pathways: synapsis surveillance, DNA repair, and transcriptional silencing. The earliest known marker of MSCI/MSUC is phosphorylation of the histone variant H2AX on the serine 139 (γH2AX) (Fernandez-Capetillo et al, 2003), which in somatic cells can be performed by the protein kinases DNA PKcs, ATM and ATR (ATM Rad3-related). Based on its specific localization to the sex body, ATR seems to be the major player in γH2AX formation on the sex chromosomes (Turner et al, 2004), although its activity appears not to be necessary for maintenance of meiotic silencing after the XY body has been formed (Royo et al, 2013). In SPO11-deficient spermatocytes, formation of such a domain is also observed, and thought to be a response to the presence of unsynapsed chromosome areas, due to impaired homologous chromosome pairing and synapsis (Bellani et al, 2005). This domain does not correspond to the X and Y chromatin and it is therefore called a pseudo XY body. However, the pseudo XY body accumulates the same markers as the proper sex body and undergoes the same silencing mechanism via ATR (Bellani et al, 2005). Activity of ATR in the sex/unsynapsed chromatin is dependent on functional BRCA1 (Turner et al, 2004), which is also an important component of the DSB repair pathway (Cressman et al, 1999; Welcsh et al, 2000; Xu et al, 2003). This suggests a relationship between the presence of DNA damage and silencing of the sex chromosomes. Indeed, several RAD51 and DMC1 foci can be observed on the unsynapsed region of the X chromosome in spermatocytes, even when almost all autosomal foci have already disappeared. Accordingly, also 53BP1, TOPBP1, and MDC1, which are involved in DNA repair pathways, specifically localize to the X and Y chromosomes at pachytene (Ahmed et al, 2007; Perera et

al, 2004). In particular MDC1 has been shown to be required for chromatin-wide spreading of γH2AX on the sex chromosomes. In the absence of MDC1, H2AX phosphorylation is not amplified and only decorates the chromosomal axes, resulting in incomplete MSCI and subsequent meiotic failure (Ichijima et al, 2011). An explanation for such extensive recruitment of DNA damage response proteins to the unsynapsed X and Y likely relates to the fact that DSBs on the X chromosome lack a homologous counterpart for repair, even when the X is paired and connected to the Y through synapsis between the PARs of both sex chromosomes. These X chromosome-associated DSBs therefore persist. In this situation, the X might rely on DSB repair using the sister chromatid, but this pathway apparently is suppressed. Analysis of meiosis in SPO11-deficient mouse spermatocytes has shown that MSUC can no longer occur in the absence of HORMADs (Kogo et al, 2012). These proteins that localize to unsynapsed regions are essential for establishment of meiotic silencing in the pseudo XY body. This hints to a role of HORMADs also in formation of the XY body proper, by helping to restrict the MSCI response only to the XY pair. Transcriptional silencing is achieved by deposition of histone modifications that characterize heterochromatin, such as H3K27me3. At mid-pachytene, very active transcription in spermatocytes can be observed by an increased level of histone acetylation on autosomes (Hazzouri et al, 2000; Kuo and Allis, 1998; Wade et al, 1997), but not on the XY. The sex chromosomes are enriched for markers of heterochromatin and compartimentalized to the periphery of the nucleus . Such phenomenon can be observed at the DNA level, by looking at pachytene nuclei stained with the intercalating agent DAPI. The XY body is seen as a DAPI-dense domain, clearly set aside from the rest of the chromatin. As a result of the chromatin modifications, transcription of genes from the sex chromosomes is prevented, as can be observed also by analysis of RNA polymerase II localization in pachytene spermatocytes (Baarends et al, 2005).

1.5 ANALYSIS OF MOUSE MEIOTIC PROPHASE BY FLUORESCENCE MICROSCOPY

Mechanisms of meiotic recombination and homologous chromosome interactions in mouse are generally investigated using a genetic approach. So far it was not possible to establish and in vitro system to culture mouse meiotic cells and follow their development. Thus, studies of mouse meiosis strongly rely on the use of

fixed bioptic material from mouse gonads to analyse the features of meiosis-specific mechanisms in wild type and genetically modified mouse models. In addition to the (immuno)histochemistry approach, a very efficient method of preparation of meiotic spread nuclei has been developed (Peters et al, 1997), which allows detailed analysis of meiotic events by using a fluorescence immunocytochemistry approach. Immunolabelling of proteins of interest can be performed in spread meiotic nuclei and can convey a substantial amount of information (Figure 4). Analysis of the pattern of SC protein components is widely used to stage meiotic prophase nuclei (as previously shown in figure 2). In addition, accumulation of proteins involved in DSB repair (RPA, RAD51, DMC1, MSH4/5) on the DSB sites results in a dotted pattern of foci. Each DSB repair protein focus is thought to correspond to a single DSB, and foci quantification has been instrumental to estimate the amount of induced DSBs in mouse meiotic prophase (figure 4A-C) (Cole et al, 2012). As DSB repair progresses, the repair proteins RAD51 and DMC1 will no longer be needed and their foci will gradually disappear. Dynamics of DSB repair foci can then be used to evaluate the extent and the efficiency of DSB repair in meiotic cells. Part of these DSBs will yield formation of a crossover via the activity of MutL protein complexes. Using immunofluorescent staining for MLH1 (of MLH3), crossing over sites can be visualized as foci that localize on the SC in spread meiotic nuclei. Beside DSB repair proteins, also a DNA damage response is triggered upon SPO11 activity (as discussed before). As in mitotic cells, the main marker of DNA damage is γH2AX accumulation (Rogakou et al, 1998) which occurs nucleus-wide in early meiotic prophase nuclei. Similar to RAD51/DMC1 and RPA foci, this histone mark will also gradually disappear, parallel to DSB repair. Indeed, at pachytene, only very small foci of γH2AX are observed in association with chromosomes in oocytes, and with autosomes in spermatocytes. The XY pair, on the contrary, shows intense γH2AX presence on the entire XY chromatin from pachytene onwards, which is a mark of MSCI. Silencing of the X and Y chromosomes can be appreciated by fluorescent immunostaining of RNA polymerase II, which is present on the autosomes but depleted from the sex chromosomes. In principle, immunofluorescence microscopy can be widely used to extensively study several aspects of meiosis. The groundbreaking progress in increasing the resolution of optical microscopy techniques opens even broader perspectives for future research in the field of meiosis.

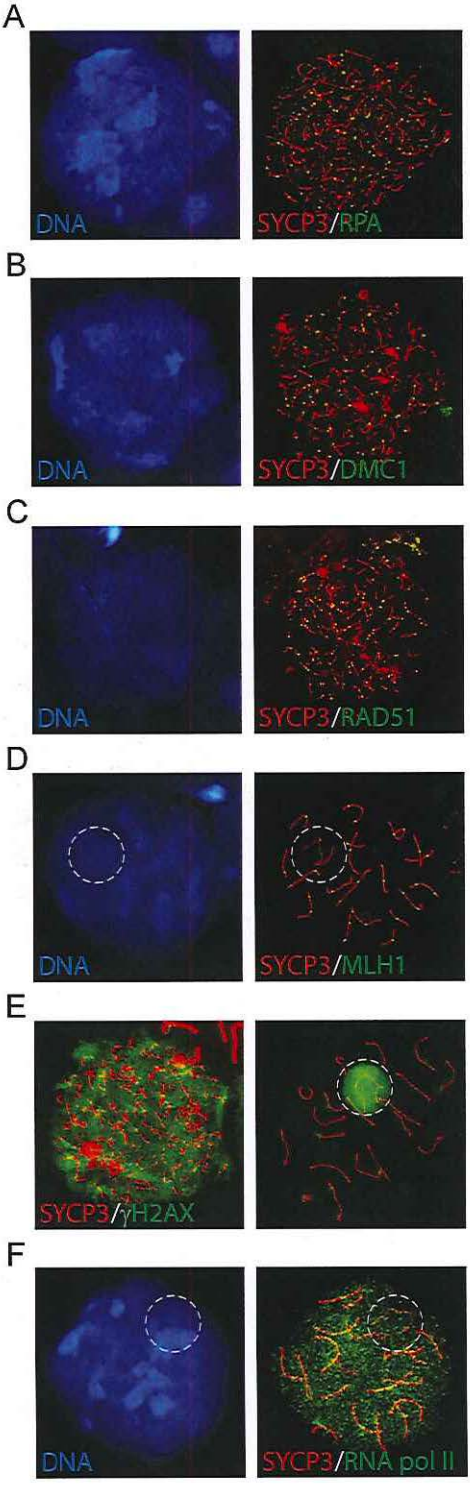

Figure 4: Meiotic prophase I can be studied by immunofluorescent stainings and fluorescent microscopy analysis

Representative images are shown of spread spermatocyte nuclei immunostained for proteins of interest during meiotic prophase.

(A-C) Double immunostaining of leptotene spermatocyte nuclei with anti-SYCP3 (red) and anti-RPA (A), anti-DMC1 (B), and anti-RAD51 (C), all in green. The DNA is counterstained with DAPI (blue). Small patches of axial elements can be observed by SYCP3 staining. Proteins involved in the processing of the DSBs form foci that associate with the synaptonemal complex. These images can be used for quantification of DSB repair protein foci. (D) Double immunostaining of pachytene spermatocyte nucleus with anti-SYCP3 (red) and anti-MLH1 (green). MLH1 marks crossover sites and can be observed as protein foci localizing on the synaptonemal complex. Every pair of synapsed homologs shows at least one MLH1 focus. The dashed circle indicates the X and Y chromosomes, which are largely unsynapsed, but show an MLH1 focus in the synapsed pseudoautosomal region. From the DAPI staining the compartimentalization and the heterochromatic state of the sex chromosomes can be appreciated. (E) Double immunostaining of spermatocyte nuclei with anti-SYCP3 (red) and anti-γH2AX green. At leptotene (left panel), many DSBs have been induced eliciting nucleus-wide accumulation of γH2AX. By pachytene most autosomal DSBs have been repaired, so that only limited γH2AX can be detected on autosomes. The dashed circle indicates the X and Y chromosomes which are undergoing MSCI, therefore the entire XY chromatin accumulates γH2AX. (F) Double immunostaining of pachytene spermatocyte nucleus with anti-SYCP3 (red) and anti-RNA polymerase II (green). At pachytene, transcriptional reactivation occurs in spermatocyte nuclei. However, the X and Y chromosomes (dashed circle) are transcriptionally silenced by MSCI. Depletion of RNA polymerase II can be observed on the XY chromatin, compared to the overall level in the nucleus.

Aim and scope of this thesis

In sexually reproducing species, the recombination events occurring in meiosis greatly contribute to genetic diversity among the progeny. Without such diversity, species would have a reduced chance of evolutionary adaptation and would be more susceptible to extinction. During meiosis, the genome faces the double-edged sword of induction of double strand DNA breaks (DSBs) by the transesterase SPO11, which are potentially detrimental to genomic integrity but also instrumental for proper meiotic division. Repair of SPO11-dependent DSBs by homologous recombination (HR) favours homologous interactions between chromosomes, instead of interactions between sister chromatids. This phenomenon is referred to as the interhomolog bias. Repair of the majority of meiotic DSBs by interaction of the broken DNA strand with one of the chromatids of the homologous chromosome, will therefore facilitate chromosome pairing and synapsis, which in turn is expected to allow more rapid DSB repair. In the largely heterologous pair of the sex chromosomes achievement of synapsis is limited to a very small region. This causes activation of surveillance mechanisms due to the lack of synapsis, which mediate transcriptional silencing of unsynapsed chromatin (MSUC), a process that most likely evolved into a specialized transcriptional silencing mechanism to inactivate the unsynapsed X and Y chromosomes (MSCI). As an additional consequence of such extensive chromosome asynapsis of the X and Y chromosomes, repair of meiotic DSBs in the heterologous regions cannot occur through the regular meiotic HR pathway, in view of lack of a homologous chromosome region. This is associated with persistence of DSB repair foci along the X chromosome, during progress of the meiotic prophase, where autosomal DSBs are repaired at an earlier stage. The general scope and aim of this thesis is to explore the pivotal role of DSBs in the meiosis-specific processes of homologous chromosome pairing and meiotic silencing. In Chapter 2, we address the relationship between the presence of persistent DSBs and the establishment of MSUC in mouse meiosis, and extend our findings to the XY-specific silencing mechanism of MSCI in male mouse meiosis. To uncover specific features of SPO11-dependent DSBs in triggering meiosis-specific processes, we compare the fate of SPO11-induced DSBs to that of exogenous radiation-induced DSBs, as described in Chapter 3, with respect to the mechanism and efficiency of DSB repair, and to the contribution of such repair to the establish-

ment of chromosomal interactions. In Chapter 4, the organization of recombination foci is investigated. A special aspect of meiotic homologous recombination is that, unlike HR repair in mitotic cells, it requires the presence of two recombinases: RAD51 which is essential in both mitotic and meiotic cells, and its paralog DMC1, that is meiosis-specific. DMC1 shares only about 50% amino acid sequence homology with RAD51. In other model species for meiosis, such as the yeast *S. cerevisiae* and the plant *A. thaliana*, RAD51 and DMC1 seem to play a specific role in homologous recombination partner choice, and in mediating the formation of recombination intermediates that can develop into crossovers. Super-resolution microscopy techniques are applied in the study described in Chapter 4, to determine the precise localization of RAD51 relative to DMC1 in meiotic foci. We try to establish a mechanistic link between the architecture of RAD51/DMC1 foci and the progression of meiotic recombination. Ultimately this study is expected to help deciphering the mechanism by which RAD51 and DMC1 may contribute to the bias towards the homolog in partner choice during meiosis. Chapter 5 provides a comprehensive discussion of the two main aspects of meiosis in which DSBs play a key role: transcriptional silencing and homologous chromosome interactions. The findings presented in this thesis are discussed in the context of the recent advances in clarifying the molecular mechanisms that mediate meiotic silencing and recombination partner choice. In addition, possible future directions are proposed for further studies aimed at unraveling the dynamics of meiotic recombination in the framework of meiotic chromosome structure.

References

Acquaviva L, Szekvolgyi L, Dichtl B, Dichtl BS, de La Roche Saint Andre C, Nicolas A, and Geli V (2013). The COMPASS subunit Spp1 links histone methylation to initiation of meiotic recombination. Science 339:215-218.

Ahmed EA, van der Vaart A, Barten A, Kal HB, Chen J, Lou Z, Minter-Dykhouse K, Bartkova J, Bartek J, de Boer P, et al. (2007). Differences in DNA double strand breaks repair in male germ cell types: lessons learned from a differential expression of Mdc1 and 53BP1. DNA Repair (Amst) 6:1243-1254.

Albiez H, Cremer M, Tiberi C, Vecchio L, Schermelleh L, Dittrich S, Kupper K, Joffe B, Thormeyer T, von Hase J, et al. (2006). Chromatin domains and the interchromatin compartment form structurally defined and functionally interacting nuclear networks. Chromosome Res 14:707-733.

Anderson LK, Reeves A, Webb LM, and Ashley T (1999). Distribution of crossing over on mouse synaptonemal complexes using immunofluorescent localization of MLH1 protein. Genetics 151:1569-1579.

Arbel A, Zenvirth D, and Simchen G (1999). Sister chromatid-based DNA repair is mediated by RAD54, not by DMC1 or TID1. EMBO J 18:2648-2658.

Arnheim N, Calabrese P, and Tiemann-Boege I (2007). Mammalian meiotic recombination hot spots. Annu Rev Genet 41:369-399.

Baarends WM, and Grootegoed JA (2003). Chromatin dynamics in the male meiotic prophase. Cytogenet Genome Res 103:225-234.

Baarends WM, Wassenaar E, van der Laan R, Hoogerbrugge JW, Sleddens-Linkels E, Hoeijmakers JH, de Boer P, and Grootegoed JA (2005). Silencing of unpaired chromatin and histone H2A ubiquitination in mammalian meiosis. Molecular and Cellular Biology 25:1041-1053.

Baker CL, Walker M, Kajita S, Petkov PM, and Paigen K (2014). PRDM9 binding organizes hotspot nucleosomes and limits Holliday junction migration. Genome Res 24:724-732.

Bannister LA, Reinholdt LG, Munroe RJ, and Schimenti JC (2004). Positional cloning and characterization of mouse mei8, a disrupted allelle of the meiotic cohesin Rec8. Genesis 40:184-194.

Bannister LA, and Schimenti JC (2004). Homologous recombinational repair proteins in mouse meiosis. Cytogenet Genome Res 107:191-200.

Barchi M, Roig I, Di Giacomo M, de Rooij DG, Keeney S, and Jasin M (2008). ATM promotes the obligate XY crossover and both crossover control and chromosome axis integrity on autosomes. PLoS Genet 4:e1000076.

Baudat F, Buard J, Grey C, Fledel-Alon A, Ober C, Przeworski M, Coop G, and de Massy B (2010). PRDM9 is a major determinant of meiotic recombination hotspots in humans and mice. Science 327:836-840.

Baudat F, and de Massy B (2007). Regulating double-stranded DNA break repair towards crossover or non-crossover during mammalian meiosis. Chromosome Res 15:565-577.

Baudat F, Manova K, Yuen JP, Jasin M, and Keeney S (2000). Chromosome synapsis defects and sexually dimorphic meiotic progression in mice lacking spo11. Mol Cell 6:989-998.

Bellani MA, Romanienko PJ, Cairatti DA, and Camerini-Otero RD (2005). SPO11 is required for sex-body formation, and Spo11 heterozygosity rescues the prophase arrest of Atm-/- spermatocytes. J Cell Sci 118:3233-3245.

Berr A, Pecinka A, Meister A, Kreth G,

Fuchs J, Blattner FR, Lysak MA, and Schubert I (2006). Chromosome arrangement and nuclear architecture but not centromeric sequences are conserved between Arabidopsis thaliana and Arabidopsis lyrata. Plant J 48:771-783.

Bertucat G, Lavery R, and Prevost C (2000). A Mechanism for RecA-Promoted Sequence Homology Recognition and Strand Exchange Between Single-Stranded DNA and Duplex DNA, via Triple-Helical Intermediates. J Biomol Struct Dyn 17 Suppl 1:147-153.

Billings T, Parvanov ED, Baker CL, Walker M, Paigen K, and Petkov PM (2013). DNA binding specificities of the long zinc-finger recombination protein PRDM9. Genome Biol 14:R35.

Billings T, Sargent EE, Szatkiewicz JP, Leahy N, Kwak IY, Bektassova N, Walker M, Hassold T, Graber JH, Broman KW, et al. (2010). Patterns of recombination activity on mouse chromosome 11 revealed by high resolution mapping. PLoS One 5:e15340.

Bishop DK (1994). RecA homologs Dmc1 and Rad51 interact to form multiple nuclear complexes prior to meiotic chromosome synapsis. Cell 79:1081-1092.

Boateng KA, Bellani MA, Gregoretti IV, Pratto F, and Camerini-Otero RD (2013). Homologous Pairing Preceding SPO11-Mediated Double-Strand Breaks in Mice. Dev Cell 24:196-205.

Bolcun-Filas E, Costa Y, Speed R, Taggart M, Benavente R, De Rooij DG, and Cooke HJ (2007). SYCE2 is required for synaptonemal complex assembly, double strand break repair, and homologous recombination. J Cell Biol 176:741-747.

Bolcun-Filas E, Hall E, Speed R, Taggart M, Grey C, de Massy B, Benavente R, and Cooke HJ (2009). Mutation of the mouse Syce1 gene disrupts synapsis and suggests a link between synaptonemal complex structural components and DNA repair. PLoS Genet 5:e1000393.

Bolzer A, Kreth G, Solovei I, Koehler D, Saracoglu K, Fauth C, Muller S, Eils R, Cremer C, Speicher MR, et al. (2005). Three-dimensional maps of all chromosomes in human male fibroblast nuclei and prometaphase rosettes. PLoS Biol 3:e157.

Borde V, Robine N, Lin W, Bonfils S, Geli V, and Nicolas A (2009). Histone H3 lysine 4 trimethylation marks meiotic recombination initiation sites. Embo J 28:99-111.

Borum K (1961). Oogenesis in the mouse. A study of the meiotic prophase. Exp Cell Res 24:495-507.

Boulton A, Myers RS, and Redfield RJ (1997). The hotspot conversion paradox and the evolution of meiotic recombination. Proc Natl Acad Sci U S A 94:8058-8063.

Brianna Caddle L, Grant JL, Szatkiewicz J, van Hase J, Shirley BJ, Bewersdorf J, Cremer C, Arneodo A, Khalil A, and Mills KD (2007). Chromosome neighborhood composition determines translocation outcomes after exposure to high-dose radiation in primary cells. Chromosome Res 15:1061-1073.

Brick K, Smagulova F, Khil P, Camerini-Otero RD, and Petukhova GV (2012). Genetic recombination is directed away from functional genomic elements in mice. Nature 485:642-645.

Buard J, Barthes P, Grey C, and de Massy B (2009). Distinct histone modifications define initiation and repair of meiotic recombination in the mouse. EMBO J 28:2616-2624.

Busygina V, Sehorn MG, Shi IY, Tsubouchi H, Roeder GS, and Sung P (2008). Hed1 regulates Rad51-mediated recombination via a novel mechanism. Genes Dev 22:786-795.

Bystricky K, Laroche T, van Houwe G, Blaszczyk M, and Gasser SM (2005). Chromosome looping in yeast: telomere pairing and coordinated movement reflect anchoring efficiency and territorial organization. J Cell Biol 168:375-387.

Bzymek M, Thayer NH, Oh SD, Kleckner N, and Hunter N (2010). Double Holliday junctions are intermediates of DNA break repair. Nature 464:937-941.

Carballo JA, Panizza S, Serrentino ME, Johnson AL, Geymonat M, Borde V, Klein F, and Cha RS (2013). Budding yeast ATM/ATR control meiotic double-strand break (DSB) levels by down-regulating Rec114, an essential component of the DSB-machinery. PLoS Genet 9:e1003545.

Chen YK, Leng CH, Olivares H, Lee MH, Chang YC, Kung WM, Ti SC, Lo YH, Wang AH, Chang CS, et al. (2004). Heterodimeric complexes of Hop2 and Mnd1 function with Dmc1 to promote meiotic homolog juxtaposition and strand assimilation. Proc Natl Acad Sci U S A 101:10572-10577.

Clermont Y (1972). Kinetics of spermatogenesis in mammals: seminiferous epithelium cycle and spermatogonial renewal. Physiol Rev 52:198-236.

Clift D, and Schuh M (2013). Restarting life: fertilization and the transition from meiosis to mitosis. Nat Rev Mol Cell Biol 14:549-562.

Cloud V, Chan YL, Grubb J, Budke B, and Bishop DK (2012). Rad51 is an accessory factor for Dmc1-mediated joint molecule formation during meiosis. Science 337:1222-1225.

Cole F, Kauppi L, Lange J, Roig I, Wang R, Keeney S, and Jasin M (2012). Homeostatic control of recombination is implemented progressively in mouse meiosis. Nat Cell Biol 14:424-430.

Conway AB, Lynch TW, Zhang Y, Fortin GS, Fung CW, Symington LS, and Rice PA (2004). Crystal structure of a Rad51 filament. Nat Struct Mol Biol 11:791-796.

Coop G, and Przeworski M (2007). An evolutionary view of human recombination. Nat Rev Genet 8:23-34.

Costa Y, Speed R, Ollinger R, Alsheimer M, Semple CA, Gautier P, Maratou K, Novak I, Hoog C, Benavente R, et al. (2005). Two novel proteins recruited by synaptonemal complex protein 1 (SYCP1) are at the centre of meiosis. J Cell Sci 118:2755-2762.

Cremer M, Grasser F, Lanctot C, Muller S, Neusser M, Zinner R, Solovei I, and Cremer T (2008). Multicolor 3D fluorescence in situ hybridization for imaging interphase chromosomes. Methods Mol Biol 463:205-239.

Cremer T, and Cremer C (2001). Chromosome territories, nuclear architecture and gene regulation in mammalian cells. Nat Rev Genet 2:292-301.

Cressman VL, Backlund DC, Avrutskaya AV, Leadon SA, Godfrey V, and Koller BH (1999). Growth retardation, DNA repair defects, and lack of spermatogenesis in BRCA1-deficient mice. Mol Cell Biol 19:7061-7075.

Crone M, Levy E, and Peters H (1965). The duration of the premeiotic DNA synthesis in mouse oocytes. Exp Cell Res 39:678-688.

Daniel K, Lange J, Hached K, Fu J, Anastassiadis K, Roig I, Cooke HJ, Stewart AF, Wassmann K, Jasin M, et al. (2011). Meiotic homologue alignment and its quality surveillance are controlled by mouse HORMAD1. Nat Cell Biol 13:599-610.

de Boer E, Stam P, Dietrich AJ, Pastink A, and Heyting C (2006). Two levels of interference in mouse meiotic recombination. Proc Natl Acad Sci U S A 103:9607-9612.

De Vlaminck I, van Loenhout MT, Zweifel L, den Blanken J, Hooning K, Hage

S, Kerssemakers J, and Dekker C (2012). Mechanism of homology recognition in DNA recombination from dual-molecule experiments. Mol Cell 46:616-624.

de Vries FA, de Boer E, van den Bosch M, Baarends WM, Ooms M, Yuan L, Liu JG, van Zeeland AA, Heyting C, and Pastink A (2005). Mouse Sycp1 functions in synaptonemal complex assembly, meiotic recombination, and XY body formation. Genes Dev 19:1376-1389.

Di Carlo AD, Travia G, and De Felici M (2000). The meiotic specific synaptonemal complex protein SCP3 is expressed by female and male primordial germ cells of the mouse embryo. Int J Dev Biol 44:241-244.

Donahue RP (1972). Fertilization of the mouse oocyte: sequence and timing of nuclear progression to the two-cell stage. J Exp Zool 180:305-318.

Edelmann W, Cohen PE, Kneitz B, Winand N, Lia M, Heyer J, Kolodner R, Pollard JW, and Kucherlapati R (1999). Mammalian MutS homologue 5 is required for chromosome pairing in meiosis. Nat Genet 21:123-127.

Eijpe M, Offenberg H, Jessberger R, Revenkova E, and Heyting C (2003). Meiotic cohesin REC8 marks the axial elements of rat synaptonemal complexes before cohesins SMC1beta and SMC3. J Cell Biol 160:657-670.

Farah JA, Cromie GA, and Smith GR (2009). Ctp1 and Exonuclease 1, alternative nucleases regulated by the MRN complex, are required for efficient meiotic recombination. Proc Natl Acad Sci U S A 106:9356-9361.

Fernandez-Capetillo O, Mahadevaiah SK, Celeste A, Romanienko PJ, Camerini-Otero RD, Bonner WM, Manova K, Burgoyne P, and Nussenzweig A (2003). H2AX is required for chromatin remodeling and inactivation of sex chromosomes in male mouse meiosis. Dev Cell 4:497-508.

Fukuda T, Daniel K, Wojtasz L, Toth A, and Hoog C (2009). A novel mammalian HORMA domain-containing protein, HORMAD1, preferentially associates with unsynapsed meiotic chromosomes. Exp Cell Res 316:158-171.

Fukuda T, Fukuda N, Agostinho A, Hernandez-Hernandez A, Kouznetsova A, and Hoog C (2014). STAG3-mediated stabilization of REC8 cohesin complexes promotes chromosome synapsis during meiosis. EMBO J 33:1243-1255.

Garcia V, Phelps SE, Gray S, and Neale MJ (2011). Bidirectional resection of DNA double-strand breaks by Mre11 and Exo1. Nature 479:241-244.

Goedecke W, Eijpe M, Offenberg HH, van Aalderen M, and Heyting C (1999). Mre11 and Ku70 interact in somatic cells, but are differentially expressed in early meiosis. Nat Genet 23:194-198.

Gordon JW, and Ruddle FH (1981). Mammalian gonadal determination and gametogenesis. Science 211:1265-1271.

Gotoh H, Zhu D, and Eddy EM (1999). Protein binding to meiotic recombination hotspots in mouse testis. Ann N Y Acad Sci 870:351-353.

Grey C, Barthes P, Chauveau-Le Friec G, Langa F, Baudat F, and de Massy B (2011). Mouse PRDM9 DNA-binding specificity determines sites of histone H3 lysine 4 trimethylation for initiation of meiotic recombination. PLoS Biol 9:e1001176.

Hamer G, Gell K, Kouznetsova A, Novak I, Benavente R, and Hoog C (2006). Characterization of a novel meiosis-specific protein within the central element of the synaptonemal complex. J Cell Sci 119:4025-4032.

Hamer G, Wang H, Bolcun-Filas E, Cooke HJ, Benavente R, and Hoog C (2008). Progression of meiotic recombina-

tion requires structural maturation of the central element of the synaptonemal complex. J Cell Sci 121:2445-2451.

Handel MA, and Hunt PA (1992). Sex-chromosome pairing and activity during mammalian meiosis. BioEssays 14:817-822.

Hartsuiker E, Mizuno K, Molnar M, Kohli J, Ohta K, and Carr AM (2009). Ctp1CtIP and Rad32Mre11 nuclease activity are required for Rec12Spo11 removal, but Rec12Spo11 removal is dispensable for other MRN-dependent meiotic functions. Mol Cell Biol 29:1671-1681.

Hassold T, Sherman S, and Hunt P (2000). Counting cross-overs: characterizing meiotic recombination in mammals. Hum Mol Genet 9:2409-2419.

Hayashi K, Yoshida K, and Matsui Y (2005). A histone H3 methyltransferase controls epigenetic events required for meiotic prophase. Nature 438:374-378.

Hazzouri M, Pivot-Pajot C, Faure AK, Usson Y, Pelletier R, Sele B, Khochbin S, and Rousseaux S (2000). Regulated hyperacetylation of core histones during mouse spermatogenesis: involvement of histone deacetylases. Eur J Cell Biol 79:950-960.

Henry JM, Camahort R, Rice DA, Florens L, Swanson SK, Washburn MP, and Gerton JL (2006). Mnd1/Hop2 facilitates Dmc1-dependent interhomolog crossover formation in meiosis of budding yeast. Mol Cell Biol 26:2913-2923.

Herran Y, Gutierrez-Caballero C, Sanchez-Martin M, Hernandez T, Viera A, Barbero JL, de Alava E, de Rooij DG, Suja JA, Llano E, et al. (2011). The cohesin subunit RAD21L functions in meiotic synapsis and exhibits sexual dimorphism in fertility. EMBO J 30:3091-3105.

Heyer WD, Ehmsen KT, and Liu J (2010). Regulation of homologous recombination in eukaryotes. Annu Rev Genet 44:113-139.

Hong S, Sung Y, Yu M, Lee M, Kleckner N, and Kim KP (2013). The logic and mechanism of homologous recombination partner choice. Mol Cell 51:440-453.

Hopkins J, Hwang G, Jacob J, Sapp N, Bedigian R, Oka K, Overbeek P, Murray S, and Jordan PW (2014). Meiosis-Specific Cohesin Component, Stag3 Is Essential for Maintaining Centromere Chromatid Cohesion, and Required for DNA Repair and Synapsis between Homologous Chromosomes. PLoS Genet 10:e1004413.

Hunter N, and Borts RH (1997). Mlh1 is unique among mismatch repair proteins in its ability to promote crossing-over during meiosis. Genes Dev 11:1573-1582.

Ichijima YI, M., Lou Z, Nussenzweig A, Camerini-Otero RD, Chen J, Andreassen PR, and Namekawa SH (2011). MDC1 directs chromosome-wide silencing of the sex chromosomes in male germ cells. Genes Dev 25:959-971.

Ishiguro K, Kim J, Shibuya H, Hernandez-Hernandez A, Suzuki A, Fukagawa T, Shioi G, Kiyonari H, Li XC, Schimenti J, et al. (2014). Meiosis-specific cohesin mediates homolog recognition in mouse spermatocytes. Genes Dev 28:594-607.

Kauppi L, Barchi M, Lange J, Baudat F, Jasin M, and Keeney S (2013). Numerical constraints and feedback control of double-strand breaks in mouse meiosis. Genes Dev 27:873-886.

Keeney S, Baudat F, Angeles M, Zhou ZH, Copeland NG, Jenkins NA, Manova K, and Jasin M (1999). A mouse homolog of the Saccharomyces cerevisiae meiotic recombination DNA transesterase Spo11p. Genomics 61:170-182.

Keeney S, Giroux CN, and Kleckner N (1997). Meiosis-specific DNA double-strand breaks are catalyzed by Spo11, a member of a widely conserved protein family. Cell 88:375-384.

Keeney S, and Neale MJ (2006). Initiation

of meiotic recombination by formation of DNA double-strand breaks: mechanism and regulation. Biochem Soc Trans 34:523-525.

Khalil A, Grant JL, Caddle LB, Atzema E, Mills KD, and Arneodo A (2007). Chromosome territories have a highly nonspherical morphology and nonrandom positioning. Chromosome Res 15:899-916.

Khil PP, Smagulova F, Brick KM, Camerini-Otero RD, and Petukhova GV (2012). Sensitive mapping of recombination hotspots using sequencing-based detection of ssDNA. Genome Res 22:957-965.

Kim KP, Weiner BM, Zhang L, Jordan A, Dekker J, and Kleckner N (2010). Sister cohesion and structural axis components mediate homolog bias of meiotic recombination. Cell 143:924-937.

Kinebuchi T, Kagawa W, Enomoto R, Tanaka K, Miyagawa K, Shibata T, Kurumizaka H, and Yokoyama S (2004). Structural basis for octameric ring formation and DNA interaction of the human homologous-pairing protein Dmc1. Mol Cell 14:363-374.

Kneitz B, Cohen PE, Avdievich E, Zhu L, Kane MF, Hou H, Jr., Kolodner RD, Kucherlapati R, Pollard JW, and Edelmann W (2000). MutS homolog 4 localization to meiotic chromosomes is required for chromosome pairing during meiosis in male and female mice. Genes Dev 14:1085-1097.

Kogo H, Tsutsumi M, Ohye T, Inagaki H, Abe T, and Kurahashi H (2012). HORMAD1-dependent checkpoint/surveillance mechanism eliminates asynaptic oocytes. Genes Cells 17:439-454.

Kolas NK, Svetlanov A, Lenzi ML, Macaluso FP, Lipkin SM, Liskay RM, Greally J, Edelmann W, and Cohen PE (2005). Localization of MMR proteins on meiotic chromosomes in mice indicates distinct functions during prophase I. J Cell Biol 171:447-458.

Kolodner RD, and Marsischky GT (1999). Eukaryotic DNA mismatch repair. Curr Opin Genet Dev 9:89-96.

Kouznetsova A, Wang H, Bellani M, Camerini-Otero RD, Jessberger R, and Hoog C (2009). BRCA1-mediated chromatin silencing is limited to oocytes with a small number of asynapsed chromosomes. J Cell Sci 122:2446-2452.

Kumar R, Bourbon HM, and de Massy B (2010). Functional conservation of Mei4 for meiotic DNA double-strand break formation from yeasts to mice. Genes Dev 24:1266-1280.

Kuo MH, and Allis CD (1998). Roles of histone acetyltransferases and deacetylases in gene regulation. Bioessays 20:615-626.

Lai YJ, Lin FM, Chuang MJ, Shen HJ, and Wang TF (2011). Genetic requirements and meiotic function of phosphorylation of the yeast axial element protein Red1. Mol Cell Biol 31:912-923.

Lamarche BJ, Orazio NI, and Weitzman MD (2010). The MRN complex in double-strand break repair and telomere maintenance. FEBS Lett 584:3682-3695.

Lange J, Pan J, Cole F, Thelen MP, Jasin M, and Keeney S (2011). ATM controls meiotic double-strand-break formation. Nature 479:237-240.

Lee CY, Conrad MN, and Dresser ME (2012). Meiotic chromosome pairing is promoted by telomere-led chromosome movements independent of bouquet formation. PLoS Genet 8:e1002730.

Lin FM, Lai YJ, Shen HJ, Cheng YH, and Wang TF (2010). Yeast axial-element protein, Red1, binds SUMO chains to promote meiotic interhomologue recombination and chromosome synapsis. EMBO J 29:586-596.

Lipkin SM, Moens PB, Wang V, Lenzi

M, Shanmugarajah D, Gilgeous A, Thomas J, Cheng J, Touchman JW, Green ED, et al. (2002). Meiotic arrest and aneuploidy in MLH3-deficient mice. Nat Genet 31:385-390.

Llano E, Herran Y, Garcia-Tunon I, Gutierrez-Caballero C, de Alava E, Barbero JL, Schimenti J, de Rooij DG, Sanchez-Martin M, and Pendas AM (2012). Meiotic cohesin complexes are essential for the formation of the axial element in mice. J Cell Biol 197:877-885.

Mahadevaiah SK, Turner JM, Baudat F, Rogakou EP, de Boer P, Blanco-Rodriguez J, Jasin M, Keeney S, Bonner WM, and Burgoyne PS (2001). Recombinational DNA double-strand breaks in mice precede synapsis. Nat Genet 27:271-276.

Marangos P, and Carroll J (2004). Fertilization and InsP3-induced Ca2+ release stimulate a persistent increase in the rate of degradation of cyclin B1 specifically in mature mouse oocytes. Dev Biol 272:26-38.

Masson JY, Davies AA, Hajibagheri N, Van Dyck E, Benson FE, Stasiak AZ, Stasiak A, and West SC (1999). The meiosis-specific recombinase hDmc1 forms ring structures and interacts with hRad51. EMBO J 18:6552-6560.

Mazin AV, and Kowalczykowski SC (1998). The function of the secondary DNA-binding site of RecA protein during DNA strand exchange. EMBO J 17:1161-1168.

McClellan KA, Gosden R, and Taketo T (2003). Continuous loss of oocytes throughout meiotic prophase in the normal mouse ovary. Dev Biol 258:334-348.

McMahill MS, Sham CW, and Bishop DK (2007). Synthesis-dependent strand annealing in meiosis. PLoS Biol 5:e299.

Mimitou EP, and Symington LS (2009). DNA end resection: many nucleases make light work. DNA Repair (Amst) 8:983-995.

Moens PB, Chen DJ, Shen Z, Kolas N, Tarsounas M, and Heng HHQ (1997). Rad51 immunocytology in rat and mouse spermatocytes and oocytes. Chromosoma 106:207-215.

Molnar M, and Kleckner N (2008). Examination of interchromosomal interactions in vegetatively growing diploid Schizosaccharomyces pombe cells by Cre/loxP site-specific recombination. Genetics 178:99-112.

Nasmyth K, and Haering CH (2005). The structure and function of SMC and kleisin complexes. Annu Rev Biochem 74:595-648.

Nasmyth K, and Haering CH (2009). Cohesin: its roles and mechanisms. Annu Rev Genet 43:525-558.

Neale MJ, Pan J, and Keeney S (2005). Endonucleolytic processing of covalent protein-linked DNA double-strand breaks. Nature 436:1053-1057.

Neusser M, Schubel V, Koch A, Cremer T, and Muller S (2007). Evolutionarily conserved, cell type and species-specific higher order chromatin arrangements in interphase nuclei of primates. Chromosoma 116:307-320.

Neyton S, Lespinasse F, Moens PB, Paul R, Gaudray P, Paquis-Flucklinger V, and Santucci-Darmanin S (2004). Association between MSH4 (MutS homologue 4) and the DNA strand-exchange RAD51 and DMC1 proteins during mammalian meiosis. Mol Hum Reprod 10:917-924.

Niu H, Li X, Job E, Park C, Moazed D, Gygi SP, and Hollingsworth NM (2007). Mek1 kinase is regulated to suppress double-strand break repair between sister chromatids during budding yeast meiosis. Mol Cell Biol 27:5456-5467.

Niu H, Wan L, Baumgartner B, Schaefer D, Loidl J, and Hollingsworth NM (2005).

Partner choice during meiosis is regulated by Hop1-promoted dimerization of Mek1. Mol Biol Cell 16:5804-5818.

Niu H, Wan L, Busygina V, Kwon Y, Allen JA, Li X, Kunz RC, Kubota K, Wang B, Sung P, et al. (2009). Regulation of meiotic recombination via Mek1-mediated Rad54 phosphorylation. Mol Cell 36:393-404.

Novak I, Wang H, Revenkova E, Jessberger R, Scherthan H, and Hoog C (2008). Cohesin Smc1beta determines meiotic chromatin axis loop organization. J Cell Biol 180:83-90.

Padhukasahasram B, and Rannala B (2013). Meiotic gene-conversion rate and tract length variation in the human genome. Eur J Hum Genet.

Page SL, and Hawley RS (2004). The genetics and molecular biology of the synaptonemal complex. Annu Rev Cell Dev Biol 20:525-558.

Panizza S, Mendoza MA, Berlinger M, Huang L, Nicolas A, Shirahige K, and Klein F (2011). Spo11-accessory proteins link double-strand break sites to the chromosome axis in early meiotic recombination. Cell 146:372-383.

Parada LA, McQueen PG, and Misteli T (2004). Tissue-specific spatial organization of genomes. Genome Biol 5:R44.

Parada LA, McQueen PG, Munson PJ, and Misteli T (2002). Conservation of relative chromosome positioning in normal and cancer cells. Curr Biol 12:1692-1697.

Pecinka A, Schubert V, Meister A, Kreth G, Klatte M, Lysak MA, Fuchs J, and Schubert I (2004). Chromosome territory arrangement and homologous pairing in nuclei of Arabidopsis thaliana are predominantly random except for NOR-bearing chromosomes. Chromosoma 113:258-269.

Perera D, Perez-Hidalgo L, Moens PB, Reini K, Lakin N, Syvaoja JE, San-Segundo PA, and Freire R (2004). TopBP1 and ATR colocalization at meiotic chromosomes: role of TopBP1/Cut5 in the meiotic recombination checkpoint. Mol Biol Cell 15:1568-1579.

Perry J, Palmer S, Gabriel A, and Ashworth A (2001). A short pseudoautosomal region in laboratory mice. Genome Res 11:1826-1832.

Peters AH, Plug AW, van Vugt MJ, and de Boer P (1997). A drying-down technique for the spreading of mammalian meiocytes from the male and female germline. Chromosome Res 5:66-68.

Petukhova G, Sung P, and Klein H (2000). Promotion of Rad51-dependent D-loop formation by yeast recombination factor Rdh54/Tid1. Genes Dev 14:2206-2215.

Pezza RJ, Voloshin ON, Volodin AA, Boateng KA, Bellani MA, Mazin AV, and Camerini-Otero RD (2014). The dual role of HOP2 in mammalian meiotic homologous recombination. Nucleic Acids Res 42:2346-2357.

Pittman D, Lu W, and Malone RE (1993). Genetic and molecular analysis of REC114, an early meiotic recombination gene in yeast. Curr Genet 23:295-304.

Pittman DL, Cobb J, Schimenti KJ, Wilson LA, Cooper DM, Brignull E, Handel MA, and Schimenti JC (1998). Meiotic prophase arrest with failure of chromosome synapsis in mice deficient for Dmc1, a germline-specific RecA homolog. Mol Cell 1:697-705.

Plug AW, Xu J, Reddy G, Golub EI, and Ashley T (1996). Presynaptic association of Rad51 protein with selected sites in meiotic chromatin. Proc Natl Acad Sci USA 11:5920-5924.

Prieto I, Pezzi N, Buesa JM, Kremer L, Barthelemy I, Carreiro C, Roncal F, Martinez A, Gomez L, Fernandez R, et al. (2002). STAG2 and Rad21 mammalian mitotic cohesins are implicated in meiosis. EMBO Rep 3:543-550.

Prieto I, Suja JA, Pezzi N, Kremer L, Martinez AC, Rufas JS, and Barbero JL (2001). Mammalian STAG3 is a cohesin specific to sister chromatid arms in meiosis I. Nat Cell Biol 3:761-766.

Rathke C, Baarends WM, Awe S, and Renkawitz-Pohl R (2014). Chromatin dynamics during spermiogenesis. Biochim Biophys Acta 1839:155-168.

Revenkova E, Eijpe M, Heyting C, Gross B, and Jessberger R (2001). Novel meiosis-specific isoform of mammalian SMC1. Mol Cell Biol 21:6984-6998.

Revenkova E, Eijpe M, Heyting C, Hodges CA, Hunt PA, Liebe B, Scherthan H, and Jessberger R (2004). Cohesin SMC1 beta is required for meiotic chromosome dynamics, sister chromatid cohesion and DNA recombination. Nat Cell Biol 6:555-562.

Rogacheva MV, Manhart CM, Chen C, Guarne A, Surtees J, and Alani E (2014). Mlh1-Mlh3, a meiotic crossover and DNA mismatch repair factor, is a Msh2-Msh3-stimulated endonuclease. J Biol Chem 289:5664-5673.

Rogakou EP, Pilch DR, Orr AH, Ivanova VS, and Bonner WM (1998). DNA double-stranded breaks induce histone H2AX phosphorylation on serine 139. J Biol Chem 273:5858-5868.

Roix JJ, McQueen PG, Munson PJ, Parada LA, and Misteli T (2003). Spatial proximity of translocation-prone gene loci in human lymphomas. Nat Genet 34:287-291.

Romanienko PJ, and Camerini-Otero RD (2000). The mouse spo11 gene is required for meiotic chromosome synapsis. Mol Cell 6:975-987.

Royo H, Prosser H, Ruzankina Y, Mahadevaiah SK, Cloutier JM, Baumann M, Fukuda T, Hoog C, Toth A, de Rooij DG, et al. (2013). ATR acts stage specifically to regulate multiple aspects of mammalian meiotic silencing. Genes Dev 27:1484-1494.

Sakaguchi K, Ishibashi T, Uchiyama Y, and Iwabata K (2009). The multi-replication protein A (RPA) system--a new perspective. FEBS J 276:943-963.

San Filippo J, Sung P, and Klein H (2008). Mechanism of eukaryotic homologous recombination. Annu Rev Biochem 77:229-257.

Sasaki H, and Matsui Y (2008). Epigenetic events in mammalian germ-cell development: reprogramming and beyond. Nat Rev Genet 9:129-140.

Schaetzlein S, Chahwan R, Avdievich E, Roa S, Wei K, Eoff RL, Sellers RS, Clark AB, Kunkel TA, Scharff MD, et al. (2013). Mammalian Exo1 encodes both structural and catalytic functions that play distinct roles in essential biological processes. Proc Natl Acad Sci U S A 110:E2470-2479.

Schalk JA, Dietrich AJ, Vink AC, Offenberg HH, van Aalderen M, and Heyting C (1998). Localization of SCP2 and SCP3 protein molecules within synaptonemal complexes of the rat. Chromosoma 107:540-548.

Schoenmakers S, Wassenaar E, de Boer P, Laven JSE, Grootegoed JA, and Baarends WM (2008). Increased efficiency of meiotic silencing of unsynapsed chromatin in the presence of irradiation-induced extra DNA double strand breaks. Reproductive Sciences 15:46.

Schramm S, Fraune J, Naumann R, Hernandez-Hernandez A, Hoog C, Cooke HJ, Alsheimer M, and Benavente R (2011). A novel mouse synaptonemal complex protein is essential for loading of central element proteins, recombination, and fertility. PLoS Genet 7:e1002088.

Schwacha A, and Kleckner N (1994). Identification of joint molecules that form frequently between homologs but rarely between sister chromatids during yeast

meiosis. Cell 76:51-63.

Sehorn MG, Sigurdsson S, Bussen W, Unger VM, and Sung P (2004). Human meiotic recombinase Dmc1 promotes ATP-dependent homologous DNA strand exchange. Nature 429:433-437.

Sen A, and Caiazza F (2013). Oocyte maturation: a story of arrest and release. Front Biosci (Schol Ed) 5:451-477.

Sheridan S, and Bishop DK (2006). Red-Hed regulation: recombinase Rad51, though capable of playing the leading role, may be relegated to supporting Dmc1 in budding yeast meiosis. Genes Dev 20:1685-1691.

Shin YH, Choi Y, Erdin SU, Yatsenko SA, Kloc M, Yang F, Wang PJ, Meistrich ML, and Rajkovic A (2007). Hormad1 mutation disrupts synaptonemal complex formation, recombination, and chromosome segregation in mammalian meiosis. PLoS Genet 6:e1001190.

Shin YH, McGuire MM, and Rajkovic A (2013). Mouse HORMAD1 is a meiosis i checkpoint protein that modulates DNA double- strand break repair during female meiosis. Biol Reprod 89:29.

Shiu PK, and Metzenberg RL (2002). Meiotic silencing by unpaired DNA: properties, regulation and suppression. Genetics 161:1483-1495.

Shiu PK, Raju NB, Zickler D, and Metzenberg RL (2001). Meiotic silencing by unpaired DNA. Cell 107:905-916.

Smagulova F, Gregoretti IV, Brick K, Khil P, Camerini-Otero RD, and Petukhova GV (2011). Genome-wide analysis reveals novel molecular features of mouse recombination hotspots. Nature 472:375-378.

Sung P, Krejci L, Van Komen S, and Sehorn MG (2003). Rad51 recombinase and recombination mediators. J Biol Chem 278:42729-42732.

Sutton E, Hughes J, White S, Sekido R, Tan J, Arboleda V, Rogers N, Knower K, Rowley L, Eyre H, et al. (2011). Identification of SOX3 as an XX male sex reversal gene in mice and humans. J Clin Invest 121:328-341.

Symington LS, and Gautier J (2011). Double-strand break end resection and repair pathway choice. Annu Rev Genet 45:247-271.

Szostak JW, Orr-Weaver TL, Rothstein RJ, and Stahl FW (1983). The double-strand-break repair model for recombination. Cell 33:25-35.

Tarsounas M, Morita T, Pearlman RE, and Moens PB (1999). RAD51 and DMC1 form mixed complexes associated with mouse meiotic chromosome cores and synaptonemal complexes. J Cell Biol 147:207-220.

Tesse S, Storlazzi A, Kleckner N, Gargano S, and Zickler D (2003). Localization and roles of Ski8p protein in Sordaria meiosis and delineation of three mechanistically distinct steps of meiotic homolog juxtaposition. Proc Natl Acad Sci U S A 100:12865-12870.

Thacker D, Mohibullah N, Zhu X, and Keeney S (2014). Homologue engagement controls meiotic DNA break number and distribution. Nature 510:241-246.

Tsubouchi H, and Roeder GS (2006). Budding yeast Hed1 down-regulates the mitotic recombination machinery when meiotic recombination is impaired. Genes Dev 20:1766-1775.

Turner JM (2007). Meiotic sex chromosome inactivation. Development 134:1823-1831.

Turner JM, Aprelikova O, Xu X, Wang R, Kim S, Chandramouli GV, Barrett JC, Burgoyne PS, and Deng CX (2004). BRCA1, histone H2AX phosphorylation, and male meiotic sex chromosome inactivation. Curr Biol 14:2135-2142.

Turner JM, Mahadevaiah SK, Ellis PJ, Mitchell MJ, and Burgoyne PS (2006). Pachytene asynapsis drives meiotic sex chromosome inactivation and leads to substantial postmeiotic repression in spermatids. Dev Cell 10:521-529.

Turner JM, Mahadevaiah SK, Fernandez-Capetillo O, Nussenzweig A, Xu X, Deng CX, and Burgoyne PS (2005). Silencing of unsynapsed meiotic chromosomes in the mouse. Nat Genet 37:41-47.

Visser AE, Jaunin F, Fakan S, and Aten JA (2000). High resolution analysis of interphase chromosome domains. J Cell Sci 113 (Pt 14):2585-2593.

Wade PA, Pruss D, and Wolffe AP (1997). Histone acetylation: chromatin in action. Trends Biochem Sci 22:128-132.

Wan L, de los Santos T, Zhang C, Shokat K, and Hollingsworth NM (2004). Mek1 kinase activity functions downstream of RED1 in the regulation of meiotic double strand break repair in budding yeast. Mol Biol Cell 15:11-23.

Wang CC, Wu CH, Shieh JY, and Wen CY (2002). Microglial distribution and apoptosis in fetal rat brain. Brain Res Dev Brain Res 139:337-342.

Wang TF, Kleckner N, and Hunter N (1999). Functional specificity of MutL homologs in yeast: evidence for three Mlh1-based heterocomplexes with distinct roles during meiosis in recombination and mismatch correction. Proc Natl Acad Sci U S A 96:13914-13919.

Wang Y, Putnam CD, Kane MF, Zhang W, Edelmann L, Russell R, Carrion DV, Chin L, Kucherlapati R, Kolodner RD, et al. (2005). Mutation in Rpa1 results in defective DNA double-strand break repair, chromosomal instability and cancer in mice. Nat Genet 37:750-755.

Wassmann K (2013). Sister chromatid segregation in meiosis II: deprotection through phosphorylation. Cell Cycle 12:1352-1359.

Watanabe Y (2005). Shugoshin: guardian spirit at the centromere. Curr Opin Cell Biol 17:590-595.

Wei K, Kucherlapati R, and Edelmann W (2002). Mouse models for human DNA mismatch-repair gene defects. Trends Mol Med 8:346-353.

Welcsh PL, Owens KN, and King MC (2000). Insights into the functions of BRCA1 and BRCA2. Trends Genet 16:69-74.

Wojtasz L, Cloutier JM, Baumann M, Daniel K, Varga J, Fu J, Anastassiadis K, Stewart AF, Remenyi A, Turner JM, et al. (2012). Meiotic DNA double-strand breaks and chromosome asynapsis in mice are monitored by distinct HORMAD2-independent and -dependent mechanisms. Genes Dev 26:958-973.

Wojtasz L, Daniel K, Roig I, Bolcun-Filas E, Xu H, Boonsanay V, Eckmann CR, Cooke HJ, Jasin M, Keeney S, et al. (2009). Mouse HORMAD1 and HORMAD2, two conserved meiotic chromosomal proteins, are depleted from synapsed chromosome axes with the help of TRIP13 AAA-ATPase. PLoS Genet 5:e1000702.

Wu H, Mathioudakis N, Diagouraga B, Dong A, Dombrovski L, Baudat F, Cusack S, de Massy B, and Kadlec J (2013). Molecular basis for the regulation of the H3K4 methyltransferase activity of PRDM9. Cell Rep 5:13-20.

Wu HY, Ho HC, and Burgess SM (2010). Mek1 kinase governs outcomes of meiotic recombination and the checkpoint response. Curr Biol 20:1707-1716.

Wu TC, and Lichten M (1994). Meiosis-induced double-strand break sites determined by yeast chromatin structure. Science 263:515-518.

Xu H, Beasley MD, Warren WD, van der Horst GT, and McKay MJ (2005). Ab-

sence of mouse REC8 cohesin promotes synapsis of sister chromatids in meiosis. Dev Cell 8:949-961.

Xu X, Aprelikova O, Moens P, Deng CX, and Furth PA (2003). Impaired meiotic DNA-damage repair and lack of crossing-over during spermatogenesis in BRCA1 full-length isoform deficient mice. Development 130:2001-2012.

Yang F, De La Fuente R, Leu NA, Baumann C, McLaughlin KJ, and Wang PJ (2006). Mouse SYCP2 is required for synaptonemal complex assembly and chromosomal synapsis during male meiosis. J Cell Biol 173:497-507.

Yang F, and Wang PJ (2009). The Mammalian synaptonemal complex: a scaffold and beyond. Genome Dyn 5:69-80.

Yao X, Buermeyer AB, Narayanan L, Tran D, Baker SM, Prolla TA, Glazer PM, Liskay RM, and Arnheim N (1999). Different mutator phenotypes in Mlh1- versus Pms2-deficient mice. Proc Natl Acad Sci USA 96:6850-6855.

Yoshida K, Kondoh G, Matsuda Y, Habu T, Nishimune Y, and Morita T (1998). The mouse RecA-like gene Dmc1 is required for homologous chromosome synapsis during meiosis. Mol Cell 1:707-718.

Yu X, Jacobs SA, West SC, Ogawa T, and Egelman EH (2001). Domain structure and dynamics in the helical filaments formed by RecA and Rad51 on DNA. Proc Natl Acad Sci U S A 98:8419-8424.

Yuan L, Liu JG, Zhao J, Brundell E, Daneholt B, and Hoog C (2000). The murine SCP3 gene is required for synaptonemal complex assembly, chromosome synapsis, and male fertility. Mol Cell 5:73-83.

Yuan L, Pelttari J, Brundell E, Bjorkroth B, Zhao J, Liu JG, Brismar H, Daneholt B, and Hoog C (1998). The synaptonemal complex protein SCP3 can form multistranded, cross-striated fibers in vivo. J Cell Biol 142:331-339.

Zaitseva EM, Zaitsev EN, and Kowalczykowski SC (1999). The DNA binding properties of Saccharomyces cerevisiae Rad51 protein. J Biol Chem 274:2907-2915.

Zakharyevich K, Ma Y, Tang S, Hwang PY, Boiteux S, and Hunter N (2010). Temporally and biochemically distinct activities of Exo1 during meiosis: double-strand break resection and resolution of double Holliday junctions. Mol Cell 40:1001-1015.

Zanders S, Sonntag Brown M, Chen C, and Alani E (2011). Pch2 modulates chromatid partner choice during meiotic double-strand break repair in Saccharomyces cerevisiae. Genetics 188:511-521.

2

SPO11-independent DNA repair foci and their role in meiotic silencing

PLoS Genet. 2013 Jun; 9(6): e1003538. Epub 2013 June 6

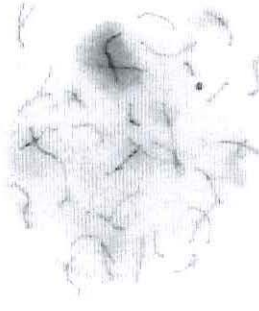

Author Summary

Meiosis is a special cell division that generates genetically divergent haploid germ cells. At the very beginning of this process, during meiotic prophase, the enzyme SPO11 generates hundreds of DNA double-strand breaks (DSBs). Meiotic DSBs are repaired via a mechanism that requires the presence of an intact homologous template. This repair process stimulates homologous chromosome pairing, and the formation of a protein complex that connects the paired chromosome axes, reaching a state called synapsis. Male mammals carry a pair of largely heterologous sex chromosomes, the X and Y, which show delayed DSB repair and extensive asynapsis. In addition, the X and Y chromosomes are transcriptionally silenced by a mechanism named Meiotic Sex Chromosome Inactivation (MSCI). This mechanism is a specialization of a more general silencing mechanism, named Meiotic Silencing of Unsynapsed Chromatin (MSUC), that is induced when any pairing problem between homologous chromosomes results in asynapsis, in male as well as female meiotic prophase cells. Here, we demonstrate that in addition to asynapsis, the persistent presence of DNA repair foci is a hallmark of meiotic silencing. In addition, we show that SPO11-independent DNA repair foci form during normal oocyte development. We propose that these foci represent sites of unrepaired DSBs that are capable of inducing transcriptional silencing, irrespective of synapsis.

SPO11-independent DNA repair foci and their role in meiotic silencing

Fabrizia Carofiglio[1], Akiko Inagaki[1,6], Sandra de Vries[2], Evelyne Wassenaar[1], Sam Schoenmakers[3], Christie Vermeulen[2], Wiggert A. van Cappellen[1,4], Esther Sleddens-Linkels[1], J. Anton Grootegoed[1], Hein P. J. te Riele[2], Bernard de Massy[5], and Willy M Baarends[1*]

[1]Department of Reproduction and Development, Erasmus MC - University Medical Center, Rotterdam, The Netherlands

[2]Division of Molecular Biology, Netherlands Cancer Institute, Amsterdam, The Netherlands

[3]Department of Obstetrics and Gynaecology, Erasmus MC - University Medical Center, Rotterdam, The Netherlands

[4]Erasmus Optical Imaging Centre, Department of Pathology, Erasmus MC - University Medical Center, Rotterdam, The Netherlands

[5]Institut de Génétique Humaine, CNRS UPR 1142, Montpellier, France

[6]Current address: Laboratory of Chromosome Biology, Memorial Sloan Kettering Cancer Center, New York, USA

**E-mail address: w.baarends@erasmusmc.nl*

Abstract

In mammalian meiotic prophase, the initial steps in repair of SPO11-induced DNA double-strand breaks (DSBs) are required to obtain stable homologous chromosome pairing and synapsis. The X and Y chromosomes pair and synapse only in the short pseudo-autosomal regions. The rest of the chromatin of the sex chromosomes remains unsynapsed, contains persistent meiotic DSBs, and the whole so-called XY body undergoes meiotic sex chromosome inactivation (MSCI). A more general mechanism, named meiotic silencing of unsynapsed chromatin (MSUC), is activated when autosomes fail to synapse. In the absence of SPO11, many chromosomal regions remain unsynapsed, but MSUC takes place only on part of the unsynapsed chromatin. We asked if spontaneous DSBs occur in meiocytes that lack a functional SPO11 protein, and if these might be involved in targeting the MSUC response to part of the unsynapsed chromatin. We generated mice carrying a point mutation that disrupts the predicted catalytic site of SPO11 (*Spo11*$^{YF/YF}$), and blocks its DSB-inducing activity. Interestingly, we observed foci of proteins involved in the processing of DNA damage, such as RAD51, DMC1, and RPA, both in *Spo11*$^{YF/YF}$ and *Spo11* knockout meiocytes. These foci preferentially localized to the areas that undergo MSUC and form the so-called pseudo XY body. In SPO11-deficient oocytes, the number of repair foci increased during oocyte development, indicating the induction of S phase-independent, *de novo* DNA damage. In wild type pachytene oocytes we observed meiotic silencing in two types of pseudo XY bodies, one type containing DMC1 and RAD51 foci on unsynapsed axes, and another type containing only RAD51 foci, mainly on synapsed axes. Taken together, our results indicate that in addition to asynapsis, persistent SPO11-induced DSBs are important for the initiation of MSCI and MSUC, and that SPO11-independent DNA repair foci contribute to the MSUC response in oocytes.

Introduction

During meiotic prophase in yeast and mammals, the induction of DNA double-strand breaks (DSBs) by the transesterase SPO11 precedes stable pairing and synapsis of homologous chromosomes (Kleckner, 1996; Mahadevaiah et al, 2001). Synapsis between chromosomes is achieved by the formation of a specific protein complex, consisting of lateral elements along the chromosomal axes that contain SYCP2, SYCP3 (Offenberg et al, 1998; Schalk et al, 1998), different components of the cohesin complex (Eijpe et al, 2000; Eijpe et al, 2003), and (before synapsis is achieved, on axial elements) the HORMA-domain proteins HORMAD1 and HORMAD2 (Fukuda et al, 2009; Wojtasz et al, 2009). Lateral elements are connected by a central element containing SYCP1 (Meuwissen et al, 1992) and several other meiosis-specific proteins, including SYCE1, SYCE2 (Costa et al, 2005) and TEX12 (Hamer et al, 2006); reviewed by Yang and Wang (Yang and Wang, 2009). Parallel to synaptonemal complex formation, meiotic DSBs are repaired, thereby facilitating homologous chromosomes interaction and the achievement of complete synapsis.

In male mammals, the X and Y chromosomes form a very special pair; they can synapse only in their short pseudoautosomal regions, and localize to the periphery of the nucleus. Furthermore, the XY chromatin is silenced, forming the XY body, by a process named meiotic sex chromosome inactivation (MSCI). This requires the expression of the histone variant H2AX (Fernandez-Capetillo et al, 2003). The checkpoint kinase ATR phosphorylates H2AX at S139, generating γH2AX (Turner et al, 2004). γH2AX is the earliest known marker of MSCI. This specific histone modification is also found in somatic cells, usually at sites of DNA DSB repair (Rogakou et al, 1998). Interestingly, H2AX phosphorylation in response to DNA damage has been coupled to reduced levels of RNA polymerase II activity in somatic cells (Solovjeva et al, 2007).

MSCI is considered a specialized form of a more general mechanism termed meiotic silencing of unsynapsed chromatin (MSUC), which silences unsynapsed chromatin in male and female meiotic prophase cells (Baarends et al, 2005; Schimenti, 2005; Turner et al, 2005). The exact cascade of events that leads to this transcriptional silencing is not known, but it has been established that there is a tight correlation between the presence of unsynapsed chromosomal axes coated by

HORMAD1 and HORMAD2 (the two mammalian orthologs, of the yeast protein Hop1 (Chen et al, 2005; Fukuda et al, 2009; Pangas et al, 2004)), the accumulation of ATR along these axes, the formation of γH2AX, and the transcriptional silencing. Indeed, it was recently reported that efficient accumulation of ATR on the XY body requires the HORMAD1 and HORMAD2 proteins (Daniel et al, 2011; Wojtasz et al, 2012). Many DNA repair proteins accumulate at the XY body, together with histone modifications such as specific methylation, sumoylation and ubiquitylation (reviewed by Inagaki et al. (Inagaki et al, 2010)). The accumulation of DSB repair proteins may be caused by delayed or stalled DSB repair in regions that fail to synapse. Persistent meiotic DSBs can indeed be observed on the X, but not on the Y chromosome, via immunocytochemical detection of the homologous recombination proteins RAD51 and its meiosis-specific paralogue DMC1 (Moens et al, 1997; Moens et al, 2002; Plug et al, 1996; Tarsounas et al, 1999). RAD51 and DMC1 have DNA-dependent ATPase activity and form filaments on single-stranded resected DNA-ends at DSB repair sites, and are essential for homologous recombination repair in mitotic and meiotic cells, respectively (Lim and Hasty, 1996; Pittman et al, 1998; Tsuzuki et al, 1996; Yoshida et al, 1998).

Evidence for a relationship between meiotic DSBs and homologous synapsis is provided by the observation that synapsis is severely affected in the absence of SPO11-induced meiotic DSBs (Baudat et al, 2000; Romanienko and Camerini-Otero, 2000). Some heterologous synapsis can occur in *Spo11* knockout meiocytes, but both spermatocytes and oocytes do not proceed beyond a zygotene-like stage (Baudat et al, 2000; Romanienko and Camerini-Otero, 2000). In *Spo11* knockout spermatocytes, a pseudo XY body is formed, which most often does not localize to the X and Y chromosomes, but to part of the unsynapsed chromatin (Barchi et al, 2005; Bellani et al, 2005). It has been defined as a condensed chromatin structure that, similar to the XY body, is marked by γH2AX and ATR, and is transcriptionally silenced (Barchi et al, 2005; Mahadevaiah et al, 2008). Based upon these characteristics, it has been proposed that the pseudo XY body is a manifestation of MSUC (Mahadevaiah et al, 2008). However, in *Spo11* knockout spermatocytes, HORMAD1 and HORMAD2 coat all unsynapsed axes, but the pseudo XY body forms only on part of the unsynapsed chromatin, indicating that somehow the MSUC response is not complete (Fukuda et al, 2009; Wojtasz et al, 2009) In addition, although more than 60% of the spermatocyte nuclei in *Spo11* knockout

testes contain a pseudo XY body, only 11% show clear accumulation of ATR along the unsynapsed axes in the pseudo XY body, compared to 100% ATR accumulation along the axes of true XY bodies in wild type spermatocytes (Wojtasz et al, 2012). The restriction of MSUC to only part of the unsynapsed chromatin is surprising, and raises the possibility that, apart from asynapsis, also other mechanisms may contribute to the activation of MSUC and MSCI. Since all known players in these processes function also in DNA repair we hypothesized that persistent DSBs on unsynapsed axes may contribute to the activation of MSUC and MSCI. This would then suggest that, even in the absence of SPO11, perhaps some damage-induced DSBs are frequently present, and could play a role in restricting the MSUC response to those areas that contain both unsynapsed axes and DNA damage. This notion is supported by the fact that radiation-induced DSBs in mouse leptotene cells enhance the efficiency of MSUC of a small translocation bivalent that carries a heterologous region of approximately 35-40 Mb (Schoenmakers et al, 2008). In addition, recent data also provide a link between DSB repair, the checkpoint kinase ATM, and transcriptional silencing of surrounding chromatin in somatic cells (Shanbhag et al, 2010).

Herein, we have generated a mouse model with a point mutation, which inactivates the catalytical site of SPO11. We used this mouse model to obtain more insight in the relation between the presence of DSBs and MSUC.

As expected based on our hypothesis, we found that SPO11-independent DNA repair foci are present in spermatocytes and oocytes. Moreover, we observed *de novo* induction of DNA repair foci in zygotene-like SPO11-deficient oocytes. Together with the results of a thorough analysis of the relationship between the localisation of DSB repair proteins and the MSUC response, our data reveal a direct link between the presence of persistent damage and the activation of MSUC and MSCI.

Results

Generation and initial analysis of the Spo11 Y138F mutation

We used a *Spo11* knock-in mouse model in which the catalytically active tyrosine (Tyr) 138 residue is replaced by a phenylalanine (Phe) ($Spo11^{YF/YF}$) (Figure S1A, B). In yeast and plants, mutation of the analogous Tyr residue abolished meiotic DSB formation (Bergerat et al, 1997; Cha et al, 2000; Hartung et al, 2007), and a similar

mouse mutant was recently described (Boateng et al). Presence of the point mutation and normal expression of the mutant protein were verified by sequence analyses, RT-PCR, and Western blot analyses (Figure S1C, D, E). The amount of mutant and/or wild type SPO11 protein in the testis of +/+, +/YF and YF/YF animals was comparable. Identical to the *Spo11* knockout (Baudat et al, 2000; Romanienko and Camerini-Otero, 2000), male and female $Spo11^{YF/YF}$ mice are infertile, and leptotene and zygotene nuclei display global absence of markers of DSB formation and repair (Figure 1A, B, and C). Spermatocytes and oocytes reach a zygotene-like stage with variable degrees of heterologous synapsis (Figure S2A, B, C).

A two-fold reduction in the amount of functional SPO11 reduces the number of RAD51 foci at leptotene but not at zygotene

We analyzed the formation of meiotic DSBs in wild type, heterozygote and homozygote $Spo11^{YF/YF}$ mice through immunocytochemical analysis of the formation of RAD51 foci. The number of RAD51 foci was quantified in leptotene and zygotene spermatocyte and oocyte nuclei (Figure 1). In wild type leptotene, many DSBs are formed, concomitant with the assembly of short patches of axial element along the chromosomal axes (Figure 1A, B, left panels, 1C). In zygotene, repair of meiotic DSBs occurs, parallel to the pairing of homologous chromosomes. Axial elements of paired homologous chromosomes then synapse (and are therefore termed lateral elements), through the formation of the central element of the synaptonemal complex (SC) (Figure 1A, B, left panel). The number of RAD51 foci gradually decreases, from leptotene to zygotene (Figure 1 A, C), as has been observed before (Tarsounas et al, 1999). It should be noted that, in mouse, male meiosis induction occurs throughout postpubertal life, whereas female meiosis is initiated only once during embryonic development (around embryonic day 13 (E13)). Oocytes progress through leptotene and zygotene in 15-20 h (Crone et al, 1965; McClellan et al, 2003). At E17, the vast majority of oocytes has reached the pachytene stage, and around E19, oocytes enter diplotene, reaching the first meiotic arrest. Spermatocytes require a longer time span between leptotene (induction of DSBs) and early pachytene (synapsis) of approximately 48 h (Oakberg, 1956). In $Spo11^{+/YF}$ leptotene spermatocyte nuclei, the number of RAD51 foci was approximately 30% lower compared to wild type (Figure 1C). However, in zygotene nuclei, no difference in the number of RAD51 foci between wild type and heterozygote nuclei was ob-

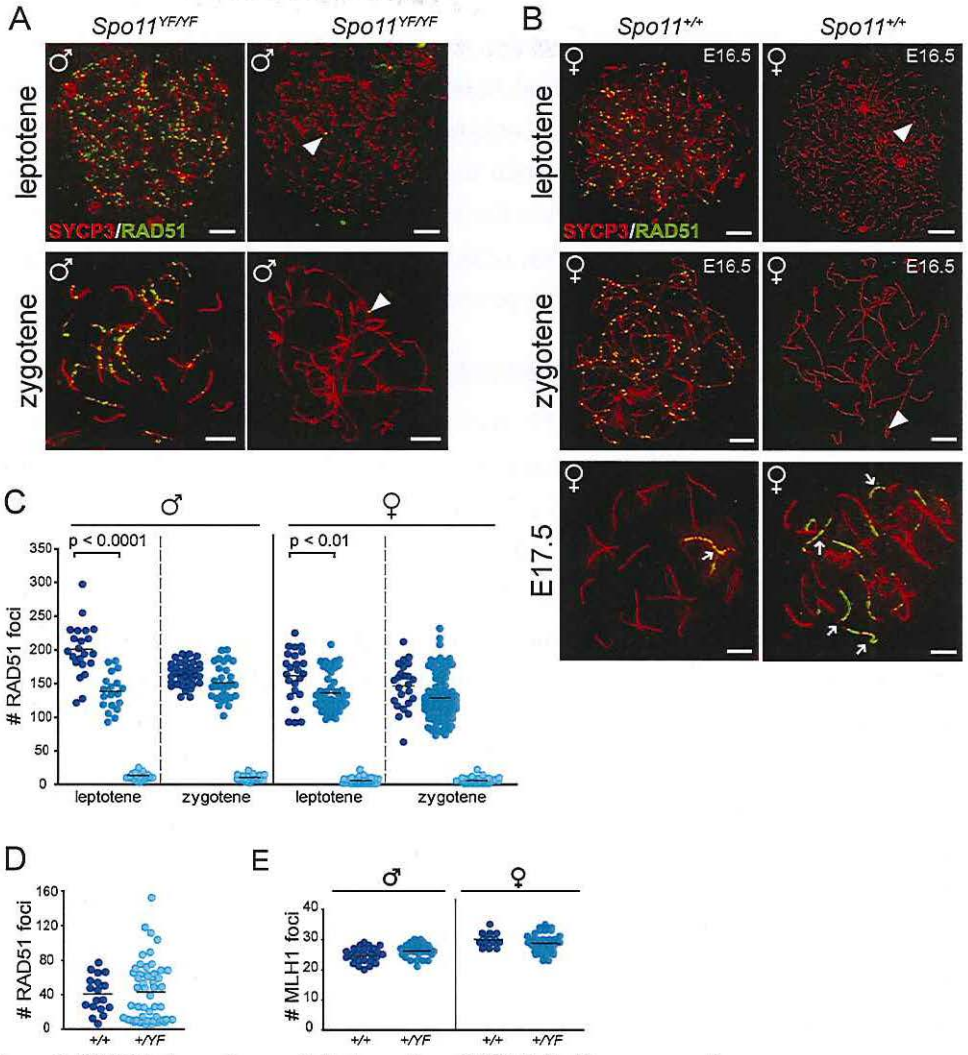

Figure 1: SPO11-dependent and -independent RAD51 foci in mouse meiocytes

(A-C) The number of RAD51 foci decreases from leptotene to zygotene in *Spo11*$^{+/+}$ and *Spo11*$^{+/YF}$ spermatocytes, whereas a few foci are detected in *Spo11*$^{YF/YF}$ spermatocytes and oocytes at both stages. **(A-B)** Double immunostaining with anti-SYCP3 (red), anti-RAD51 (green) of spermatocyte **(A)** and oocyte **(B)** nuclei from *Spo11*$^{+/+}$ (A-B, left panel) and *Spo11*$^{YF/YF}$ (A-B, right panel) mice. Arrowheads point to RAD51 foci in *Spo11*$^{YF/YF}$ spermatocytes and oocytes, both leptotene and zygotene. Extensive accumulation of RAD51 along axial elements of one or few chromosomes (arrows) can be observed in both *Spo11*$^{+/+}$ and *Spo11*$^{YF/YF}$ oocyte nuclei (B, lower panel). Size bars represent 10 μm. **(C)** The number of RAD51 foci was counted in *Spo11*$^{+/+}$, *Spo11*$^{+/YF}$, and *Spo11*$^{YF/YF}$ leptotene and zygotene spermatocytes and oocytes. Each dot represents the focus count of one nucleus. Black bars indicate mean number of foci. P values for the indicated comparisons (Mann-Whitney, two-tailed), and genotypes are indicated in the plot. **(D)** The number of MLH1 foci in pachytene spermatocyte nuclei was counted in *Spo11*$^{+/+}$and *Spo11*$^{+/YF}$ mice. Black bars indicate the mean values. **(E)** Number of RAD51 foci at E17.5 in *Spo11*$^{+/+}$ and *Spo11*$^{YF/YF}$ oocytes.

served (Figure 1C). Similar to the males, the number of RAD51 foci was lower in *Spo11*$^{+/YF}$ leptotene oocytes, compared to the wild type, and a small difference between the wild type and heterozygote oocytes was still observed at zygotene (Figure 1C). MLH1 is mismatch repair protein that is a well-known marker of crossover sites (Anderson et al, 1999), and functions in the resolution of joint molecules at the final phase of crossover formation (Zakharyevich et al). The number of MLH1 foci was not different between wild type and *Spo11*$^{+/YF}$ spermatocytes (Figure 1D).

SPO11-independent DNA repair foci in *Spo11*$^{YF/YF}$ and *Spo11*$^{-/-}$ meiocytes

In *Spo11*$^{YF/YF}$ animals, a few RAD51 foci were observed on the axial elements in leptotene and zygotene-like spermatocytes (average foci number 12 ± 4.4, n=54) and oocytes (average foci number 5 ± 3.7, n=50) (Figure 1A-C). Surprisingly, from E17.5 onwards, when oocytes should have reached the pachytene stage, we observed *de novo* RAD51 accumulation (Figure 1E), in oocytes from *Spo11*$^{YF/YF}$ mice. These RAD51 foci formed along most of the length of one or more axes (Figure 1B, lower panel, right). Such marked accumulation of RAD51 is also observed in wild type and *Spo11*$^{+/YF}$ pachytene oocytes (Figure 1B, lower panel, left), but in a relatively small proportion of the nuclei (around 20%, see also below). To confirm the specificity of this pattern of RAD51 accumulation, we also used a commercial RAD51 antibody previously reported to mark RAD51 foci in spread meiotic nuclei (Shin et al, 2007). This antibody yielded a similar pattern of RAD51 accumulation in oocytes (Compare Figure 1B to Figure S3). To ensure that the RAD51 foci that are observed in *Spo11*$^{YF/YF}$ spermatocytes and oocytes are not caused by remnant SPO11 activity, we also analysed RAD51 localisation in *Spo11* knockout meiocytes. As expected, the pattern of RAD51 foci staining in *Spo11* knockout spermatocytes and oocytes was similar to what was observed in meiocytes of *Spo11*$^{YF/YF}$ animals (Figure S4). This confirms that the observed RAD51 foci in our *Spo11*$^{YF/YF}$ model are SPO11-independent.

A pseudo XY body is present in *Spo11*$^{YF/YF}$ spermatocytes, and in *Spo11*$^{+/+}$ and *Spo11*$^{YF/YF}$ oocytes

Extensive asynapsis is thought to elicit an MSUC response, which can be observed in *Spo11*$^{-/-}$ spermatocytes as a γH2AX positive domain in the nucleus (Bellani et al, 2005; Mahadevaiah et al, 2008). This domain has been termed pseudo XY body,

since it does not necessarily include chromatin from the X and Y chromosomes.

Similar to what has been described for *Spo11* knockout mice, we observed one or two pseudo XY bodies in late zygotene-like spermatocytes from *Spo11*$^{YF/YF}$ mice (Figure S5A). In addition to γH2AX, other components of the DNA repair machinery are known to accumulate on the unsynapsed axes of the pseudo XY body (BRCA1, TOPBP1), or on the surrounding chromatin (MDC1) in *Spo11* knockout spermatocytes (Ichijima et al, 2011; Mahadevaiah et al, 2008), and this was also observed for the pseudo XY bodies in *Spo11*$^{YF/YF}$ spermatocytes (Figure S5B-D).

As recently reported, pseudo XY body-like structures can also be detected in *Spo11* knockout oocytes (Daniel et al, 2011), and even wild type oocytes have been reported to contain a MSUC region in a small percentage of the pachytene oocytes that fails to correctly synapse all chromosomes (Kouznetsova et al, 2009). We also observed areas of MSUC in a minority of wild type and *Spo11*$^{-/YF}$oocytes at E16.5 and E17.5 (Table 1). In addition, in *Spo11*$^{YF/YF}$ ovaries we observed a γH2AX-positive chromatin domain in about 14% of oocytes at E16.5 (Table 2), and in more than 80% of oocytes derived from *Spo11*$^{YF/YF}$ ovaries at E17.5 (Table 2).

The transcriptional silencing in the XY body can be immunocytochemically visualized as an area that is relatively depleted of RNA polymerase II (Baarends et al, 2005). To verify that the γH2AX domain detected in SPO11-deficient spermatocytes and oocytes is a transcriptionally silenced region, we performed RNA polymerase II (RNA pol II) staining and indeed observed a depletion of this enzyme from the areas enriched for γH2AX in *Spo11*$^{-/-}$ and *Spo11*$^{YF/YF}$spermatocytes and oocytes (Figure 2A and B). To verify the results, we quantified the relative average

Table 1 - Number of different subtypes of meiotic nuclei and frequency of pachytene nuclei with a pseudo-XY body in E16.5 and E17.5 oocytes from *Spo11*$^{+/+}$ and *Spo11*$^{+/YF}$ embryos

	genotype	#leptotene (%)*	#zygotene (%)*	#pachytene (%)*		fraction of pachytenes with pseudo XY body
				pseudo XY (+)	pseudo XY (-)	
E16.5	*Spo11*$^{+/+}$	13 (8.4)	77 (50)	10 (6.5)	54 (35)	0.16
	Spo11$^{+/YF}$	10 (6.5)	105 (68)	7 (4.5)	32 (21)	0.18
E17.5	*Spo11*$^{+/+}$	0 (0)	6 (4.3)	32 (23)	103 (73)	0.24
	Spo11$^{+/YF}$	0 (0)	6 (3.8)	34 (22)	118 (75)	0.23

*percentage of the total number of counted nuclei

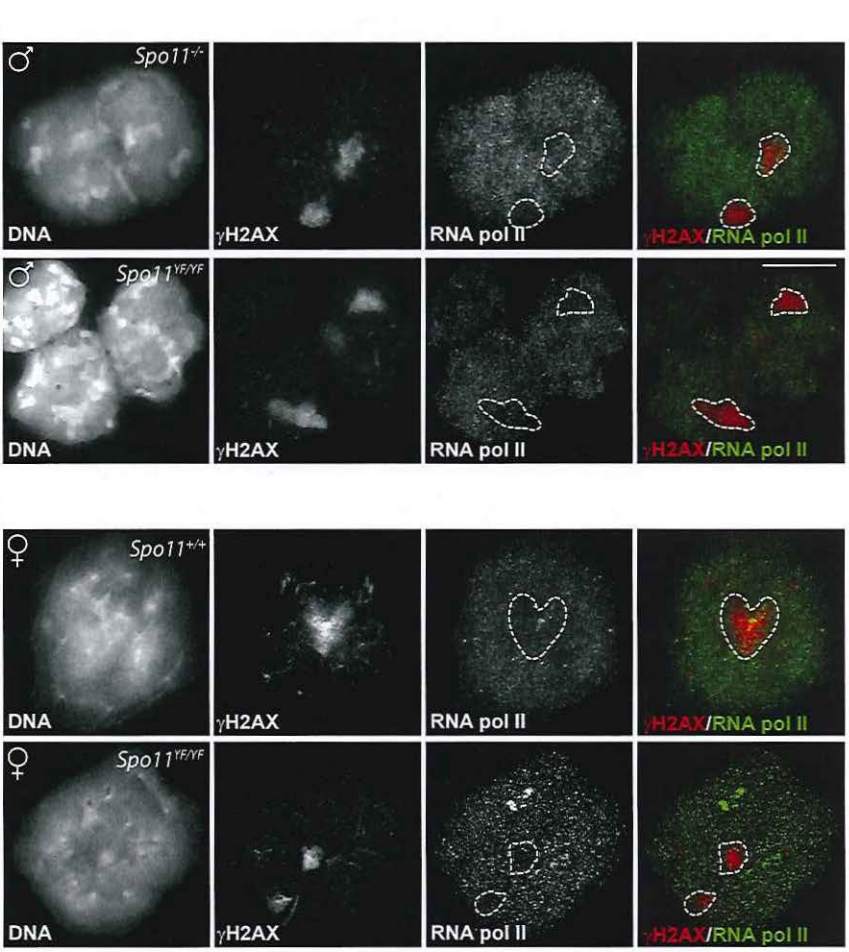
A
♂ Spo11-/-
DNA
γH2AX
RNA pol II
γH2AX/RNA pol II
♂ Spo11YF/YF
DNA
γH2AX
RNA pol II
γH2AX/RNA pol II
B
♀ Spo11+/+
DNA
γH2AX
RNA pol II
γH2AX/RNA pol II
♀ Spo11YF/YF
DNA
γH2AX
RNA pol II
γH2AX/RNA pol II
C
Relative amount of RNA pol II in (pseudo) XY body
1
0.8
0.6
0.4
0.2
0
♂ Spo11+/+
♀ E17.5 Spo11+/+
♀ E17.5 Spo11YF/YF

Figure 2: Transcriptional silencing of the pseudo XY body in spermatocytes and oocytes
(A-B) Double immunostaining with anti-γH2AX and anti-RNA polymerase II of spermatocyte (A) and oocyte (B) nuclei from *Spo11*$^{-/-}$ (A, upper panel), *Spo11*$^{YF/YF}$ (A-B, lower panels), and *Spo11*$^{+/+}$ (B, upper panel) animals.
Nuclear domains enriched in γH2AX are marked by a dashed circle.
(C) Scatter plots of the relative amount of RNA polII in a γH2AX domain normalized to the RNA polII level in a non-heterochromatic area of the same nucleus. Every dot represents a nucleus. RNA polII levels are compared between γH2AX domains (pseudo XY body) of *Spo11*$^{+/+}$ and *Spo11*$^{YF/YF}$ E17.5 oocytes, and the proper sex body in *Spo11*$^{+/+}$ mid-pachytene spermatocytes. Grey lines indicate the average. No significant difference between the wild type pachytene spermatocyte nuclei and either E17.5 oocyte nuclei group was observed (Mann-Whitney, confidence interval $p<0.01$).

intensity of RNA pol II staining in the γH2AX domain in oocytes, and compared it to the relative intensity in the true XY body of wild type pachytene spermatocytes (Figure 2C). Despite the fact that we observed variable depletion levels within each of the three analysed categories, the relative average level of RNA pol II in γH2AX domains of wild type (0.77 ± 0.16, n=30) and *Spo11*$^{YF/YF}$ (0.76 ± 0.18, n=30) oocytes is similar, and also comparable to what is observed for the XY body in male wild type spermatocytes (0.69 ± 0.14, n=30) (Mann-Whitney, confidence interval $p<0.001$), indicating a significant transcriptional silencing.

Based on these results, we will refer to the γH2AX domains that are observed in both *Spo11*$^{YF/YF}$ and *Spo11*$^{+/+}$ oocytes as pseudo XY bodies.

RAD51 foci frequently localize to the pseudo XY body in *Spo11*$^{YF/YF}$ spermatocytes

Having established that both SPO11-independent DNA repair foci and pseudo XY bodies are present in SPO11-deficient spermatocytes and oocytes, we subsequently analysed whether these foci are indeed associated with the MSUC are-

Table 2 - Number of different subtypes of meiotic nuclei and frequency of nuclei with a pseudo-XY body in E16.5 and E17.5 oocytes from *Spo11*$^{YF/YF}$ embryos

	genotype	#leptotene (%)*	#zygotene (%)*	
			pseudo XY (+)	pseudo XY (-)
E16.5	*Spo11*$^{+/+}$	13 (8.4)	10 (6.5)	54 (35)
E17.5	*Spo11*$^{+/+}$	0 (0)	32 (23)	103 (73)

*percentage of the total number of counted nuclei

as. Such an association would be expected, if SPO11-independent DNA damage, present on part of the unsynapsed axes, plays a role in nucleating the formation of the pseudo XY body. To investigate this, we performed co-immunostaining experiments for RAD51 to visualize DSB repair sites, γH2AX to visualize the pseudo XY body and SYCP3 to assess the stages of the cells.

Due to the severe impairment of meiotic prophase progression in *Spo11*$^{YF/YF}$ animals, spermatogenesis is arrested at stage IV, but spermatocytes never reach a true pachytene stage. We performed our analyses on a subpopulation of spermatocytes which displayed one or more areas of (heterologous) synapsis and showed no signs of SC fragmentation, in order to select healthy spermatocytes which had already entered the zygotene stage.

First of all we determined the frequency of spermatocytes with RAD51 foci and with a pseudo XY body. We split our population (n=240) in four classes (Figure 3A): 1) cells having both a pseudo XY body and RAD51 foci; 2) cells having only a pseudo XY body; 3) cells having only RAD51 foci; and 4) cells lacking both a pseudo XY body and RAD51 foci (Figure 3A, B). The results indicate that the vast majority of nuclei (78.3%) contain both a pseudo XY body as well as RAD51 foci. Although RAD51 is a well-known marker of sites of DSB repair (Haaf et al, 1995), it may also accumulate on ssDNA that is formed in a different context of DNA damage, such as observed during collapse of a replication fork in S phase (Long et al, 2011). To obtain additional evidence for the presence of DNA damage in *Spo11*$^{YF/YF}$ spermatocytes, we performed the same analysis by staining for two more markers of DNA damage and repair: DMC1 and RPA. DMC1 is the meiosis-specific homolog of RAD51 which participates in the process of repair of meiotic DSBs via homologous recombination. Hence, we expected the results for DMC1 and RAD51 to be similar. Indeed, comparable percentages of the analyzed nuclei were found to fall in each of the four classes (Figure 3A). In addition, we observed colocalization between RAD51 and DMC1 foci in the γH2AX domains (Figure S6A).

Unlike RAD51 and DMC1, RPA is not a recombinase but a single-stranded DNA (ssDNA) binding protein which takes part in many processes involving DNA metabolism (reviewed by Sakaguchi et al. (Sakaguchi et al, 2009)). At meiotic DSBs, the dynamics of RPA foci differ from those of DMC1, and although both proteins are enriched on the XY body, this occurs at different developmental

time points (Figure S7). Nevertheless, similar to what was found for RAD51 and DMC1, 72.3% of the cells (n=108) showed presence of both RPA foci and γH2AX domains (Figure 3A, lower panel).

The high percentages of cells with a pseudo XY body and DNA damage markers, provided an indication for a possible correlation between the presence of DNA damage, in particular DSBs, and the formation of the pseudo XY body. To further test the hypothesis for such a correlation, we determined the colocalization between each DNA repair marker and the γH2AX domain, in the fraction of spermatocytes that was positive for both of these features. We counted similar average numbers of RAD51, DMC1 and RPA foci (5.7, 5.2 and 6.4, respectively) in the nuclei, and the percentages of colocalization with the γH2AX domain(s) ranged between 70.8% (RAD51) and 82.2% (DMC1) (Figure 3B). Furthermore, up to 89-98% of the analysed pseudo XY bodies contained at least one focus of RAD51, DMC1 or RPA (Figure 3B).

To validate that the frequent localization of RAD51 in the pseudo XY body is not coincidental, we compared the relative area of the nucleus that was positive for γH2AX (pseudo XY body) to the fraction of RAD51 foci that was found inside that area. We observed that the fraction of RAD51 that localized inside the pseudo XY body (more than 70%) was much larger than the fraction of the nucleus that was taken up by this chromatin domain (20% of the total area). In addition, there was no specific correlation (Pearson linear correlation coefficient [Pcorr] = 0.0704) between the size of the pseudo XY body and the percentage of RAD51 foci that was found in the pseudo XY body (Figure 3C). In *Spo11* knockout spermatocytes, a similar pattern of colocalization between RAD51, DMC1, and RPA foci and the pseudo XY body was observed (Figure S8).

Radiation induced DSBs elicit an MSUC response in *Spo11*$^{YF/YF}$ spermatocytes

The localised presence of DNA repair foci in one or a few pseudo XY bodies indicates that DNA damage in spermatocytes tends to concentrate in a single, transcriptionally silenced area. To test this hypothesis, we induced exogenous DSBs in *Spo11*$^{YF/YF}$ spermatocyte nuclei by whole-body irradiation, and analysed the presence of DSB markers at different time points following the treatment. We observed approximately 120 (± 5.3, n=30) RAD51 foci and a nucleus-wide accumulation of γH2AX at 1h following irradiation. Interestingly, 48 hours after irradiation, we still

A

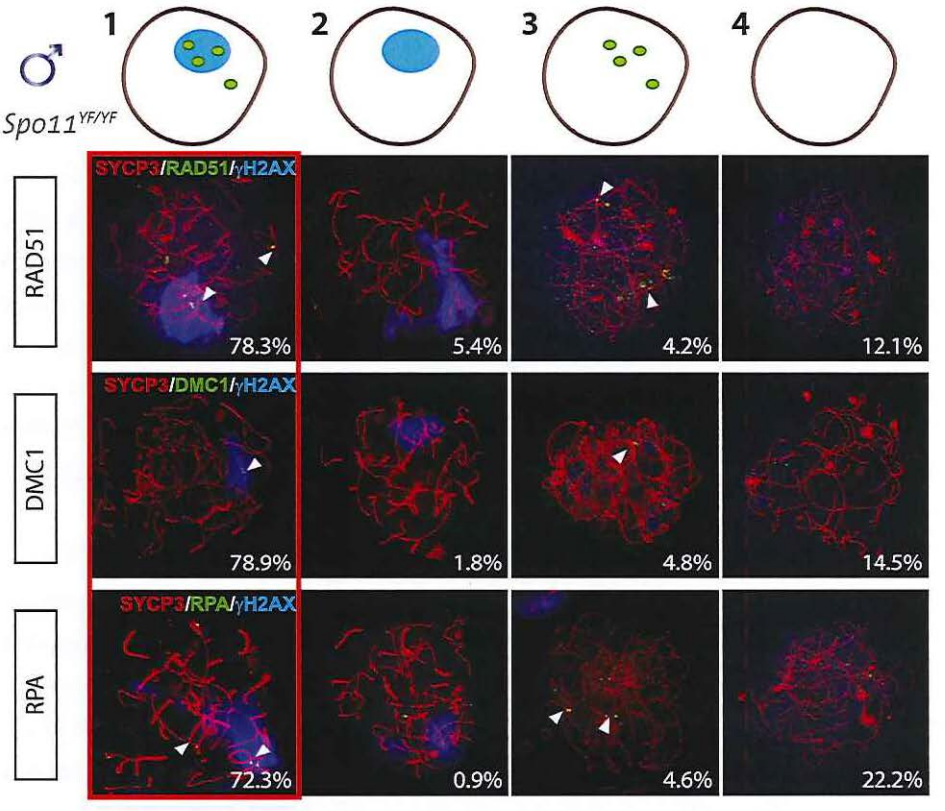

B

	average #foci	% foci in γH2AX domain	% γH2AX domains with foci
RAD51	5.8	70.8	89.9
DMC1	5.2	82.2	97.5
RPA	6.4	75.0	95.1

C

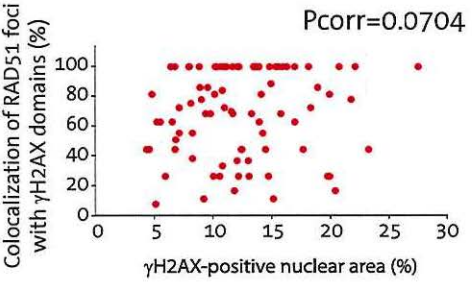

◀ Figure 3: Enrichment of DNA repair markers in the pseudo XY body of *Spo11*$^{YF/YF}$ spermatocytes

(A) Nuclei of *Spo11*$^{YF/YF}$zygotene spermatocytes were divided in four subgroups depending on their positivity for the pseudo XY body and for foci of one of the three DNA repair proteins RAD51 (n=120), DMC1 (n=227) or RPA (n=108) as follows: 1) with pseudo XY body and with foci, 2) with pseudo XY body and without foci, 3) without pseudo XY body and with foci, 4) without pseudo XY body and without foci. Spermatocyte nuclei were immunostained with anti-SYCP3 (red), anti-γH2AX (blue), and one of the following antibodies: anti-RAD51 (green, upper panel), anti-DMC1 (green, middle panel) or RPA (green, lower panel). Every panel shows a representative nucleus for each of the four subgroups mentioned above. Numbers in the bottom left corner of every picture represent the percentage of nuclei of this type in the analyzed cell population. **(B)** The average number of RAD51, DMC1 and RPA foci per nucleus was counted in spermatocytes of the first subgroup (outlined in red). The table also shows the percentage of foci located within a pseudo XY body and the percentage of pseudo XY bodies which contained at least one focus. **(C)** Scatter plot representing the colocalization percentage in relation to the fraction of the nuclear area occupied by the pseudo XY body. Every dot represents a nucleus. Pearson linear correlation coefficient [Pcorr] = 0.0741.

observed extensive H2AX phosphorylation emanating from the many RAD51 foci (Figure 4A). However, 120h following irradiation, when cells that were irradiated at leptotene would have progressed to pachytene in a wild type background, a pseudo XY body was observed in about 90 % (n=70) of the analysed nuclei (Figure 4B). These pseudo XY bodies always contained RAD51 foci (25.1 ± 1.73, n=50), and the majority of the radiation-induced RAD51 foci that are still present at this time point (65.7 %) localized in the pseudo XY body (Figure 4A). These data show that the persistent radiation-induced DSBs tend to relocalize in a specific nuclear subdomain. This phenomenon is in accordance with the colocalization of unsynapsed or partially synapsed translocation chromosomes, carrying persistent meiotic DSBs, with the XY body (Schoenmakers et al, 2008).

To confirm that the pseudo XY body in these irradiated spermatocytes is an MSUC area, as observed in non-irradiated *Spo11*$^{YF/YF}$ spermatocytes, we performed co-immunostaining for γH2AX and RNA pol II. We detected a depletion of this enzyme in the areas enriched for γH2AX, indicating that they are transcriptionally silenced (Figure 4C).

Pseudo XY bodies in *Spo11*$^{YF/YF}$ oocytes correlate with DSB markers

Next, we asked if RAD51, DMC1, and RPA foci also preferentially localized in the pseudo XY bodies in E17.5 *Spo11*$^{YF/YF}$ oocytes.

As discussed above, RAD51 was found to accumulate extensively on some chro-

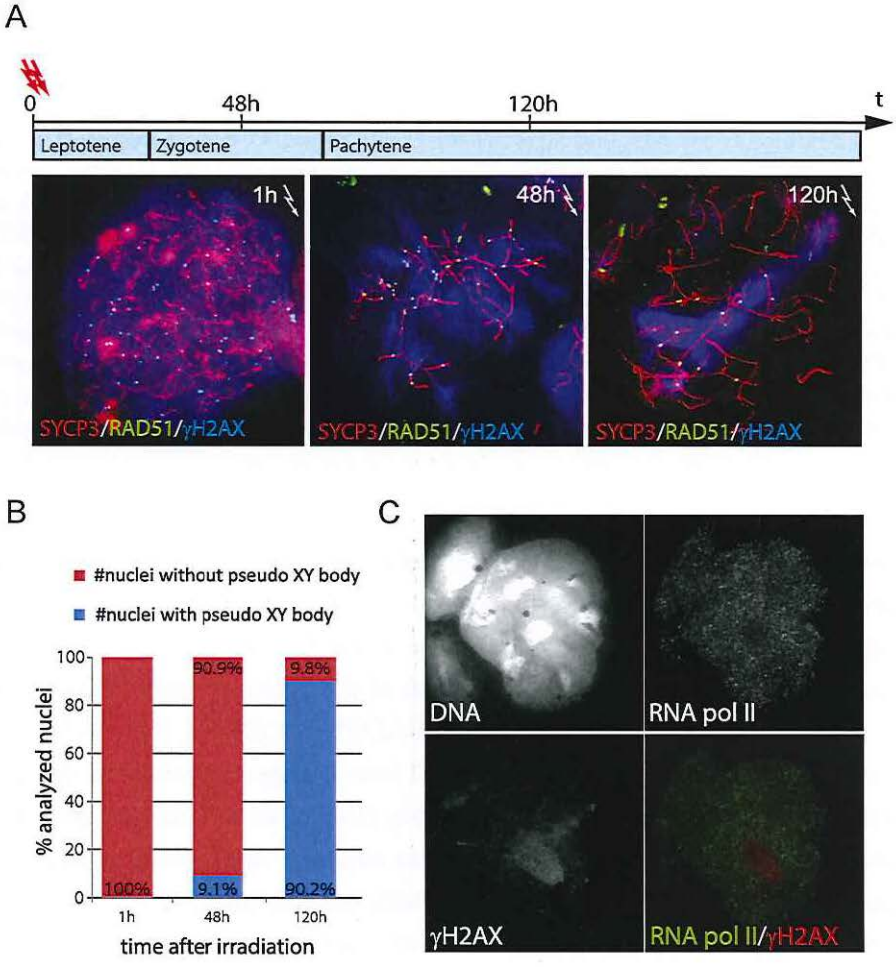

Figure 4: Relocalisation of persistent radiation-induced DSBs into a pseudo XY body
(A) Irradiated *Spo11*$^{YF/YF}$ spermatocytes were collected 1h, 48h and 120h upon irradiation and immunostained for RAD51 (green), SYCP3 (red), and γH2AX (blue). Spermatocytes that were irradiated at the leptotene stage, should have reached zygotene and pachytene with respect to the pattern of γH2AX, at 48 and 120h following irradiation, respectively. **(B)** Fraction of cells showing a pseudo XY body upon irradiation at the analysed time-points (n=50). **(C)** Immunostaining of *Spo11*$^{YF/YF}$ spermatocyte 120 hours after irradiation with anti-RNA pol II (green) and anti-γH2AX (red). The intense γH2AX domain (pseudo XY body) corresponds to a nuclear area depleted for RNA pol II.

mosomal axes, often coating them completely, so that single foci could not be easily resolved. Such marked accumulation was not observed for DMC1 or RPA, which are forming fewer foci (average number of 5.6 ± 2.3, n=20 and 7.4 ± 6.9, n=30, respectively). Despite this difference in foci pattern, the percentage of oocyte nuclei that contained both a γH2AX domain and RAD51 foci (79.2%, n=120) was similar to the percentage of oocyte nuclei with a γH2AX domain and RPA foci (83.1%, n=89) (Figure 5A, upper and lower panel respectively). In contrast, only 25.9 % of the analysed *Spo11*$^{YF/YF}$ oocytes (n=54) displayed DMC1 foci, but all these cells also had a γH2AX domain. The rest of the nuclei had only a pseudo XY body (57.41%) or were negative for both DMC1 and γH2AX (16.67%) (Figure 5A, middle panel).

In the group of nuclei that contained both RAD51 foci and a γH2AX domain, the pseudo XY body always contained RAD51 foci that coated part of the axes (Figure 5B). Also, in E17.5 *Spo11*$^{YF/YF}$ oocytes that contained a pseudo XY body and DMC1 or RPA foci, more than 90% of the pseudo XY bodies contained DMC1 or RPA foci, respectively. Conversely, the vast majority of RAD51, DMC1, and RPA foci in this subgroup of nuclei were located in the pseudo XY body, similar to what was observed for *Spo11*$^{YF/YF}$ spermatocyte nuclei. Furthermore, the DMC1 foci were found to colocalize with some of the (more abundant) RAD51 foci in the pseudo XY bodies of oocytes (Figure S6B).

For comparison, these analyses were also performed on *Spo11* knockout E17.5 oocytes and this provided similar results (Figure S8, right).

DSB repair proteins mark pseudo XY bodies that are occasionally observed in wild type oocytes

Interestingly, also in wild type and *Spo11*$^{YF/+}$ oocyte nuclei, RAD51 coats the axial elements in γH2AX-positive domains (Table 1). These pseudo XY bodies were observed in approximately 20% of pachytene oocytes, similar to what was previously reported by Koutznetsova et al. (Kouznetsova et al, 2009) who observed BRCA1 and ATR on unsynapsed axes in around 15% of the oocyte population from E17 wild type embryos.

To analyse this further, we studied the localisation of other proteins involved in homologous recombination (DMC1 and RPA) in relation to the formation of a γH2AX domain. Again we divided the oocyte population in four subgroups, based on the detection of γH2AX and the three DNA repair markers. As expected, the

A

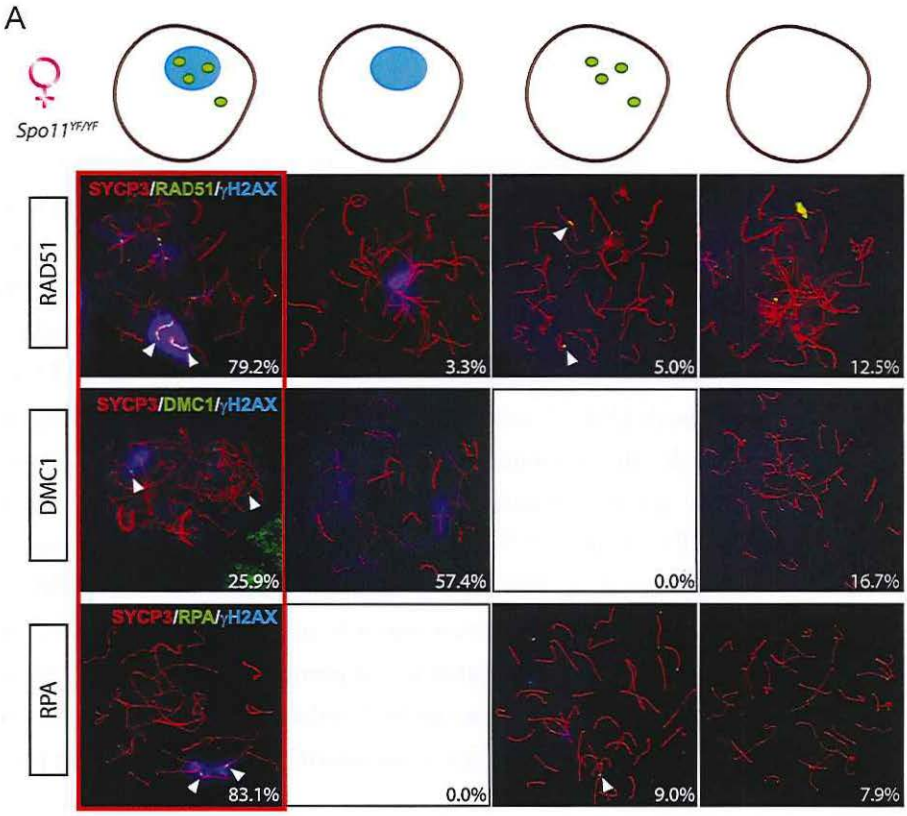

B

	average # foci	% foci in γH2AX domain	% γH2AX domains with foci
RAD51	45.0	76.4	100
DMC1	5.6	73.5	95.9
RPA	7.4	75.4	92.8

Figure 5: Enrichment of DNA repair markers in the pseudo XY body of *Spo11*$^{YF/YF}$ oocytes
(A) Oocyte nuclei from *Spo11*$^{YF/YF}$ E17.5 embryos were immunostained with anti-SYCP3 (red), anti-γH2AX (blue), and one of the following antibodies: anti-RAD51 (green, upper panel), anti-DMC1 (green, middle panel), or RPA (green, lower panel). Foci of each marker listed above are indicated with arrowheads. Quantification of the four fractions (defined in the legend to Figure 3A) was performed in 120, 54, and 89 oocyte nuclei, for RAD51, DMC1, and RPA protein foci, respectively. Numbers in the bottom left corner of every picture represent the percentage of nuclei of this type in the analyzed cell population. **(B)** The number of RAD51, DMC1 and RPA foci was counted in oocyte nuclei showing both a pseudo XY body and foci (red circle). The average total number of foci of each protein per nucleus is reported in the first column of the table. The second and the third column show the percentage of foci located within a pseudo XY body and the percentage of pseudo XY bodies that contained at least one focus.

A

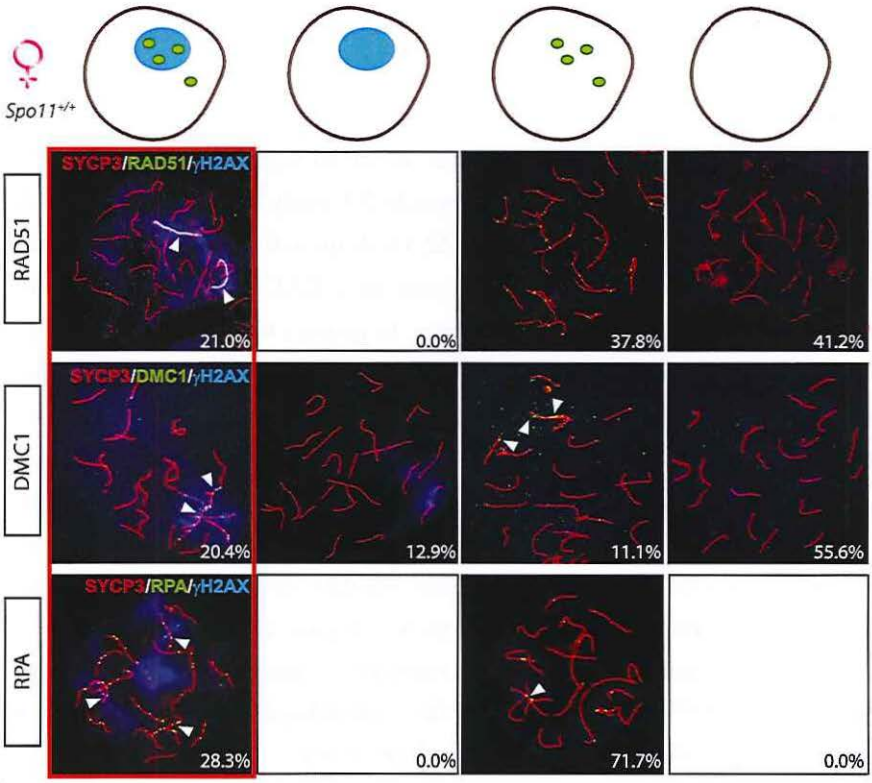

B

	average # foci	% foci in γH2AX domain	% γH2AX domains with foci
RAD51	40.6	81.3	100
DMC1	16.7	68.3	80.0
RPA	59.1	41.2	100

Figure 6: Enrichment of DNA repair markers in the pseudo XY bodies of *Spo11*$^{+/+}$ oocytes
(A) Oocyte nuclei from *Spo11*$^{+/+}$ E17.5 embryos were immunostained with anti-SYCP3 (red), anti-γH2AX (blue) and anti-RAD51 (green, upper panel) or anti-DMC1 (green, middle panel) or RPA (green, lower panel). Foci of each marker listed above are indicated with arrowheads. Numbers in the bottom left corner of every picture represent the percentage of nuclei of the respective type in the analyzed cell population. Quantification of the four fractions (defined in Figure 3A) was performed in 271, 54, and 53 oocyte nuclei, for RAD51, DMC1, and RPA protein foci, respectively. **(B)** The number of RAD51, DMC1, and RPA foci was counted in pachytene oocyte nuclei showing both a pseudo XY body and foci (red circle). The average total number of foci of each protein per nucleus is reported in the first column of the table. The second and the third column show the percentage of foci located within a pseudo XY body-like domain and the percentage of pseudo XY body-like domains which contained at least one focus.

majority of pachytene oocytes showed complete synapsis of all chromosomes and no clear γH2AX-positive domain. Around 20-30% of nuclei showed pseudo XY bodies, as defined by the presence of one or a few distinct γH2AX-positive domains (Figure 6A). Approximately half of the pachytene nuclei lacked both γH2AX domains and RAD51 or DMC1 foci, whereas no nuclei were found without RPA foci (Figure 6A, B). We did not observe any pseudo XY body in nuclei without RAD51 foci, but 13% of the nuclei contained a γH2AX domain but no DMC1 foci (Figure 6A). RPA is known to mark DSB repair spots after RAD51-mediated strand invasion and during homologous recombination, to protect the ssDNA regions generated during this process (Plug et al, 1998). This explains the fact that RPA foci are always present in E17.5 oocyte nuclei which are at a mid-meiotic stage and have not yet completed the homologous recombination process at all DSB repair sites. Also, since RPA is engaged in completing recombination at synapsed autosomal sites, a relatively small fraction of the RPA foci colocalizes with pseudo XY bodies. In contrast, most DMC1 and RAD51 foci localize to γH2AX domains, similar to what was found for *Spo11*$^{YF/YF}$ oocyte nuclei (Figure 6B), although DMC1 foci are found more frequently and in higher numbers in pseudo XY bodies in *Spo11*$^{+/+}$ compared to *Spo11*$^{YF/YF}$ oocytes. DMC1 foci colocalized with RAD51 foci when both were present in the pseudo XY body (Figure S6C).

Pseudo XY bodies overlapping synapsed axes contain RAD51 foci but lack DMC1

Since we observed some differences between the patterns of RAD51 and DMC1 accumulation in pseudo XY bodies of wild type oocytes, we wondered whether pseudo XY bodies that contain both DMC1 and RAD51 foci differ from those that show only RAD51 foci. First, we analysed the relation between DMC1 accumulation, formation of the pseudo XY body and synapsis, using an antibody directed against the central element protein TEX12. The results in Figure 7A and B show that DMC1 foci in oocyte pseudo XY bodies localize mainly (58.6%) on unsynapsed axes (inferred from the absence of TEX12, and placement of DMC1 foci in an axis-like pattern), and rarely (12.8%) on synapsed areas (Figure 7B). It is important to note that 28.6% of oocytes with a pseudo XY body did not show any DMC1 foci (Figure 7A, B) and that all these nuclei were also characterized by complete synapsis (based on the presence of 20 TEX12-positive bivalents) (Figure 7B). In

A

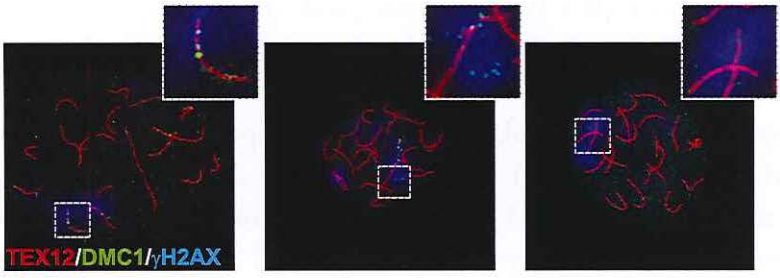

B

	DMC1 foci detected		DMC1 foci not detected	
	synapsed axes	asynapsed axes	synapsed axes	asynapsed axes
#chromosomal axes in pseudo XY body (%)	9 (12.8)	41 (58.6)	20 (28.6)	0 (0.0)

C

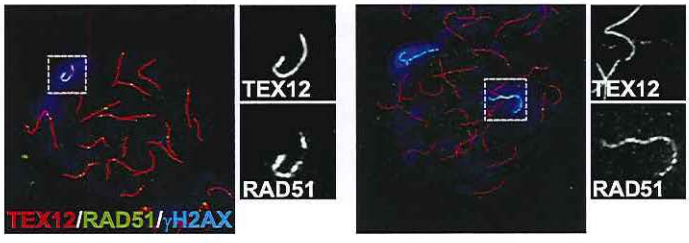

Figure 7: DMC1 preferentially localizes to unsynapsed axes in wild type pachytene oocytes
(A) Triple immunostaining with anti-TEX12 (red), anti-DMC1 (green), and anti-γH2AX (blue) of pachytene oocyte nuclei from E17.5 wild type embryos. DMC1 foci are detected in the pseudo XY body and localize to synapsed axes (left, close-up), or to unsynapsed axes (middle, close-up). The pseudo XY body is often devoid of DMC1 foci (right, close-up). **(B)** Quantification of the number of synapsed and unsynapsed axes, present in pseudo XY bodies, that are positive or negative for DMC1 foci (n=70). Percentages are shown in brackets. **(C)** Triple immunostaining with anti-TEX12 (red), anti-RAD51 (green), and anti-γH2AX (blue) of oocytes from E17.5 wild type embryos. Axis-wide accumulation of RAD51 in the pseudo XY body was observed on both synapsed (left) and unsynapsed (right) axes. Close-ups separately show TEX12 and RAD51 patterns in the pseudo XY body.

contrast, RAD51 always coats the chromosomal axes of the pseudo XY body, irrespective of synapsis (Figure 7C). These observations prompted us to further analyse the occurrence of pseudo XY bodies in association with complete synapsis. For this, we used an antibody directed against the HORMAD1 protein, together with anti-TEX12 as well as anti-γH2AX to identify the pseudo XY body. As reported previously, HORMAD1 covered all unsynapsed axes at zygotene, and was lost once

the cells reached complete synapsis at pachytene (Wojtasz et al, 2009) (Figure 8A). Conversely, TEX12 gradually accumulated as synapsis progressed, consistent with earlier reports (Hamer et al, 2006) (Figure 8A). When we analysed the pachytene population in more detail, we observed unsynapsed axes that were positive for HORMAD1 in a pseudo XY body in 9.8% of the pachytene nuclei, and another 13.1% that showed partial (5.7%) or no (7.4%) colocalisation of the pseudoXY body with HORMAD1 (Figure 8B). Whenever HORMAD1 was absent from the pseudo XY body, TEX12 was present, indicating complete synapsis. To verify that synapsis was complete in the nuclei that lacked HORMAD1 but contained a pseudo XY body, we measured the total length of synapsed axes, visualized as TEX12 stretches, in pachytene oocyte nuclei. We found that the total SC length was comparable in pachytene oocytes without any HORMAD1 staining, independent of the presence of a pseudo XY body. On the contrary, the total synapsis length was significantly lower in pachytene oocyte nuclei which showed both a pseudo XY body and HORMAD1 (Figure 8C). Finally, to confirm that these pseudo XY bodies elicit true meiotic silencing, despite the absence of asynapsis, we performed a triple staining for RNA polII, TEX12 and γH2AX. As shown in Figure 8D and 8E, RNA polII is depleted from the pseudo XY body, irrespective of synapsis.

► **Figure 8: Pseudo XY bodies containing synapsed axes in wild type embryonic oocytes**
(A-B) Triple immunostaining with anti-HORMAD1 (red), anti-TEX12 (green) and anti-γH2AX (blue) of oocyte nuclei from E17.5 wild type embryos. In the lower right corner percentages are reported, representing the frequency of each type of cell in the pachytene oocyte population (n=244). **(A)** Representative pictures of early zygotene (EZ), late zygotene (LZ), early pachytene (EP) and pachytene (P) oocytes, from left to right. HORMAD1 levels are decreasing while TEX12 accumulates as synapsis progresses. Parallel to the increase of synapsis and HORMAD1 removal, γH2AX accumulation decreases. **(B)** Representative pictures of pachytene oocytes with a pseudo XY body. HORMAD1 positive axes totally (left picture) or partially (middle picture) colocalize with the pseudo XY body, or are not present (right picture) in the pseudo XY body. **(C)** Scatter plot of the total length of synapsed axes in E17.5 wild type pachytene oocytes, belonging to the following categories: HORMAD1 and pseudo XY body absent (blue); HORMAD1 absent and pseudo XY body present (light blue); presence of both HORMAD1 and a pseudo XY body. Every dot represents a nucleus. Black bars indicate the mean values. P values for the indicated comparison (Mann-Whitney, two-tailed) are shown in the plot. **(D-E)** Triple immunostaining with anti-TEX12 (white), anti-RNA polymerase II (green), and anti-γH2AX (red) of pachytene oocytes from E17.5 wild type embryos, imaged with the Zeiss LSM700 confocal microscope. Depletion of RNA pol II can be observed in the area of the the pseudo XY body marked by γH2AX, both when synapsis is complete **(D)** and when unsynapsed axes **(E)** are present in this region. Size bars represent 10 μm.

A

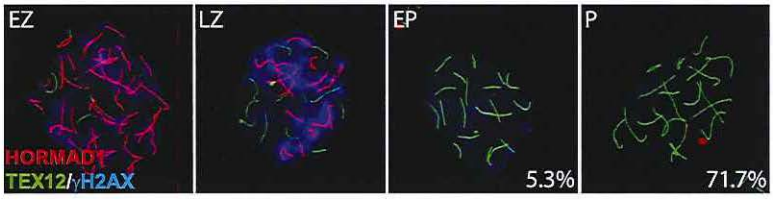
EZ
LZ
EP
P
HORMAD1
TEX12/γH2AX
5.3%
71.7%

B

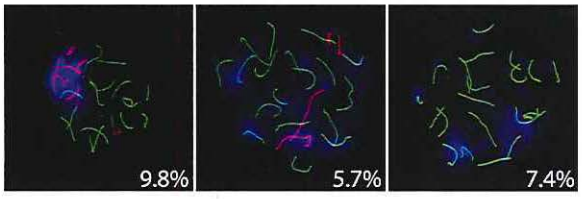
9.8%
5.7%
7.4%

C

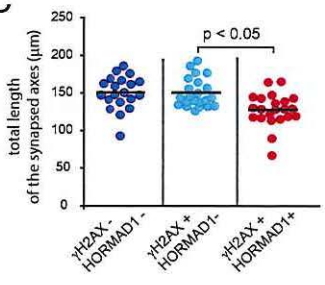
250
200
150
100
50
0
total length of the synapsed axes (µm)
p < 0.05
γH2AX - HORMAD1 -
γH2AX + HORMAD1-
γH2AX + HORMAD1+

D

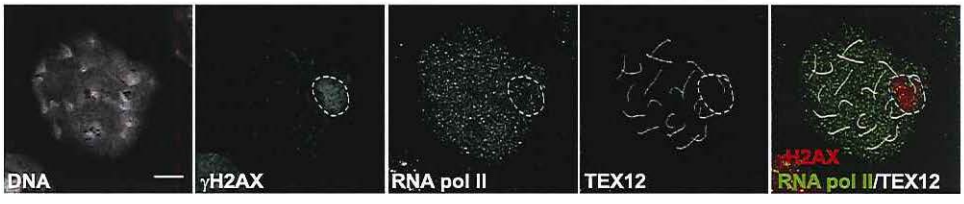
DNA
γH2AX
RNA pol II
TEX12
γH2AX
RNA pol II/TEX12

E

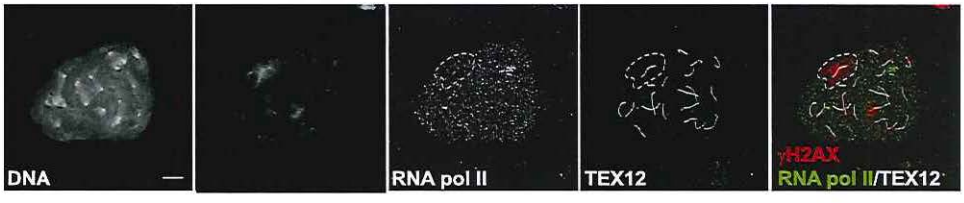
DNA
RNA pol II
TEX12
γH2AX
RNA pol II/TEX12

Discussion

SPO11-dependent DSB formation

A point mutation in the *Spo11* gene that results in the replacement of Tyr 138 by Phe in the catalytic site of the enzyme leads to the absence of detectable SPO11-dependent meiotic DSBs in oocytes and spermatocytes. This observation is in accordance with recent findings of Boateng et al. (Boateng et al), who analysed a mouse mutant carrying a mutation in the *Spo11* gene that leads to replacement of both Tyr 137 and Tyr138 by Phe.

Although having half the amount of functional SPO11 is sufficient to generate a normal number of crossovers, as evidenced by the analysis of MLH1 foci in $Spo11^{+/YF}$ spermatocytes and oocytes, the dynamics of DSB induction was clearly altered. The lower number of RAD51 foci that was observed in leptotene $Spo11^{+/YF}$ oocytes and spermatocytes may indicate that fewer breaks are made. However, near normal numbers of RAD51 foci are observed in zygotene $Spo11^{+/YF}$ spermatocytes and oocytes. These data are consistent with the homeostatic control mechanism that has been observed in yeast (Martini et al, 2006) and mouse spermatocytes, allowing maintenance of normal crossover frequencies when the number of DSBs is reduced (Cole et al, 2012). In addition, or alternatively, the recently identified feedback mechanism, requiring ATM activity, which regulates the number of breaks that can be formed by SPO11 (Lange et al, 2011) may ensure that a similar level of DSB formation is reached in the heterozygote, albeit with different kinetics when compared to the wild type.

SPO11-independent DNA repair foci

In the absence of SPO11, no meiotic DSBs are formed, and accumulation of RAD51, DMC1 and RPA proteins is therefore not expected. Nevertheless we observed significant numbers of RAD51, DMC1 and RPA foci in $Spo11^{YF/YF}$ and $Spo11^{-/-}$ oocytes and spermatocytes that preferentially localized in the pseudo XY body, identified on the basis of the γH2AX staining pattern. In $Spo11^{YF/YF}$ oocytes, we observed a clear increase in the number of RAD51 foci in oocytes at E17.5, compared to oocytes at E16.5. However, the number of DMC1 and RPA foci was much lower than the number of RAD51 foci in these nuclei. The number of DMC1 foci in particular would be expected to follow the same pattern as RAD51, because

DMC1 has been reported to participate in the formation of recombination filaments (Tarsounas et al, 1999). Nevertheless, it has been recently shown that the dynamics of accumulation of DMC1 and RAD51 are different when extra DSBs are induced by a supplemental copy of the SPO11β-isoform (Cole et al, 2012). Cole et al. (Cole et al, 2012) suggested that, in this situation, the extra DSBs may be more likely to engage in a mitotic pathway of HR repair, and thus less likely to recruit DMC1. In oocytes that completely lack a synaptonemal complex, DMC1 was found to be lost from persistent DSBs, whereas RAD51 foci were still observed (Kouznetsova et al, 2011). Based on this, it was suggested that DMC1 can only stably associate with meiotic DSBs in the context of synapsed chromatin and normal progression of repair (Kouznetsova et al, 2011). Our own observations also indicate that DMC1 is lost from SPO11-induced DSB repair sites before RAD51 (data not shown). Together, these observations are in accordance with the notion that the sites that recruit RAD51 foci in E17.5 oocytes can no longer recruit DMC1 with equal efficiency. This may be due to differences in the composition of the repair complexes at (persistent) DSBs in late compared to early pachytene oocytes, or is possibly caused by a drop in the level of DMC1 protein expression.

Nature of the SPO11-independent DNA repair foci

It is important to establish if the DNA repair foci represent actual sites of DNA damage. The increase in the number of RAD51 foci in oocytes between E16.5 and E17.5 may be due to a DNA-damage independent association of RAD51 to chromosomal axes, or foci formation might be induced by the specific chromatin structure that is formed upon γH2AX formation, which would explain why the foci tend to colocalize in a single subnuclear region. However, we have observed that radiation-induced DSBs, that localize throughout the nucleus, first lead to a nucleus wide accumulation of γH2AX, and subsequently to a more concentrated presence of RAD51 foci and γH2AX in a specific subdomain of the nucleus (the pseudo XY body). In addition, it is known that in spermatocytes that carry autosomes with a pairing problem, meiotic DSBs persist on the unsynapsed regions, in association with MSUC, and these regions then also tend to colocalize with the XY body, indicating that persistent DSBs in the context of MSUC have a tendency to reside together in a single nuclear area (Schoenmakers et al, 2008). The preferred presence of DMC1 and RPA in addition to RAD51 in the pseudo XY bodies supports the

hypothesis of the presence of a DNA damage event. One particular feature of the SPO11-independent repair foci in *Spo11*$^{YF/YF}$ oocytes is their inefficient processing. In fact, in oocytes from E17.5 *Spo11*$^{YF/YF}$ mice, RAD51 appears to coat unsynapsed axial elements, so that individual foci are no longer clearly observed, indicating that the RAD51 filament formation is not regulated as in a normal homologous DSB repair event. Upon replacement of RPA by RAD51/DMC1, and subsequent persistence of a DSB without further processing to a recombination intermediate, such an axis-wide pattern for RAD51 may develop, possibly due to an abnormal regulation of the foci dynamics, compared to conventional DSB repair events. The spreading of RAD51 along axial elements may result from spreading of RAD51 onto double-stranded DNA, a phenomenon that has also been described for persistent DSBs in yeast (Kalocsay et al, 2009). Based upon these considerations, we favour the conclusion that the SPO11-independent DNA repair foci represent true sites of persistent DNA damage.

Origin of SPO11-independent DNA repair foci

To explain what might cause spontaneous DNA damage in *Spo11*$^{YF/YF}$ and knockout spermatocytes and oocytes, and possibly also in wild type meiocytes, different mechanisms can be proposed. First, during S phase in somatic cells, and most likely also in meiocytes, DSBs can form at stalled replication forks. In human cells, 50 endogenous DSBs have been proposed to occur in every cell cycle (Vilenchik and Knudson, 2003). Most of these DSBs will be repaired before the cells enter G2, but some may persist, and the number of persisting breaks appears to vary between different cell types (Inagaki et al, 2009; Xue et al, 2009). A second mechanism that could generate endogenous DSBs is transcription-associated recombination (TAR). The causes of DSBs that form in association with ongoing gene transcription are thought to be related either to generation of stalled replication forks in association with transcription, or to increased accessibility of DNA during transcription, making it more vulnerable to DNA-damaging agents (reviewed by (Aguilera, 2002; Gottipati and Helleday, 2009)). Meiocytes are post S phase cells, and leptotene, zygotene, and early pachytene spermatocytes and oocytes display a low level of RNA synthesis, making TAR an unlikely source of RAD51 foci in these cells (Hartung and Stahl, 1978; Monesi, 1964). A third possible endogenous source of DSBs is impaired topoisomerase II activity. Inhibition of topoisomerase II activity in pachy-

tene spermatocytes has been found to result in DSB formation, indicating that topoisomerase II is indeed functional in meiocytes (Matulis and Handel, 2006). Fourth, endonuclease activity of ORF2, encoded by *Line1* transposons, generates DSBs during the transposition of mobile elements in the genome (Belgnaoui et al, 2006; Gasior et al, 2006; Wallace et al, 2008). Derepression of transposons has been shown to cause SPO11-independent DNA damage in *Mael* mutant spermatocytes (Soper et al, 2008). In wild type oocytes and spermatocytes, transcription of *Line1* elements is transiently derepressed at the onset of meiosis (van der Heijden and Bortvin, 2009). Finally, we cannot exclude that DNA damage may occur as a result of unknown environmental or endogenous factors such as reactive oxygen species (ROS). ROS generation has been described for normal rat spermatocytes (Fisher and Aitken, 1997), but it is not clear to what extent such damage also results in RAD51 foci formation.

In *Spo11*$^{YF/YF}$ spermatocytes, it appears most likely that some or all of the SPO11-independent RAD51 foci result from carry-over of spontaneous DSBs that were induced in the previous S phase. In oocytes this may also occur, and the observed *de novo* generation of RAD51 foci post S phase in *Spo11*$^{YF/YF}$ oocytes indicates that (additional) spontaneous DSBs in oocytes may arise either from impaired topoisomerase II activity or from ORF2 mediated endonuclease activity in cells that should have progressed already to pachytene. Such SPO11-independent DNA damage may also be induced in wild type pachytene oocytes, but the close proximity of the homologous template in these oocytes may facilitate homologous recombination repair of most of the *de novo* induced DNA damage. In *Spo11*$^{YF/YF}$ oocytes the appropriate template for repair is not directly available due to almost complete lack of homologous chromosome pairing. This difference in homologous template availability readily explains the higher relative frequency of pseudo XY body formation in *Spo11*$^{YF/YF}$ oocytes compared to oocytes from wild type or heterozygote littermate controls. At present, it is not clear whether the persistent repair foci are resolved at some later time point, or whether the persistent presence of these foci and the associated γH2AX signaling triggers a checkpoint that induces apoptosis. Daniel et al. (Daniel et al, 2011) reported increased apoptosis of oocytes in ovaries of newborn *Spo11* knockout mice compared to controls. In addition, it has been reported that only 10-20% of the normal number of oocytes is present in *Spo11* knockout ovaries at postnatal days 4 and day 8 (Baudat et al, 2000; Di Giacomo et

al, 2005). This percentage nicely corresponds to the 19% of oocytes that do not contain a pseudo XY body at E17.5 in our *Spo11*$^{YF/YF}$ model. However, although these data confirm that oocytes with a pseudo XY body are lost shortly after birth, cell death may also be caused by a so-called synapsis checkpoint, mediated by HORMAD proteins, rather than by a DNA repair checkpoint (Daniel et al, 2011; Kogo et al, 2012; Wojtasz et al, 2012).

Two types of pseudo XY bodies in wild type oocytes

Our analyses of RAD51 and DMC1 foci in relation to MSUC and synapsis in pachytene oocytes from *Spo11*$^{+/YF}$ and wild type E17.5 embryos has shown that two different types of equally silenced pseudo XY bodies exist in wild type pachytene oocytes. Approximately two-third of the pseudo XY bodies accumulate DMC1 as well as RAD51 and form on unsynapsed chromatin (Type I), whereas one-third accumulate RAD51, but little or no DMC1, and form on synapsed chromatin (Type II). We propose that the Type I pseudo XY bodies represent sites that contain persistent SPO11-induced DSBs in areas that failed to synapse, whereas the Type II pseudo XY bodies represent sites where SPO11-independent damage has persisted that elicited a MSUC response, independent of synapsis.

Persistent DSBs nucleate meiotic silencing

The percentage of cells with γH2AX accumulation in a pseudo XY body is highly reduced in *Spo11*$^{-/-}$ *Hormad1*$^{-/-}$ or *Spo11*$^{-/-}$ *Hormad2*$^{-/-}$ double mutant spermatocytes (Daniel et al, 2011; Wojtasz et al, 2012). This illustrates the important role of HORMAD proteins in the MSUC response. Yet the localization of HORMAD1 to all unsynapsed chromatin in *Spo11* knockout spermatocytes (Daniel et al, 2011; Wojtasz et al, 2012)), and the presence of some nuclei with a proper MSUC response in *Spo11*$^{-/-}$ *Hormad1*$^{-/-}$ spermatocytes indicate that, apart from HORMAD proteins, an additional localizing event is needed for pseudo XY body nucleation. Taken together, these and our observations support the hypothesis that both asynapsis, detected by HORMADs, and persistent SPO11-independent DNA repair foci are involved in the induction of H2AX phosphorylation and the establishment of meiotic silencing in pseudo XY bodies in *Spo11*$^{YF/YF}$ oocyte nuclei. We would like to propose that MSCI in wild type spermatocytes is then also triggered by both persistent DSBs, in this case SPO11-dependent, and the presence of unsynapsed

chromatin (schematically presented in Figure 9).

If RAD51 accumulation is as extensive as observed in pseudo XY bodies in oocytes, HORMADs may not even be required, and enough ATR may be recruited by the DNA repair machinery itself, to elicit the MSUC response, as indicated by the existence of pseudo XY bodies that lack HORMAD1 in oocytes.

Despite the more prominent RAD51 accumulation on axes of the pseudo XY body in oocytes as compared to spermatocytes, we propose that the mechanism of pseudo XY body formation in *Spo11*$^{YF/YF}$ spermatocytes occurs in a similar fashion. The differences in the pattern of RAD51 accumulation may be caused by the fact that *Spo11*$^{YF/YF}$ spermatocytes are eliminated at stage IV of the spermatogenic cycle, whereas *Spo11*$^{YF/YF}$ oocytes appear to proceed normally throughout the stage that should correspond to pachytene and are eliminated later (Baudat et al, 2000). Perhaps, the few spontaneous DSBs in *Spo11*$^{YF/YF}$ spermatocytes modulate the MSUC response in a slightly different way, compared to the responses elicited by the more extensive accumulation of endogenous DSBs in *Spo11*$^{YF/YF}$ oocytes. Still, the MSUC response in both *Spo11*$^{YF/YF}$ spermatocytes and oocytes is characterized by the same intense γH2AX accumulation and by the presence of RAD51/DMC1 and RPA foci. It is interesting to note that such foci can also be observed on the unsynapsed axes of the X chromosome in wild type spermatocytes, as a hallmark of persistent DSBs. HORMAD proteins may be instrumental to spread the MSUC response along the chromosomal axes into areas that lack persistent DSBs, such as the Y chromosome. In somatic cells, formation of γH2AX chromatin domains has also been coupled to transcriptional silencing, in the context of radiation-induced damage (Solovjeva et al, 2007). More recently, Shanbhag et al. (Shanbhag et al, 2010) analysed the effect of persistence of an endonuclease-dependent DSB on transcriptional activity in the neighbouring genes. They observed that H2AX phosphorylation spreads along the DNA surrounding the DSB, and that the accumulation of this histone modification correlated with reduction of RNA polymerase II activity. Persistent DSBs were shown to trigger the silencing of neighbouring genes, and the mechanism was termed DSB-induced silencing *in cis* (DISC) (Shanbhag et al, 2010). This mechanism, that occurs in somatic cells, might have some aspects in common with MSUC and MSCI in meiocytes.

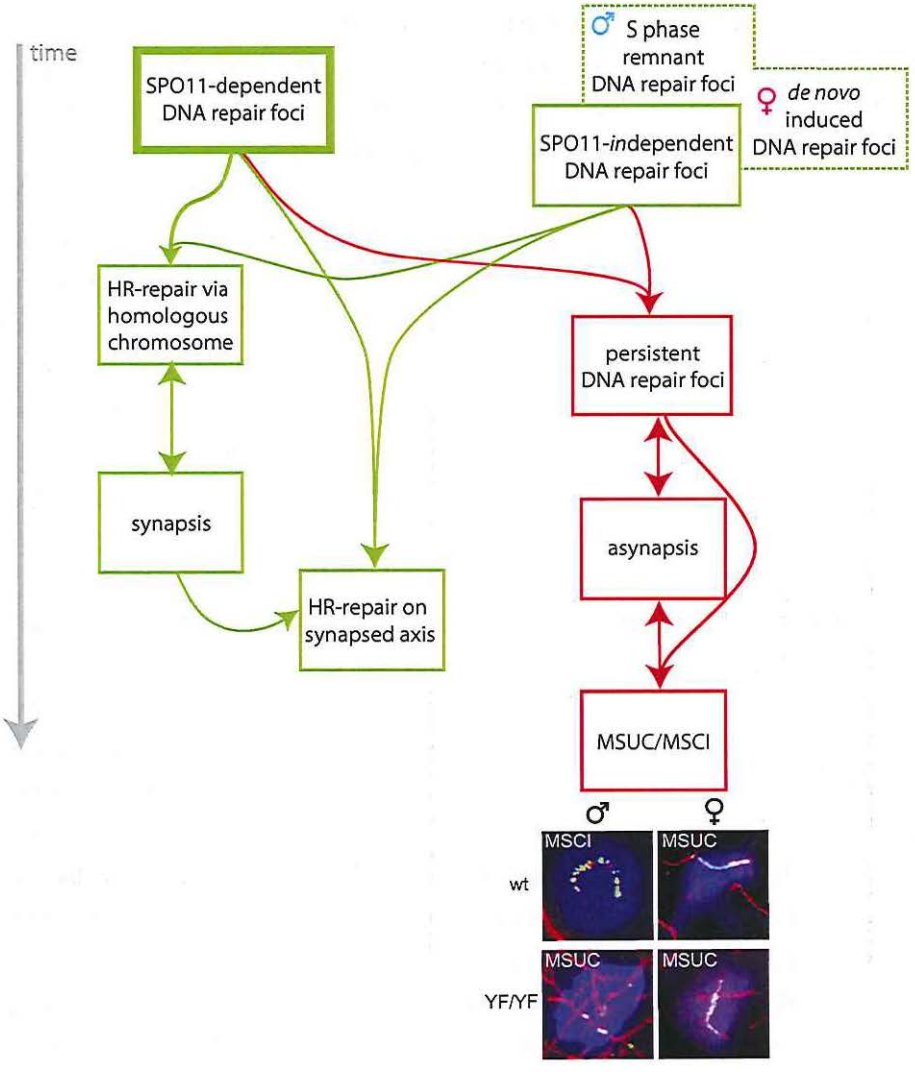
time
SPO11-dependent DNA repair foci
♂ S phase remnant DNA repair foci
♀ de novo induced DNA repair foci
SPO11-independent DNA repair foci
HR-repair via homologous chromosome
persistent DNA repair foci
synapsis
asynapsis
HR-repair on synapsed axis
MSUC/MSCI
♂
♀
wt
MSCI
MSUC
YF/YF
MSUC
MSUC

In conclusion, this study has revealed the presence of SPO11-independent DNA repair foci in oocytes and spermatocytes. In addition, we show that unrepaired DSBs most likely are the initial trigger of both MSCI and MSUC in spermatocytes and oocytes. For wild type oocytes, the possible presence of *de novo* induced DNA damage in a substantial part of the oocyte population may contribute to the massive loss of such oocytes around birth. For spermatocytes, the few SPO11-independent breaks that are present will most likely be rapidly repaired once homologous chromosome pairing is obtained with the help of the 200 or more SPO11-induced DSBs. The MSUC and MSCI response may be less unique than previously thought, and actually represent an extreme and adapted form of DISC. Therefore, knowledge about the molecular basis of meiotic silencing may also be relevant for our understanding of DNA damage-induced chromatin modifications in somatic cells.

◀ **Figure 9: Model for the roles of SPO11-dependent and -independent meiotic DSBs in synapsis and meiotic silencing**

In spermatocytes and oocytes, SPO11 generates many meiotic DSBs which are repaired via homologous recombination (HR). This repair process requires the use of the homologous chromosome as a repair template and promotes homologous chromosome synapsis. Once the homologs are in close juxtaposition, synapsis proceeds. Subsequently, repair may occur faster, perhaps now allowing the use of both the homologous chromosome and the sister chromatid as a template for repair. In the absence of a repair template, DSBs persist, inhibiting synapsis between non-homologous partners, although some repair via the sister chromatid on chromosomes that are not synapsed is not excluded. Conversely, asynapsis also contributes to the persistence of DSBs when repair via the sister chromatid remains suppressed. The presence of persistent DSBs on unsynapsed axes, may lead to local accumulation of γH2AX and activate a positive feedback mechanism that involves HORMAD activation, followed by recruitment of ATR, which will lead to rapid spreading of a signal along the unsynapsed axes that will then induce accumulation of γH2AX on the chromatin surrounding these axes. This process always occurs on the XY pair in spermatocytes and leads to MSCI. In the absence of SPO11-induced DSBs, SPO11-independent DNA damage nucleates MSUC via the same mechanism. In spermatocytes, SPO11-independent DNA repair foci may represent remnant DSBs that have formed during the premeiotic S phase. In oocytes (both wild type and SPO11-mutant), SPO11-independent DNA repair foci form late, at a time point corresponding to early pachytene. Such *de novo* induced DNA repair foci, most likely caused by some form of DNA damage, together with unrepaired SPO11-induced DSBs, and frequently in combination with occasional asynapsis, result in γH2AX accumulation and activation of MSUC. Representative images of the (pseudo) XY body in male and female nuclei from wild type (wt) and *Spo11*$^{YF/YF}$ nuclei are shown. The immunostainings show SYCP3 (red), γH2AX (blue) and RAD51 (green).

Materials and Methods

Ethics statement

All animal experiments were approved by the local animal experiments committee DEC Consult.

All animals were housed in IVC cages under supervision of the Animal Welfare Officer. Any discomfort of animals was daily scored by the animal caretakers. No more than mild or moderate discomfort of animals was expected from the treatments, and no unexpected discomfort was observed.

Mice

All animal experiments were approved by the animal experiments committee DEC-Consult.

Spo11 mutant mice were generated through a two-step recombination strategy as described by Soukharev et al., (Soukharev et al, 1999). First, two heterospecific *lox* sites flanking the selectable marker hygromycin, replacing exons 4-8, were placed in the *Spo11* gene, in ES cells by homologous recombination. Next, a targeting vector containing the same heterospecific *lox* sites flanking exon 4-8 of *Spo11* with the point mutation generating Y138F at exon 4 was used to replace the selection marker by a site-specific double cross-over event (Figure S1A). The final modified *Spo11* locus carries a *loxP* site between exons 3 and 4, the point mutation generating Y138F at exon 4, and a *lox511* site between exons 8 and 9. ES cells carrying a single modified *Spo11* allele were used for blastocyst injection to generate chimeras, and heterozygotes were obtained upon germ line transmission of the mutated allele. Correct targeting was verified using Southern blotting with 5'and 3'probes outside the targeted region (Figure S1B), and sequencing (Figure S1C). This *Spo11* allele has been registered at Mouse Genome Informatics (MGI) as *Spo11<tm1Bdm>* (Allele Accession ID: MGI:5432496). Wild type, heterozygote and homozygote *Spo11* mutant mice were kept on a FVB background. To genotype the animals, the following primers were used: forward, 5'CTGGTCGATGCAGATCCCTACGG3'; reversed, 5'TAGATGCACATTATCTCGATGCC3' (Figure S1B)

Spo11 knockout mice carried the $Spo11^{tm1M}$ allele described in (Baudat et al, 2000).

For the analysis of radiation-induced DSBs in spermatocytes, $Spo11^{YF/YF}$ male adult mice were exposed to 5Gy whole body radiation and sacrificed 1h, 48h, and

120h after the treatment to collect the testes.

Antibodies

For primary antibodies, we used mouse monoclonal antibodies anti-phosphorylated H2AX, anti-BRCA1, anti-TOPBP1, anti-MDC1, anti-phospho H2AX (all from Upstate), anti-DMC1 (DMC1-specific), anti-RAD51, anti-RNA Polymerase II (all from Abcam); rabbit polyclonal antibodies anti-RAD51 (recognizing both DMC1 and RAD51) (Essers et al, 2002), anti-RPA (gift from P. De Boer, described in Schaarmidt et al., ((Schaarschmidt et al, 2002)), anti-SYCP3 (gift from C. Heyting), anti-HORMAD1 (gift from A. Tóth) and anti-phosphorylated H2AX (Upstate); rat polyclonal anti-SYCP3 (Baarends et al, 2007); guinea pig anti-TEX12 (gift from Christer Höög). SPO11 antibody (Spo11L56S9) was raised from rabbits immunized with GST-Spo11α produced by the service of recombinant protein of CRBM (UMR5237-CNRS). For secondary antibodies, we used a goat anti-rabbit IgG alexa 405/488/546/633, goat anti-mouse alexa IgG 350/488/546/633, goat anti-rat IgG alexa 546, goat anti-guinea pig 405/555 (Molecular Probes).

Expression analysis

RNA was extracted and reverse transcribed according to standard procedures. PCR amplifications were performed with forward primer 5'AATAGTCGAGAAGGATGCAACA3'and reversed primer 5'TAGATGCACATTATCTCGATGC3'

Immunoprecipitations were carried out with rabbit polyclonal anti-SPO11 antibody, followed by western blot detection with the same primary antibody and Trueblot secondary antibody (eBioscience).

Histology

Testes were fixed and stained with hematoxilin and eosin using standard histological methods.

Meiotic spread nuclei preparations and immunocytochemistry

Testis tissues were processed to obtain spread nuclei for immunocytochemistry as described by Peters et al. (1997) (Peters et al, 1997). Spread nuclei of spermatocytes were stained with antibodies mentioned above. Before incubation with antibodies, slides were washed in PBS (3x10 min), and non-specific sites were blocked with

0.5% w/v BSA and 0.5% w/v milk powder in PBS. Primary antibodies were diluted in 10% w/v BSA in PBS, and incubations were overnight at room temperature in a humid chamber. Subsequently, slides were washed (3x10 min) in PBS, blocked in 10% v/v normal goat serum (Sigma) in blocking buffer (supernatant of 5% w/v milk powder in PBS centrifuged at 14,000 rpm for 10 min), and incubated with secondary antibodies in 10% normal goat serum in blocking buffer at room temperature for 2 hours. Finally, slides were washed (3x10 min) in PBS (in the dark) and embedded in Prolong Gold with or without DAPI (invitrogen). Fluorescent images were observed by using a fluorescence microscope (Axioplan 2; Carl Zeiss) equipped with a digital camera (Coolsnap-Pro; Photometrics). To distinguish zygotenes from aberrant pachytenes, we used specific parameters defined in Figure S9. Aberrant pachytene oocytes,have also been described in previous publications (Fukuda et al, 2009; Kouznetsova et al, 2009), and are characterized by the presence of one to three chromosome pairs lacking synapsis. We also included rare nuclei in which some chromosomes are entangled and not fully synapsed. Normal (late) zygotene nuclei are characterized by a higher proportion of homologs that have not completed synapsis, compared to what is observed in the aberrant pachytenes, and SYCP1/TEX12 patches can be observed which have not yet converged to become a single complete central element. In addition to specific characteristics of the SC, the labelling patterns of the repair associated recombinase RAD51 and phosphorylated H2AX are also helpful to distinguish late zygotenes from aberrant pachytenes. Single, isolated RAD51 foci are observed in zygotene nuclei, whereas multiple closely adjacent foci are present in aberrant pachytenes. H2AX phosphorylation,occurs in a nucleus-wide pattern at zygotene. In contrast, aberrant pachytene oocytes have one to three bright and defined γH2AX domains.

Fluorescent images were taken under identical conditions for all slides, and images were analyzed using the ImageJ (Fiji) software (Rasband, W.S., ImageJ, U.S. National Institutes of Health, Bethesda, Maryland, USA [http://rsb.info.nih.gov/ij/]). Confocal imaging was performed on a Zeiss LSM700 microscope (Carl Zeiss, Jena): we used 63X oil immersion objective lens (N.A. 1.4), pinhole 1AU. DAPI was excited at 405 nm and imaged with a short pass filter (SP) 490 nm; Alexa 488 was excited at 490 nm and imaged SP 555 nm; Alexa 546 was excited at 555 nm and imaged SP 640 nm; Alexa 633 was excited at 639 nm and for the imaging no filter was required.

Quantification of repair foci, synaptonemal complex length, and RNA pol II intensity

Imaging of nuclei immunostained for RAD51 or DMC1 or RPA and SYCP3 was performed with the same exposure time for each nucleus. Images were analysed without any manipulation of brightness and contrast. Foci were subsequently counted using Image J software, including the Fiji plug-in. We used the analyze particles function and set the threshold manually, in order to include the smallest visible focus in the analysis. The average area of one RAD51 focus was assessed to be 40-50 pixels, therefore foci with an area larger than 100 pixels were counted as multiple foci to allow approximate quantification of RAD51 foci also when it was observed as a continuous signal along the axial elements.

Measurement of synaptonemal complex length was performed using a homemade ImageJ macro. The macro generates a skeletonized image of the original picture and measures the length of that skeleton.

Relative quantification of the RNA polII levels in the (pseudo) XY body was performed comparing the average intensity per pixel area in the γH2AX domain with the average intensity in a non-heterochromatic nuclear area of the same shape and size.

Acknowledgements

We would like to thank dr. Godfried van der Heijden for advice and technical assistance. We thank dr. S. Soukharev for the gift of plasmids carrying two heterologous lox sites, dr Attila Tóth for the gift of the antibody against HORMAD1 and dr Christer Höög for the gift of the antibody against TEX12.

References

Aguilera A (2002). The connection between transcription and genomic instability. Embo J 21:195-201.

Anderson LK, Reeves A, Webb LM, and Ashley T (1999). Distribution of crossing over on mouse synaptonemal complexes using immunofluorescent localization of MLH1 protein. Genetics 151:1569-1579.

Baarends WM, Wassenaar E, Hoogerbrugge JW, Schoenmakers S, Sun ZW, and Grootegoed JA (2007). Increased phosphorylation and dimethylation of XY body histones in the Hr6b-knockout mouse is associated with derepression of the X chromosome. J Cell Sci 120:1841-1851.

Baarends WM, Wassenaar E, van der Laan R, Hoogerbrugge JW, Sleddens-Linkels E, Hoeijmakers JH, de Boer P, and Grootegoed JA (2005). Silencing of unpaired chromatin and histone H2A ubiquitination in mammalian meiosis. Molecular and Cellular Biology 25:1041-1053.

Barchi M, Mahadevaiah S, Di Giacomo M, Baudat F, de Rooij DG, Burgoyne PS, Jasin M, and Keeney S (2005). Surveillance of different recombination defects in mouse spermatocytes yields distinct responses despite elimination at an identical developmental stage. Mol Cell Biol 25:7203-7215.

Baudat F, Manova K, Yuen JP, Jasin M, and Keeney S (2000). Chromosome synapsis defects and sexually dimorphic meiotic progression in mice lacking spo11. Mol Cell 6:989-998.

Belgnaoui SM, Gosden RG, Semmes OJ, and Haoudi A (2006). Human LINE-1 retrotransposon induces DNA damage and apoptosis in cancer cells. Cancer Cell Int 6:13.

Bellani MA, Romanienko PJ, Cairatti DA, and Camerini-Otero RD (2005). SPO11 is required for sex-body formation, and Spo11 heterozygosity rescues the prophase arrest of Atm-/- spermatocytes. J Cell Sci 118:3233-3245.

Bergerat A, de Massy B, Gadelle D, Varoutas PC, Nicolas A, and Forterre P (1997). An atypical topoisomerase II from Archaea with implications for meiotic recombination. Nature 386:414-417.

Boateng KA, Bellani MA, Gregoretti IV, Pratto F, and Camerini-Otero RD (2013). Homologous Pairing Preceding SPO11-Mediated Double-Strand Breaks in Mice. Dev Cell 24:196-205.

Cha RS, Weiner BM, Keeney S, Dekker J, and Kleckner N (2000). Progression of meiotic DNA replication is modulated by interchromosomal interaction proteins, negatively by Spo11p and positively by Rec8p. Genes Dev 14:493-503.

Chen YT, Venditti CA, Theiler G, Stevenson BJ, Iseli C, Gure AO, Jongeneel CV, Old LJ, and Simpson AJ (2005). Identification of CT46/HORMAD1, an immunogenic cancer/testis antigen encoding a putative meiosis-related protein. Cancer Immun 5:9.

Cole F, Kauppi L, Lange J, Roig I, Wang R, Keeney S, and Jasin M (2012). Homeostatic control of recombination is implemented progressively in mouse meiosis. Nat Cell Biol 14:424-430.

Costa Y, Speed R, Ollinger R, Alsheimer M, Semple CA, Gautier P, Maratou K, Novak I, Hoog C, Benavente R, et al. (2005). Two novel proteins recruited by synaptonemal complex protein 1 (SYCP1) are at the centre of meiosis. J Cell Sci 118:2755-2762.

Crone M, Levy E, and Peters H (1965). The duration of the premeiotic DNA synthesis in mouse oocytes. Exp Cell Res 39:678-688.

Daniel K, Lange J, Hached K, Fu J, Ana-

stassiadis K, Roig I, Cooke HJ, Stewart AF, Wassmann K, Jasin M, et al. (2011). Meiotic homologue alignment and its quality surveillance are controlled by mouse HORMAD1. Nat Cell Biol 13:599-610.

Di Giacomo M, Barchi M, Baudat F, Edelmann W, Keeney S, and Jasin M (2005). Distinct DNA-damage-dependent and -independent responses drive the loss of oocytes in recombination-defective mouse mutants. Proceedings of the National Academy of Sciences of the United States of America 102:737-742.

Eijpe M, Heyting C, Gross B, and Jessberger R (2000). Association of mammalian SMC1 and SMC3 proteins with meiotic chromosomes and synaptonemal complexes. J Cell Sci 113:673-682.

Eijpe M, Offenberg H, Jessberger R, Revenkova E, and Heyting C (2003). Meiotic cohesin REC8 marks the axial elements of rat synaptonemal complexes before cohesins SMC1beta and SMC3. J Cell Biol 160:657-670.

Essers J, Hendriks RW, Wesoly J, Beerens CE, Smit B, Hoeijmakers JH, Wyman C, Dronkert ML, and Kanaar R (2002). Analysis of mouse Rad54 expression and its implications for homologous recombination. DNA Repair (Amst) 1:779-793.

Fernandez-Capetillo O, Mahadevaiah SK, Celeste A, Romanienko PJ, Camerini-Otero RD, Bonner WM, Manova K, Burgoyne P, and Nussenzweig A (2003). H2AX is required for chromatin remodeling and inactivation of sex chromosomes in male mouse meiosis. Dev Cell 4:497-508.

Fisher HM, and Aitken RJ (1997). Comparative analysis of the ability of precursor germ cells and epididymal spermatozoa to generate reactive oxygen metabolites. J Exp Zool 277:390-400.

Fukuda T, Daniel K, Wojtasz L, Toth A, and Hoog C (2009). A novel mammalian HORMA domain-containing protein, HORMAD1, preferentially associates with unsynapsed meiotic chromosomes. Exp Cell Res 316:158-171.

Gasior SL, Wakeman TP, Xu B, and Deininger PL (2006). The human LINE-1 retrotransposon creates DNA double-strand breaks. J Mol Biol 357:1383-1393.

Gottipati P, and Helleday T (2009). Transcription-associated recombination in eukaryotes: link between transcription, replication and recombination. Mutagenesis 24:203-210.

Haaf T, Golub EI, Reddy G, Radding CM, and Ward DC (1995). Nuclear foci of mammalian Rad51 recombination protein in somatic cells after DNA damage and its localization in synaptonemal complexes. Proc Natl Acad Sci U S A 92:2298-2302.

Hamer G, Gell K, Kouznetsova A, Novak I, Benavente R, and Hoog C (2006). Characterization of a novel meiosis-specific protein within the central element of the synaptonemal complex. J Cell Sci 119:4025-4032.

Hartung F, Wurz-Wildersinn R, Fuchs J, Schubert I, Suer S, and Puchta H (2007). The catalytically active tyrosine residues of both SPO11-1 and SPO11-2 are required for meiotic double-strand break induction in Arabidopsis. Plant Cell 19:3090-3099.

Hartung M, and Stahl A (1978). Autoradiographic study of RNA synthesis during meiotic prophase in the human oocyte. Cytogenet Cell Genet 20:51-58.

Ichijima YI, M., Lou Z, Nussenzweig A, Camerini-Otero RD, Chen J, Andreassen PR, and Namekawa SH (2011). MDC1 directs chromosome-wide silencing of the sex chromosomes in male germ cells. Genes Dev 25:959-971.

Inagaki A, Schoenmakers S, and Baarends WM (2010). DNA double strand break repair, chromosome synapsis and transcriptional silencing in meiosis. Epigenetics 5:255-266.

Inagaki A, van Cappellen WA, van der Laan R, Houtsmuller AB, Hoeijmakers JH, Grootegoed JA, and Baarends WM (2009). Dynamic localization of human RAD18 during the cell cycle and a functional connection with DNA double-strand break repair. DNA Repair (Amst) 8:190-201.

Kalocsay M, Hiller NJ, and Jentsch S (2009). Chromosome-wide Rad51 spreading and SUMO-H2A.Z-dependent chromosome fixation in response to a persistent DNA double-strand break. Mol Cell 33:335-343.

Kleckner N (1996). Meiosis: how could it work? Proc Natl Acad Sci U S A 93:8167-8174.

Kogo H, Tsutsumi M, Ohye T, Inagaki H, Abe T, and Kurahashi H (2012). HORMAD1-dependent checkpoint/surveillance mechanism eliminates asynaptic oocytes. Genes Cells 17:439-454.

Kouznetsova A, Benavente R, Pastink A, and Hoog C (2011). Meiosis in mice without a synaptonemal complex. PloS one 6:e28255.

Kouznetsova A, Wang H, Bellani M, Camerini-Otero RD, Jessberger R, and Hoog C (2009). BRCA1-mediated chromatin silencing is limited to oocytes with a small number of asynapsed chromosomes. J Cell Sci 122:2446-2452.

Lange J, Pan J, Cole F, Thelen MP, Jasin M, and Keeney S (2011). ATM controls meiotic double-strand-break formation. Nature 479:237-240.

Lim DS, and Hasty P (1996). A mutation in mouse rad51 results in an early embryonic lethal that is suppressed by a mutation in p53. Mol Cell Biol 16:7133-7143.

Long DT, Raschle M, Joukov V, and Walter JC (2011). Mechanism of RAD51-dependent DNA interstrand cross-link repair. Science 333:84-87.

Mahadevaiah SK, Bourc'his D, de Rooij DG, Bestor TH, Turner JM, and Burgoyne PS (2008). Extensive meiotic asynapsis in mice antagonises meiotic silencing of unsynapsed chromatin and consequently disrupts meiotic sex chromosome inactivation. J Cell Biol 182:263-276.

Mahadevaiah SK, Turner JM, Baudat F, Rogakou EP, de Boer P, Blanco-Rodriguez J, Jasin M, Keeney S, Bonner WM, and Burgoyne PS (2001). Recombinational DNA double-strand breaks in mice precede synapsis. Nat Genet 27:271-276.

Martini E, Diaz RL, Hunter N, and Keeney S (2006). Crossover homeostasis in yeast meiosis. Cell 126:285-295.

Matulis S, and Handel MA (2006). Spermatocyte responses in vitro to induced DNA damage. Mol Reprod Dev 73:1061-1072.

McClellan KA, Gosden R, and Taketo T (2003). Continuous loss of oocytes throughout meiotic prophase in the normal mouse ovary. Dev Biol 258:334-348.

Meuwissen RL, Offenberg HH, Dietrich AJ, Riesewijk A, van Iersel M, and Heyting C (1992). A coiled-coil related protein specific for synapsed regions of meiotic prophase chromosomes. Embo J 11:5091-5100.

Moens PB, Chen DJ, Shen Z, Kolas N, Tarsounas M, and Heng HHQ (1997). Rad51 immunocytology in rat and mouse spermatocytes and oocytes. Chromosoma 106:207-215.

Moens PB, Kolas NK, Tarsounas M, Marcon E, Cohen PE, and Spyropoulos B (2002). The time course and chromosomal localization of recombination-related proteins at meiosis in the mouse are compatible with models that can resolve the early DNA-DNA interactions without reciprocal recombination. J Cell Sci 115:1611-1622.

Monesi V (1964). Ribonucleic Acid Synthesis During Mitosis and Meiosis in the

Mouse Testis. J Cell Biol 22:521-532.

Oakberg EF (1956). Duration of spermatogenesis in the mouse and timing of stages of the cycle of the seminiferous epithelium. Am J Anat 99:507-516.

Offenberg HH, Schalk JA, Meuwissen RL, van Aalderen M, Kester HA, Dietrich AJ, and Heyting C (1998). SCP2: a major protein component of the axial elements of synaptonemal complexes of the rat. Nucleic Acids Res 26:2572-2579.

Pangas SA, Yan W, Matzuk MM, and Rajkovic A (2004). Restricted germ cell expression of a gene encoding a novel mammalian HORMA domain-containing protein. Gene Expr Patterns 5:257-263.

Peters AH, Plug AW, van Vugt MJ, and de Boer P (1997). A drying-down technique for the spreading of mammalian meiocytes from the male and female germline. Chromosome Res 5:66-68.

Pittman DL, Cobb J, Schimenti KJ, Wilson LA, Cooper DM, Brignull E, Handel MA, and Schimenti JC (1998). Meiotic prophase arrest with failure of chromosome synapsis in mice deficient for Dmc1, a germline-specific RecA homolog. Mol Cell 1:697-705.

Plug AW, Peters AH, Keegan KS, Hoekstra MF, de Boer P, and Ashley T (1998). Changes in protein composition of meiotic nodules during mammalian meiosis. J Cell Sci 111:413-423.

Plug AW, Xu J, Reddy G, Golub EI, and Ashley T (1996). Presynaptic association of Rad51 protein with selected sites in meiotic chromatin. Proc Natl Acad Sci USA 11:5920-5924.

Rogakou EP, Pilch DR, Orr AH, Ivanova VS, and Bonner WM (1998). DNA double-stranded breaks induce histone H2AX phosphorylation on serine 139. J Biol Chem 273:5858-5868.

Romanienko PJ, and Camerini-Otero RD (2000). The mouse spo11 gene is required for meiotic chromosome synapsis. Mol Cell 6:975-987.

Sakaguchi K, Ishibashi T, Uchiyama Y, and Iwabata K (2009). The multi-replication protein A (RPA) system--a new perspective. FEBS J 276:943-963.

Schaarschmidt D, Ladenburger EM, Keller C, and Knippers R (2002). Human Mcm proteins at a replication origin during the G1 to S phase transition. Nucleic Acids Res 30:4176-4185.

Schalk JA, Dietrich AJ, Vink AC, Offenberg HH, van Aalderen M, and Heyting C (1998). Localization of SCP2 and SCP3 protein molecules within synaptonemal complexes of the rat. Chromosoma 107:540-548.

Schimenti J (2005). Synapsis or silence. Nat Genet 37:11-13.

Schoenmakers S, Wassenaar E, van Cappellen WA, Derijck AA, de Boer P, Laven JS, Grootegoed JA, and Baarends WM (2008). Increased frequency of asynapsis and associated meiotic silencing of heterologous chromatin in the presence of irradiation-induced extra DNA double strand breaks. Dev Biol 317:270-281.

Shanbhag NM, Rafalska-Metcalf IU, Balane-Bolivar C, Janicki SM, and Greenberg RA (2010). ATM-dependent chromatin changes silence transcription in cis to DNA double-strand breaks. Cell 141:970-981.

Shin YH, Choi Y, Erdin SU, Yatsenko SA, Kloc M, Yang F, Wang PJ, Meistrich ML, and Rajkovic A (2007). Hormad1 mutation disrupts synaptonemal complex formation, recombination, and chromosome segregation in mammalian meiosis. PLoS Genet 6:e1001190.

Solovjeva LV, Svetlova MP, Chagin VO, and Tomilin NV (2007). Inhibition of transcription at radiation-induced nuclear foci of phosphorylated histone H2AX

in mammalian cells. Chromosome Res 15:787-797.

Soper SF, van der Heijden GW, Hardiman TC, Goodheart M, Martin SL, de Boer P, and Bortvin A (2008). Mouse maelstrom, a component of nuage, is essential for spermatogenesis and transposon repression in meiosis. Dev Cell 15:285-297.

Soukharev S, Miller JL, and Sauer B (1999). Segmental genomic replacement in embryonic stem cells by double lox targeting. Nucleic Acids Res 27:e21.

Tarsounas M, Morita T, Pearlman RE, and Moens PB (1999). RAD51 and DMC1 form mixed complexes associated with mouse meiotic chromosome cores and synaptonemal complexes. J Cell Biol 147:207-220.

Tsuzuki T, Fujii Y, Sakumi K, Tominaga Y, Nakao K, Sekiguchi M, Matsushiro A, Yoshimura Y, and MoritaT (1996). Targeted disruption of the Rad51 gene leads to lethality in embryonic mice. Proc Natl Acad Sci USA 93:6236-6240.

Turner JM, Aprelikova O, Xu X, Wang R, Kim S, Chandramouli GV, Barrett JC, Burgoyne PS, and Deng CX (2004). BRCA1, histone H2AX phosphorylation, and male meiotic sex chromosome inactivation. Curr Biol 14:2135-2142.

Turner JM, Mahadevaiah SK, Fernandez-Capetillo O, Nussenzweig A, Xu X, Deng CX, and Burgoyne PS (2005). Silencing of unsynapsed meiotic chromosomes in the mouse. Nat Genet 37:41-47.

van der Heijden GW, and Bortvin A (2009). Transient relaxation of transposon silencing at the onset of mammalian meiosis. Epigenetics 4:76-79.

Vilenchik MM, and Knudson AG (2003). Endogenous DNA double-strand breaks: production, fidelity of repair, and induction of cancer. Proc Natl Acad Sci U S A 100:12871-12876.

Wallace NA, Belancio VP, and Deininger PL (2008). L1 mobile element expression causes multiple types of toxicity. Gene 419:75-81.

Wojtasz L, Cloutier JM, Baumann M, Daniel K, Varga J, Fu J, Anastassiadis K, Stewart AF, Remenyi A, Turner JM, et al. (2012). Meiotic DNA double-strand breaks and chromosome asynapsis in mice are monitored by distinct HORMAD2-independent and -dependent mechanisms. Genes Dev 26:958-973.

Wojtasz L, Daniel K, Roig I, Bolcun-Filas E, Xu H, Boonsanay V, Eckmann CR, Cooke HJ, Jasin M, Keeney S, et al. (2009). Mouse HORMAD1 and HORMAD2, two conserved meiotic chromosomal proteins, are depleted from synapsed chromosome axes with the help of TRIP13 AAA-ATPase. PLoS Genet 5:e1000702.

Xue L, Yu D, Furusawa Y, Okayasu R, Tong J, Cao J, and Fan S (2009). Regulation of ATM in DNA double strand break repair accounts for the radiosensitivity in human cells exposed to high linear energy transfer ionizing radiation. Mutat Res 670:15-23.

Yang F, and Wang PJ (2009). The Mammalian synaptonemal complex: a scaffold and beyond. Genome Dyn 5:69-80.

Yoshida K, Kondoh G, Matsuda Y, Habu T, Nishimune Y, and Morita T (1998). The mouse RecA-like gene Dmc1 is required for homologous chromosome synapsis during meiosis. Mol Cell 1:707-718.

Zakharyevich K, Tang S, Ma Y, and Hunter N Delineation of joint molecule resolution pathways in meiosis identifies a crossover-specific resolvase. Cell 149:334-347.

Supplemental figures

Figure S1: Generation of *Spo11*$^{YF/YF}$ mice

(A) Intron/exon structure of the *Spo11* gene. Step I: homologous recombination using a NotI fragment that replaces exons 5-9 and part of the flanking introns for a HYG/TK positive/negative selectable marker cassette and two heterologous lox sites, loxC33 and lox511. Step II: Cre-mediated cassette exchange using a donor plasmid that replaces the HYG/TK cassette for a mutated *Spo11* fragment carrying the F138 codon in exon 5.

(B) (left) Southern blot to visualize a diagnostic BclI fragment using the 5' probe as indicated in A. Correct integration enlarges the BclI fragment from 12 kb to 18 kb (right). PCR using primers in exon 9 and 10 distinguishes the wild-type allele (394 bp) from the mutant allele carrying the lox511 site in intron 9 (482 bp).

(C) Sequencing of *Spo11* cDNA from wild-type (+/+), heterozygote (+/YF) and homozygote (YF/YF) knock-in mice. The A-T mutation that changes the TAC codon for Tyrosine into a TTC codon for Phenylalanin is boxed.

(D) RT-PCR to analyse mRNA expression using testis RNA from 15 day-old-mice, wild-type (+/+), heterozygote (+/YF) and homozygote (YF/YF). Using a forward primer in exon 8 and a reversed primer in exon 10, two splice variants can be detected in wild type and knock-in testes (drawing on the left). Due to the fact that a Loxp site resides between exon 9 and 10, the splice variant that includes these intronic sequences is larger in the *Spo11*$^{YF/YF}$.

(E) Immunoprecipitation and detection of SPO11 in testis extracts from adult wild type (+/+) and *Spo11* knockout (-/-) and 16 days old wild-type (+/+), heterozygote (+/YF) and homozygote (YF/YF) knock-in mice (16d). The positions of the two SPO11 isoforms (β and α) are shown. M: molecular weight marker.

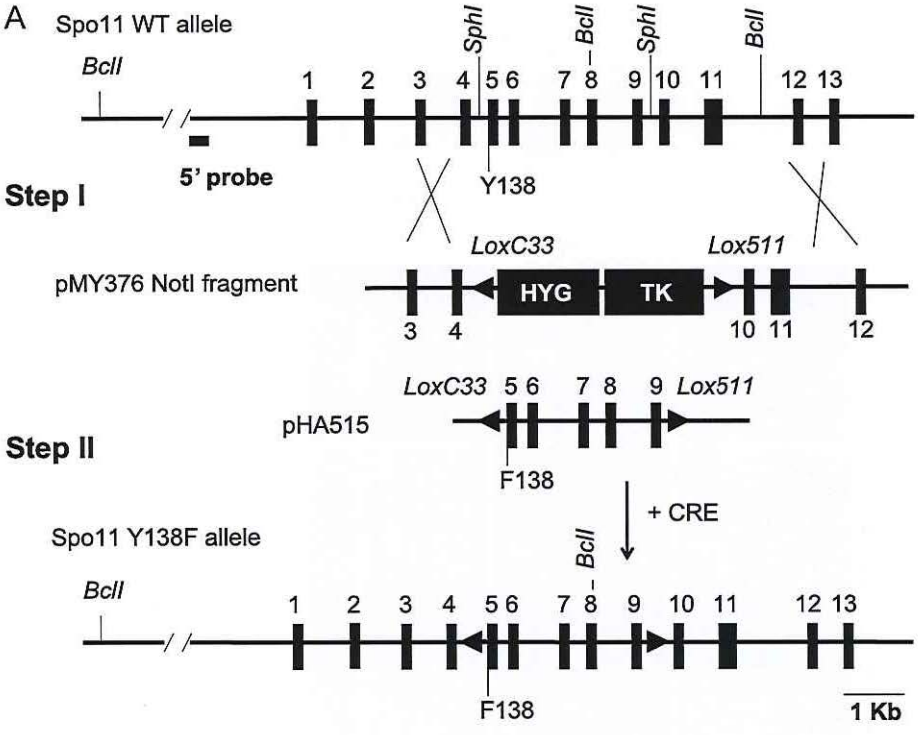
A
Spo11 WT allele
BclI
SphI
BclI
SphI
BclI
1 2 3 4 5 6 7 8 9 10 11 12 13
5' probe
Y138
Step I
LoxC33
Lox511
pMY376 NotI fragment
HYG
TK
3 4 10 11 12
LoxC33 5 6 7 8 9 Lox511
pHA515
Step II
F138
+ CRE
Spo11 Y138F allele
BclI
1 2 3 4 5 6 7 8 9 10 11 12 13
F138
1 Kb

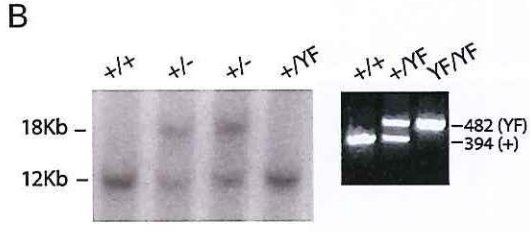
B
+/+ +/- +/- +/YF
18Kb
12Kb
+/+ +/YF YF/YF
482 (YF)
394 (+)

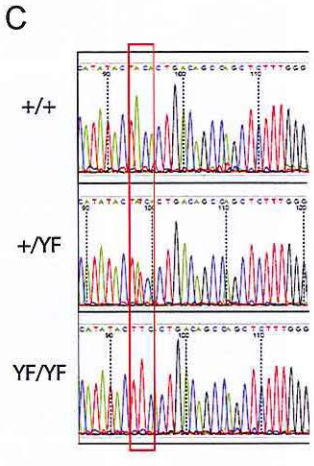
C
+/+
+/YF
YF/YF

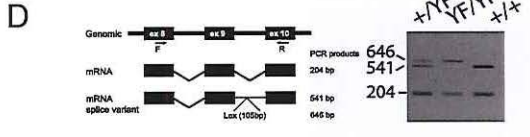
D
Genomic
ex 8
ex 9
ex 10
F
R
mRNA
mRNA splice variant
Lox (105bp)
PCR products
204 bp
541 bp
646 bp
+/YF YF/YF +/+
646
541
204

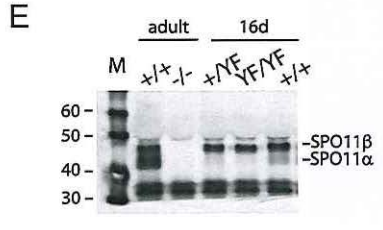
E
adult
16d
M
+/+ -/- +/YF YF/YF +/+
60
50
40
30
SPO11β
SPO11α

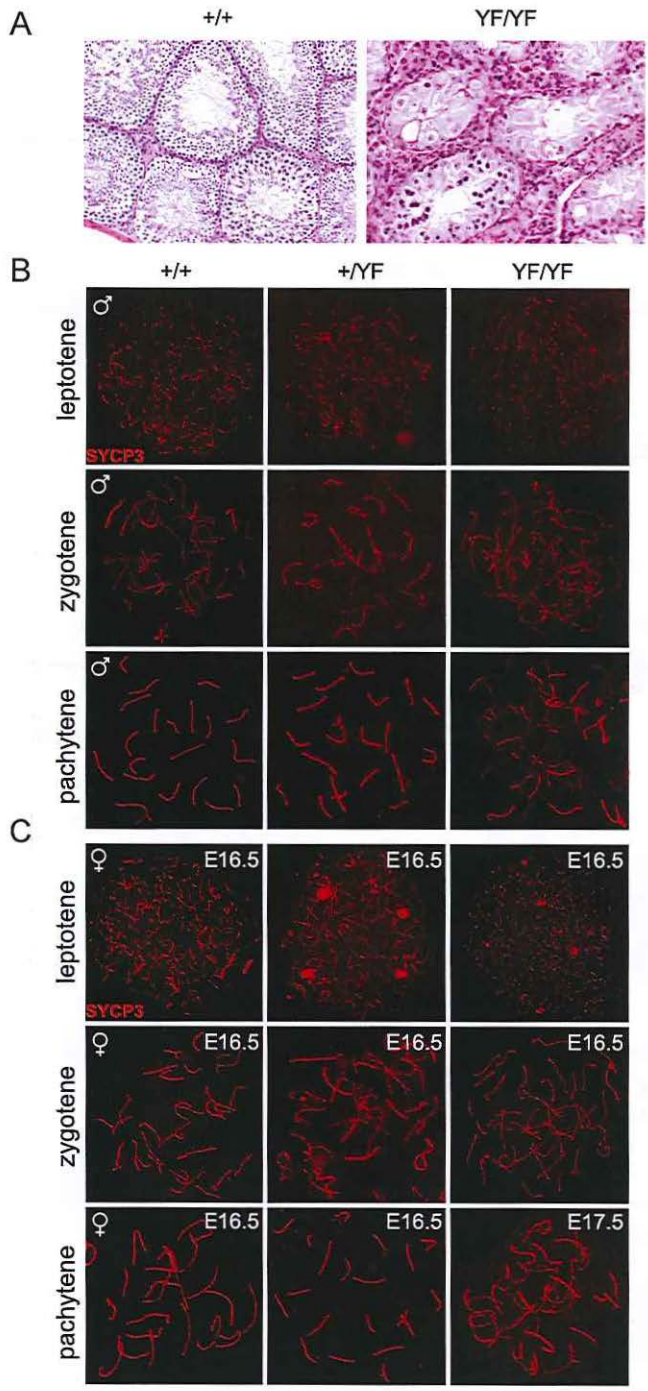

Figure S2: Spermatogenesis and oogenesis are blocked at a zygotene-like stage in *Spo11*$^{YF/YF}$ mice

(A) Hematoxylin-eosin staining of testis from adult wild type (+/+) and *Spo11*$^{YF/YF}$ (YF/YF) mice. Immunostaining of spread nuclei of spermatocytes **(B)** and oocytes **(C)** of wild-type (+/+), *Spo11*$^{+/YF}$ (+/YF) and *Spo11*$^{YF/YF}$ (YF/YF) mice. For wild type and heterozygote mice, leptotene, zygotene and pachytene nuclei are shown. For the *Spo11*$^{YF/YF}$ mice, leptotene, zygotene and late zygotene -like nuclei are shown.

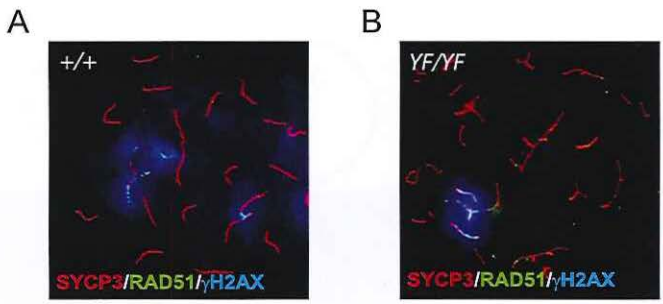

Figure S3: Pattern of RAD51 foci in E17.5 oocyte nuclei is confirmed by ab1837 Abcam antibody
(A-B) Double immunostaining of pseudo XY body-positive *Spo11*$^{YF/YF}$ **(A)** and *Spo11*$^{+/+}$ **(B)** E17.5 oocyte nuclei with anti-SYCP3 (red), anti-RAD51 (green), and anti-γH2AX (blue).

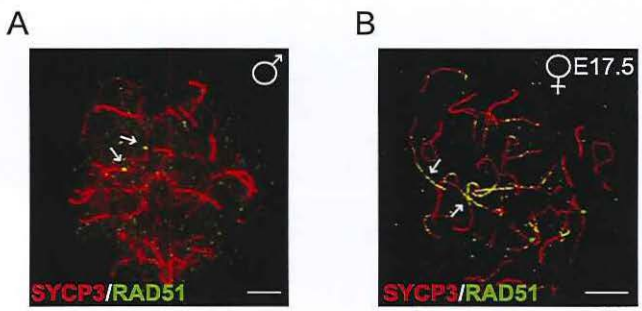

Figure S4: RAD51 foci in *Spo11*$^{-/-}$ spermatocyte and E17.5 oocyte nuclei
(A-B) Double immunostaining of *Spo11*$^{-/-}$ spermatocyte **(A)** and E17.5 oocyte **(B)** nuclei with anti-SYCP3 (red) and anti-RAD51 (green). Arrows indicate RAD51 foci **(A)** and axis-wide RAD51 accumulation **(B)**.

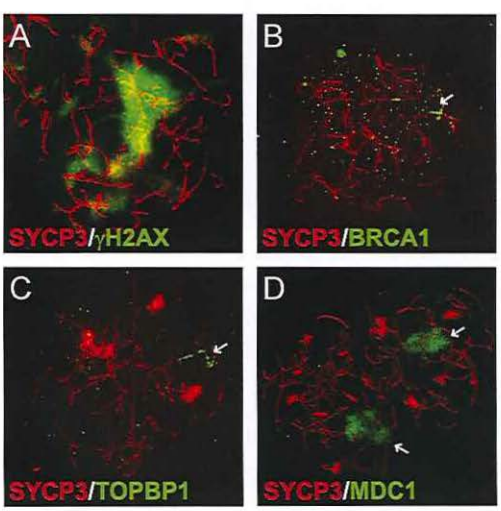

Figure S5: Pseudo XY body in *Spo11*$^{YF/YF}$ spermatocytes
(A-D) Double immunostaining of *Spo11*$^{YF/YF}$ spermatocytes with anti-SYCP3 (red) and different DNA repair proteins or histone modifications (green). Antibodies used for immunostaining are indicated. Arrows mark the localization of the pseudo XY body.

A

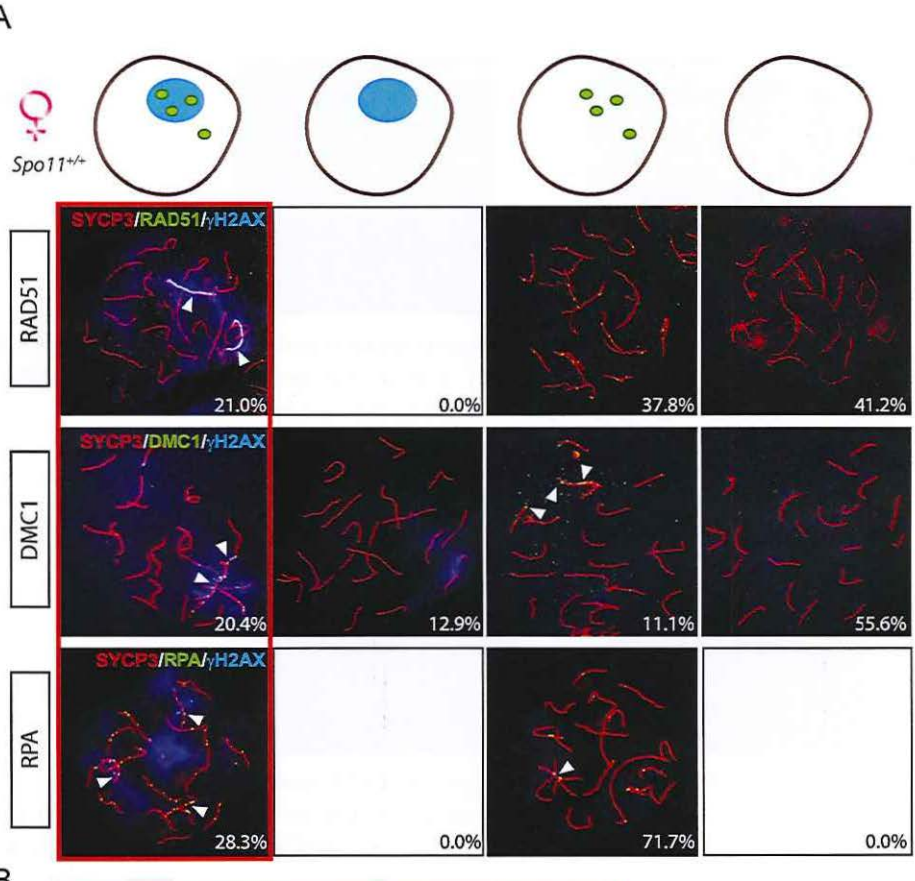

B

	average # foci	% foci in γH2AX domain	% γH2AX domains with foci
RAD51	40.6	81.3	100
DMC1	16.7	68.3	80.0
RPA	59.1	41.2	100

Figure S6: RAD51 and DMC1 foci colocalize in mouse meiocytes
(A-C) Immunostaining of *Spo11*$^{YF/YF}$ spermatocyte **(A)**, *Spo11*$^{YF/YF}$ E17.5 oocyte **(B)**, and *Spo11*$^{+/+}$ E17.5 oocyte **(C)** nuclei with anti-RAD51 (red), anti-DMC1 (green) and anti-γH2AX (blue). Close-ups show RAD51 and DMC1 foci in the area of the pseudo XY body next to every nucleus: red and green channels overlaid (top) and offset (bottom).

► **Figure S7: Limited colocalization of RPA and DMC1 during spermatogenesis**
Mouse spermatocyte nuclei were stained with anti-DMC1 (green) and anti-RPA (red). DAPI was used to visualize the DNA and stage spermatocytes from leptotene (L) through zygotene (Z) to

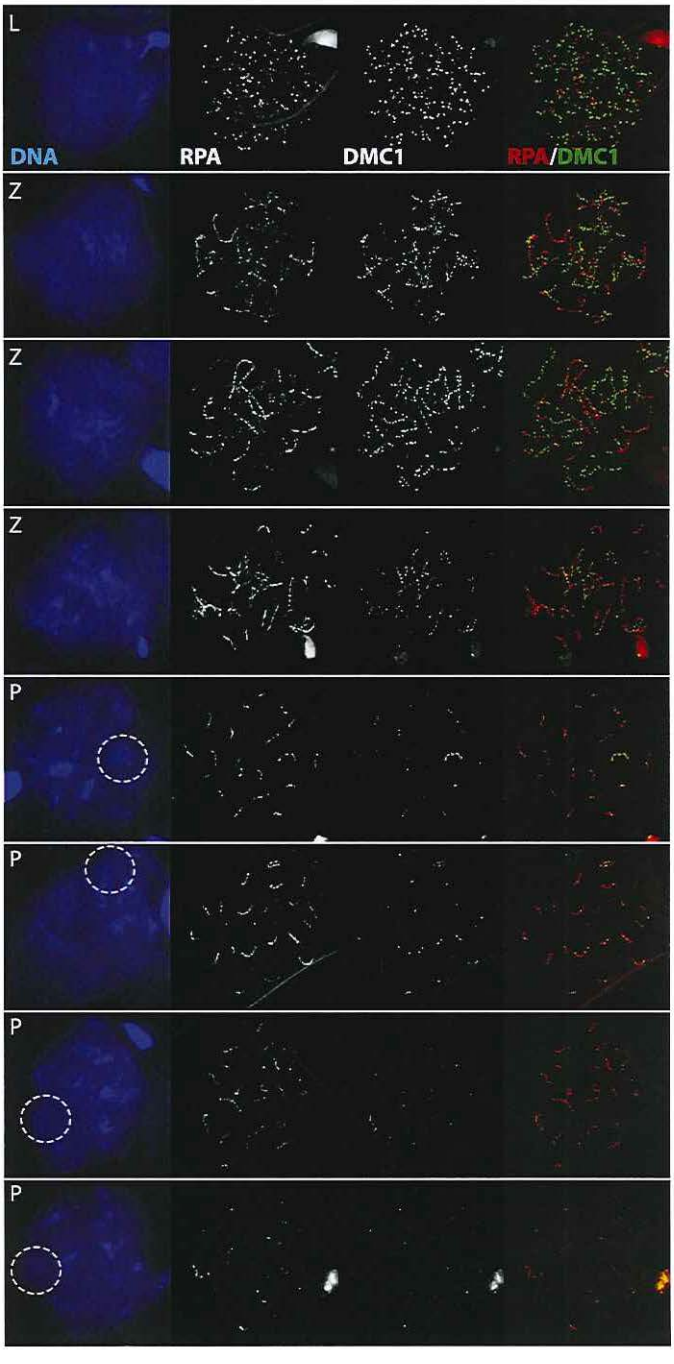

pachytene (P). Early to late pachytene spermatocytes were distinguished based on the conformation of the X and Y chromosomal axes, that were visible in the DAPI image. Consecutive prophase stages are shown from top to bottom. Dashed circles show the nuclear area of the sex body. Both RPA and DMC1 are very abundant at the onset of meiosis. Most likely, RPA is first loaded on the processed 3' ssDNA strands, and then replaced by DMC1 and RAD51. Starting from late zygotene onwards, DMC1 foci decrease in number, presumably because the recombinase has accomplished its function and its presence is no longer needed. At the same time RPA is recruited again to protect areas of ssDNA generated during the recombination process. Note that at early pachytene, the X chromosome is clearly enriched for DMC1 but not for RPA foci. However, RPA foci increase on the X at late pachytene, when almost all DMC1 and autosomal RPA foci have disappeared. In general, colocalization of DMC1 and RPA is only sporadically observed at all stages examined.

A

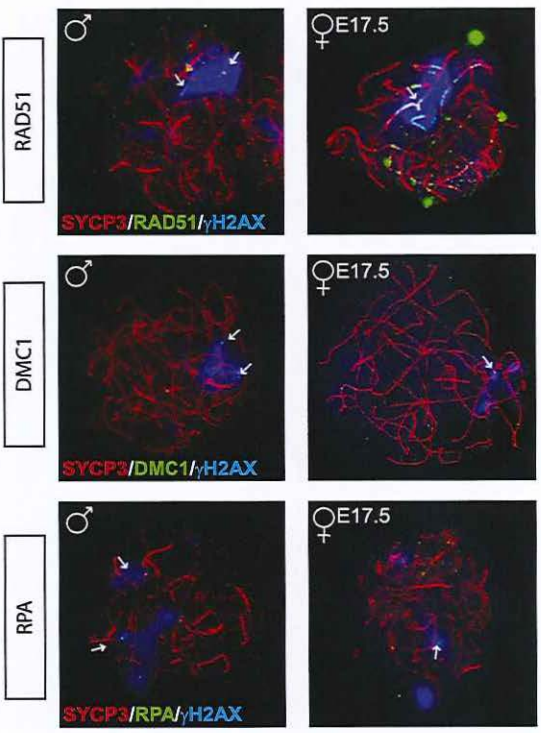

B

	1	2	3	4
RAD51	78.5	8.3	4.9	8.3
DMC1	74.6	1.7	4.4	19.3
RPA	73.7	0.0	4.4	21.9

C

	Average # foci	% foci in γH2AX domain	% γH2AX domains with foci
RAD51	6.5	80.0	96.2
DMC1	5.6	79.6	97.9
RPA	6.2	78.4	95.1

Figure S8: Correlation between DNA repair markers and pseudo XY body formation in *Spo11*$^{-/-}$ spermatocytes and oocytes

(A) Immunostaining of spermatocyte (left) and E17.5 oocyte (right) nuclei from *Spo11*$^{-/-}$ animals with anti-SYCP3 (red), anti-γH2AX (blue) and anti-RAD51 (green, upper panel) or anti-DMC1 (green, middle panel) or anti-RPA (green, lower panel). SPO11-independent foci are observed in the same pattern as in *Spo11*$^{YF/YF}$ meiocytes

(B) Quantification of pseudo XY body and DNA repair marker foci positive spermatocytes (n=120) in *Spo11*$^{-/-}$ animals. Nuclei with four different staining patterns were distinguished as indicated by the cartoons above the colums. Numbers indicate percentages.

(C) The number of RAD51, DMC1, and RPA foci was counted in the subpopulation of spermatocytes showing both foci and a pseudo XY body. The average total number of foci is reported in the first column of the table. The percentage of colocalization of RAD51, DMC1 or RPA foci with pseudo XY body is shown in the second column. The percentage of pseudo XY bodies which also contain at least one focus of RAD51, DMC1 or RPA is reported in the third column.

A

	Zygotene	Aberrant pachytene
SYCP1 (or TEX12)	Incomplete synapsis for more than 3 chromosomes	Asynapsis or Incomplete synapsis for 1-3 chromosomes
SYCP3	Presence of V-shaped axial elements protruding from lateral elements that colocalize with SYCP1/TEX12	Entangled areas involving more than 1pair of homologs OR totally unsynapsed pairs (No central element)
γH2AX	Nucleus-wide pattern, with broad areas of variable intensity	1-3 well-delimited domains, often in the nuclear peripher
RAD51	Isolated foci pattern	Pattern of multiple RAD51 foci that localize in closely adjacent positions along the axis

B

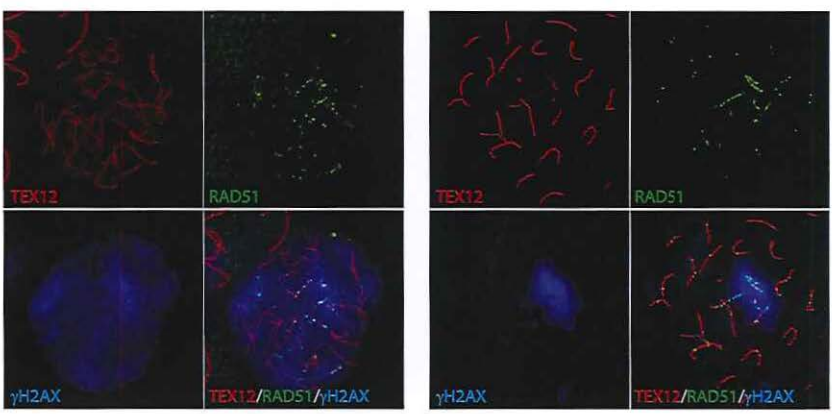

Figure S9: Parameters to discriminate between zygotene and aberrant pachytene wild type oocytes **(A)** Summary of the applied parameters to discriminate between zygotene oocytes and aberrant pachytene oocytes. Patterns of SYCP3, SYCP1 (or TEX12), γH2AX, and RAD51 are described for both categories. **(B)** Representative images of the described oocyte categories. Oocytes were immunostained for TEX12 (red), RAD51 (green), and γH2AX (blue).

3

Interhomolog repair of exogenous DNA double-strand breaks promotes chromosome synapsis in SPO11-mutant mouse meiocytes

Submitted

Interhomolog repair of exogenous DNA double-strand breaks promotes chromosome synapsis in SPO11-mutant mouse meiocytes

Fabrizia Carofiglio[1], Akiko Inagaki[1,3], Evelyne Wassenaar[1], Wiggert A. van Cappellen[2], J. Anton Grootegoed[1], and Willy M Baarends[1]*

1Department of Reproduction and Development, Erasmus MC - University Medical Center, Rotterdam, The Netherlands

2Erasmus Optical Imaging Centre, Department of Pathology, Erasmus MC - University Medical Center, Rotterdam, The Netherlands

3Current address: Laboratory of Chromosome Biology, Memorial Sloan Kettering Cancer Center, New York, USA

**Author for correspondence*

Abstract

Repair of SPO11-dependent DNA double-strand breaks (DSBs) via homologous recombination (HR) is essential for stable homologous chromosome pairing and synapsis during meiotic prophase. Here, we induced radiation-induced DSBs to study meiotic recombination and homologous chromosome pairing in mouse meiocytes, in the absence of SPO11 activity (*Spo11*$^{YF/YF}$ model). Within 30 minutes after irradiation of *Spo11*$^{YF/YF}$ mice, 140-160 DSB repair foci were detected, which specifically localized to the synaptonemal complex axes. Repair of radiation-induced DSBs was incomplete in *Spo11*$^{YF/YF}$ compared to *Spo11*$^{+/YF}$ meiocytes, although the HR machinery is intact and the sister chromatid is available as repair template in both genetic backgrounds. This suggests that template choice is biased towards the homologous chromosome in meiotic recombination. Accordingly, repair of exogenous DSBs promoted partial recovery of chromosome pairing and synapsis in *Spo11*$^{YF/YF}$ meiocytes. Together, these results suggest that recruitment of exogenous DSBs to the synaptonemal complex, in conjunction with preferential repair of exogenous DSBs via the homologous chromosome, contribute to homology recognition. This implies that the meiotic interhomolog bias in mouse, acts not only on SPO11-induced DSBs but also on exogenous DSBs.

Introduction

Meiosis is a reductional cell division that takes place during gametogenesis, to allow generation of haploid gametes. In the first meiotic division, recombination and segregation of homologous chromosomes takes place, whereas sister chromatids are separated in the second division. At the onset of meiotic prophase I, more than 200 meiotically regulated DNA double-strand breaks (DSBs) are induced by the transesterase SPO11 in the mouse (Baudat et al, 2000; Cole et al, 2012; Romanienko and Camerini-Otero, 2000). Essential components of non-homologous end joining (NHEJ), an error-prone DSB repair mechanism, are suppressed in early meiotic prophase of mouse spermatocytes (Goedecke et al, 1999), and meiotic DSBs should be repaired via homologous recombination (HR), although a contribution of pathways such as alternative NHEJ or single-strand annealing cannot be excluded (Bennardo et al, 2008; Stark et al, 2004). HR repair is mediated by recombinases, proteins that have DNA-dependent ATPase activity and form filaments on the single-stranded resected DNA ends at DSB sites. In meiotic cells, two recombinases are expressed: RAD51 and DMC1. RAD51 is known to be essential for homologous recombination repair in mitotic cells (Lim and Hasty, 1996; Tsuzuki et al, 1996), and is thought to perform an accessory function in mouse meiosis, in analogy to what has been described for yeast RAD51 (Cloud et al, 2012). DMC1 has indispensable meiosis-specific activity (Pittman et al, 1998; Yoshida et al, 1998). Repair via homologous recombination implies the use of an intact DNA template to recover the missing genetic information. In meiotic prophase I cells, three templates can be used: the sister chromatid, that is tethered to its counterpart by (meiosis-specific) cohesins which are loaded during (Eijpe et al, 2000; Eijpe et al, 2003) and after (Ishiguro et al, 2011; Ishiguro et al, 2014; Lee and Hirano, 2011) pre-meiotic S phase, and either one of the two chromatids of the homologous chromosome. For meiosis in *S. cerevisiae*, it was shown that the homologous chromosome is preferably used as a meiotic recombination partner, a phenomenon that is named interhomolog bias (Schwacha and Kleckner, 1997). This condition requires several proteins which are associated with the synaptonemal complex scaffold (Red1, Hed1, Rec8, Mek1), or function in the homologous recombination pathway (Rad51, Dmc1) (Hong et al, 2013). In mouse, no direct evidence of interhomolog bias has been provided so far. However, in spermatocytes, several DSB repair foci

are present on the unsynapsed arm of the X chromosome, that only has the sister chromatid available as repair template, long after autosomal breaks have been fully repaired (Moens et al, 1997; Plug et al, 1998). Although it has been recently shown that new DSBs may be induced on chromatin areas that fail to synapse (Kauppi et al, 2013), such X chromosome-associated foci could also represent persistent unrepaired DSBs, indicating that the sister chromatid is not used as a repair template, at least till the end of pachytene. Based on this observation, such an interhomolog bias is expected to be operational on mouse autosomes as well. This would imply that the vast majority of mouse meiotic DSBs is repaired via homologous recombination using one of the chromatids of the homologous chromosome, rather than the sister chromatid, as a template. As an important consequence, recombinational DSB repair can thereby promote homology recognition and juxtaposition of pairing chromosomes, and subsequently contribute to the achievement of tighter interactions between the paired chromosomes. This leads to synapsis, which is established by the accumulation of central and transverse element proteins of the synaptonemal complex, such as SYCP1, TEX12, SYCE2, and SYCE3 (Costa et al, 2005; Hamer et al, 2006; Meuwissen et al, 1992; Yang and Wang, 2009). These synaptonemal complex components zip together the lateral elements (composed of SYCP2 and SYCP3 complexes) that form along the bases of the chromatin loops of each chromosome (Offenberg et al, 1998; Schalk et al, 1998).

In the absence of SPO11-induced meiotic DSBs, homologous pairing and synapsis in mouse meiocytes are severely impaired; some heterologous synapsis can occur, but both spermatocytes and oocytes do not proceed beyond a zygotene-like stage (Baudat et al, 2000; Carofiglio et al, 2013; Romanienko and Camerini-Otero, 2000). Recent evidence indicates that SPO11 may be necessary for premeiotic chromosome pairing, independent of its catalytic activity, but such pairing is not maintained throughout meiotic prophase when DSBs are not induced (Boateng et al, 2013). However, in a similar study Ishiguro et al (Ishiguro et al, 2014) showed that early meiotic chromosome pairing occurs to a certain extent independent of DSBs and SPO11, and they proposed that the architecture of chromatin established by cohesins contributes to homology recognition, prior to meiotic recombination.

In a yeast strain carrying a SPO11 mutation, partial rescue of the meiotic defect was achieved by X-irradiation, with a six-fold increase of spore viability, showing that exogenous DNA lesions can partially substitute for SPO11-activity (Thorne

and Byers, 1993). Similarly, improved centromeric interactions have been observed in *Spo11* knockout spermatocytes upon cisplatin treatment (Romanienko and Camerini-Otero, 2000).

Herein, we aimed to study the role of meiotic HR repair in favouring homologous chromosome synapsis in mouse. First, we investigated if meiosis-specific processing of DSBs depends on SPO11-mediated formation of these breaks. Second, we determined whether processing of radiation-induced DSBs can contribute to homology recognition and synapsis. We used mice carrying a SPO11 amino acid replacement (Y138F, hereafter referred to as $Spo11^{YF/YF}$), which abrogates the enzymatic activity of SPO11 and results in a synapsis-deficient phenotype (Carofiglio et al., 2013), but should allow DSB-independent homologous chromosome associations (Boateng et al, 2013; Ishiguro et al, 2014). We generated exogenous DSBs by γ-irradiation of leptotene meiocytes. When we studied the early processing of the radiation-induced DSBs, we observed that the DNA repair foci were specifically localized on the axial elements. Irradiation is expected to generate DSBs randomly in the genome, therefore this observation indicates relocalization of DSBs to the chromosomal axes. Subsequently, we analysed the dynamics of exogenous DSB repair in $Spo11^{YF/YF}$ spermatocytes and oocytes, compared to $Spo11^{+/YF}$ controls. We found that homozygous mutant meiocytes repaired exogenous DSBs less efficiently, although the machinery to repair DSBs by HR is intact in both $Spo11^{YF/YF}$ and $Spo11^{+/YF}$ meiocytes, and the sister chromatid is also available as template for repair. This result indicates that use of the sister chromatid is inhibited. As expected, homologous chromosome pairing and synapsis on the $Spo11^{YF/YF}$ mutant background were partially rescued by the irradiation treatment, suggesting that the subpopulation of breaks that is repaired via the homolog contributes to the establishment of interhomolog interactions. Taken together, our data show that exogenous DSBs recruit the meiosis-specific HR repair machinery, are translocated to the axial elements, then most likely undergo the interhomolog bias, and thereby contribute to homology recognition.

Results

Radiation-induced DSBs rapidly localize on the synaptonemal complex

We treated *Spo11*$^{+/YF}$ and *Spo11*$^{YF/YF}$ adult male mice with γ-irradiation, at a dose of 5Gy, and analysed DSB markers in leptotene spermatocytes isolated from mice sacrificed 30 and 60 minutes after irradiation.

Replication protein A (RPA) specifically binds to single-stranded DNA (Heyer et al, 1990; Wang et al, 2005; Wold et al, 1989) and it forms foci in meiotic cells as soon as meiotic DSBs are resected (Ashley et al, 2004; Carofiglio et al, 2013). We observed RPA foci in irradiated *Spo11*$^{YF/YF}$ leptotene spermatocytes (for selection criteria of nuclei see Materials and Methods) by 30 minutes after irradiation (Figure 1A). In a previous study, we reported that RPA foci are almost completely absent in non-irradiated spermatocytes and oocytes from *Spo11*$^{YF/YF}$ mice (Carofiglio et al, 2013); therefore, we deduced that we could refer to RPA foci as a proxy of radiation-induced DSBs. Radiation-induced DSBs are expected to be randomly distributed in the nucleus, and to elicit repair foci formation without specific localization. Interestingly, we observed that RPA foci, although scattered around the nuclear volume, were always associated with the axial elements, both in *Spo11*$^{YF/YF}$ and *Spo11*$^{+/YF}$ spermatocytes (Figure 1A, close-ups). In the *Spo11*$^{YF/YF}$ spermatocytes, the maximum number of foci (167±30, n=40) was reached 30 minutes after irradiation, and only 6 foci were observed in the non-irradiated nuclei, which indicates that around 161 DSBs were induced (Table I). A comparable increase in the total number of RPA foci was observed in irradiated *Spo11*$^{+/YF}$ spermatocytes (Figure 1B; Table I), albeit with slower kinetics compared to the *Spo11*$^{YF/YF}$ spermatocytes. This may indicate that more time is required to process the radiation-induced DSBs in *Spo11*$^{+/YF}$ compared to *Spo11*$^{YF/YF}$ spermatocytes, perhaps due to limiting amounts of the involved proteins.

During meiotic prophase I in wild type meiocytes, RAD51 and its meiosis-specific homolog DMC1 are recruited to SPO11-dependent DSBs (Ashley et al, 1995; Plug et al, 1996; Tarsounas et al, 1999). These two recombinases have been shown to colocalize in DSB repair foci (Tarsounas et al, 1999). We observed similar patterns of accumulation using RAD51 and DMC1 antibodies in *Spo11*$^{YF/YF}$ leptotene spermatocytes, at the 30 and 60 minutes timepoints (Figure 2A,B), indicating that both RAD51 and DMC1 are recruited to the exogenous DSBs to form repair foci.

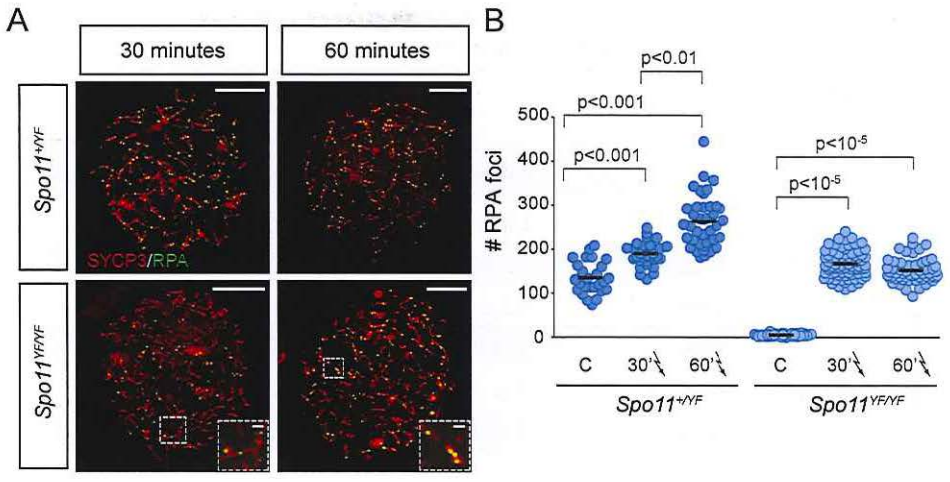

Figure 1: DNA repair protein foci upon irradiation of *Spo11*$^{+/YF}$ and *Spo11*$^{YF/YF}$ spermatocytes
(A) Co-staining of RPA (green) and SYCP3 (red) in irradiated *Spo11*$^{+/YF}$ (upper panel) and *Spo11*$^{YF/YF}$ (lower panel) leptotene spermatocyte nuclei, 30 (left panels) and 60 (right panels) minutes after irradiation. At both timepoints, all RPA foci were found in association with the chromosomal axes; the close-ups show representative areas of the nucleus. Scale bar represents 10 mm in pictures of whole nuclei, and 1 mm in close-ups. **(B)** The number of RPA foci was counted in *Spo11*$^{+/YF}$ and *Spo11*$^{YF/YF}$ leptotene spermatocytes, control (C = non-irradiated), and 30 and 60 minutes after irradiation. Statistically significant differences are marked in the plot (Mann-Whitney). **(C)** Triple immunostaining with anti-SYCP2, anti-RAD51, and anti-DMC1 of a *Spo11*$^{YF/YF}$ leptotene spermatocyte nucleus from a mouse that was killed 60 minutes after irradiation. RAD51 foci (green) localize to patches of SYCP2 (red) in the assembling axial elements. The expanded view of two areas of the nucleus shows RAD51 foci associated to the short fragments of axial elements. In the middle panels, RAD51 and DMC1 (grayscale) foci show very similar patterns. In the rightmost panel RAD51 foci (red) and DMC1 foci (green) colocalization can be appreciated in an overlaid image. The enlarged view of two areas of the nucleus shows some of the overlapping foci in an artificial offset channel. Scale bar represents 10 mm in pictures of whole nuclei, and 1 mm in close-ups. **(D)** The number of DMC1 (green), and RAD51 (red) foci was counted in *Spo11*$^{+/YF}$ and *Spo11*$^{YF/YF}$ leptotene nuclei 30 and 60 minutes after irradiation. Every dot represents one nucleus. Statistically significant increases in repair foci are observed between non-irradiated (C) and irradiated (60') spermatocytes of both genotypes (Mann-Whitney).

It should be noted that the RAD51 antibody may also recognize DMC1 to some extent, but the DMC1 antibody does not cross-react with RAD51. For simplicity we refer to RAD51 foci and DMC1 foci to indicate foci that were observed with the RAD51 or DMC1 antibody, respectively. Our observations are coherent with previous studies in which we showed that γ-irradiation results in formation of additional RAD51/DMC1 foci in wild type leptotene spermatocytes (Inagaki et al, 2011; Schoenmakers et al, 2008). Similar to what we observed for RPA, the

Table I - Protein foci formation shortly after irradiation in *Spo11*$^{+/YF}$ and *Spo11*$^{YF/YF}$ leptotene spermatocytes (averages ± standard deviation; n=80)

	genotype	protein foci	time after irradiation	
			control*	30 minutes	60 minutes
spermatocytes	*Spo11*$^{+/YF}$	RPA	136 ± 37	190 ± 26	263 ± 58
		RAD51	138 ± 27**	137 ± 20	222 ± 54
		DMC1	93 ± 35	114 ± 20	149 ± 64
	Spo11$^{YF/YF}$	RPA	6 ± 3**	167 ± 30	152 ± 27
		RAD51	6 ± 3**	128 ± 32	150 ± 40
		DMC1	5 ± 3**	115 ± 39	143 ± 45

*control was not irradiated
**data from (Carofiglio et al, 2013)

RAD51/DMC1 foci were always associated with the axial elements (Figure 2A,B), suggesting that DSBs are tethered to the axes before presynaptic recombinase filaments can be formed. In addition, the dynamics of RPA versus RAD51/DMC1 accumulation are consistent with a model in which RPA accumulates first, and is subsequently replaced by RAD51 and DMC1, as suggested previously (Inagaki et al, 2010).

In *Spo11*$^{YF/YF}$ leptotene spermatocyte nuclei, the number of RAD51 and DMC1 foci both increased from an average of 6 and 5 in non-irradiated nuclei (Fig 2C, (Carofiglio et al, 2013)) to 128 and 115 at 30 minutes and 150 and 143 at 60 minutes following irradiation, respectively (Figure 2C, Table I). This would indicate that 138-144 exogenous DSBs can be visualized by RAD51/DMC1 immunostaining upon irradiation. This is a bit less than what we observed for RPA, which could be due to differences in signal-to-noise ratio between immunostaining of

► **Figure 2: RAD51 and DMC1 foci upon irradiation of *Spo11*$^{+/YF}$ and *Spo11*$^{YF/YF}$ spermatocytes**
(A) Irradiated *Spo11*$^{+/YF}$ (upper panels) and *Spo11*$^{YF/YF}$ (lower panels) leptotene spermatocytes 30 minutes after irradiation were immunostained for RAD51, DMC1, and SYCP3. Overlayed images of the same nuclei show localization of RAD51 and DMC1 (green) to the axes (red), colocalization of RAD51 (red) and DMC1 (green) foci, and a merge of the foci with SYCP3 (blue). **(B)** Triple immunostaining with anti-SYCP2, anti-RAD51, and anti-DMC1 of a *Spo11*$^{YF/YF}$ leptotene spermatocyte nucleus from a mouse that was killed 60 minutes after irradiation. RAD51 foci (green) localize to patches of SYCP2 (red) in the assembling axial elements. The expanded view of two areas of the nucleus shows RAD51 foci associated to the short fragments of axial elements. In the middle panels,

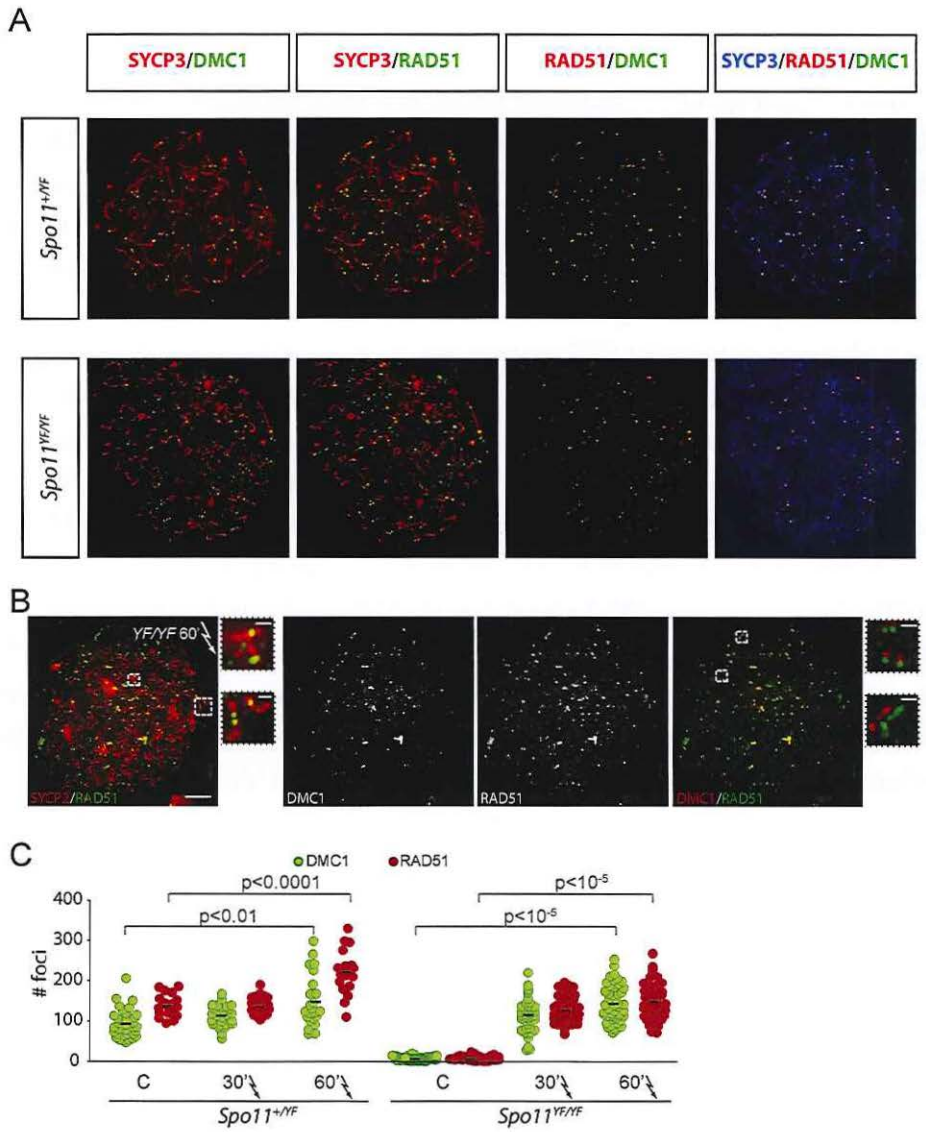

RAD51 and DMC1 (grayscale) foci show very similar patterns. In the rightmost panel RAD51 foci (red) and DMC1 foci (green) colocalization can be appreciated in an overlaid image. The enlarged view of two areas of the nucleus shows some of the overlapping foci in an artificial offset channel. Scale bar represents 10 μm in pictures of whole nuclei, and 1 μm in close-ups. **(C)** The number of DMC1 (green), and RAD51 (red) foci was counted in *Spo11*$^{+/YF}$ and *Spo11*$^{YF/YF}$ leptotene nuclei 30 and 60 minutes after irradiation. Every dot represents one nucleus. Statistically significant increases in repair foci are observed between non-irradiated (C) and irradiated (60') spermatocytes of both genotypes (Mann-Whitney).

the different proteins, or might be related to differences in life-time of RPA and RAD51/DMC1 foci.

In *Spo11*$^{+/YF}$ and *Spo11*$^{YF/YF}$ leptotene nuclei, it is expected that the same number of DSBs is induced by the same radiation dose. However, the number of RAD51 and DMC1 foci in irradiated *Spo11*$^{+/YF}$ leptotene spermatocytes were increased by only 56 for DMC1 and 84 for RAD51 at 60 minutes following irradiation (Table I). This indicates that RAD51 and DMC1 foci formation on radiation-induced breaks on the *Spo11*$^{+/YF}$ background is more delayed, or less efficient, compared to what is observed on the *Spo11*$^{YF/YF}$ background. In mouse meiotic prophase, SPO11 activity is restrained by ATM via a negative feedback loop (Lange et al, 2011), to limit the number of meiotic DSBs. If exogenous DSBs contribute to activate such feedback response, this would reduce the number of SPO11-dependent DSBs in irradiated *Spo11*$^{+/YF}$ spermatocytes. Phosphorylation of the histone variant H2AX into γH2AX is a direct effect of ATM activation upon DSB formation (Rogakou et al, 1998) also in meiocytes (Mahadevaiah et al, 2001), and can therefore be used as a readout for ATM activity. We measured the level of γH2AX intensity in *Spo11*$^{+/YF}$ leptotene nuclei 30 minutes after irradiation and found that it was 36 % higher than in non-irradiated controls (mean intensity controls=31.9±11 (n=25), mean intensity irradiated nuclei=43.6±14.6 (n=25)). It has been reported that overexpression of SPO11 in spermatocytes resulted in 100 additional RAD51 foci, and a two-fold increase in γH2AX mean intensity compared to wild type spermatocytes (Cole et al, 2012). Thus, in this model, the ATM-dependent feedback mechanism did not nullify the effect of SPO11 overexpression. In our system, a more limited effect on γH2AX was observed upon irradiation, strongly suggesting that radiation-induced DSBs may not be able to significantly enhance ATM-mediated SPO11-down-regulation. Still, repair factors might become limiting when extra DSBs are induced, either by irradiation or by SPO11 overexpression, and in order to avoid overestimation of the amount of radiation-induced damage in *Spo11*$^{+/YF}$ spermatocytes, we used the observed numbers of radiation-induced RAD51 foci in *Spo11*$^{YF/YF}$ spermatocytes (144) and in *Spo11*$^{+/YF}$ spermatocytes (84) at the 1h timepoint as estimates of the total number of radiation-induced DSB repair foci in leptotene spermatocytes as well as oocytes of the respective genotypes, and as a reference for further analysis of the repair dynamics (see below).

Repair of radiation-induced DSBs is delayed in *Spo11*$^{YF/YF}$ spermatocytes and oocytes

We wished to analyse the dynamics of radiation-induced DSB repair as meiotic prophase progresses from leptotene onwards. A time period of 48h and 120h is required for the transition from leptotene to late zygotene and to midpachytene, respectively. Thus, male mice were sacrificed at 48h or 120h following 5Gy irradiation (Figure 3A). A dose of 5 Gy will kill most of the spermatogonia and preleptotene spermatocytes, but more than half of the spermatocytes at later stages will survive, and progress through meiotic prophase with normal timing of subsequent events (Oakberg and Diminno, 1960). Thus, the zygotene and midpachytene (like) spermatocytes analysed at the chosen timepoints will have developed from cells that were at the leptotene stage at the time of irradiation. To analyse repair of radiation-induced DSBs in oocytes, we followed a different experimental time schedule, coherent with the timing of female meiotic prophase which is initiated during embryonic development. Pregnant *Spo11*$^{+/YF}$ female mice which had mated with *Spo11*$^{+/YF}$ males were irradiated at embryonic day 15.5 (E15.5), when most oocytes are in leptotene (Crone et al, 1965; McClellan et al, 2003). These pregnant females were sacrificed to prepare spread oocyte nuclei from female embryos, 24 (E16.5) and 48 (E17.5) hours later, when the majority of oocytes that were at leptotene at the time of irradiation has reached late zygotene and pachytene, respectively (Figure 3A). We counted the number of RAD51 foci in spermatocytes (Fig 3B-E) and in oocytes (Figure 3F-I) at the above-mentioned timepoints following irradiation (Table II), selecting nuclei of the appropriate stage, based on synapsis extent as described in the Materials and Methods section. In adult *Spo11*$^{YF/YF}$ mice, the population of meiotic cells will include different stages, thus also zygotene and pachytene-like spermatocytes will be hit at the moment of irradiation. However, these cells will have progressed to different stages than those that we analysed, or be eliminated by apoptosis, and are therefore not represented in this analysis.

To measure the degree of repair of radiation-induced breaks, we subtracted the number of foci in non-irradiated cells from those observed in irradiated cells of the same stage and genotype. We assumed that the irradiation treatment did not affect the total number of SPO11-induced breaks that was reached in the *Spo11*$^{+/YF}$ leptotenes of which we followed the fate. Thus we ascribed the higher number of foci in irradiated nuclei, compared to non-irradiated control, to persistence of ra-

Table II - Time-course of RAD51 foci in control and irradiated *Spo11*$^{+/YF}$ and *Spo11*$^{YF/YF}$ meiocytes (averages ± standard deviation; n=60)

			Spo11$^{+/YF}$ (%)*	*Spo11*$^{YF/YF}$ (%)*
spermatocytes	zygotene	control	151 ± 26**	6 ± 4**
		48h	162 ± 27 (13.1%)	63 ± 14$^{\#\#}$ (39.6%)
	mid-pachytene (-like)	control	40 ± 19**	6 ± 4
		120h	41 ± 19 (1.2%)	47 ± 12$^{\#\#}$ (28.5%)
oocytes	E16.5	control	129 ± 35**	5 ± 4
		24h	156 ± 45$^{\#}$ (32.1%)	94 ± 16$^{\#\#}$ (61.8%)
	E17.5	control	41 ± 23**	43 ± 45
		48h	59 ± 24$^{\#}$ (21.4%)	112 ± 24$^{\#\#}$ (47.9%)

*control was not irradiated

**data from (Carofiglio et al, 2013)

#,## Significantly different from non-irradiated control of the same genotype (# p≤0.05; ## p<0.001, Mann–Whitney)

diation-induced DSBs up to the analysed stage. Interestingly, the absolute number of foci did not significantly differ between irradiated and non-irradiated *Spo11*$^{+/YF}$ spermatocytes at both indicated timepoints after irradiation, meaning that cells were able to process exogenous DSBs quite rapidly (Table II). This was not the case for irradiated *Spo11*$^{YF/YF}$ spermatocytes, which had much more abundant foci than non-irradiated matched controls. (Table II). We calculated the percentage of radiation-induced DSBs that persisted at the analysed stages by dividing the average number of residual radiation-induced breaks at zygotene or pachytene (or pachytene-like) stages in each genotype by the average number of radiation-induced repair foci in leptotene shortly after irradiation (84 for *Spo11*$^{+/YF}$ and 144 for *Spo11*$^{YF/YF}$, see above), and multiplied this by 100%. Using this calculation, it is easier to compare the repair efficiency between *Spo11*$^{+/YF}$ and *Spo11*$^{YF/YF}$ meiocytes. Indeed we observed that approximately 40% of the DSBs induced in leptotene persisted in zygotene and pachytene-like *Spo11*$^{YF/YF}$ spermatocytes, whereas the percentage was

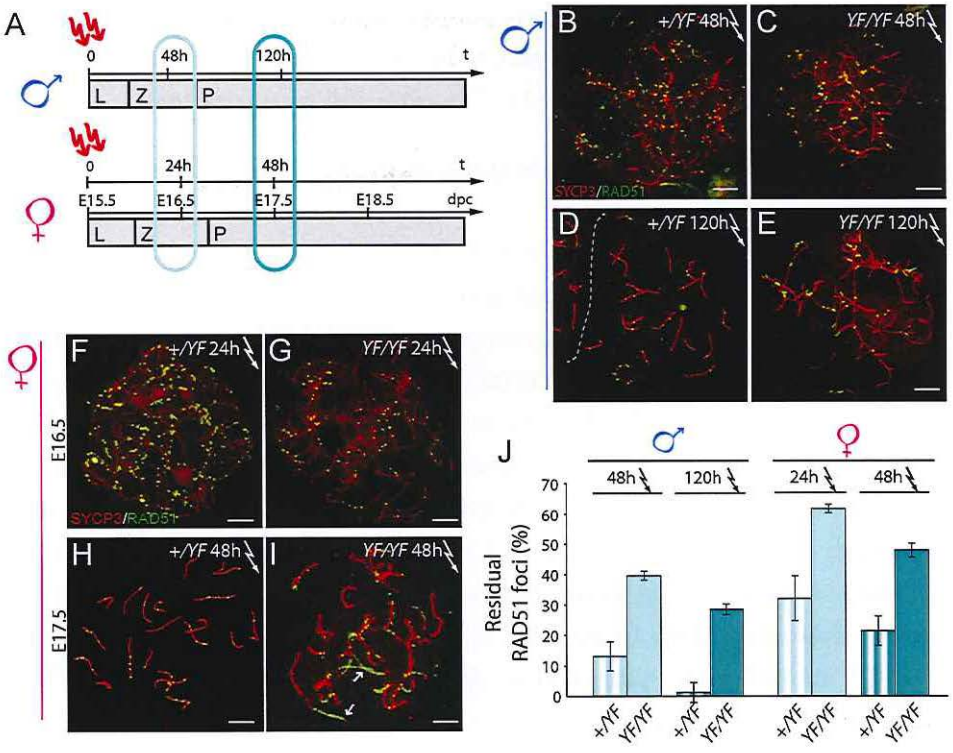

Figure 3: Repair dynamics of radiation-induced DSBs in *Spo11*$^{+/YF}$ and *Spo11*$^{YF/YF}$ spermatocytes and oocytes

(A) The number of RAD51 foci was counted in control and irradiated *Spo11*$^{+/YF}$ and *Spo11*$^{YF/YF}$ zygotene spermatocyte and oocyte nuclei. A timeline of male and female meiotic prophase in mouse is shown to indicate the correspondence between each analyzed timepoint and the meiotic substage, both in spermatocytes (Oakberg, 1956) and in oocytes (Crone et al, 1965; McClellan et al, 2003). **(B-I)** Irradiated spermatocytes **(B-E)** and oocytes **(F-I)** from *Spo11*$^{+/YF}$ **(B, D, F, H)** and *Spo11*$^{YF/YF}$ **(C, E, G, I)** mice, immunostained for RAD51 (green) and SYCP3 (red). Size bars represent 10 μm. **(B-E)** Spermatocytes were collected 48 **(B-C)** and 120 **(D-E)** hours after irradiation, to analyze late zygotene and pachytene-like stages, respectively. **(F-I)** Oocytes were collected 24h (E16.5) **(F-G)** and 48 (E17.5) **(H-I)** hours post irradiation, to analyze late zygotene and pachytene-like stages, respectively. **(J)** Bar graph showing the percentage of residual radiation-induced RAD51 foci detected at the noted time-points in irradiated spermatocytes and oocytes from *Spo11*$^{+/YF}$ (striped bars) and *Spo11*$^{YF/YF}$ (solid bars) mice. Error bars indicate SEM for 40 nuclei from 2 mice.

reduced from 13.1 to 1.2 when irradiated *Spo11*$^{+/YF}$ spermatocytes had progressed from leptotene to zygotene or pachytene, respectively (Figure 3C, J; Table II). Similar results were obtained for oocytes at both the analysed timepoints, albeit a higher percentage of residual foci was present in oocytes compared to spermatocytes for

all corresponding genotypes and time points (Figure 3F-J; Table II). Thus, both in *Spo11*$^{YF/YF}$ oocytes and spermatocytes, radiation-induced DSBs are repaired with reduced efficiency compared to *Spo11*$^{+/YF}$ oocytes and spermatocytes.

Radiation-induced DSBs stimulate synapsis in *Spo11*$^{YF/YF}$ spermatocytes and oocytes

To evaluate the effect of radiation-induced DSBs on synapsis, we analysed SC formation using antibodies directed against the axial/lateral element component SYCP3 and the transverse filament component SYCP1 (Meuwissen et al, 1992). In non-irradiated *Spo11*$^{YF/YF}$ spermatocytes and E16.5 oocytes, the degree of synapsis is variable, with some nuclei showing no synapsis, whereas others showed diverse degrees of heterologous, rather than homologous, synapsis (Figure 4A, C, E). Occasionally, in spermatocytes, complete synapsis between one or two chromosomes appears to occur (Figure 4A, arrows). On average, the degree of synapsis is more extensive in *Spo11*$^{YF/YF}$ zygotene spermatocytes compared to *Spo11*$^{YF/YF}$ zygotene oocytes isolated at E16.5 (Figure 4A, C, E). However, *Spo11*$^{YF/YF}$ oocytes isolated at E17.5 showed more synapsis than *Spo11*$^{YF/YF}$ zygotene spermatocytes (Figure 4C, G). Subsequently, we measured the total length of synapsed SC (SYCP1 positive) per nucleus in spermatocytes and oocytes after irradiation. Both in *Spo11*$^{YF/YF}$ spermatocytes and oocytes, the degree of synapsis was increased upon irradiation. In spermatocytes, the SC length was increased 1.5-fold and 2.3-fold compared to non-irradiated controls, at 48h and 120h after irradiation, respectively (Figure 4A-D, I). In oocytes, the SC length was increased approximately two-fold compared to non-irradiated oocytes at 24h after irradiation (Figure 4E-F, I). At E17.5, the extensive heterologous synapsis in non-irradiated *Spo11*$^{YF/YF}$ oocytes obscured most of the effect of the irradiation (Figure 4G-H, I). However, the number of completely synapsed axes (not entangled) was higher in irradiated compared to non-irradiated *Spo11*$^{YF/YF}$ oocytes at 48h after irradiation (Figure 4G-H, arrows, and Figure 4J).

Radiation-induced DSBs stimulate homologous chromosome interactions in *Spo11*$^{YF/YF}$ meiocytes

To assess whether the observed increased synapsis in irradiated *Spo11*$^{YF/YF}$ meiocytes included increased interactions between homologous chromosomes, we performed FISH experiments using BAC probes for chromosomes 1 and 8 in irradi-

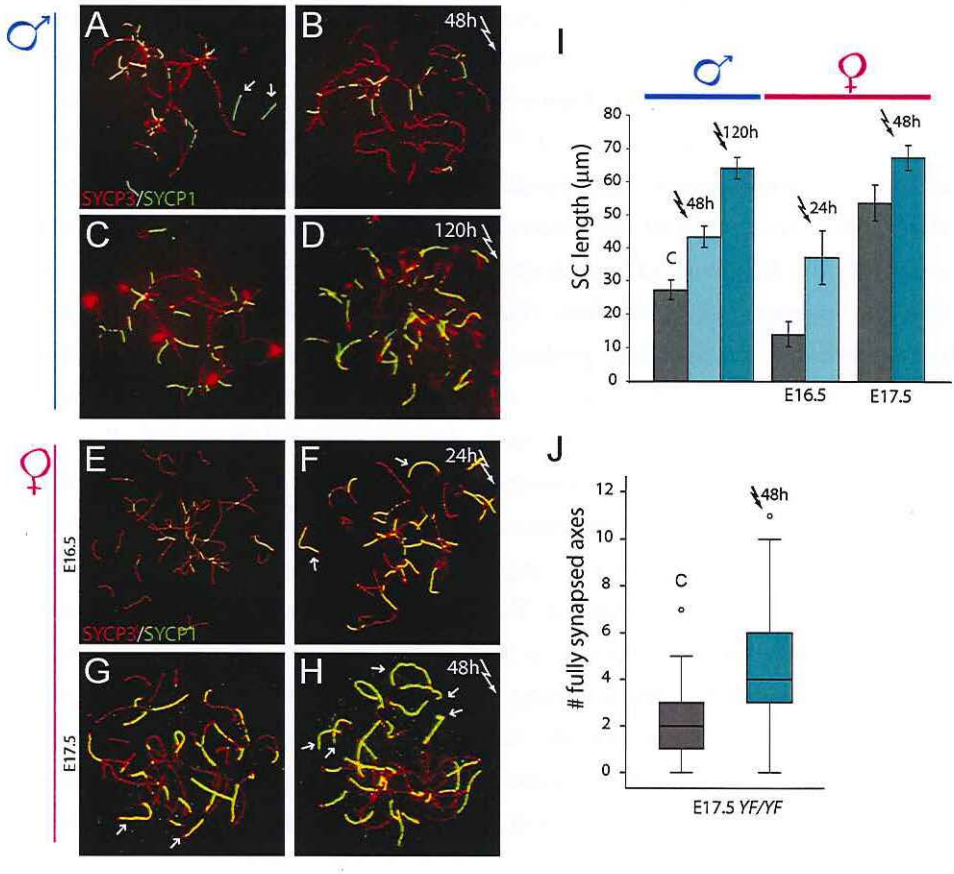

Figure 4: Radiation-induced DSBs stimulate synapsis in *Spo11*$^{YF/YF}$ spermatocytes and oocytes
(A-H) Spread zygotene-like spermatocyte **(A-D)** and oocyte **(E-H)** nuclei of *Spo11*$^{YF/YF}$ mice, either non-irradiated **(A, C, E, G)**, or exposed to 5 Gy irradiation **(B, D, F, H)**. Spermatocytes were fixed at 48h **(B)** or 120h **(D)**, and oocytes at 24h **(F)** or 48h **(H)** following irradiation. Synapsis was analyzed via double-immunostaining for SYCP1 (green) and SYCP3 (red). Arrows indicate fully synapsed axes. Scale bars represent 10 µm. **(I)** The total SC length (measured via SYCP1-signal analysis) in zygotene-like nuclei of *Spo11*$^{YF/YF}$ mice irradiated as described above was measured. Error bars indicate SEM for 40 nuclei from 2 mice. C = non-irradiated controls. **(J)** The number of fully synapsed (not entangled) axes was counted in E17.5 *Spo11*$^{YF/YF}$ control (grey plot) and irradiated (turquoise plot) oocytes. P ≤0.0001.

ated and non-irradiated *Spo11*$^{YF/YF}$ spermatocytes and oocytes (Figure 5A-D). We measured the distance between homologous (1-1, 8-8) and heterologous probes (1-8) (schematically shown in Figure 5A'-D'). Based on the average distance between homologous probes in *Spo11*$^{+/YF}$ pachytene spermatocytes and oocytes, we defined a threshold length (see Materials and Methods for extensive explanation) below which we considered the chromosomes to be paired, and used this threshold to quantify the frequency of homologous chromosome interactions. We also quantified the frequency of interactions that are defined as non-specific, based on the distance between heterologous probes. It is important to note that this frequency was considerable (around 10 %) even in *Spo11*$^{+/YF}$ pachytene nuclei that we analysed as positive controls (Figure 5E-F). This is due to the fact that, even if all homologous chromosomes are properly synapsed, chromosomes 1 and 8 may be in close proximity. However, non-specific interactions are expected to occur more often in a random mixture of chromosomes compared to a situation in which all homologous chromosomes are properly arranged. Therefore, for each genotype we compared the frequency of non-specific interactions to the frequency of specific interactions.

In *Spo11*$^{YF/YF}$ spermatocytes, homologous pairing frequency was significantly higher than the frequency of nonspecific interactions (two-fold increase) only at 120h following irradiation ($p<0.001$, Figure 5E). This was mainly due to the markedly reduced level of non-specific pairing at this timepoint, compared to non-irradiated matched controls ($p<0.001$), and indicates that specific interactions indeed exist in *Spo11*$^{YF/YF}$ pachytene-like spermatocyte nuclei 120h after irradiation.

In *Spo11*$^{YF/YF}$ spread oocyte nuclei, non-specific interactions between chromosomes 1 and 8 were overall less frequent than in spermatocytes. Indeed, the homologous pairing frequency of chromosome 1 significantly exceeded the non-homologous 1-8 pairing frequency, already at 24h after irradiation ($p<0.001$, Figure 5F). Improved homologous pairing of chromosomes 1 and 8 at the pachytene-like timepoint ($p<0.001$) was also more evident in irradiated *Spo11*$^{YF/YF}$ oocytes, compared to irradiated *Spo11*$^{YF/YF}$ spermatocytes (Figure 5F). Furthermore, the pairing frequency of approximately 8-12% above the background that was observed in irradiated *Spo11*$^{YF/YF}$ oocytes at E17.5 corresponds well with the 10% increase in complete synapsis frequency in this oocyte population (2 versus 4 fully synapsed chromosomes out of 20 chromosome pairs in control versus irradiated oocytes at E17.5) (Figure 4).

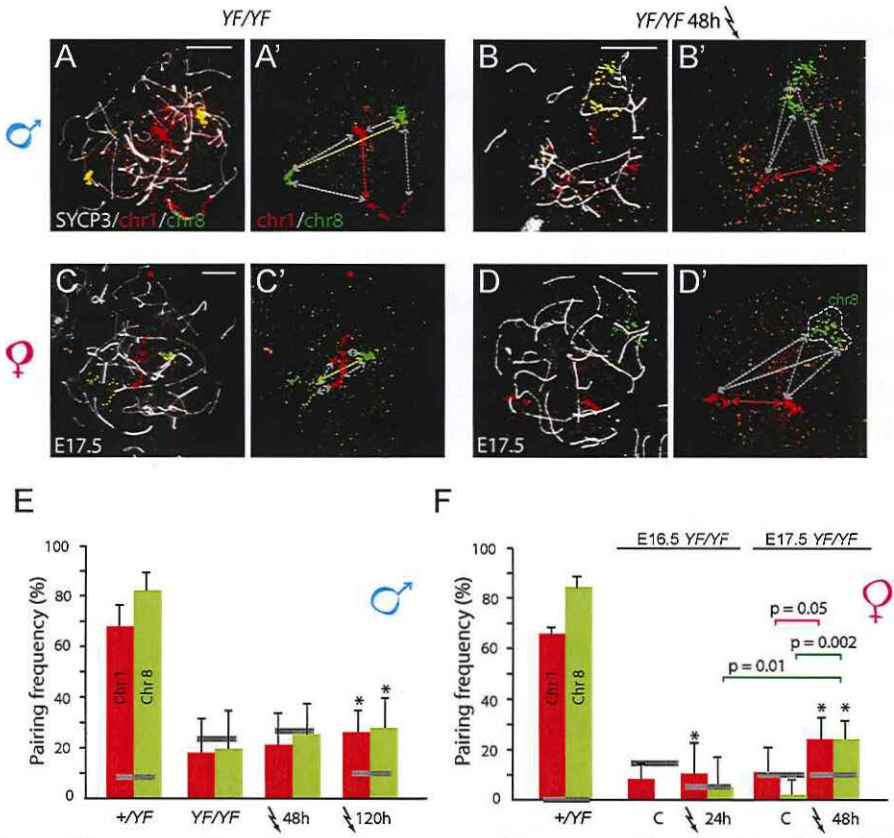

Figure 5: Frequency of homologous chromosome pairing in control and irradiated *Spo11*$^{YF/YF}$ spermatocytes and oocytes

(A-D) *Spo11*$^{YF/YF}$ control (*YF/YF*) and irradiated (*YF/YF* 48h) spermatocytes **(A, B)** and oocytes **(C, D)** were immunostained with anti-SYCP3 (white) and subjected to FISH using BAC probes for chromosomes 1 (red) and 8 (green). The FISH signals for chromosomes 1 and 8 are shown separately in **(A'-D')**. Arrows draw the minimum distance between homologous probes for chromosomes 1 (red) and 8 (green) and heterologous probes (grey, all combinations). In D' both probe signals for chromosome 8 formed a single domain inside the nucleus marked by the dashed white line. Scale bars represent 10 μm. **(E-F)** Frequency of paired probe signals in *Spo11*$^{YF/YF}$ control and irradiated spermatocytes **(E)** and oocytes **(F)** (n=80). Red and green bars represent homologous pairing frequency for chromosomes 1 and 8 respectively. Grey lines represent the frequency of heterologous pairing. Statistically significant differences between homologous pairing frequencies are marked on the plots (Mann-Whitney). Error bars indicate standard deviations calculated for the frequency datasets of the two animals used for each measurement. Asterisk indicates a significant difference between the frequency of specific and nonspecific frequencies (P values are described in the main text).

Discussion

Radiation-induced DSBs are tethered to the axial elements shortly after induction

A recent study conducted in yeast indicates that SPO11-induced breaks are most likely formed on the axes through an interaction with the DSB machinery components Mer2/Rec114/Mei4 (Panizza et al, 2011). In mouse, the Mei4 ortholog MEI4 is required for SPO11-mediated induction of DSBs, and has also been localized on axes before and at the time of DSB formation (Kumar et al, 2010). Interestingly, the present immunocytochemical analysis of RPA, RAD51, and DMC1 foci shortly after irradiation, shows that radiation-induced DSBs are rapidly recruited to the axes in leptotene, coherent with our previous observations in irradiated wild type pachytene spermatocytes (Inagaki et al, 2011). It is thus possible that a specific mechanism is responsible for recognizing radiation-induced DSBs and tethering them to the chromosome axis. Tethering the damaged site to the axial elements appears to occur rapidly and may be a prerequisite for proper loading of repair proteins, since we do not observe damage-induced RPA, RAD51, and DMC1 foci that are not associated with the axial elements.

Kinetics of repair protein recruitment to radiation-induced breaks differ between *Spo11*$^{+/YF}$ and *Spo11*$^{YF/YF}$ spermatocytes

In somatic cells, irradiation has been reported to induce approximately 35 DSBs/Gy in G1 cells *in vitro*, with some variation in the extent of damage depending on oxygen level and DNA compaction (Barnard et al, 2013; Cowell et al, 2007; Warters and Lyons, 1992). In our model, we compared accumulation of recombinases at damage-induced DSBs between *Spo11*$^{+/YF}$ and *Spo11*$^{YF/YF}$ leptotene spermatocytes. At this stage of meiosis, there are no gross differences between the two genotypes in the chromatin structure in the nuclei, and the mice have similar sizes. Thus, we suggest that irradiation induces a comparable level of damage in leptotene nuclei of the *Spo11*$^{+/YF}$ and *Spo11*$^{YF/YF}$ genotypes. This is also reflected by the fact that the average number of damage-induced RPA foci is similar in both genotypes. However, on a *Spo11*$^{+/YF}$ background, radiation-induced recombinase foci appeared in lower numbers, compared to the *Spo11*$^{YF/YF}$ background. In irradiated *Spo11*$^{+/YF}$ spermatocytes, part of the pool of DSB repair proteins is engaged in repair of SPO11-induced breaks, and the amount of one or more of the components of the whole machin-

ery may become limiting. The dynamics of recombinase recruitment to DSBs may therefore be delayed in irradiated versus non-irradiated *Spo11*$^{+/YF}$ spermatocytes. Indeed, the accumulation of repair proteins occurred with slower kinetics in *Spo11*$^{+/YF}$ compared to *Spo11*$^{YF/YF}$ leptotene spermatocytes.

Delayed repair of radiation-induced DSBs in a SPO11-deficient background may reflect the interhomolog bias mechanism in mouse meiosis

RAD51 foci disappearance over time indicates that HR progresses to a stage where recombinases are no longer needed and DSBs have been repaired. Here we used the analysis of RAD51 foci at different timepoints after irradiation as a proxy for progression of damage-induced DSB repair. The use of damage-induced DSBs to study repair dynamics in meiotic cells has two major advantages. First, the same amount of damage is inflicted, at a fixed timepoint, whether SPO11 protein is present or not. Second, SPO11 protein is absent from the sites of damage-induced DSB formation on both backgrounds. This means that, even if SPO11 protein played plays a role in meiotic recombination events downstream of DSB induction, radiation-induced DSBs would be as capable of recruiting DSB repair factors in either the *Spo11*$^{+/YF}$ or *Spo11*$^{YF/YF}$ background. However, we observed that the dynamics of radiation-induced RAD51 foci disappearance over time clearly differed between *Spo11*$^{+/YF}$ and *Spo11*$^{YF/YF}$ meiocytes, in particular at the late timepoints following irradiation. Indeed, we do not observe significant differences in the numbers of DSBs between irradiated and non-irradiated *Spo11*$^{+/YF}$ zygotene and pachytene meiocytes, indicating that (almost) all radiation-induced DSBs have been repaired. In contrast, a large significant difference between irradiated and non-irradiated nuclei is observed for zygotene and pachytene-like *Spo11*$^{YF/YF}$ meiocytes that were irradiated at leptotene, indicating that many radiation-induced DSBs persisted. These conclusions are built on the assumption that the total number of SPO11-induced DSBs is not significantly altered between irradiated and non-irradiated leptotene nuclei as they proceed to zygotene. This is supported by published data which indicate that negative feedback from increased ATM activation, which is expected when SPO11 is overexpressed, still allows for an increase of approximately 100 endogenous DSBs (Cole et al, 2012). The present analysis of γH2AX accumulation upon irradiation indicates that the degree of ATM activation in our model is even lower than what has been reported for the SPO11-overexpression model (Cole

et al, 2012). In addition, the ATM-induced feedback on SPO11 is thought to act locally, perhaps by phosphorylating nearby SPO11-containing complexes (Lange et al, 2011). ATM activation at damage-induced DSBs may not occur in close enough proximity to SPO11-complexes to efficiently mediate downregulation of their activity. Finally, our previous analyses of the processing of radiation-induced breaks showed that midpachytene cells that were irradiated in leptotene did not display evidence of remaining radiation-induced breaks, whereas cells that were irradiated at early pachytene and reached diplotene at 120h after damage induction did show persistent γH2AX domains that were not observed in non-irradiated cells (Schoenmakers et al., 2008). In the current irradiation experiment we also observed no difference in the γH2AX staining pattern between irradiated and non-irradiated *Spo11*$^{+/YF}$ pachytene nuclei at the 120h time-point, whereas remaining damage was observed in diplotene nuclei (not shown). These previous and current observations also indicate that there is complete repair of DSBs that were induced by irradiation at leptotene on the *Spo11*$^{+/YF}$ background.

When subjected to γ-radiation, somatic G2 cells can choose different DSB repair pathways (as reviewed by (Thompson, 2012)). It has been shown that HR is preferred during and after S phase, when a template to recover the missing genetic information is available (Hinz et al, 2005; Rothkamm et al, 2003). During G2 phase, exogenous DSBs are repaired within 4-5 hours, by using the sister chromatid as a DNA template which is in close proximity thanks to sister chromatid cohesion (Saha et al, 2013). Meiotic prophase nuclei have also completed S phase, and therefore the sister chromatid is available both in *Spo11*$^{+/YF}$ and in *Spo11*$^{YF/YF}$ meiocytes. Nevertheless, we found that repair of radiation-induced DSBs in *Spo11*$^{YF/YF}$ meiocytes is much slower than in somatic cells, and also slower than on the *Spo11*$^{+/YF}$ background. In *Spo11*$^{YF/YF}$ meiotic cells, the DSB repair machinery is still intact. It cannot be excluded that SPO11 may play a specific role in recombinase loading (Neale et al, 2005). However, we do observe both recombinases together at most foci in *Spo11*$^{YF/YF}$ irradiated nuclei, strongly indicating that SPO11 is not required for assembly of the recombinase filaments. In addition, neither the wild type nor the mutant SPO11 protein will be present at radiation-induced DSB sites. Thus, we anticipate that *Spo11*$^{YF/YF}$ and *Spo11*$^{+/YF}$ meiocytes do not differ in the capability of processing radiation-induced DSBs. Still, in wild type or heterozygous nuclei, homologous synapsis is ongoing with the aid of SPO11-induced DSBs. As a conse-

quence, the homologous chromosome will more frequently be nearby and available as a repair template for the exogenous DSBs in *Spo11*$^{+/YF}$, compared to *Spo11*$^{YF/YF}$ nuclei, thus allowing more rapid repair of radiation-induced DSBs. The higher repair efficiency in *Spo11*$^{+/YF}$ spermatocytes could also indicate that progression of synapsis releases the interhomolog bias through an effect in *cis*, further contributing to rapid repair of remaining DSBs in the synapsed region via either the sister chromatid or the homolog. Taken together, these observations indicate that repair of exogenous DSBs in *Spo11*$^{YF/YF}$ meiotic cells is inefficient because the use of the sister chromatid as a template for HR is repressed, and thus provide evidence for the interhomolog bias in mouse, that can be imposed on exogenous DSBs.

Repair of exogenous DSBs stimulates chromosome synapsis and favours homologous pairing

In mouse, lack of SPO11-induced DSBs results in loss of homologous chromosome pairing and extensive heterologous synapsis (Baudat et al, 2000; Carofiglio et al, 2013; Romanienko and Camerini-Otero, 2000). Various DNA damaging agents have been used previously to induce meiotic recombination in *Spo11* mutants in different species. It was shown that cisplatin treatment, which induces DSBs, had an effect on centromeric interactions in *Spo11* knockout spermatocytes (Romanienko and Camerini-Otero, 2000). Moreover, in yeast, fungi and worms, radiation-induced DSBs can partially or completely rescue the *spo11* mutant phenotype (Thorne and Byers, 1993); (Bowring et al, 2006; Celerin et al, 2000; Dernburg et al, 1998; Storlazzi et al, 2003).

Similarly to what has been found for the species described above, the induction of DSBs via γ-radiation in *Spo11*$^{YF/YF}$ mouse meiocytes, would be expected to contribute to homologous chromosome pairing and synapsis. Indeed, we observed a clear increase in the degree of synapsis and homologous chromosome interactions upon irradiation, indicating that repair of exogenous DSBs improves synapsis, even if this repair occurs less efficiently compared to repair of endogenous DSBs.

We have obtained no evidence for homologous synapsis in non-irradiated *Spo11*$^{YF/YF}$ oocytes and spermatocytes. This finding matches with observations of Boateng et al. (2013) (Boateng et al, 2013) in *Spo11*$^{FF/FF}$ spermatocytes which also express a catalytically inactive SPO11 enzyme. In these mice, homologous chromosome premeiotic pairing is observed, but is later lost due to the absence of meiotic DSBs

that are required to achieve stable homologous chromosome interactions. Furthermore, it was recently reported that in early *Spo11*$^{-/-}$ spermatocytes, homologous chromosome pairing is also occurring to some extent, but it never reaches wild type levels, again confirming that HR-mediated repair of meiotic DSBs is important to facilitate stable homologous interactions (Ishiguro et al, 2014). In our model, the premeiotic/early meiotic DSB-independent homologous interactions should also still occur and it is possible that the induction of exogenous DSBs via irradiation contributes to the stabilization of such interactions by initiating the homologous recombination processes. Rescue of homologous chromosome pairing was far from complete, and we suggest that this may be caused by the fact that irradiation may induce DSBs relatively frequently in regions of the genome that contain repetitive DNA. Homology-mediated repair at such sites may involve the homologous sequence of repetitive DNA located on a non-homologous chromosome. In this case, the homology search would still show a bias for a non-sister template, but would not guarantee interaction between homologous chromosomes.

Taken together, the data presented in this manuscript show that damage-induced DSBs are processed by the meiosis-specific HR machinery, relocate to chromosome axes, thereby undergo the interhomolog bias, and contribute to homology recognition and synapsis.

Materials and Methods

Ethics Statement

All animal experiments were approved by the local animal experiments committee DEC-Consult. All animals were housed in IVC cages under supervision of the Animal Welfare Officer. Any discomfort of animals was daily scored by the animal caretakers. No more than mild or moderate discomfort of animals was expected from the treatments, and no unexpected discomfort was observed.

Mice

Spo11 mutant mice were generated as described previously (Carofiglio et al, 2013). *Spo11*$^{YF/YF}$ males and age matched controls were irradiated with 5 Gy with Elekta linear accelerator from a ^{137}Cs source (Crawley). At 30 minutes, 1h, 48h, and 120h following irradiation, male mice were sacrificed to prepare spermatocyte nuclei spread preparations for immunocytochemical and FISH analyses. Testes were collected and spermatocytes were spread as described below. Pregnant heterozygote *Spo11*$^{+/YF}$ females were also irradiated with a dose of 5 Gy at E15.5. At the timepoints 24h and 48h after irradiation, pregnant females were sacrificed, embryos were collected, and oocytes were spread from the ovaries. Tails from each embryo were used to genotype the embryos as described (Carofiglio et al, 2013).

Meiotic spread nuclei preparations and immunocytochemistry

Testis tissues were processed to obtain spread nuclei for immunocytochemistry as described by (Peters et al, 1997). Spread nuclei of spermatocytes were stained with antibodies mentioned below. Before incubation with antibodies, slides were washed in PBS (3x10 min), and non-specific sites were blocked with 0.5% w/v BSA and 0.5% w/v milk powder in PBS. Primary antibodies were diluted in 10% w/v BSA in PBS, and incubations were overnight at room temperature in a humid chamber. Subsequently, slides were washed (3x10 min) in PBS, blocked in 10% v/v normal goat serum (Sigma) in blocking buffer (supernatant of 5% w/v milk powder in PBS centrifuged at 14,000 rpm for 10 min), and incubated with secondary antibodies in 10% normal goat serum in blocking buffer at room temperature for 2 hours. Finally, slides were washed (3x10 min) in PBS (in the dark) and embedded in Prolong Gold with or without DAPI (invitrogen). Fluorescent images were observed by using a

fluorescence microscope (Axioplan 2; Carl Zeiss) equipped with a digital camera (Coolsnap-Pro; Photometrics). Fluorescent images were taken under identical conditions for all slides, and images were analyzed using the ImageJ (Fiji) software (Rasband, W.S., ImageJ, U.S. National Institutes of Health, Bethesda, Maryland, USA [http://rsb.info.nih.gov/ij/]).

Antibodies

For primary antibodies, we used mouse monoclonal antibodies anti-phosphorylated H2AX (Upstate), anti-DMC1 (DMC1-specific) (Abcam), and anti-MLH1 (Becton and Dickinson); rabbit polyclonal antibodies anti-53BP1 (Novus Biologicals), anti-RAD51 (raised against full length hRAD51, therefore it may recognize DMC1) (Essers et al, 2002), anti-RPA (gift from dr. Peter de Boer) anti-SYCP3 and anti SYCP1 (gift from dr. C. Heyting), and anti-phosphorylated H2AX (Upstate); rat polyclonal anti-SYCP3 (Baarends et al, 2007); guinea pig anti-SYCP2 (gift from dr. P. J. Wang (Yang et al, 2006)). For secondary antibodies, we used a goat anti-rabbit IgG Alexa 405/488/546/633, goat anti-mouse Alexa IgG 350/488/546/633, goat anti-rat IgG Alexa 546, goat anti-guinea pig Alexa 405 (Molecular Probes).

Selection criteria for staging mutant meiocytes

To quantify the amount of induced DSBs shortly after irradiation, repair protein foci were counted in leptotene nuclei. We only included leptotene nuclei that had short patches of synaptonemal complex already formed (1-3 μm length), which is the same stage analysed for quantification of the endogenous SPO11-dependent protein foci in heterozygous controls.

For the time-course analysis of recombination foci upon irradiation, *Spo11*$^{YF/YF}$ nuclei were selected based on the extent of synapsed areas, in order to consistently select similar meiotic stages at the analysed timepoints. Spermatocytes with a total synapsis length below 21 μm (average length of 13 μm) were selected to count foci 48h after irradiation (early zygotene) and with a total synapsis length above 21 μm (average 24 μm) to count foci 120h after irradiation (mid-pachytene).

With the same threshold as for the 48h timepoint in spermatocytes, we selected zygotene-like *Spo11*$^{YF/YF}$ irradiated oocytes at E16.5 (average synapsis length 14 μm), and oocytes with synapsis extending over at least 22 μm at E17.5 (average 42

μm), to select cells that would have progressed to mid-pachytene.

To measure the increase of synapsis extent upon irradiation, we included in the quantitative analysis the nuclei that showed extensive synapsis at the visual inspection, both for non-irradiated and for irradiated *Spo11*$^{YF/YF}$ meiocytes.

The same class of nuclei that were analysed for synapsis extent was used for quantification of homologous pairing frequency. First, synapsis was assessed by SYCP1/SYCP3 immunostaining, and positions of the selected nuclei in the specimen were recorded. Subsequently, FISH was performed and FISH signals distances (see below) were measured in the previously selected nuclei.

Quantification of protein foci and γH2AX intensity

Imaging of immunostained nuclei (RPA, RAD51, DMC1, SYCP1, SYCP3, γH2AX) was performed with the same exposure time for each nucleus. Foci were subsequently counted using Image J software, including the Fiji plugin. We used the analyze particles function and set the threshold manually, in order to include the smallest visible focus in the analysis. The average area of one focus was assessed to be 40-50 pixels, so that foci with an area larger than 100 pixels were counted as multiple foci to allow approximate quantification of foci also when they were not resolved in the analysed image. Intensity of γH2AX was assessed selecting the nuclear area of leptotene cells based on DAPI staining. Using the measure function of ImageJ, the mean intensity (arbitrary units) of γH2AX per pixel area was quantified.

FISH analyses

BAC probes were used both for chromosome 1 (RP23-82C21) and chromosome 8 (CH26-18P14). BACs were labelled with biotin (Biotin-Nick Translation Kit, Roche) and digoxigenin (DIG-Nick Translation Kit, Roche) respectively. After alcohol precipitation in the presence of mouse Cot-1 DNA and salmon sperm DNA, the labeled DNA was resuspended in formamide. An amount of 1 μg per probe was used to perform FISH as described by Mahadevaiah et al. (2009) (Mahadevaiah et al, 2009) on slides that were first immunostained with SYCP1/SYCP3 (see above). Detection of the digoxigenin-labelled probe was performed with a primary antibody sheep anti-DIG (Roche diagnosics) and a secondary rabbit anti-sheep-FITC (Jackson labs). Detection of the biotin-labelled probe was performed with a primary antibody mouse anti-BIO (Roche diagnostics) and a secondary goat anti-mouse

Alexa 633 (Molecular Probes).

FISH signals were analysed in Image J software (Fiji), measuring the minimum distance between domains belonging to homologous probes (1-1, 8-8) and heterologous probes (1-8, all combinations). Due to variation in nuclear size, the measured absolute distances were normalized to the nuclear diameter as follows: the average nuclear diameter size was established to be 40 μm, and this reference size was divided by the measured diameter of each analysed nucleus. The number obtained was used as a conversion factor for the probe distances measured for the respective nucleus.

The average distance between probe signals from homologously paired and synapsed chromosome 1 and 8 plus the standard deviation in heterozygous pachytene spermatocytes and oocytes was used as threshold to discriminate between paired and unpaired chromosomes. For spermatocytes, the threshold was set at 3.38 μm, whereas for oocytes, we used a threshold distance of 2.45 μm.

Acknowledgements:

We thank Dr. Bernard de Massy (CNRS, Montpellier, France) for critical reading of the manuscript.

References

Ashley T, Gaeth AP, Creemers LB, Hack AM, and de Rooij DG (2004). Correlation of meiotic events in testis sections and microspreads of mouse spermatocytes relative to the mid-pachytene checkpoint. Chromosoma *113*:126-136.

Ashley T, Plug AW, Xu J, Solari AJ, Reddy G, Golub EI, and Ward DC (1995). Dynamic changes in Rad51 distribution on chromatin during meiosis in male and female vertebrates. Chromosoma *104*:19-28.

Baarends WM, Wassenaar E, Hoogerbrugge JW, Schoenmakers S, Sun ZW, and Grootegoed JA (2007). Increased phosphorylation and dimethylation of XY body histones in the Hr6b-knockout mouse is associated with derepression of the X chromosome. J Cell Sci *120*:1841-1851.

Barnard S, Bouffler S, and Rothkamm K (2013). The shape of the radiation dose response for DNA double-strand break induction and repair. Genome Integr *4*:1.

Baudat F, Manova K, Yuen JP, Jasin M, and Keeney S (2000). Chromosome synapsis defects and sexually dimorphic meiotic progression in mice lacking spo11. Mol Cell *6*:989-998.

Bennardo N, Cheng A, Huang N, and Stark JM (2008). Alternative-NHEJ is a mechanistically distinct pathway of mammalian chromosome break repair. PLoS Genet *4*:e1000110.

Boateng KA, Bellani MA, Gregoretti IV, Pratto F, and Camerini-Otero RD (2013). Homologous Pairing Preceding SPO11-Mediated Double-Strand Breaks in Mice. Dev Cell *24*:196-205.

Bowring FJ, Yeadon PJ, Stainer RG, and Catcheside DE (2006). Chromosome pairing and meiotic recombination in Neurospora crassa spo11 mutants. Curr Genet *50*:115-123.

Carofiglio F, Inagaki A, de Vries S, Wassenaar E, Schoenmakers S, Vermeulen C, van Cappellen WA, Sleddens-Linkels E, Grootegoed JA, Te Riele HP, *et al.* (2013). SPO11-independent DNA repair foci and their role in meiotic silencing. PLoS Genet *9*:e1003538.

Celerin M, Merino ST, Stone JE, Menzie AM, and Zolan ME (2000). Multiple roles of Spo11 in meiotic chromosome behavior. Embo J *19*:2739-2750.

Cloud V, Chan YL, Grubb J, Budke B, and Bishop DK (2012). Rad51 is an accessory factor for Dmc1-mediated joint molecule formation during meiosis. Science *337*:1222-1225.

Cole F, Kauppi L, Lange J, Roig I, Wang R, Keeney S, and Jasin M (2012). Homeostatic control of recombination is implemented progressively in mouse meiosis. Nat Cell Biol *14*:424-430.

Costa Y, Speed R, Ollinger R, Alsheimer M, Semple CA, Gautier P, Maratou K, Novak I, Hoog C, Benavente R, *et al.* (2005). Two novel proteins recruited by synaptonemal complex protein 1 (SYCP1) are at the centre of meiosis. J Cell Sci *118*:2755-2762.

Cowell IG, Sunter NJ, Singh PB, Austin CA, Durkacz BW, and Tilby MJ (2007). gammaH2AX foci form preferentially in euchromatin after ionising-radiation. PLoS One *2*:e1057.

Crone M, Levy E, and Peters H (1965). The duration of the premeiotic DNA synthesis in mouse oocytes. Exp Cell Res *39*:678-688.

Dernburg AF, McDonald K, Moulder G, Barstead R, Dresser M, and Villeneuve AM (1998). Meiotic recombination in C. elegans initiates by a conserved mechanism and is dispensable for homologous chromosome synapsis. Cell *94*:387-398.

Eijpe M, Heyting C, Gross B, and Jessberger R (2000). Association of mammalian SMC1 and SMC3 proteins with meiotic chromosomes and synaptonemal complexes. J Cell Sci *113*:673-682.

Eijpe M, Offenberg H, Jessberger R, Revenkova E, and Heyting C (2003). Meiotic cohesin REC8 marks the axial elements of rat synaptonemal complexes before cohesins SMC1beta and SMC3. J Cell Biol *160*:657-670.

Essers J, Hendriks RW, Wesoly J, Beerens CE, Smit B, Hoeijmakers JH, Wyman C, Dronkert ML, and Kanaar R (2002). Analysis of mouse Rad54 expression and its implications for homologous recombination. DNA Repair (Amst) *1*:779-793.

Goedecke W, Eijpe M, Offenberg HH, van Aalderen M, and Heyting C (1999). Mre11 and Ku70 interact in somatic cells, but are differentially expressed in early meiosis. Nat Genet *23*:194-198.

Hamer G, Gell K, Kouznetsova A, Novak I, Benavente R, and Hoog C (2006). Characterization of a novel meiosis-specific protein within the central element of the synaptonemal complex. J Cell Sci *119*:4025-4032.

Heyer WD, Rao MR, Erdile LF, Kelly TJ, and Kolodner RD (1990). An essential Saccharomyces cerevisiae single-stranded DNA binding protein is homologous to the large subunit of human RP-A. EMBO J *9*:2321-2329.

Hinz JM, Yamada NA, Salazar EP, Tebbs RS, and Thompson LH (2005). Influence of double-strand-break repair pathways on radiosensitivity throughout the cell cycle in CHO cells. DNA Repair (Amst) *4*:782-792.

Hong S, Sung Y, Yu M, Lee M, Kleckner N, and Kim KP (2013). The logic and mechanism of homologous recombination partner choice. Mol Cell *51*:440-453.

Inagaki A, Schoenmakers S, and Baarends WM (2010). DNA double strand break repair, chromosome synapsis and transcriptional silencing in meiosis. Epigenetics *5*:255-266.

Inagaki A, Sleddens-Linkels E, Wassenaar E, Ooms M, van Cappellen WA, Hoeijmakers JH, Seibler J, Vogt TF, Shin MK, Grootegoed JA, *et al.* (2011). Meiotic functions of RAD18. J Cell Sci *124*:2837-2850.

Ishiguro K, Kim J, Fujiyama-Nakamura S, Kato S, and Watanabe Y (2011). A new meiosis-specific cohesin complex implicated in the cohesin code for homologous pairing. EMBO Rep *12*:267-275.

Ishiguro K, Kim J, Shibuya H, Hernandez-Hernandez A, Suzuki A, Fukagawa T, Shioi G, Kiyonari H, Li XC, Schimenti J, *et al.* (2014). Meiosis-specific cohesin mediates homolog recognition in mouse spermatocytes. Genes Dev *28*:594-607.

Kauppi L, Barchi M, Lange J, Baudat F, Jasin M, and Keeney S (2013). Numerical constraints and feedback control of double-strand breaks in mouse meiosis. Genes Dev *27*:873-886.

Kumar R, Bourbon HM, and de Massy B (2010). Functional conservation of Mei4 for meiotic DNA double-strand break formation from yeasts to mice. Genes Dev *24*:1266-1280.

Lange J, Pan J, Cole F, Thelen MP, Jasin M, and Keeney S (2011). ATM controls meiotic double-strand-break formation. Nature *479*:237-240.

Lee J, and Hirano T (2011). RAD21L, a novel cohesin subunit implicated in linking homologous chromosomes in mammalian meiosis. J Cell Biol *192*:263-276.

Lim DS, and Hasty P (1996). A mutation in mouse rad51 results in an early embryonic lethal that is suppressed by a mutation in p53. Mol Cell Biol *16*:7133-7143.

Mahadevaiah SK, Costa Y, and Turner

JM (2009). Using RNA FISH to study gene expression during mammalian meiosis. Methods Mol Biol *558*:433-444.

Mahadevaiah SK, Turner JM, Baudat F, Rogakou EP, de Boer P, Blanco-Rodriguez J, Jasin M, Keeney S, Bonner WM, and Burgoyne PS (2001). Recombinational DNA double-strand breaks in mice precede synapsis. Nat Genet *27*:271-276.

McClellan KA, Gosden R, and Taketo T (2003). Continuous loss of oocytes throughout meiotic prophase in the normal mouse ovary. Dev Biol *258*:334-348.

Meuwissen RL, Offenberg HH, Dietrich AJ, Riesewijk A, van Iersel M, and Heyting C (1992). A coiled-coil related protein specific for synapsed regions of meiotic prophase chromosomes. Embo J *11*:5091-5100.

Moens PB, Chen DJ, Shen Z, Kolas N, Tarsounas M, and Heng HHQ (1997). Rad51 immunocytology in rat and mouse spermatocytes and oocytes. Chromosoma *106*:207-215.

Neale MJ, Pan J, and Keeney S (2005). Endonucleolytic processing of covalent protein-linked DNA double-strand breaks. Nature *436*:1053-1057.

Oakberg EF (1956). Duration of spermatogenesis in the mouse and timing of stages of the cycle of the seminiferous epithelium. Am J Anat *99*:507-516.

Oakberg EF, and Diminno RL (1960). X-ray sensitivity of primary spermatocytes of the mouse.int. International journal of radiation biology *2*:196-209.

Offenberg HH, Schalk JA, Meuwissen RL, van Aalderen M, Kester HA, Dietrich AJ, and Heyting C (1998). SCP2: a major protein component of the axial elements of synaptonemal complexes of the rat. Nucleic Acids Res *26*:2572-2579.

Panizza S, Mendoza MA, Berlinger M, Huang L, Nicolas A, Shirahige K, and Klein F (2011). Spo11-accessory proteins link double-strand break sites to the chromosome axis in early meiotic recombination. Cell *146*:372-383.

Peters AH, Plug AW, van Vugt MJ, and de Boer P (1997). A drying-down technique for the spreading of mammalian meiocytes from the male and female germline. Chromosome Res *5*:66-68.

Pittman DL, Cobb J, Schimenti KJ, Wilson LA, Cooper DM, Brignull E, Handel MA, and Schimenti JC (1998). Meiotic prophase arrest with failure of chromosome synapsis in mice deficient for Dmc1, a germline-specific RecA homolog. Mol Cell *1*:697-705.

Plug AW, Peters AH, Keegan KS, Hoekstra MF, de Boer P, and Ashley T (1998). Changes in protein composition of meiotic nodules during mammalian meiosis. J Cell Sci *111*:413-423.

Plug AW, Xu J, Reddy G, Golub EI, and Ashley T (1996). Presynaptic association of Rad51 protein with selected sites in meiotic chromatin. Proc Natl Acad Sci USA *11*:5920-5924.

Rogakou EP, Pilch DR, Orr AH, Ivanova VS, and Bonner WM (1998). DNA double-stranded breaks induce histone H2AX phosphorylation on serine 139. J Biol Chem *273*:5858-5868.

Romanienko PJ, and Camerini-Otero RD (2000). The mouse spo11 gene is required for meiotic chromosome synapsis. Mol Cell *6*:975-987.

Rothkamm K, Kruger I, Thompson LH, and Lobrich M (2003). Pathways of DNA double-strand break repair during the mammalian cell cycle. Mol Cell Biol *23*:5706-5715.

Saha J, Wang M, and Cucinotta FA (2013). Investigation of switch from ATM to ATR signaling at the sites of DNA damage induced by low and high LET radiation. DNA Repair (Amst) *12*:1143-

1151.

Schalk JA, Dietrich AJ, Vink AC, Offenberg HH, van Aalderen M, and Heyting C (1998). Localization of SCP2 and SCP3 protein molecules within synaptonemal complexes of the rat. Chromosoma *107*:540-548.

Schoenmakers S, Wassenaar E, de Boer P, Laven JSE, Grootegoed JA, and Baarends WM (2008). Increased efficiency of meiotic silencing of unsynapsed chromatin in the presence of irradiation-induced extra DNA double strand breaks. Reproductive Sciences *15*:46.

Schwacha A, and Kleckner N (1997). Interhomolog bias during meiotic recombination: meiotic functions promote a highly differentiated interhomolog-only pathway. Cell *90*:1123-1135.

Stark JM, Pierce AJ, Oh J, Pastink A, and Jasin M (2004). Genetic steps of mammalian homologous repair with distinct mutagenic consequences. Mol Cell Biol *24*:9305-9316.

Storlazzi A, Tesse S, Gargano S, James F, Kleckner N, and Zickler D (2003). Meiotic double-strand breaks at the interface of chromosome movement, chromosome remodeling, and reductional division. Genes Dev *17*:2675-2687.

Tarsounas M, Morita T, Pearlman RE, and Moens PB (1999). RAD51 and DMC1 form mixed complexes associated with mouse meiotic chromosome cores and synaptonemal complexes. J Cell Biol *147*:207-220.

Thompson LH (2012). Recognition, signaling, and repair of DNA double-strand breaks produced by ionizing radiation in mammalian cells: the molecular choreography. Mutat Res *751*:158-246.

Thorne LW, and Byers B (1993). Stage-specific effects of X-irradiation on yeast meiosis. Genetics *134*:29-42.

Tsuzuki T, Fujii Y, Sakumi K, Tominaga Y, Nakao K, Sekiguchi M, Matsushiro A, Yoshimura Y, and MoritaT (1996). Targeted disruption of the Rad51 gene leads to lethality in embryonic mice. Proc Natl Acad Sci USA *93*:6236-6240.

Wang Y, Putnam CD, Kane MF, Zhang W, Edelmann L, Russell R, Carrion DV, Chin L, Kucherlapati R, Kolodner RD, *et al.* (2005). Mutation in Rpa1 results in defective DNA double-strand break repair, chromosomal instability and cancer in mice. Nat Genet *37*:750-755.

Warters RL, and Lyons BW (1992). Variation in radiation-induced formation of DNA double-strand breaks as a function of chromatin structure. Radiat Res *130*:309-318.

Wold MS, Weinberg DH, Virshup DM, Li JJ, and Kelly TJ (1989). Identification of cellular proteins required for simian virus 40 DNA replication. J Biol Chem *264*:2801-2809.

Yang F, De La Fuente R, Leu NA, Baumann C, McLaughlin KJ, and Wang PJ (2006). Mouse SYCP2 is required for synaptonemal complex assembly and chromosomal synapsis during male meiosis. J Cell Biol *173*:497-507.

Yang F, and Wang PJ (2009). The Mammalian synaptonemal complex: a scaffold and beyond. Genome Dyn *5*:69-80.

Yoshida K, Kondoh G, Matsuda Y, Habu T, Nishimune Y, and Morita T (1998). The mouse RecA-like gene Dmc1 is required for homologous chromosome synapsis during meiosis. Mol Cell *1*:707-718.

4

Dynamic changes in the localization of RAD51 and DMC1 in mouse meiosis

Work in progress

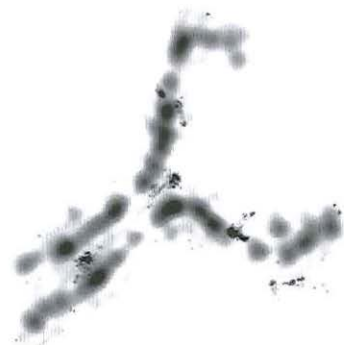

Dynamic changes in the localization of RAD51 and DMC1 in mouse meiosis

Fabrizia Carofiglio[1#], Maarten W Paul[2#], Johan A Slotman[2,3#], H Martijn de Gruiter[2], Wiggert A van Cappellen[2], J Anton Grootegoed[1], Adriaan Houtsmuller[2,3], Willy M Baarends[1*]

1Department of Reproduction and Development, Erasmus MC - University Medical Center, Rotterdam, The Netherlands

2Erasmus Optical Imaging Centre, Department of Pathology, Erasmus MC - University Medical Center, Rotterdam, The Netherlands

3Department of Pathology, Erasmus MC - University Medical Center, Rotterdam, The Netherlands

#These authors contributed equally to this work

**Author for correspondence*

Abstract

Programmed DNA double strand breaks (DSBs) are induced in meiotic prophase, and their repair by homologous recombination is essential for homologous chromosome pairing and synapsis in yeast and mouse meiosis. In meiotic cells, two recombinases are expressed: RAD51, and its meiosis-specific paralog DMC1. Genetic studies in budding yeast have indicated that both proteins are required for proper meiotic recombination. Here, we applied two different super-resolution microscopy techniques (3D-SIM and dSTORM) to investigate the dynamic relationship between RAD51 and DMC1 at DSB repair foci in mouse spermatocytes. Single molecule localization microscopy analysis of meiotic recombination foci showed that RAD51 and DMC1 each localize to distinct domains within recombination foci, and that the distribution patterns of these proteins change as meiotic prophase progresses. We identified two major configurations of recombination foci, that appeared to represent a very early intermediate, with a single cluster of both DMC1 and RAD51, and a more advanced intermediate consisting of two DMC1 clusters and a single RAD51 cluster. In *Sycp1* knockout mouse spermatocytes, that lack the transverse filament of the synaptonemal complex, both these configurations were present, but the two separate DMC1 clusters in the later intermediate were localized further apart, compared to what was observed for the wild type. Based on the present results, we propose a model in which DMC1 is loaded first on both resected ends of a DSB, followed by preferential loading of RAD51 on either one of the two ends. The DNA end that is loaded with both RAD51 and DMC1 may subsequently search for and interact with the homologous DNA template. It is discussed that the present combination of genetic models with super-resolution imaging represents a novel and highly useful approach to investigate the mechanism of homologous recombination in mouse meiosis.

Introduction

DNA double strand breaks (DSBs) are highly detrimental and hazardous lesions that can lead to genetic and chromosomal aberrations, cell cycle arrest, and eventually cell death (Schipler and Iliakis, 2013). For this reason, cells are equipped with proteins that are responsible for restoring genomic integrity. Cells can execute two main pathways of DSB repair: non-homologous end joining (NHEJ) and homologous recombination (HR) (Kass and Jasin, 2010; Shrivastav et al, 2008). The latter is an error-free repair process that uses an intact DNA molecule to recover the genetic information that may have been lost upon DSB formation (San Filippo et al, 2008). In this pathway, the DSB ends are resected, generating 3'-single-stranded DNA (ssDNA) overhangs which are first bound by the ssDNA-binding protein replication protein A (RPA) (San Filippo et al, 2008). RPA is then replaced by RAD51, an ATP-driven recombinase that forms a right-handed helical filament on the 3' overhang (presynaptic phase) (Heyer et al, 2010). When the nucleoprotein filament associates with a homologous DNA sequence, strand invasion occurs (synaptic phase), which is observed as the formation of the displacement loop (D-loop) in *in vitro* assays. In the postsynaptic phase, DNA synthesis is primed by the 3' end of the invading strand, and the genetic content of the damaged DNA molecule will be reconstituted from the homologous template. Due to the need for an intact repair template, HR is especially important during S/G2 phases, when the sister chromatid is available.

In meiotic cells, hundreds of DSBs are induced in a regulated fashion by a transesterase named SPO11 (Baudat et al, 2000; Keeney et al, 1999; Keeney et al, 1997; Romanienko and Camerini-Otero, 2000). Due to repression of NHEJ, repair of such DSBs occurs mainly via HR (Goedecke et al, 1999). Since meiotic cells have just undergone DNA replication (premeiotic S phase), three repair templates are available: one (identical) DNA sequence from the newly synthesized sister chromatid, and two DNA sequences from the homologous chromosome. When strand invasion involves the homologous chromosome, the formation of a repair intermediate brings the homologs in close proximity, and thereby contributes to homologous chromosome pairing and synapsis (Mahadevaiah et al, 2001), which are essential for proper chromosome segregation at the end of meiosis I. Synapsis is achieved by formation of the synaptonemal complex (SC) (Page and Hawley, 2004; Yang and

Wang, 2009). First, axial elements form along the basis of the chromatin loops of each chromosome (Di Carlo et al, 2000; Yang et al, 2006; Yuan et al, 2000; Yuan et al, 1998). Then the axial elements (now called lateral elements) are connected by transverse filaments and central element proteins, to achieve full synapsis (Bolcun-Filas et al, 2007; Bolcun-Filas et al, 2009; Costa et al, 2005; de Vries et al, 2005; Hamer et al, 2006; Schramm et al, 2011). DSBs persist in meiotic cells lacking any of the components of the SC (Bolcun-Filas et al, 2007; de Vries et al, 2005; Pelttari et al, 2001; Schramm et al, 2011; Yuan et al, 2002; Yuan et al, 2000), indicating that progression of DSB repair not only stimulates SC formation, but that full assembly of the SC (synapsis) is also needed to complete DSB repair. In meiotic prophase, two recombinases are known to be active: RAD51 and its meiosis-specific homolog DMC1 (Bishop, 1994; Gupta et al, 2001; Habu et al, 1996; Shinohara and Shinohara, 2004; Yoshida et al, 1998). Both proteins form right-handed nucleoprotein filaments that coat the resected ssDNA ends and can drive homology search. Accumulation of recombinases at sites of DSBs can be observed as protein foci, which generally associate with the chromosomal axes in spread meiotic nuclei (Moens et al, 1997; Tarsounas et al, 1999). In yeast and in mouse, foci of RAD51 and DMC1 detected by immunofluorescent labelling seem to overlap in wide field microscopy (resolution of around 300 nm). Based on this observation it is generally assumed that both RAD51 and DMC1 participate in the same recombination event.

Genetic studies in *S. cerevisiae* led to the conclusion that both RAD51 and DMC1 perform meiotic recombination, yielding joint molecules (JMs) (Hong et al, 2013; Lao et al, 2013). However, in the absence of Dmc1, no recombination intermediates are observed, unless Rad51 is overexpressed (Lao et al, 2013; Liu et al, 2014), meaning that its activity is tightly regulated. Indeed, several proteins appear to specifically suppress the activity of Rad51 in yeast meiosis (Lai et al, 2011; Lin et al, 2010; Niu et al, 2007; Wan et al, 2004; Wu et al, 2010). When Rad51 is active in the absence of Dmc1, meiotic recombination preferentially involves the sister chromatid rather than the homologous chromosome, showing an intrinsic intersister bias for Rad51-mediated template choice (Hong et al, 2013). Unexpectedly, lack of Rad51 also leads to exclusive formation of intersister JMs (Hong et al, 2013), suggesting that both Rad51 and Dmc1 are necessary for interhomolog recombination in wild type cells. Recent additional genetic experiments have shown that Rad51, but not its strand invasion activity, is required for meiotic progression and

for JM formation with the normal IH:IS ratio. This strongly indicates that Rad51 has an accessory role, to stimulate interhomolog strand invasion by Dmc1 in yeast meiosis (Cloud et al, 2012). A similar finding has been reported in plants, where the recombination phenotype of a *AtRad51* knockout strain could be rescued by the expression of a catalytically inactive RAD51-GFP fusion protein (Da Ines et al, 2013). Despite evidence of functional crosstalk between AtRAD51 and AtDMC1 in *A. thaliana*, immunofluorescent analysis of AtRAD51 and AtDMC1 foci by confocal microscopy showed that the two proteins do not colocalize within one and the same recombination nodule. In particular, it was speculated that each one locates at a different end of the DSB, and that DMC1 drives one side of the break into strand-invasion (Kurzbauer et al, 2012). In mouse, Tarsounas et al. (1999) reported colocalization of RAD51- and DMC1-associated immunogold grains in meiotic nuclei (Tarsounas et al, 1999) analysed by electron microscopy (resolution 1 nm). However, we feel that the EM images suggest that, although the two proteins are enriched in common areas, there is little or no mixing of the two labels, so that each of the two proteins may occupy specific subdomains of this area.

Here, we used super-resolution microscopy to determine to what extent RAD51 and DMC1 proteins might accumulate in discrete domains within repair foci during mouse meiotic recombination. We performed direct Stochastic Optical Reconstruction Microscopy (dSTORM) and Structured Illumination Microscopy (3D-SIM) to image spread mouse meiotic nuclei, immunostained for DMC1, RAD51 and the axial/lateral element component protein SYCP3. Applying super-resolution microscopy techniques allows imaging of a specimen at a resolution below the diffraction limit of a fluorescence light microscope. In dSTORM imaging, this is obtained by the stochastic reactivation of fluorophores which were first put in the dark state. This allows to analyse the localization of individual molecules in the specimen, rather than measuring the intensity of fluorescence (Sauer, 2013). Fluorescence emitters, reactivated in turns over a time interval, are analysed in number, time, space and frequency of emission. Based on these parameters, it is possible to identify the most probable localization of fluorophores. In the present experimental setup, fluorophores are connected to the proteins of interest (RAD51 and DMC1) by immunofluorescent labelling, thus multiple fluorophores may track back to the same molecule. Further analysis is therefore employed to define the localization of the molecules at a lateral resolution that can reach 20 nm (van de Linde et al, 2011).

The localized molecules form a pattern that will help define the composition and organization of recombination foci. Due to the extensive calculations and statistical analyses that are applied to dSTORM data, some artefacts in the reconstruction of the image may be introduced. 3D-SIM imaging is an optics-based microscopy technique, that exploits the moiré effect obtained by interposing diffracting grids between the excitation light and the specimen, to increase the resolution by 2-fold in all dimensions, compared to widefield microscopy. The obtained 3D-SIM image is more comparable to the images used for previously reported analysis of meiotic foci and for this reason it was used as a positive control of the data obtained by dSTORM imaging. The resolution power of dSTORM imaging allowed to observe that RAD51 and DMC1 occupy specific distinct domains within a single recombination nodule. Furthermore, we found that such foci evolve during meiotic prophase, as observed from the changes in their composition and spatial organization. Early and late recombinase configurations were identified, based on their relative abundance at each analysed meiotic substage, and we infer that they correspond to the presynaptic and synaptic steps of the HR process, respectively. In *Sycp1* knockout spermatocytes, which lack the transverse filaments (TF) of the SC, axial elements align but do not synapse (de Vries et al, 2005). Herein, we describe experimental results indicating that, in this mutant, the synaptic step of homologous recombination may be affected. Using super-resolution imaging of wild type and mutant mouse spermatocytes, critical configurations of RAD51 and DMC1 in the initiation of meiotic recombination may be defined. As indicated by the new insight in the dynamics of meiotic DSB repair foci presented herein, we anticipate that super-resolution imaging will be a powerful tool to investigate more proteins involved in meiotic recombination and in crossing over formation, in particular when the advanced microscopic technology is used in combination with mouse genetic models showing meiotic phenotypes related to homologous chromosome interactions (SC mutants) and DSB repair.

Results

Features of meiotic recombination foci revealed by super-resolution imaging

Recombination foci were analysed in spread meiotic nuclei immunostained for RAD51, DMC1, and SYCP3, using 3D-structured illumination microscopy (3D-SIM) and direct stochastic optical reconstruction microscopy (dSTORM). As reported before, SIM allows discrimination between the two lateral elements interacting in synapsed areas of chromosomes (Qiao et al, 2012) (Figure 1A-B), which cannot be appreciated in widefield imaging of similar spermatocyte nuclei samples. In widefield microscopy studies, recombination foci have been described as circular spots both in RAD51 and in DMC1 immunofluorescent stainings. When analyzing the patterns for both proteins in the same nucleus, foci seem to colocalize, meaning that signals from the two proteins largely overlap (Figure 1A-B). 3D-SIM images showed recombination foci as aggregates of proteins, in which the distribution of DMC1 and RAD51 was not homogeneous and not completely overlapping throughout the focus (Figure 1C, D, F). In DMC1 and RAD51 co-staining experiments, the two proteins displayed distinct localization patterns, indicating that the used antibodies do not crossreact under these conditions. By utilizing a microscope that combines 3D-SIM and dSTORM functionalities within the same instrument, we were able to image the same field applying both techniques with the same lens. The obtained images could therefore be easily overlaid and compared: in particular, the 3D-SIM image was used as a reference for the image acquired via the dSTORM.

All DSB repair foci were manually selected in the 3D-SIM image and marked as regions of interest (ROIs) to be further analysed in the dSTORM image of the same nucleus. Detections of fluorescent events acquired in dSTORM imaging were analysed (see Materials and Methods) and grouped to define localizations. Every localization is assumed to be derived from a single fluorophore. The results of the dSTORM analysis depend on the chemical properties of the used fluorophores and their environment. We tested what would be the best set up for our analysis of recombination foci in spermatocyte nuclei immunostained for RAD51 and DMC1. As described in Materials and Methods, we used Alexa488 and Alexa647 dyes coupled to the secondary antibodies to detect RAD51 and DMC1, respectively, and vice versa. Using either fluorophore combination, we consistently detected ~3 times

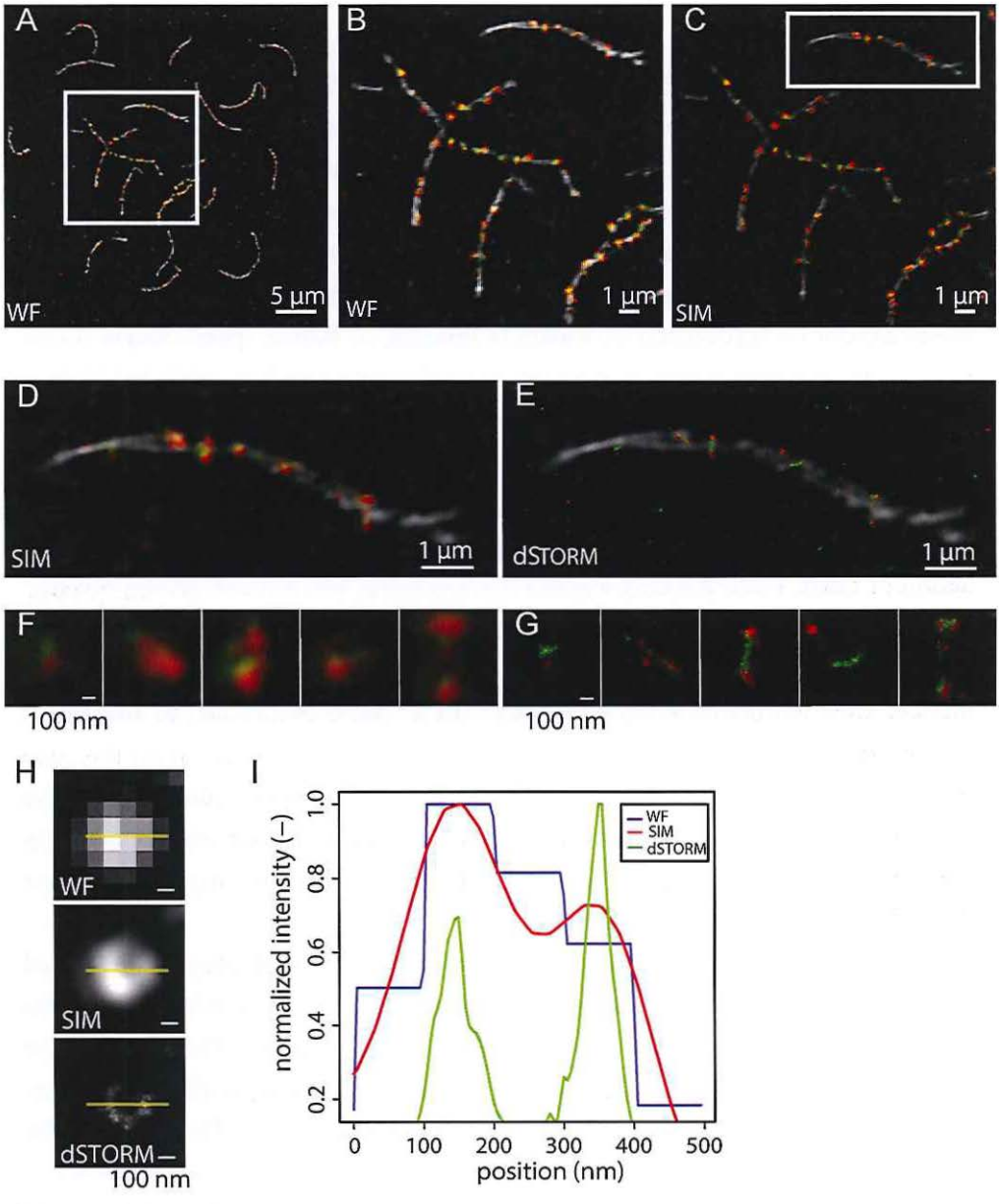

Figure 1: Meiotic DSB foci in super-resolution

Spread mouse late zygotene nucleus immunostained with primary antibodies for RAD51, DMC1, and SYCP3, and appropriate secondary antibodies labelled with Alexa-488 (green), Alexa-647 (red), and Alexa-555 (white), respectively. **(A)** widefield image; **(B-C)** widefield and 3D-SIM of boxed region in **A**. **(D-E)** 3D-SIM and dSTORM images of boxed region in **C**. **(F)** Close-up of single foci

more localization events for RAD51 than DMC1. As expected, we observed more localizations for Alexa647 compared to Alexa488, due to a more optimal switching behavior of the former (van de Linde et al, 2011). To obtain the most informative data, we decided to use the more efficient Alexa647 dye to detect DMC1 (red), that is either less abundant or less well recognized by the primary antibody compared to RAD51, and the Alexa488 dye to detect RAD51 (green). A total dataset of 1787 ROIs was generated by analysis of 12 nuclei in different meiotic substages, imaged in three independent experiments (Figure S1). The maximum number of foci/ROIs per nucleus was observed in early zygotene, and corresponds well with what we and others have reported in quantitative analyses of RAD51 foci numbers at different substages of meiotic prophase (Carofiglio et al, 2013; Cole et al, 2012).

The dSTORM technique allows determination of the position of individual fluorescent objects at the single molecule level with a lateral resolution of about 20 nm. Due to the use of immunofluorescent stainings, more than one fluorophore may be associated with every recombinase monomer, precluding absolute quantification of molecules. Still, single molecule localization revealed that meiotic recombination foci are composed of partially separate DMC1 and RAD51 domains (Figure 1E, G). This observation was unprecedented in several widefield studies of meiotic recombination foci, but could be roughly appreciated in the 3D-SIM images, and appeared more defined upon dSTORM analysis of foci, which have a resolution ~2-fold and ~10-fold higher than widefield microscopy, respectively (Figure 1H, I). The spatial separation of RAD51 areas from DMC1 excludes the possibility that the filament formed by recombinases on DSB ends consists of a random mixture of RAD51 and DMC1 monomers. In addition, we observed that the reciprocal position and orientation of DMC1 and RAD51 domains was highly heterogeneous in the population of analysed foci. These observations prompted us to examine the spatial distribution of localizations of DMC1 and RAD51 within DSB repair foci in more detail, to identify possible predominant patterns.

present on the chromosome pair shown in **D** in 3D-SIM and dSTORM. **(G-I)** Example of ROI imaged in widefield, 3D-SIM, and dSTORM showing the difference in resolution of a fluorescent item in deconvolved images **(G)** and the precision of localization of fluorescence emitters **(I)** across the image (yellow line in **G**).

RAD51 and DMC1 cluster organization occurs in two most prominent configurations

To quantify and categorize the different patterns of RAD51 and DMC1 localizations, we used a Kernel density estimation function (Wand, 2013) to analyse the dSTORM images. In this way we identified specific domains within the ROIs that were enriched for either or both proteins. Such a domain is termed a cluster. The experimental setup of the immunofluorescence analysis of RAD51 and DMC1 in the present study was not compatible with quantification of the number of molecules forming these domains, therefore a cluster was defined as an area larger than 50 nm^2 in which the density of RAD51 or DMC1 was at least 5 localizations per 10 nm^2 (see Materials and Methods). We quantified the number of clusters within each ROI and observed that for both RAD51 and DMC1 a single cluster within a ROI was most frequently observed. Foci with multiple RAD51 or DMC1 clusters are also present, but are more frequent for DMC1 compared to RAD51 (Figure 2A). Using the above described definition of clusters, ROIs with low localization counts of either RAD51 or DMC1 will be classified as having 0 clusters of RAD51 or DMC1 respectively, even if a signal appears visible in the SIM. In addition, labelling of the proteins may be heterogeneous due to variability in the antibody binding to the epitopes (of the target protein and/or of the primary antibody), and in the number of fluorophores conjugated to the secondary antibodies. This variability may generate artefacts in the data, such as dips in the signal to levels below the set threshold. When these gaps are bigger than the minimum distance between clusters (20 nm), it may result in splitting of single clusters in multiple areas, and may be interpreted as the presence of multiple distinct complexes of the same recombinase within the same focus. The few ROIs that contain 0 or more than 2 DMC1 or RAD51 clusters may in part be explained as the consequence of such artefacts. Next, we quantified the different RAD51 and DMC1 clustering combinations in our ROIs dataset in order to assess how the two recombinases related to each other within each ROI. We observed that ROIs composed of a combination of maximum two clusters per protein were the most represented, whereas ROIs composed of more than two clusters of either protein occurred at a frequency lower than 5%. In the distribution of cluster combinations, more than 50 % of the total population of ROIs fell within two specific groups: a single DMC1 domain with a single RAD51 domain (D1R1), and two DMC1 clusters with a single RAD51

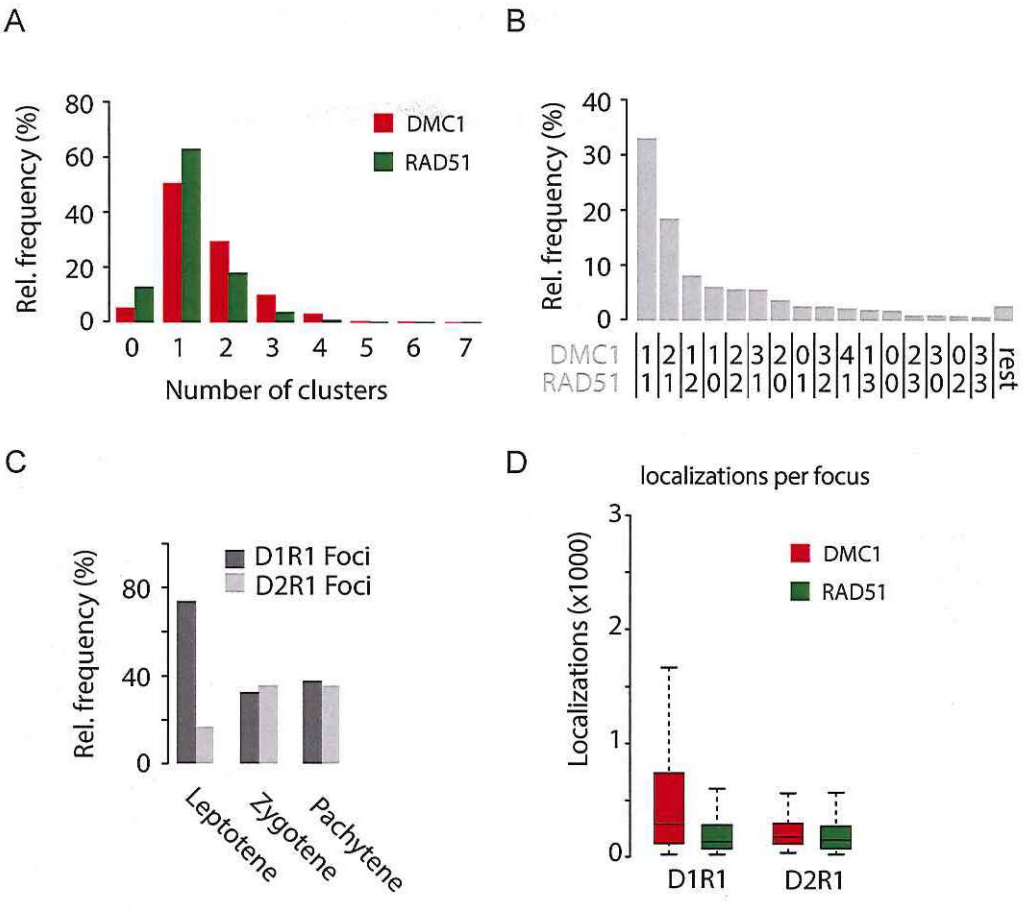

Figure 2: Abundance of cluster configurations

Numbers of clusters within foci were determined on images from 2-dimensional Kernel density estimations (KDE2D fitted). **(A)** Relative frequency of foci containing 0-7 RAD51 or DMC1 clusters per focus as a percentage of the total number of foci. **(B)** Relative frequency of foci containing the indicated combinations of RAD51 and DMC1 clusters per focus as a percentage of the total number of foci. Combinations that were present in less than 10 foci were grouped in the category referred to as rest. **(C)** Relative number of foci in the group D1R1 (one DMC1 cluster and one RAD51 cluster) and D2R1 (two DMC1 clusters and one RAD51 cluster) per stage as percentage of total number of foci per stage. **(D)** Boxplot of the number of RAD51 and DMC1 localizations in the D1R1 and D2R2 groups

cluster (D2R1) (Figure 2B). Given their high relative frequencies, we investigated these two configurations in more detail.

Timecourse analysis of D1R1 and D2R1 foci during meiotic prophase

While meiotic prophase progresses, recombination foci gradually disappear, indicating that repair reaches a stage at which recombinases are no longer required (Cole et al, 2012). Based on this, we inferred that later meiotic substages would be enriched for more advanced recombination intermediates compared to early meiotic prophase nuclei. We therefore quantified the frequency of the D1R1 group compared to the D2R1 group throughout meiotic substages, in order to assess their frequency in time. The D1R1 group was most abundant at leptotene, the early meiotic stage at which the majority of SPO11-induced DSBs are generated, suggesting that this configuration could represent the initial step of meiotic recombination, when DMC1 and RAD51 are forming filaments on the resected DSB ends. In the transition to zygotene and then to pachytene, a dramatic reduction of the D1R1 configuration frequency was observed, parallel to a more than 2-fold increase in the relative frequency of D2R1 (Figure 2C). This finding indicates that the D2R1 configuration could represent the evolution of the D1R1 configuration. The appearance of a second DMC1 domain could occur through accumulation of additional DMC1 molecules, or might involve a redistribution of the present DMC1 molecules within the focus. To further explore this, we compared the number of DMC1 localizations per focus in either one of the most abundant groups. This analysis showed that the number of localizations per focus was constant for RAD51, and was slightly reduced for DMC1 in the D2R1 group compared to the D1R1 group (Figure 2D). This observation suggests that the second DMC1 cluster is not likely to form through additional accumulation of this protein, but is more likely the result of a redistribution of the initial pool of DMC1 that was already present in the D1R1 configuration. This may occur by relocation of DMC1 on the DNA or upon movement of DMC1-coated DNA, which could take place to perform the homology search.

The D1R1 foci occur more frequently on non-synapsed axes at zygotene

During meiotic prophase, homologous chromosome synapsis and repair of meiotic DSBs are intertwined processes that positively regulate each other: homolo-

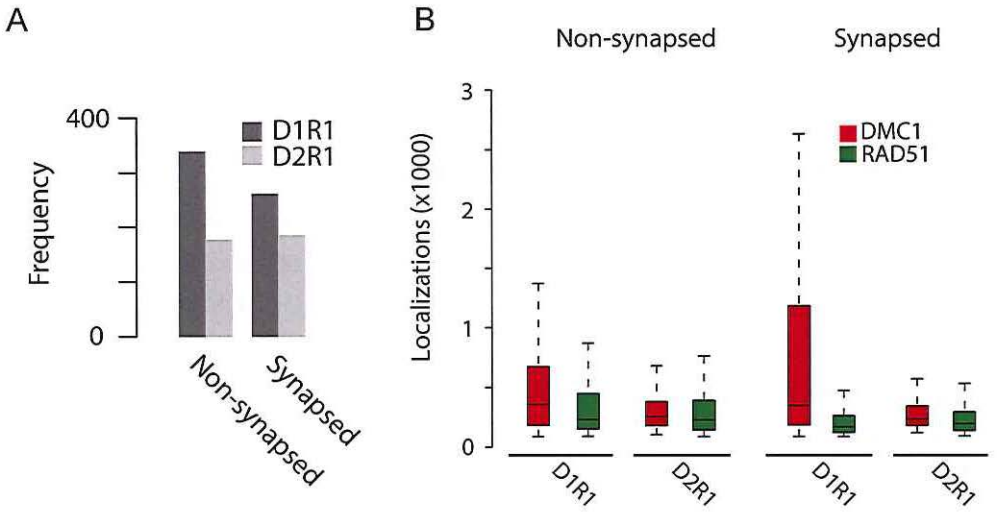

Figure 3: D1R1 and D2R1 configurations on synapsed versus non-synapsed axes
The presence of individual foci on synapsed or non-synapsed regions of the synaptonemal complex was assessed based on the SYCP3 signal in the 3D-SIM images. **(A)** Frequency of foci and **(B)** number of localizations for DMC1 and RAD51 of the D1R1 and D2R2 group on synapsed and non-synapsed regions of the SC.

gy search and strand invasion to mediate meiotic DSB repair favour homologous chromosome alignment and synapsis (Baudat et al, 2000; Mahadevaiah et al, 2001; Romanienko and Camerini-Otero, 2000). Concomitantly, achievement of synapsis allows more rapid repair of DSBs by providing a homologous template for repair in closer proximity. We therefore hypothesized that D1R1 foci could be specifically located on axial elements of chromosomes that have not yet synapsed (herein referred to as non-synapsed, to distinguish them from unsynapsed, which concerns regions that are not able to reach synapsis), whereas D2R1 foci would preferentially be found on synapsed axes. To test this hypothesis we compared the frequency of both configurations between synapsed and non-synapsed chromosomes in early and mid zygotene nuclei. At this stage, homologous chromosomes are partially engaged in pairing, but have not yet synapsed along their full length. In these nuclei, we found that D2R1 foci are equally frequent on synapsed and non-synapsed chromosomes. However, D1R1 foci appeared more often in association with non-synapsed chromosomal areas (Figure 3A), further supporting the idea that this configuration precedes the D2R1 configuration. Next, we compared the number of localizations per focus for both RAD51 and DMC1 in D1R1 foci that were present on synapsed

versus non-synapsed axes, but no significant difference in the mean values was detected (Figure 3B). However, it appears that on synapsed axes, there is a wider variability in the number of DMC1 localizations for the D1R1 configuration.

Asymmetrical distribution of RAD51 compared to DMC1

To gain better understanding of the spatial organization of protein clusters in the identified configurations, we determined the center of mass of every cluster in the ROI and measured the distance between the center of RAD51 cluster(s) and DMC1 cluster(s) (Figure 4A-C). The mean RAD51-DMC1 distances in all the foci analysed followed a clear bimodal distribution with data clustering around a mean distance of about 50 nm and 180 nm. By measuring the mean RAD51-DMC1 distance in the D1R1 group only, we found that this frequency distribution graph overlapped with the 50 nm peak of the distribution of mean DMC1-RAD51 distances of all ROIs (Figure 4D). Conversely, we observed that the 180 nm peak corresponded well with the distribution of mean distances between RAD51 and DMC1 in the D2R1 group. We also analysed the distribution of the maximum distance between RAD51 and DMC1 per focus, which also clustered in two peaks, of about 50 nm and 300 nm in size.

Since only a single domain is present per protein in the D1R1 group, the distribution of the maximum distance was the same as for the mean distance. Importantly, it corresponded with the first peak of the distribution of maximum distances, suggesting that all foci with more than one cluster per protein contain RAD51 and DMC1 clusters that are larger (localizations are more spread) or that are spatially more separated. Interestingly, minimum distances coherently clustered around 50 nm. This indicates that also in foci with more than one DMC1 domain, RAD51

► **Figure 4: Internal distribution of RAD51 and DMC1 clusters within foci**
(A-C) Representations of 3 different visualization methods for single molecule localization data, for a typical example of the D1R1 (top) and D2R2 (bottom) groups, RAD51 (green), DMC1 (red). Bars 100nm. **(A)** Scatter plot localizations. **(B)** Normalized Gaussian plot: each localization is plotted as a 2D Gaussian with a sigma (standard deviation) corresponding to the precision of the detection, and a fixed integrated intensity. **(C)** Representation of the binary image obtained by fitting a 2-dimensional Kernel density estimation (KDE2D) function on the localizations. Asterisks indicate the centers of mass of each cluster. White double arrows indicate the measured RAD51-DMC1 distances. **(D)** Distribution of the mean, maximum, and minimum distances between the center of mass of RAD51 and DMC1 clusters (white arrows in **C**). Yellow and red lines represent the D1R1 and D2R2 subgroups, respectively.

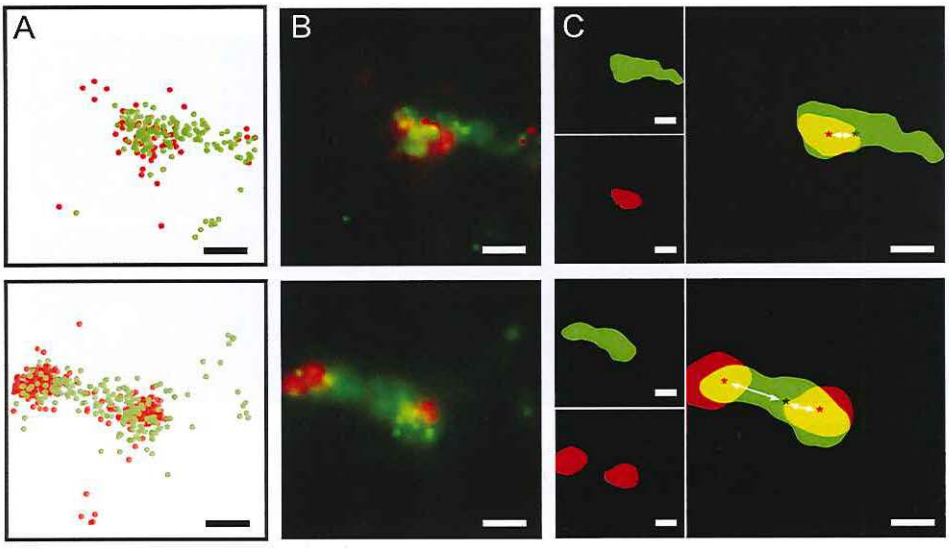
A
B
C

D

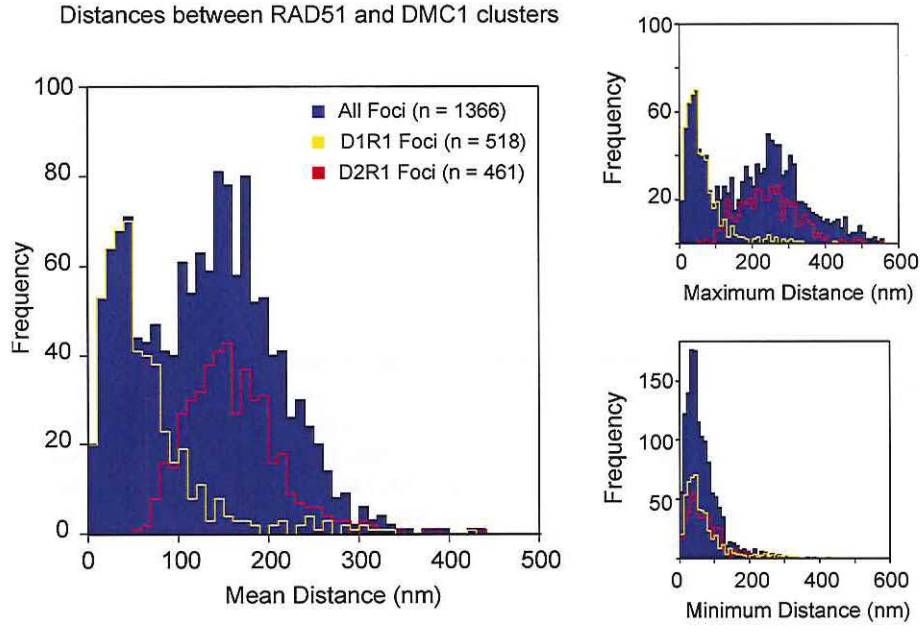
Distances between RAD51 and DMC1 clusters
All Foci (n = 1366)
D1R1 Foci (n = 518)
D2R1 Foci (n = 461)
Frequency
Mean Distance (nm)
Maximum Distance (nm)
Minimum Distance (nm)

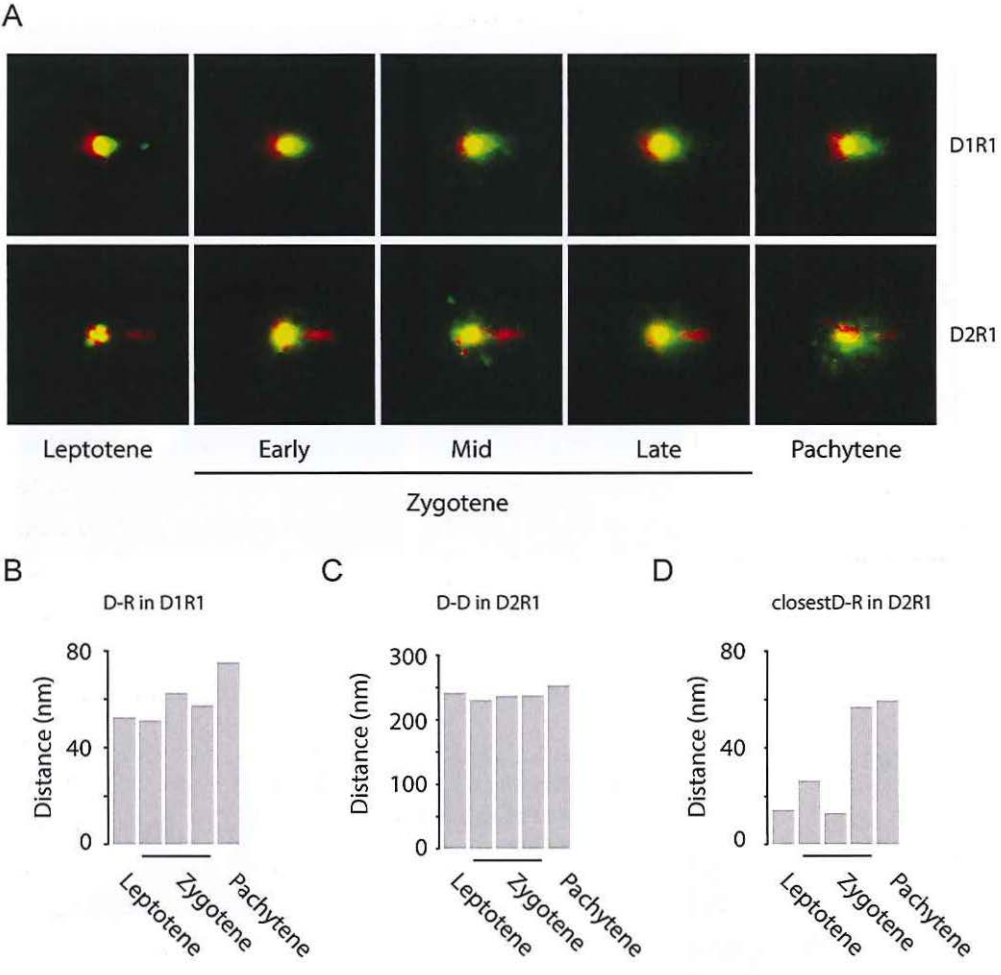

Figure 5: Conformation of subgroups through the stages of meiotic prophase I
(A) Summed images of all aligned foci within the D1R1 (top) and D2R1 (bottom) group per stage. Images were rotated around the closest DMC1 cluster and aligned in such a fashion that the center of the RAD51 cluster (D1R1) or the center of the far DMC1 cluster (D2R1) is in line with, and on the right side of the center of the close DMC1 cluster. **(B-D)** Mean distances between clusters for the indicated group per stage. Mean distance between DMC1 and RAD51 (D-R) in the D1R1 configuration **(B)**, between the two DMC1 clusters (D-D) in the D2R1 configuration **(C)**, and mean of the shortest distance between DMC1 and RAD51 in the D2R1 configuration **(D)**.

is very close to DMC1 on one side. Hence, the D2R1 configuration appears to be asymmetrical with respect to the position of the RAD51 cluster relative to the two DMC1 clusters. In addition, the DMC1-RAD51 distance is around 50 nm in both the D1R1 and on one side in the D2R1 ROIs reinforces the idea that D1R1 foci evolve into D2R1 foci when DMC1 localizations separate into two separate clusters, one of which remains closely associated with RAD51.

Consensus pattern of the spatial organization in D2R1 foci

To further evaluate the shape and organization of DMC1 and RAD51 clusters within a ROI, we aligned all the D1R1 and the D2R1 foci, by rotation. For the D1R1 group, the DMC1 cluster was used as an anchor point, and for D2R1 group we used the DMC1 cluster which was closest to the RAD51 cluster as an anchor point. We generated a summed image of all the aligned foci divided per meiotic stage, in order to appreciate variations in the structure of the foci throughout meiotic progression (Figure 5A). The D1R1 group showed partial overlap of RAD51 and DMC1 clusters in the summed images. It is important to note that spread spermatocytes are extremely flat preparations (~400 nm thickness) of the three-dimensional nuclear structure. This implies that the nuclear volume is flattened on a surface, clashing chromatin areas on each other, and thereby potentially also superimposing different domains of recombination nodules. Interestingly, D1R1 foci also seemed to undergo elongation through time, as shown by the slight increase in the distance between DMC1 and RAD51 centers of mass, as measured in the summed images (Figure 5A, B). The shorter distance in early nuclei may be related to the enrichment for very early recombination foci at leptotene, when loading of the recombinases may not yet be complete. In D2R1 foci, RAD51 signal was mainly located between the two DMC1 clusters, although the distribution of RAD51 detections seemed to be more scattered when spermatocytes had progressed to pachytene. Surprisingly, the mean distance between the two DMC1 domains in the D2R1 group did not change through time (Figure 5C). However, the center of mass of the RAD51 cluster seemed to be extending away from the closest DMC1 anchor domain as cells progressed from zygotene to pachytene (Figure 5D).

Configuration of recombination foci is affected by the absence of the transverse filament protein SYCP1

Imaging of the organization of recombinases within foci allows analysis of recombination intermediates up to the stage when DNA synthesis has to occur and RAD51 and DMC1 are removed, rendering the DNA end accessible and allowing recruitment of other proteins that perform the postsynaptic steps of homologous recombination. In meiotic cells, DSB repair is profoundly affected by the correct assembly of the synaptonemal complex (SC). This tripartite proteinaceous scaffold forms along the axis of chromosomes and is instrumental for homologs to be zipped together into synapsis (Boateng et al, 2013; Hamer et al, 2006; Hamer et al, 2008; Schramm et al, 2011). In the absence of the central or transverse filament of the SC, homologous chromosomes can pair and align their axial elements, but the distance between these elements remains larger compared to the distance between the lateral elements in normally synapsed SCs in the wild type (de Vries et al, 2005). Mutation of any component of the central element leads to this phenotype. Here, we analysed recombination foci in spermatocytes that lack the transverse filament protein SYCP1 (Figure 6A-C). It has been reported that on a *Sycp1*$^{-/-}$ background, meiotic DSB repair is severely impaired and RAD51 foci persist (Boateng et al, 2013; Hamer et al, 2006; Hamer et al, 2008; Schramm et al, 2011). Therefore we hypothesized that *Sycp1*$^{-/-}$ nuclei would be enriched for the DSB repair intermediate that corresponds to the recombination step at which repair gets stalled because of the aberrant SC. We found that the frequencies of the D1R1 and D2R1 configurations, previously identified in wild type meiosis, were similar in *Sycp1*$^{-/-}$ and wild type spermatocytes (Figure 6D). This suggests that the spatial organization of foci

Figure 6: Meiotic DSB foci in *Sycp1*$^{-/-}$ spermatocytes
Microspread pachytene-like meiotic nucleus from *Sycp1*$^{-/-}$ mouse immunostained with primary antibodies for RAD51, DMC1, and SYCP3, and appropriate secondary antibodies labelled with Alexa-488 (green), Alexa-647 (red), and Alexa-555 (white), respectively. **(A-B)** 3D-SIM image **(A)**, and close-up of the region boxed in **A (B)**. Arrowheads mark regions shown in **C**. **(C)** Close-up of chromosomal areas marked in **B**, in 3D-SIM (top), and dSTORM (bottom). **(D)** Relative frequency of foci containing the indicated combinations of RAD51 and DMC1 clusters per focus as a percentage of the total number of foci. **(E)** Frequency distribution of the mean distance between RAD51 and DMC1 clusters. Yellow and red lines represent the D1R1 and D2R1 subgroups, respectively. **(F)** Frequency distribution of the distance between the two DMC1 clusters in the D2R1 group in the *Sycp1*$^{-/-}$ (orange line), compared to the wild type (grey line).

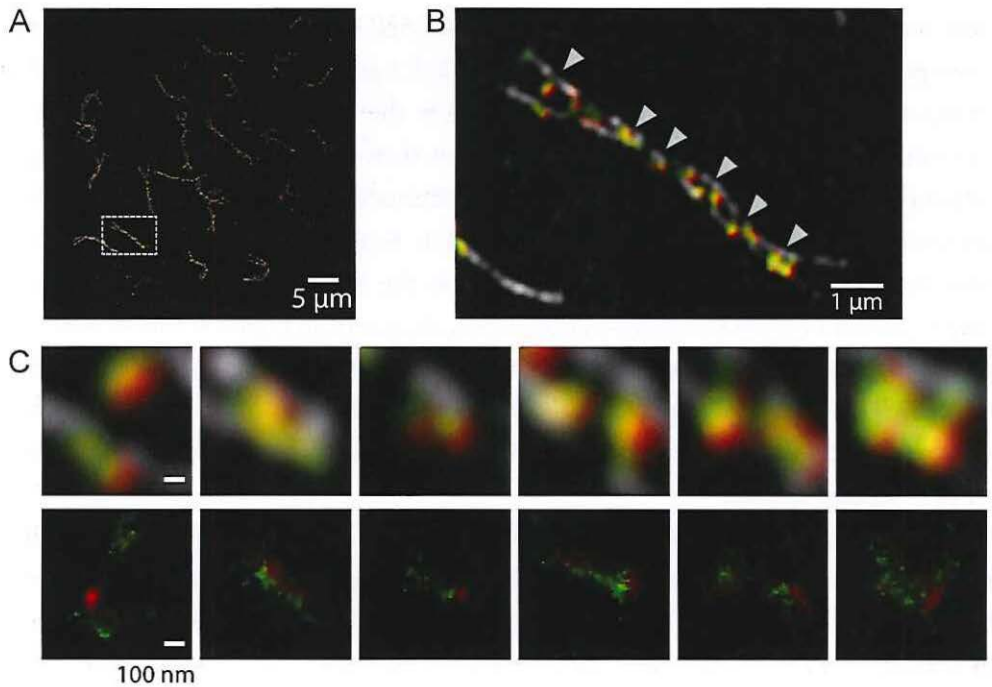
A
5 µm
B
1 µm
C
100 nm
D
Cluster distribution
Rel. frequency (%)
40
30
20
10
0
DMC1
RAD51
1 1 2 2 1 3 3 2 1 4 0 4 3 0 2 5 5 4 1 1 3 6
1 0 1 0 2 0 1 2 3 0 0 1 2 1 3 0 1 3 4 5 3 0
E
Distance distribution
All Foci (n = 801)
D1R1 Foci (n = 406)
D2D1 Foci (n = 156)
Frequency
80
40
0
0 100 200 300 400 500 600
Mean Distance (nm)
F
Distance between red clusters
WT
Sycp1-/-
Releative Frequency (%)
30
20
10
0
0 100 200 300 400 500
Distance (nm)

does not differ in the *Sycp1*$^{-/-}$ spermatocytes, and that recombination intermediates manage to reach the stage represented by the D2R1 group. Interestingly, the D1R0 group, in which RAD51 localizations fall below the threshold for cluster identification, was far more abundant in this mutant than in the wild type, suggesting impaired loading of RAD51. In addition, or alternatively, the D1R0 may actually represent the earliest configuration, if DMC1 is first loaded on both DSB ends. This configuration could be overrepresented in the collection of ROIs from the *Sycp1*$^{-/-}$, either because the analysed population derives from nuclei at earlier meiotic prophase compared to the wild type, or because SPO11-activity is prolonged due to the lack of synapsis (Kauppi et al, 2013; Thacker et al, 2014). Further experiments will be needed to assess if the enhanced frequency of the D1R0 configuration is a *Sycp1*$^{-/-}$ specific feature.

Measurement of the mean distance between RAD51 and DMC1 clusters resulted in the expected bimodal distribution, with the peak at 50 nm represented by the D1R1 group (Figure 6E). The distribution of mean distances in the D2R1 foci overlapped very well with the profile of the second peak, but it was centered at a larger distance compared to what was observed for the wild type. We therefore measured the distances between the two DMC1 clusters in the D2R1 foci of the *Sycp1*$^{-/-}$ nuclei, and we found that the size distribution of this distance was also shifted to higher values compared to the DMC1-DMC1 distance distribution of D2R1 foci from wild type nuclei (Figure 6F, $p<0.0001$). This indicates that the lack of synapsis between chromosomes leads to a structural change of the D2R1 recombination intermediate, which may cause impaired progression to the next step in the meiotic homologous recombination repair process.

Discussion

In this study we analysed meiotic recombination foci using two independent super-resolution microscopy techniques. The combination of information obtained by 3D-SIM and dSTORM imaging allowed us to gain insight in the structure of repair foci in the context of meiotic synapsis of homologous chromosomes, which is mediated by the synaptonemal complex (SC). In the analysis of dSTORM images, every detection is assumed to correspond to a single molecule (as defined in the Materials and Methods section), although the use of indirect immunofluorescence to visualize the proteins of interest precludes direct protein molecule counting. Detections relating to the two recombinases RAD51 and DMC1, that are both present in meiotic cells, were not homogeneously distributed within foci, suggesting that the two proteins do not form mixed filaments, although their vicinity may indicate a functional interaction. We identified two most represented configurations of recombination foci, based on the distribution of RAD51 and DMC1 molecules in one or more subdomains or clusters within the foci: the D1R1, composed of one DMC1 and one RAD51 cluster, and the D2R1, composed of two DMC1 and one RAD51 cluster. In addition, we observed that the frequency of such configurations changes during meiosis, suggesting an evolution of recombination foci as meiotic prophase progresses. Based on the frequency and features of the two most abundant configurations, we propose a model for DMC1 and RAD51 accumulation forming early repair intermediates in mouse meiotic prophase cells (Figure 7).

We observed that both D1R1 and D2R1 configurations are present at different meiotic prophase substages. However, D1R1 ROIs were far more abundant than D2R1 ROIs at leptotene, before they dramatically decreased in number at later stages, when the frequency of D2R1 ROIs increased. This trend suggests that the D2R1 foci replace the D1R1 foci, as meiotic prophase progresses. In addition, we found a comparable number of DMC1 detections in each of the D1R1 and D2R1 ROIs, at later meiotic prophase stages, which suggests that the DMC1 cluster in the D1R1 foci has become split into two domains in the transition from D1R1 to D2R1. Progression of meiotic prophase is marked by a gradual increase of synapsis between homologous chromosomes, concomitant with progression of the DSB repair process. A differential distribution of foci configurations was therefore expected on synapsed compared to non-synapsed chromosomes, based on the hypothesis

presented above that D2R1 configurations follow D1R1 configurations in meiotic recombination. Indeed, we observed more D1R1 configurations on non-synapsed versus synapsed axes in zygotene, although the frequencies of D2R1 and D1R1 configurations on synapsed axes was comparable. In meiotic cells, not all DSBs are synchronously generated and repaired: a subset of meiotic breaks may be formed later, or persists till later stages of meiotic prophase, which could explain the presence of more or less advanced recombination intermediates on synapsed chromosomes. Surprisingly, D2R1 configurations were equally abundant on synapsed and non-synapsed axes, meaning that recombination may proceed till such stage before synapsis is achieved, or independent of the engagement of the homologous chromosome into recombination. This may suggest that the D2R1 configuration can form before a stable interaction with the homologous chromosome is established, so that this intermediate promotes actual pairing and subsequent synapsis of the chomosomal axes. Alternatively, or in addition, D2R1 configurations may represent recombination intermediates involving either the sister chromatid (mainly on asynapsed axes) or a chromatid of the homologous chromosome (mainly on synapsed axes). Based on the data presented here, it is not yet possible to discriminate between recombination intermediates involving the sister chromatid or the chromatids of the homologous chromosome.

The separation of the DMC1 cluster may be related to progression of the meiotic recombination mechanism from protein loading to the initiation of homology search and strand invasion, upon which the D2R1 form appears. Homology search would indeed separate the two DSB ends, thereby allowing resolution of the two DMC1 clusters, located on opposite sides of the DSB. In this scenario, the accumulation of DMC1 and RAD51 at DSBs would occur asymmetrically, with one side being DMC1-only and the other side showing accumulation of both RAD51 and DMC1. This might involve a random choice, not controlled by specific properties of either of the two ends. However, the asymmetry might have significant consequences. It is tempting to speculate that this asymmetry may allow different functionalization of the DSB ends, by making one of them more competent for homology search and strand invasion. This interpretation is consistent with both the partial overlapping single clusters of RAD51 and DMC1 in the D1R1 configuration, and a split of the DMC1 cluster upon strand invasion generating the D2R1 configuration. The D1R1 configuration itself does not provide information

about a possible hierarchy in loading of RAD51 and DMC1 on resected DSB ends. However, we found a significant fraction of ROIs showing only one DMC1 cluster without any RAD51 in *Sycp1*$^{-/-}$ spermatocytes, which are expected to be enriched for early recombination intermediates due to the structural defect in the formation of the SC. Such a configuration (D1R0) may not be frequent enough or stable enough to be significantly represented in the groups of recombination foci in wild type spermatocytes, although they have been observed in plant meiocytes by confocal microscopy (Kurzbauer et al, 2012).Taking all the above into account, we would like to propose that DMC1 filaments are first formed on both DSB ends (Figure 7, (1)), although we cannot exclude that loading of recombinases may occur in a stochastic way, so that RAD51 may be recruited first, at some DSBs. We speculate that the end that preferentially accumulates RAD51 is resected further than the DMC1-only end, explaining the more elongated shape of the RAD51 domain in the D2R1 configuration (Figure 7, (2)). Notably, in this experimental set up, DNA is not visualized, therefore it is not possible to determine the position of the DSB ends relative to the recombinases. Combination of recombinase imaging together with detection of the DNA may allow determining the relative position of the DNA molecule with respect to RAD51 and DMC1 clusters, and therefore help to verify this interpretation. In budding yeast, RAD51 strand invasion activity is repressed to favour DMC1-mediated strand invasion, which involves the homologous chromosome, thereby contributing to the interhomolog bias. In addition, it is thought that RAD51 may stimulate DMC1 activity (Cloud et al, 2012; Lao et al, 2013). Based on our current observations, we speculate that a similar mechanism may be operational in mouse meiosis, with RAD51 acting as an accessory protein to DMC1. The differential distribution of recombinases on the two sides of the break would nicely fit with such distinct roles for DMC1 compared to RAD51. The presence of DMC1 on the 3' end of the 3'-overhang could be instrumental to perform strand invasion preferentially in the homologous chromosome, whereas RAD51 may serve a structural function in the nucleoprotein filament, may activate DMC1, and/or have a role in homology proofreading. On the other side of the DSB, the DMC1-only filament may be the quiescent strand. A similar scenario has been proposed for budding yeast recombination, based on genetic data (Hong et al, 2013).

In the D2R1 foci, the center of mass of the RAD51 cluster was not at equal distance from each DMC1 cluster: one DMC1 cluster was found to be closer to

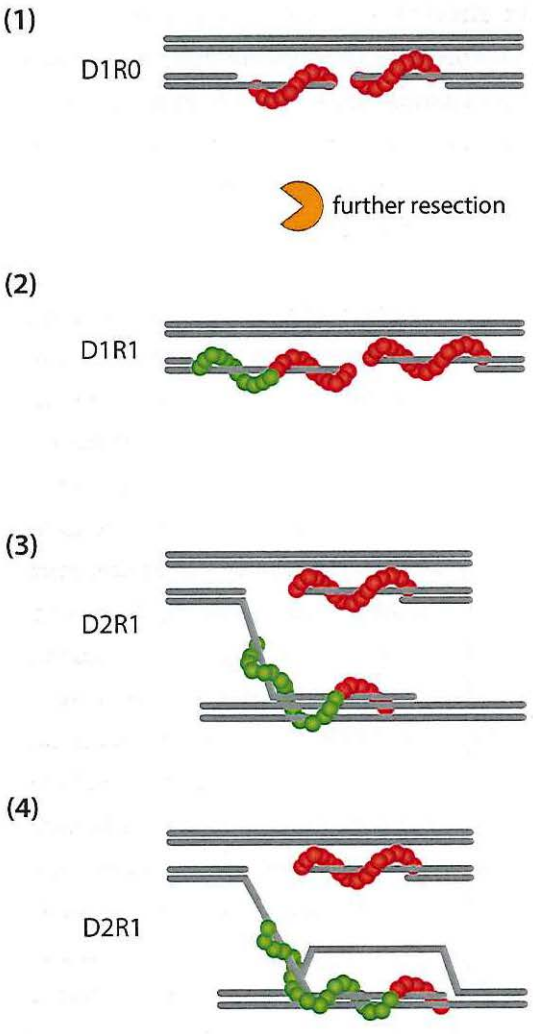

Figure 7: Schematic model of RAD51 and DMC1 cooperation in meiotic recombination foci

A speculative model is proposed, for dynamic patterns of RAD51 and DMC1 localization and organization in recombination intermediates in mouse meiotic prophase in subsequent steps. Upon initial resection of the DSB ends, we propose that DMC1 is loaded first **(1)**. This is suggested to be a very shortlived intermediate step, because it is not detected at significant levels in the wild type. Further resection of the 5'strand occurs asymmetrically, as suggested by studies in budding yeast (Neale et al, 2005). Preferential loading of RAD51 on one end leads to the D1R1 configuration, which is most frequent at leptotene, when the majority of DSBs is induced. Accumulation of RAD51 increases as long as resection progresses **(2)**, as suggested by the gradual increase of the RAD51-DMC1 distance in D1R1 foci from leptotene to pachytene. When one of the two strands begins homology search **(3)**, the two DMC1 associated ends will diverge, allowing visualization of two separate DMC1 domains (D2R1). We propose that the filament that contains both RAD51 and DMC1 performs the homology search. When homology is detected, interaction of the invading strand with the template becomes more stable **(4)**, thereby explaining the consensus configuration observed for the D2R1 group, in which RAD51 is most often localized between the two DMC1 clusters. The organization of the RAD51 filament onto dsDNA (formed by the invading strand and the template strand now paired) may stretch the DNA, extending the area of RAD51 localizations, and thereby increasing the shortest DMC1-RAD51 distance, as observed in the aligned D2R1 foci at later meiotic stages.

the RAD51 cluster, at a distance of approximately 50 nm. The distance of RAD51 cluster from the farther DMC1 cluster was measured to be 300 nm on average. In yeast, a 3' overhang generated by resection of a meiotic DSB has been estimated to be around 800 nt long (Zakharyevich et al, 2010), and in vitro studies showed that association of RAD51 with dsDNA generates a filament length of 1.5 nm per 3bp, and per monomer of RAD51 (Ristic et al, 2005). Assuming a similar ratio for interaction between RAD51 and ssDNA, a filament of around 400 nm length could be formed on ssDNA of approximately 800 bp. Based on this estimate, the size range of the maximal RAD51-DMC1 distance in the D2R1 foci fits well with the expected size of the 3' overhang, and could indicate the distance between the center of mass of DMC1 on ssDNA on one end of the DSB, and that of RAD51 on ssDNA on the other end of the DSB. Alternatively the DMC1 and RAD51 cluster with this distance could both be located on the same ssDNA molecule. It is important to note that the labelling of RAD51 and DMC1 with an unlabeled primary antibody followed by an Alexa-conjugated secondary antibody results in the formation of a molecular complex quite larger than the two proteins of interest. Given the size of antibodies and of the attached dyes, the added molecular bulk can be estimated to be around 30 nm in diameter. It is currently not possible to determine the spatial organization of such complex, therefore an accuracy error of around 30 nm needs to be taken into account, meaning that the use of indirect immunofluorescent labelling may increase the apparent size of the protein clusters and will increase the uncertainty of localization of the individual molecules. This error is in the same range as the maximum resolution achieved by dSTORM, but it affects the measurement of size and distances. In order to overcome this limitation and validate the proposed structure of recombination foci, direct labelling of the proteins would be needed which would add a modest contribution to the size of the molecule, allowing higher accuracy.

Upon rotational alignment of the D2R1 ROIs, an increase of the shortest D-R distance was observed in the progression of meiosis from leptotene to pachytene, whereas the D-D distance stays constant. Following the hypothesis put forward above, that DMC1 is loaded on both ends, and RAD51 extends the filament only on one end of the DSB, it may be suggested that the nucleoprotein filament that contains both the RAD51 and the DMC1cluster is the one that performs strand invasion. The stable average distance between the DMC1 clusters could represent the

maximum extension of the invading strand away from the parental strand, towards a potential repair template. Alternatively, the D2R1 configuration is reached very rapidly, or is most stable, thus more extended intermediate configurations could be formed but may not be detected due to a short life-span. Upon strand invasion, the nucleoprotein filament that contains both DMC1 (at the 3'end) and RAD51 may become more tightly associated with the template DNA and expand the formed D-loop. In addition, it has been shown that RAD51 tends to stretch the dsDNA when it binds to it, extending its length by 50% (Ristic et al, 2005), which would distribute the RAD51 localizations over a longer filament. This may contribute to the shifting of the center of mass of the RAD51 cluster away from the DMC1 cluster, on the same DNA strand. DMC1 interaction with the DNA also results in stretching of the molecule, but we did not assess elongation of DMC1 clusters.

The relative increase in the shortest RAD51-DMC1 distance between zygotene and pachytene also indicates that the filament that contains both RAD51 and DMC1 is undergoing structural changes as meiotic prophase progresses. When homology search is taking place, the two DSB ends will diverge from each other, thereby allowing resolution of the two areas of accumulation of DMC1 on either side of the break (Figure 7, (3)), establishing the D2R1 configuration. At this step of homologous recombination, localizations of RAD51, which is the most abundant protein in the foci, appear to form a more elongated cluster. This might be explained by a movement of the nucleoprotein filament diverging away from the other end of the DSB, to search for, and interact, with a repair template. Once stable interaction with the homologous template is established, RAD51 might further stretch and extend the heteroduplex dsDNA that is then formed (Ristic et al, 2005), and thereby expand the area occupied by the nucleoprotein filament upon its invasion and formation of joint molecules. This would lead to an increase in the distance between the center of mass of the RAD51 domain and the adjacent DMC1 domain at the 3' end of the invading strand, as observed in the alignment of the D2R1 foci at subsequent stages of meiotic prophase. Meanwhile, the DMC1-only end is still associated with the parental strand and kept quiescent (Figure 7, (4)), in agreement with the model proposed by Hong et al. (2013), wherein only one end of the DSB is performing homology search, branching away from the DSB site (Hong et al, 2013). This phenomenon is termed single-end invasion, and is considered to be a general recombination intermediate from which both synthesis-dependent strand

annealing and double Holliday junctions can evolve, depending on the fate of the newly synthesized strand (Hunter and Kleckner, 2001). Further studies will be required to identify specific features that may discriminate between intersister and interhomolog single-end invasion, perhaps by performing super-resolution imaging to analyse more proteins that play a role in meiotic recombination. In addition, we anticipate that experimental combination of meiosis-defective knockout mouse models with super-resolution microscopy will provide a promising new approach to study the dynamics of mouse meiotic recombination and meiotic defects at the molecular level.

Materials and Methods

Meiotic spread preparation and immunofluorescence

Testis tissues were processed to obtain spread nuclei for immunocytochemistry as described (Peters et al, 1997). Cells were spread on 1.5 um thickness coverslips, previously coated with 1% poly L-lysine (Sigma) and stained with antibodies mentioned above. Before incubation with antibodies, coverslips were washed in PBS (3x10 min), and non-specific sites were blocked with 0.5% w/v BSA and 0.5% w/v milk powder in PBS. Primary antibodies were diluted in 10% w/v BSA in PBS, and incubations were overnight at room temperature in a humid chamber. Subsequently, coverslips were washed (3x10 min) in PBS, blocked in 10% v/v normal swine serum (Sigma) in blocking buffer (supernatant of 5% w/v milk powder in PBS centrifuged at 14,000 rpm for 10 min), and incubated with secondary antibodies in 10% normal swine serum in blocking buffer overnight at room temperature. Finally, coverslips were washed (3x10 min) in PBS (in the dark) and immediately used for imaging.

Antibodies

For primary antibodies, we used goat antibody against SYCP3 (R&D Systems), mouse monoclonal antibody against DMC1 (Abcam ab1837), and a previously generated rabbit polyclonal anti RAD51 (Essers et al, 2002). For secondary antibodies, we used a donkey anti-rabbit IgG Alexa 488/647, donkey anti-mouse Alexa IgG 488/647, and donkey anti-goat Alexa 555 (Molecular Probes).

Sample preparation

Coverslips immunostained as described above were mounted in an Attofluor Cell Chamber (Life Technologies). For drift correction and channel alignment 100nm Goldnanoparticles (Sigma) were added to the sample. To perform dSTORM imaging, an imaging buffer was prepared containing 40mM MEA (Sigma), 0.5mg/ml Glucose Oxidase (Sigma), 40 µg/ml Catalase (Sigma) and 10% w/v Glucose in PBS pH 7.4. Samples were incubated in the imaging buffer during the entire imaging session.

3D-SIM and dSTORM imaging

Imaging was performed using a Zeiss Elyra PS1 system. Both 3D-SIM and dSTORM data were acquired using a 100x 1.49NA objective. 488, 561, 642 100mW diode lasers were used to excite the fluorophores together with respectively a BP 495-575 + LP 750, BP 570-650 + LP 75 or LP 655 excitation filter. For 3D-SIM imaging a grating was present in the light path. The grating was modulated in 5 phases and 5 rotations, and multiple z-slices were recorded on an Andor iXon DU 885, 1002x1004 EMCCD camera. dSTORM imaging was performed using near-TIRF settings while the images were recorded on Andor iXon DU 897, 512x512 EMCCD camera. dSTORM imaging was done using near-TIRF settings while the images were recorded on Andor iXon DU 897, 512x512 EMCCD camera. For the dSTORM data at least 10 000 images were acquired and frames were subsequently imaged at an interval of 33ms for Alexa 647. For Alexa488 an interval of 50ms was used to compensate for the lower photon yield of the Alexa488 dye.

Image analysis

3D- SIM images were analysed using the algorithm in the ZEN2011 (Carl Zeiss, Jena) software. Channels were aligned based on a reference sample containing 100nm Tetraspeck beads (Life Technologies). For dSTORM, individual fluorescent events were localized in the subsequent frames using a 2D Gauss fitting algorithm. Detections in subsequent frames originating from the same fluorophore were grouped. Drift was corrected using 100nm gold nanoparticles (Sigma). The same fiducials were used to align the two color dSTORM images using an affine alignment. Dual color dSTORM and triple color SIM images were aligned, based on the dSTORM and 3D-SIM Alexa647 images, using a channel alignment algo-

rithm in the ZEN2011 software. Foci were manually selected based on the SIM images, and square regions (side of 600 nm) around the foci were selected using ImageJ within the FiJI platform (Schindelin et al, 2012). The single molecule localizations of the individual foci were subsequently imported into R using the RStudio GUI for further analysis (Gregoire Pau, 2013; R Development Core Team, 2008).

Foci shape analysis

Single molecule localization data was used to fit a 2D Kernel Density Estimation (KDE) function (Wand, 2013). The KDE function estimates the density of localizations at a certain position in the image. The KDE function was applied to foci with more than 20 localizations for the given protein. The bandwidth of the density estimation was set equal to the average localization precision of our data (20 nm). The 2D KDE gives a normalized density over the image. Because we are interested to determine the absolute density of localizations, the normalized density is multiplied by the number of localizations in the focus. After fitting a 2D KDE to the data we are able to define objects by applying a threshold. The threshold is set at 0.05 localization/nm, equal to 5 localizations/10 nm, meaning we have sufficient sampling in that region. The resulting binary images were used to determine shape features (center of mass i.e.).

References

Baudat F, Manova K, Yuen JP, Jasin M, and Keeney S (2000). Chromosome synapsis defects and sexually dimorphic meiotic progression in mice lacking spo11. Mol Cell *6*:989-998.

Bishop DK (1994). RecA homologs Dmc1 and Rad51 interact to form multiple nuclear complexes prior to meiotic chromosome synapsis. Cell *79*:1081-1092.

Boateng KA, Bellani MA, Gregoretti IV, Pratto F, and Camerini-Otero RD (2013). Homologous Pairing Preceding SPO11-Mediated Double-Strand Breaks in Mice. Dev Cell *24*:196-205.

Bolcun-Filas E, Costa Y, Speed R, Taggart M, Benavente R, De Rooij DG, and Cooke HJ (2007). SYCE2 is required for synaptonemal complex assembly, double strand break repair, and homologous recombination. J Cell Biol *176*:741-747.

Bolcun-Filas E, Hall E, Speed R, Taggart M, Grey C, de Massy B, Benavente R, and Cooke HJ (2009). Mutation of the mouse Syce1 gene disrupts synapsis and suggests a link between synaptonemal complex structural components and DNA repair. PLoS Genet *5*:e1000393.

Carofiglio F, Inagaki A, de Vries S, Wassenaar E, Schoenmakers S, Vermeulen C, van Cappellen WA, Sleddens-Linkels E, Grootegoed JA, Te Riele HP, *et al.* (2013). SPO11-independent DNA repair foci and their role in meiotic silencing. PLoS Genet *9*:e1003538.

Cloud V, Chan YL, Grubb J, Budke B, and Bishop DK (2012). Rad51 is an accessory factor for Dmc1-mediated joint molecule formation during meiosis. Science *337*:1222-1225.

Cole F, Kauppi L, Lange J, Roig I, Wang R, Keeney S, and Jasin M (2012). Homeostatic control of recombination is implemented progressively in mouse meiosis. Nat Cell Biol *14*:424-430.

Costa Y, Speed R, Ollinger R, Alsheimer M, Semple CA, Gautier P, Maratou K, Novak I, Hoog C, Benavente R, *et al.* (2005). Two novel proteins recruited by synaptonemal complex protein 1 (SYCP1) are at the centre of meiosis. J Cell Sci *118*:2755-2762.

Da Ines O, Degroote F, Goubely C, Amiard S, Gallego ME, and White CI (2013). Meiotic recombination in Arabidopsis is catalysed by DMC1, with RAD51 playing a supporting role. PLoS Genet *9*:e1003787.

de Vries FA, de Boer E, van den Bosch M, Baarends WM, Ooms M, Yuan L, Liu JG, van Zeeland AA, Heyting C, and Pastink A (2005). Mouse Sycp1 functions in synaptonemal complex assembly, meiotic recombination, and XY body formation. Genes Dev *19*:1376-1389.

Di Carlo AD, Travia G, and De Felici M (2000). The meiotic specific synaptonemal complex protein SCP3 is expressed by female and male primordial germ cells of the mouse embryo. Int J Dev Biol *44*:241-244.

Essers J, Hendriks RW, Wesoly J, Beerens CE, Smit B, Hoeijmakers JH, Wyman C, Dronkert ML, and Kanaar R (2002). Analysis of mouse Rad54 expression and its implications for homologous recombination. DNA Repair (Amst) *1*:779-793.

Goedecke W, Eijpe M, Offenberg HH, van Aalderen M, and Heyting C (1999). Mre11 and Ku70 interact in somatic cells, but are differentially expressed in early meiosis. Nat Genet *23*:194-198.

Gregoire Pau AO, Mike Smith, Oleg Sklyar and Wolfgang Huber (2013). EBImage: Image processing toolbox for R. .

Gupta RC, Golub E, Bi B, and Radding CM (2001). The synaptic activity of HsDmc1, a human recombination protein specific to meiosis. Proc Natl Acad Sci U S A

98:8433-8439.

Habu T, Taki T, West A, Nishimune Y, and Morita T (1996). The mouse and human homologs of DMC1, the yeast meiosis-specific homologous recombination gene, have a common unique form of exon- skipped transcript in meiosis. Nucleic Acids Res *24*:470-477.

Hamer G, Gell K, Kouznetsova A, Novak I, Benavente R, and Hoog C (2006). Characterization of a novel meiosis-specific protein within the central element of the synaptonemal complex. J Cell Sci *119*:4025-4032.

Hamer G, Wang H, Bolcun-Filas E, Cooke HJ, Benavente R, and Hoog C (2008). Progression of meiotic recombination requires structural maturation of the central element of the synaptonemal complex. J Cell Sci *121*:2445-2451.

Heyer WD, Ehmsen KT, and Liu J (2010). Regulation of homologous recombination in eukaryotes. Annu Rev Genet *44*:113-139.

Hong S, Sung Y, Yu M, Lee M, Kleckner N, and Kim KP (2013). The logic and mechanism of homologous recombination partner choice. Mol Cell *51*:440-453.

Hunter N, and Kleckner N (2001). The single-end invasion: an asymmetric intermediate at the double-strand break to double-holliday junction transition of meiotic recombination. Cell *106*:59-70.

Kass EM, and Jasin M (2010). Collaboration and competition between DNA double-strand break repair pathways. FEBS Lett *584*:3703-3708.

Kauppi L, Barchi M, Lange J, Baudat F, Jasin M, and Keeney S (2013). Numerical constraints and feedback control of double-strand breaks in mouse meiosis. Genes Dev *27*:873-886.

Keeney S, Baudat F, Angeles M, Zhou ZH, Copeland NG, Jenkins NA, Manova K, and Jasin M (1999). A mouse homolog of the Saccharomyces cerevisiae meiotic recombination DNA transesterase Spo11p. Genomics *61*:170-182.

Keeney S, Giroux CN, and Kleckner N (1997). Meiosis-specific DNA double-strand breaks are catalyzed by Spo11, a member of a widely conserved protein family. Cell *88*:375-384.

Kurzbauer MT, Uanschou C, Chen D, and Schlogelhofer P (2012). The recombinases DMC1 and RAD51 are functionally and spatially separated during meiosis in Arabidopsis. Plant Cell *24*:2058-2070.

Lai YJ, Lin FM, Chuang MJ, Shen HJ, and Wang TF (2011). Genetic requirements and meiotic function of phosphorylation of the yeast axial element protein Red1. Mol Cell Biol *31*:912-923.

Lao JP, Cloud V, Huang CC, Grubb J, Thacker D, Lee CY, Dresser ME, Hunter N, and Bishop DK (2013). Meiotic crossover control by concerted action of Rad51-Dmc1 in homolog template bias and robust homeostatic regulation. PLoS Genet *9*:e1003978.

Lin FM, Lai YJ, Shen HJ, Cheng YH, and Wang TF (2010). Yeast axial-element protein, Red1, binds SUMO chains to promote meiotic interhomologue recombination and chromosome synapsis. EMBO J *29*:586-596.

Liu Y, Gaines WA, Callender T, Busygina V, Oke A, Sung P, Fung JC, and Hollingsworth NM (2014). Down-regulation of Rad51 activity during meiosis in yeast prevents competition with Dmc1 for repair of double-strand breaks. PLoS Genet *10*:e1004005.

Mahadevaiah SK, Turner JM, Baudat F, Rogakou EP, de Boer P, Blanco-Rodriguez J, Jasin M, Keeney S, Bonner WM, and Burgoyne PS (2001). Recombinational DNA double-strand breaks in mice precede synapsis. Nat Genet *27*:271-276.

Moens PB, Chen DJ, Shen Z, Kolas N, Tarsounas M, and Heng HHQ (1997). Rad51 immunocytology in rat and mouse spermatocytes and oocytes. Chromosoma *106*:207-215.

Neale MJ, Pan J, and Keeney S (2005). Endonucleolytic processing of covalent protein-linked DNA double-strand breaks. Nature *436*:1053-1057.

Niu H, Li X, Job E, Park C, Moazed D, Gygi SP, and Hollingsworth NM (2007). Mek1 kinase is regulated to suppress double-strand break repair between sister chromatids during budding yeast meiosis. Mol Cell Biol *27*:5456-5467.

Page SL, and Hawley RS (2004). The genetics and molecular biology of the synaptonemal complex. Annu Rev Cell Dev Biol *20*:525-558.

Pelttari J, Hoja MR, Yuan L, Liu JG, Brundell E, Moens P, Santucci-Darmanin S, Jessberger R, Barbero JL, Heyting C, *et al.* (2001). A meiotic chromosomal core consisting of cohesin complex proteins recruits DNA recombination proteins and promotes synapsis in the absence of an axial element in mammalian meiotic cells. Mol Cell Biol *21*:5667-5677.

Peters AH, Plug AW, van Vugt MJ, and de Boer P (1997). A drying-down technique for the spreading of mammalian meiocytes from the male and female germline. Chromosome Res *5*:66-68.

Qiao H, Chen JK, Reynolds A, Hoog C, Paddy M, and Hunter N (2012). Interplay between synaptonemal complex, homologous recombination, and centromeres during mammalian meiosis. PLoS Genet *8*:e1002790.

R Development Core Team (2008). R: A language and environment for statistical computing. R Foundation for Statistical Computing (Vienna, Austria, R Foundation for Statistical Computing).

Ristic D, Modesti M, van der Heijden T, van Noort J, Dekker C, Kanaar R, and Wyman C (2005). Human Rad51 filaments on double- and single-stranded DNA: correlating regular and irregular forms with recombination function. Nucleic Acids Res *33*:3292-3302.

Romanienko PJ, and Camerini-Otero RD (2000). The mouse spo11 gene is required for meiotic chromosome synapsis. Mol Cell *6*:975-987.

San Filippo J, Sung P, and Klein H (2008). Mechanism of eukaryotic homologous recombination. Annu Rev Biochem *77*:229-257.

Sauer M (2013). Localization microscopy coming of age: from concepts to biological impact. J Cell Sci *126*:3505-3513.

Schindelin J, Arganda-Carreras I, Frise E, Kaynig V, Longair M, Pietzsch T, Preibisch S, Rueden C, Saalfeld S, Schmid B, *et al.* (2012). Fiji: an open-source platform for biological-image analysis. Nat Methods *9*:676-682.

Schipler A, and Iliakis G (2013). DNA double-strand-break complexity levels and their possible contributions to the probability for error-prone processing and repair pathway choice. Nucleic Acids Res *41*:7589-7605.

Schramm S, Fraune J, Naumann R, Hernandez-Hernandez A, Hoog C, Cooke HJ, Alsheimer M, and Benavente R (2011). A novel mouse synaptonemal complex protein is essential for loading of central element proteins, recombination, and fertility. PLoS Genet *7*:e1002088.

Shinohara A, and Shinohara M (2004). Roles of RecA homologues Rad51 and Dmc1 during meiotic recombination. Cytogenet Genome Res *107*:201-207.

Shrivastav M, De Haro LP, and Nickoloff JA (2008). Regulation of DNA double-strand break repair pathway choice. Cell Res *18*:134-147.

Tarsounas M, Morita T, Pearlman RE, and Moens PB (1999). RAD51 and DMC1 form mixed complexes associated with mouse meiotic chromosome cores and synaptonemal complexes. J Cell Biol *147*:207-220.

Thacker D, Mohibullah N, Zhu X, and Keeney S (2014). Homologue engagement controls meiotic DNA break number and distribution. Nature *510*:241-246.

van de Linde S, Loschberger A, Klein T, Heidbreder M, Wolter S, Heilemann M, and Sauer M (2011). Direct stochastic optical reconstruction microscopy with standard fluorescent probes. Nat Protoc *6*:991-1009.

Wan L, de los Santos T, Zhang C, Shokat K, and Hollingsworth NM (2004). Mek1 kinase activity functions downstream of RED1 in the regulation of meiotic double strand break repair in budding yeast. Mol Biol Cell *15*:11-23.

Wand M (2013). KernSmooth: Functions for kernel smoothing for Wand & Jones.

Wu HY, Ho HC, and Burgess SM (2010). Mek1 kinase governs outcomes of meiotic recombination and the checkpoint response. Curr Biol *20*:1707-1716.

Yang F, De La Fuente R, Leu NA, Baumann C, McLaughlin KJ, and Wang PJ (2006). Mouse SYCP2 is required for synaptonemal complex assembly and chromosomal synapsis during male meiosis. J Cell Biol *173*:497-507.

Yang F, and Wang PJ (2009). The Mammalian synaptonemal complex: a scaffold and beyond. Genome Dyn *5*:69-80.

Yoshida K, Kondoh G, Matsuda Y, Habu T, Nishimune Y, and Morita T (1998). The mouse RecA-like gene Dmc1 is required for homologous chromosome synapsis during meiosis. Mol Cell *1*:707-718.

Yuan L, Liu JG, Hoja MR, Wilbertz J, Nordqvist K, and Hoog C (2002). Female germ cell aneuploidy and embryo death in mice lacking the meiosis-specific protein SCP3. Science *296*:1115-1118.

Yuan L, Liu JG, Zhao J, Brundell E, Daneholt B, and Hoog C (2000). The murine SCP3 gene is required for synaptonemal complex assembly, chromosome synapsis, and male fertility. Mol Cell *5*:73-83.

Yuan L, Pelttari J, Brundell E, Bjorkroth B, Zhao J, Liu JG, Brismar H, Daneholt B, and Hoog C (1998). The synaptonemal complex protein SCP3 can form multistranded, cross-striated fibers in vivo. J Cell Biol *142*:331-339.

Zakharyevich K, Ma Y, Tang S, Hwang PY, Boiteux S, and Hunter N (2010). Temporally and biochemically distinct activities of Exo1 during meiosis: double-strand break resection and resolution of double Holliday junctions. Mol Cell *40*:1001-1015.

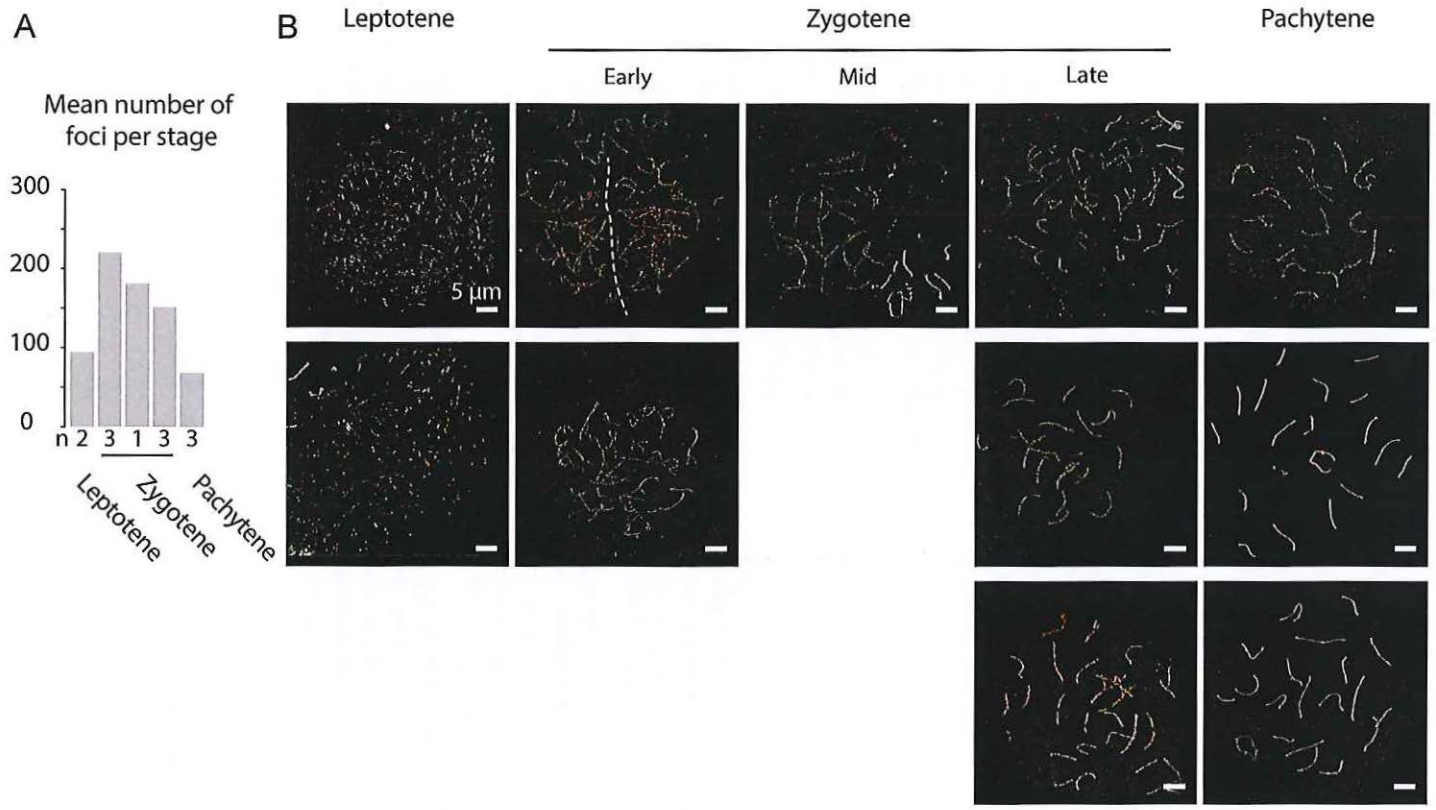

Figure S1: Mean number of foci analysed per meiotic stage

(A) Bar graph showing the average number of foci from wild type spermatocyte nuclei that were analysed in dSTORM per stage (Leptotene, Early-Mid-Late Zygotene, Pachytene). The trend mirrors the dynamics of recombinase foci reported before. The number of analysed nuclei per stage is reported underneath each bar. **(B)** 3D-SIM images of the wild type nuclei analysed per stage. Nuclei were immunostained for RAD51 (green), DMC1 (red), and SYCP3 (white). Two zygotene nuclei imaged in the same field of view are separated by the dashed line.

5

General discussion

Meiosis and DNA double strand break repair: making a connection

In yeast and mammals, correct meiotic chromosome pairing, recombination and segregation is tightly coupled to the induction and repair of meiotic DSBs. This seems to be a "no pain no gain" deal, that is associated with sexual reproduction and is exploited in evolution, because it ensures genetic diversity, which is a prerequisite for adaptation and population fitness. Meiotic cells need the induction of regulated DSBs to achieve correct chromosome pairing and segregation, although such DSBs might endanger genomic integrity (Baudat et al, 2000; Bellani et al, 2005; Keeney et al, 1997). Different pathways, error-prone or error-free, can be activated to repair spontaneous DSBs in somatic cells, depending on the stage of the cell cycle and the chromatin configuration. Meiotic prophase cells, however, have evolved in such a way that they are programmed to use mainly the error-free DSB repair mechanism: homologous recombination (HR) (Goedecke et al, 1999). In meiotic cells, the HR repair mechanism has been adapted, and it is associated with exchange of genetic material between homologous chromosomes and haploidization. The meiosis-specific features of this repair mechanism are still partially obscure and, although extensive information about evolutionary conserved aspects can be deduced from experiments that have been performed using organisms of lower complexity like budding yeast, many questions remain open in particular for mammals. In male mammals, meiotic DSB repair is not only required for homologous chromosome pairing and crossover formation, but is also implicated in correct transcriptional regulation of the heterologous X and Y chromosomes (reviewed in (Inagaki et al, 2010; Turner, 2007)). In this thesis project, we aimed to gain a better understanding of the mechanisms by which meiotic DSB repair contributes to both transcriptional silencing of heterologous sex chromosomes (Chapter 2) and homology recognition between autosomes (Chapters 3 and 4). This General Discussion will address the implications and future directions of our work related to the link between meiotic DSB formation and transcriptional silencing on the one hand, and DSB formation and chromosome pairing on the other hand.

DNA DOUBLE-STRAND BREAKS AND MEIOTIC SILENCING

A specific requirement for meiosis is the achievement of full synapsis between homologous chromosomes, and subsequent formation of at least one crossover per

chromosome pair. If one or more chromosome pairs fail to synapse, this could lead to aneuploidy in a future embryo, although meiotic check-points will be called into action to prevent progress of meiotic prophase in case of severe failure of synapsis. Intringuingly, male meiotic cells carry a chromosomal pair that is largely asynaptic by default: the X and Y sex chromosome pair. In the mammalian ancestor, 160 million years ago, the proto-X and proto-Y originated from a pair of autosomes, but in evolution the Y chromosome underwent a degenerative process whereby it lost most of its genetic content and therefore kept little sequence homology to the X chromosome (Graves, 2006). This precludes overall homologous chromosome pairing and synapsis between the sex chromosomes, except for a very small part of both X and Y, corresponding to the pseudo-autosomal region (PAR). In the PAR, significant X-Y homology has been maintained, and this region would thus be expected to behave similar to autosomal homologous chromosomes. In fact, it is thought that maintenance of a PAR region is essential to achieve meiotic pairing and thereby proper segregation of X and Y in meiosis (Shi et al, 2001). However, achievement of synapsis in the PAR does not avoid activation of a special signalling mechanism that leads to meiotic sex chromosome inactivation (MSCI). MSCI is required for progression of the male meiotic prophase in mouse (Royo et al, 2010). All known mouse mutants in which proper transcriptional silencing of X and Y is not achieved show meiotic arrest at a stage corresponding to mid-pachytene, when these cells undergo apoptosis (Ashley et al, 2004). It has been suggested that this is caused by so-called "toxic expression" of X- and Y-linked genes that are detrimental to meiotic cells (Hunt and Eicher, 1991). Proper silencing of the X and Y chromosomes by MSCI is thus essential for meiotic progression, and MSCI appears to function as a very stringent checkpoint mechanism in males.

MSCI is most likely a specialization of a more general mechanism that mediates meiotic silencing of unsynapsed chromatin (MSUC), and that operates in males as well as in females (Baarends et al, 2005; Turner et al, 2005). MSCI and MSUC have been mechanistically connected to the presence of unsynapsed chromosome regions, and require specific coating of the axial elements of the synaptonemal complex (SC) with the meiosis-specific HORMAD proteins, as well as accumulation of several DNA damage response proteins on the axes and on the surrounding chromatin (Fernandez-Capetillo et al, 2003; Ichijima et al, 2011; Shin et al, 2007; Wojtasz et al, 2012). The first known MSUC/MSCI marker is phosphorylation of the

histone variant H2AX, forming γH2AX (Mahadevaiah et al, 2001). As described in Chapter 2 of this thesis, it is most likely the combination of the presence of DSBs and unsynapsed chromatin that triggers MSUC. In SPO11-deficient spermatocytes, which lack the meiotic DSBs which are normally enzymatically induced by SPO11, many of the axial elements remain unsynapsed, but the MSUC response is usually restricted to one or two domains, that frequently do not encompass the majority of the unsynapsed axes. Such domains are termed pseudo XY bodies, even though these domains do not include any X or Y chromatin (Mahadevaiah et al, 2008). In Chapter 2, we show that there is a correlation between the subnuclear localization of the pseudo XY body and the presence of DNA damage markers in spermatocytes. We propose that, in the absence of SPO11-induced meiotic DSBs, some SPO11-independent DSBs may be present that are most likely instrumental for triggering MSUC. In addition, we provided strong indications for the occurrence of such SPO11-independent DSBs also in meiotic prophase oocytes, and activation of MSUC in areas where these DSBs were localized. In oocytes, MSUC markers could accumulate even in regions with normal synapsis, but containing many DSB repair foci, confirming the notion that DSB-detection is the initial trigger for the MSUC response. It is important to note that our work and that of others provides indications that MSCI and MSUC also may differ in several aspects, and that MSUC may have different causes, mechanistic aspects, and consequences, in male and female meiosis, as described below.

Meiotic silencing: male versus female meiosis

As indicated above, the presence of DSBs appears to elicit MSUC in oocytes, even in synapsed chromosomal areas. This is of particular interest, because HORMAD proteins, which are known to be involved in the establishment of MSCI, are not present on such synapsed chromosomes undergoing an MSUC response. An extremely high concentration of RAD51 foci along the SC in MSUC domains in oocyte nuclei (Chapter 2) may represent an amount of damage that is sufficient to recruit the players that are needed to repress transcription, although it cannot be excluded that transcriptional repression in such regions is incomplete. Alternatively, or in addition, the type of DNA damage that elicits the MSUC response in oocytes may differ from the type of damage that results in MSUC in spermatocytes. Recent data indicate that reactivation of retrotransposons, such as the LINE

transposon L1, frequently cause DNA damage in mammalian oocytes (Malki et al, 2014). Retrotransposons are repressed during germ cell development by the activity of a protein named Maelstrom (Soper et al, 2008). However, it appears that epigenetic modifications that occur during oogenesis may create a window of opportunity during which transposable elements are reactivated. A transposon-encoded endonuclease may thereby generate the DSBs observed in embryonic oocytes. Unlike transcriptional silencing in spermatocytes, which allows meiotic progression, MSUC caused by transposon-dependent DSBs in oocytes results in depletion of such cells from the ovarian pool (Malki et al, 2014). In addition, and possibly independently, L1-dependent reverse transcriptase activity provides a major contribution to death of oocytes that express too high levels of the L1 encoded L1ORF1p protein (Malki et al, 2014). This appears to be a protective mechanism that helps to select only those oocytes that carry an intact genome. In that sense, MSCI and MSUC are involved in quality control in male and female gametes, respectively, albeit through totally different mechanisms. MSCI mediates repression of the X and Y chromosomes, and it functions as a response to lack of synapsis and to persistent SPO11-dependent DSBs. However, excess of SPO11-dependent DSBs on autosomes impedes proper activation of MSCI. Toxic sex-linked gene expression then leads to cell death. MSUC in wild type oocytes appears to be triggered by unwanted and possibly harmful SPO11-independent DSBs largely derived from transposon reactivation. MSUC may therefore mediate silencing, avoiding further retrotransposon activity (Malki et al, 2014) and the resulting additional DNA damage. Oocytes with transposon activity that exceeds a certain threshold may not be able to establish as efficient MSUC, due to the need to recruit the silencing machinery to several chromatin areas. Subsequently, such oocytes would undergo apoptosis, probably as a result of the massive DNA damage induced by transposons. In this scenario, MSUC is acting similar to a genome integrity checkpoint. Taken together, it can be suggested that a threshold of autosomal SPO11-dependent DSB repair completion needs to be reached for efficient establishment of X and Y chromosomes silencing, whereas a threshold of SPO11-independent DSBs may be required for MSUC activation in oocytes. However, excessive DNA damage in oocytes will also have a detrimental effect on MSUC activation and, most likely, persistent DSBs will trigger elimination of such oocytes. Unlike in spermatocytes, in which cell depletion is caused by inefficient transcriptional silencing, oocytes

would be eliminated upon signalling by DNA damage response (DDR) proteins, as it occurs in somatic cells. From this perspective, it would be of interest to analyse female phenotypes of mouse models showing an MSCI/MSUC defect (*Mdc1*, *H2ax* genetic mutants) (Fernandez-Capetillo et al, 2003; Ichijima et al, 2011), to determine to what extent impairment of MSUC activation and signalling of DDR proteins upon transposon reactivation would affect oocyte survival, and genomic integrity and ploidy of surviving oocytes.

Another unsolved aspect of MSUC relates to the chromosome axis-wide accumulation of RAD51 in oocytes. It should be noted that separate foci are still observed on oocyte chromosomal axes that undergo MSUC, but these are in very close proximity to each other. It appears unlikely that all these sites of RAD51 accumulation represent closely adjacent DNA damage events, since the target sequences of the endonuclease L1ORF2p may most probably localize in chromatin loops, which include the vast majority of the DNA in a meiotic nucleus. The presence of RAD51 foci only on the chromosomal axes, in association with the synaptonemal complex, and in close proximity to each other, is thus unexplained. A possibility to explore is the presence of putative docking sites in the SC where RAD51 foci formation is favoured or more efficient. Such docking sites might originate from an accumulation of cofactors that help the assembly of the nucleoprotein filament, or because of specific interactions of RAD51 with the synaptonemal complex proteins SYCP3 and SYCP1 (Syrjanen et al, 2014; Tarsounas et al, 1999). This would suggest that damaged DNA is relocated to the synaptonemal complex to allow repair processes (see below). We cannot exclude that the DNA present at the bases of the chromatin loops and interacting with the SC might be a more accessible target for endonuclease activity, but no evidence is supporting this hypothesis so far.

Pseudo XY body versus XY body proper: structural and functional differences

MSUC can occur simultaneously in several chromatin areas within one nucleus, as for example has been observed in SYCP3-deficient oocytes. As described by Kouznetsova et al. (2009), this is associated with inefficient recruitment of MSUC mediators, resulting in less efficient silencing (Kouznetsova et al, 2009). Formation of multiple sites of MSUC was also observed in wild type and SPO11-deficient oocytes (Chapter 2), questioning the efficiency of transcriptional silencing, compared

to what occurs during MSCI. Although some similar chromatin marks are detected in both MSUC and MSCI areas, the chromatin of the XY body in spermatocytes is much more compact and the region of γH2AX (and other histone modifications) accumulation is more defined, compared to regions of MSUC in oocytes. This may be due to some specific mechanism that delimits the borders of the sex chromatin. Multiple chromosomes are frequently involved in the formation of the pseudo XY body in SPO11-deficient spermatocytes, owing to the severe impairment of synapsis which leads to the formation of chromosomal tangles (Baudat et al, 2000; Romanienko and Camerini-Otero, 2000). Perhaps this is affecting the spatial delimitation of the silenced area. In addition, around 15 DSB repair foci are usually present on the X chromosome when MSCI is initiated, whereas only few such foci are detected within the pseudo XY body in *Spo11* mutant spermatocytes. This may result in less robust silencing. Analyses of RNA polymerase II accumulation and Cot-1 depletion, that are usually performed to assess transcriptional activity (Baarends et al, 2005; Mahadevaiah et al, 2009), are not sensitive enough to define possible differences in silencing efficiency between MSCI and MSUC. Since MSUC in SPO11-deficient spermatocytes and wild type or SPO11-deficient oocytes does not target a specific region, RNA sequencing approaches will also not be able to provide more insight into the degree of transcriptional inactivation, unless this can be performed at single-cell level. Even in single cells it may be challenging to detect significant changes in transcriptional activity, since the half-life of mRNAs needs to be taken into account, and cells do not survive very long after MSUC has been established. It might be better to use more sensitive markers of transcriptional activity, in combination with more quantitative detection methods on fixed or even living cells. An interesting candidate is the CDK9 protein. Fluorescent-tagged CDK9 was recently shown to allow visualization of so-called transcription factories in living cells (Ghamari et al, 2013), and it would thus be expected that the degree of exclusion of this protein from regions in spermatocyte or oocyte nuclei that are silenced by MSCI or MSUC, respectively, could be a reliable quantitative indicator of silencing efficiency.

Meiotic silencing to delimit areas of genomic instability

In spermatocytes carrying a translocation between two autosome pairs, synapsis between the two derivatives cannot occur. The unsynapsed autosomes are also

subjected to meiotic silencing and tend to coalesce in the XY body (Baarends et al, 2005). The presence of multiple unsynapsed regions results in inefficient MSUC, and recruitment of unsynapsed chromosomes other than the X and Y to the XY body might allow male meiotic cells to silence the unsynapsed regions more successfully, by confining them to a single area. Similarly, in irradiated *Spo11* mutant spermatocytes, γH2AX is accumulated nucleus-wide upon irradiation, due to the high level of induced DNA damage (Chapter 2). However, a pseudo XY body is again observed 5 days later. Thus, the damaged areas seem to converge to form a single nuclear domain, where response to the insult (DNA damage and/or unsynapsed chromatin) can potentially occur more efficiently by forming a competent platform with a very high concentration of the required factors. In mitotic cells, a link between the occurrence of DNA damage and the establishment of silencing in the chromatin neighbouring the damage has already been established (Shanbhag et al, 2010). More extensive study of chromatin dynamics upon DSB-induction in mitotic cells showed that the ATM/ATR activation that follows the sensing of a DSB is not only mediating RNA polymerase II repression, but it is also instrumental for relocalization of chromosomal territories (Mehta et al, 2013). In particular chromosomal movement has been observed for gene-rich chromosomes that tend to migrate from the nuclear lamina to the core of the nucleus. This may isolate gene-rich chromatin upon DNA damage, which would avoid transcription of potentially mutated DNA, and might facilitate DNA repair by concentrating damaged DNA in nuclear areas enriched for repair proteins. Furthermore, coalescence of damaged chromatin areas has been proposed as a mechanism to favour close proximity of an appropriate DNA template for homologous recombination (Agmon et al, 2013; Dion et al, 2012), which may be what happens when a pseudo XY body is formed upon irradiation in SPO11-mutant spermatocytes. From this perspective, MSUC represents an interesting example of how chromosome dynamics may enhance the quality of DNA repair by partially rearranging the nuclear architecture. Thus, analysis of the highly specific DSB repair mechanism and chromatin structure changes that are associated with XY body formation in mouse spermatocytes may also provide a wealth of information that is relevant to our understanding of the processes that are initiated upon occurrence of the far more general and life-threatening DSB events that take place in all our cells.

MEIOTIC DNA DOUBLE-STRAND BREAKS AND CHROMOSOME PAIRING

In this thesis, the contribution of DSB repair to homology recognition recognition in meiosis was addressed from two different angles. First (Chapter 3), we used a functional approach, and asked if radiation-induced breaks would be repaired in a meiosis-specific manner in oocytes and spermatocytes, and could thereby contribute to the formation of stable homologous chromosome associations. This research led to three main findings: damage-induced DSBs are recruited to the axial elements, undergo the interhomolog bias, and contribute to homology recognition, virtually identical to the response to SPO11-induced DSBs. Second, using super resolution microscopy of immunostained spermatocyte nuclei, we aimed to dissect molecular details of the early recombination intermediates formed upon SPO11-dependent DSBs induction in spermatocytes. In particular, we wished to determine how RAD51 and its meiosis-specific paralog DMC1 accumulate relative to each other within meiotic recombination nodules. The observations clearly indicated that, although RAD51 and DMC1 foci colocalize at low resolution, the two proteins occupy different subdomains within a single repair focus, observed at high resolution. Based on analysis of the changes in RAD51 and DMC1 localisation patterns that occur as meiotic prophase progresses, we propose that DMC1 is loaded first, on both ends of the DSB, and that RAD51 is loaded subsequently, in an asymmetric manner. This would then lead to a frequently occurring repair intermediate that contains mainly DMC1 on one end of the break, and DMC1 together with an elongated RAD51 filament on the other end. We hypothesized that this is the end that mediates the strand invasion of homologous DNA. The implications of all these observations will be discussed in the next paragraphs, in the context of the chronological order of events during meiotic prophase, up to the stage of repair at which RAD51 and DMC1 are removed. In addition, we will present results of preliminary experiments and provide directions for future research.

Meiotic DSB formation

Some genomic areas are more frequently targeted for SPO11-dependent DSB induction. These regions are defined as recombination hotspots (Arnheim et al, 2007; Smagulova et al, 2011). The currently available data indicate that the DSB-inducing

SPO11-complex first tethers the hotspot from the chromatin loop to the axes, and then induces DSBs (Panizza et al, 2011). This notion is mainly based on observations in yeast, but a similar model might be proposed for mammals. In mammals, only a few components of the complex of proteins that is required for SPO11 activity have been identified so far. Interestingly, one of these proteins required for DSB formation, named MEI4, localizes to meiotic chromosome axes, independent of SPO11 expression (Kumar et al, 2010). This indicates that the actual break formation also occurs on the axes in mice. For yeast, it recently became clear that tethering of the hotspot to the chromosome axes is regulated by Spp1, a PHD finger-containing protein that localizes to chromosome axes, but recruits the hotspot by interacting with trimethylated H3K4 (H3K4me3) that is enriched in the neighbouring chromatin (Sommermeyer et al, 2013). In mammals, H3K4 trimethylation mediated by the methyl transferase PRDM9 also determines hotspot localization (Baudat et al, 2010; Grey et al, 2011), and thus it might be proposed that recruitment of trimethylated H3K4 could also be a means of connecting hotspots to the chromosomal axes in mouse. From that perspective, it is highly surprising that radiation-induced DSBs, that should occur at more or less random positions in the genome, can be recruited to the axial elements of the SC with high efficiency. Based on the expected number of DSBs that would be induced by a 5 Gy irradiation dose, it appears that almost all DSBs relocalize to the axes. The histone mark H3K4me3, which is associated with hotspots relocation to the synaptonemal complex, is very unlikely to be enriched at most of the damage-induced DSB sites, thus it is relatively safe to assume that these damaged sites are not tethered to the axes by capture of H3K4me3 marked chromatin. Therefore, our data indicate that one or more of the early components of the DSB detection and repair machinery in meiocytes should be able to interact with components of the synaptonemal complex, and thereby mediate this relocalisation. Obvious candidates for interaction on the axial elements are the structural components SYCP2 and SYCP3 (Yang et al, 2006; Yuan et al, 2002; Yuan et al, 2000), HORMAD1 and HORMAD2 (the mammalian homologs of yeast Hop1) (Shin et al, 2007; Shin et al, 2013; Wojtasz et al, 2012), and components of the meiosis-specific cohesion complex (Eijpe et al, 2003; Hopkins et al, 2014; Ishiguro et al, 2014; Revenkova et al, 2004). In single knockouts of genes encoding these components, SPO11-induced RAD51/DMC1 foci still localize on the chromosomal axes, suggesting that none of these proteins is essential for tether-

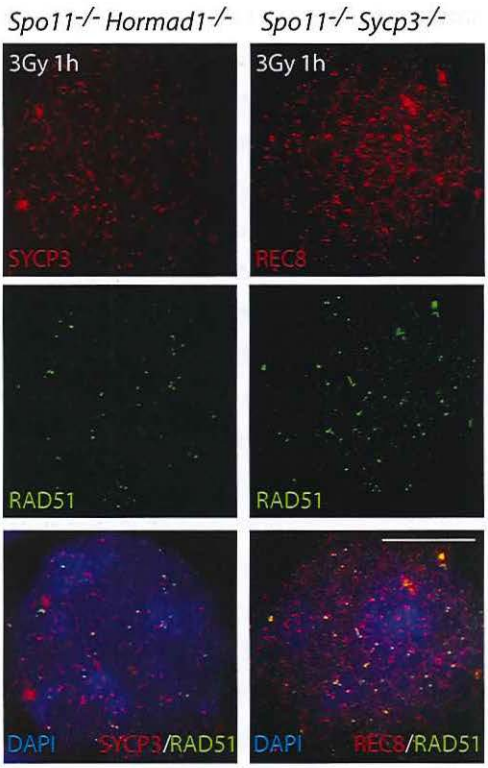

Figure 1: HORMAD1 and SYCP3 are not required to recruit damage-induced DSB foci to the chromosomal axes
Spread leptotene nuclei from *Spo11*$^{-/-}$/*Hormad1*$^{-/-}$ and *Spo11*$^{-/-}$/*Sycp3*$^{-/-}$ male mice were prepared at 1h following irradiation (3Gy), and stained for RAD51 (green) and SYCP3/REC8 (red) as indicated. The bottom panel shows overlaid images with the DAPI-stained DNA (blue). For both genotypes, the vast majority of RAD51 foci that can be observed colocalize with short patches of axial element. Scale bar represents 20μm.

ing hotspots to the synaptonemal complex before DSB formation. Recently, we analysed recruitment of radiation-induced DSBs to the chromosomal axes in double mutants for *Spo11* and either *Hormad1* or *Sycp3*. We performed immunostainings for RAD51 to localize the repair foci, in combination with visualization of the chromosomal axes by either SYCP3 or the meiosis-specific cohesin REC8. We observed that the majority of RAD51 foci appeared to colocalize with the short axial element fragments (Figure 1). This indicates that neither SYCP3 nor HORMAD1 are indispensable for relocalisation of DSB repair foci to the chromosomal axes. Since SYCP2 is lost from the chromosomal axes in *Sycp3*$^{-/-}$ spermatocytes (Pelttari et al, 2001), this also excludes a critical role for SYCP2 in relocalisation of damage-induced DSBs to the chromosomal axes. Interestingly, in spermatocytes from mice lacking the meiosis-specific cohesins REC8 and RAD21L, RAD51 accumulation was strongly reduced, but DMC1 and RPA appeared to accumulate in foci (Ishiguro et al, 2014). In the images provided in that paper, it is difficult to assess if these foci colocalize with the remnant SYCP3 fragments that are still present, pre-

venting a definite conclusion about the possible role of these cohesion components in tethering meiotic DSB forming complexes to the chromosomal axes.

In somatic cells, there is a known connection between cohesin recruitment and damage-induced DSB repair, and it appears that SCC1(also named RAD21, and paralog of REC8 and RAD21L) is required for the recruitment of extra cohesin to DSBs, perhaps to ensure close proximity of sister chromatids (Heidinger-Pauli et al, 2008). Replacement of RAD21 by REC8 abolishes damage-induced cohesin recruitment. This function of REC8 may have been adapted in meiosis, not to enhance sister chromatid cohesion, but to recruit the damaged DNA to the cohesion-enriched chromosomal axes. In budding yeast meiosis, Rec8 binding sites coincide with Spo11 binding sites, and mutation of *Rec8* reduces Spo11 recruitment (Spallanzani et al, 2013). Analysis of damage-induced DSB repair foci in combined mutants of *Spo11* and genes encoding meiotic components of the cohesin complex could provide more definite insight in this matter.

Initial accumulation of recombinases on meiotic DSBs

Once SPO11 has cut the double-stranded DNA, it becomes covalently attached to the DNA, and because of the homodimerization between two SPO11 molecules, this initially tethers the two ends together (Keeney et al, 1997). Subsequently, the combined endo- and exo-nuclease activities of CTIP, the MRN complex, and EXO1 most likely (based on observations in both budding and fission yeast meiosis) mediate formation of single-stranded DNA (Garcia et al, 2011; Milman et al, 2009) that is rapidly bound by the RPA complex (Sakaguchi et al, 2009; Wang et al, 2005). Indeed, we have observed numerous RPA foci in early leptotene nuclei (Chapter 2). Subsequently, RPA is replaced by DMC1 and RAD51. This appears to occur fairly rapidly, since RPA and DMC1 foci show hardly any overlap (Chapter 2). At low resolution, in *Spo11*$^{+/YF}$ leptotene spermatocytes (where YF refers to the SPO11 mutation, which was investigated as described in Chapters 2 and 3), we observed approximately 1.5 fold more RAD51 foci compared to DMC1 foci. At pachytene, the RAD51/DMC1 foci ratio has dropped to 1.2. This is similar to observations of Cole et al. (2012), who quantified a RAD51/DMC1 foci ratio of around 2 in leptotene, 1.5 in early zygotene, and 1.1 in late zygotene, in *Spo11*$^{+/-}$ spermatocytes (Cole et al, 2012). From this, it appears that RAD51 initially accumulates at more foci, but both RAD51 and DMC1 have their foci peak at early zygotene. By the

time pachytene is reached, the RAD51 and DMC1 foci have decreased to more or less equal numbers. In our quantifications, DMC1 foci may be underestimated because the anti-DMC1 signal to noise ratio is less optimal compared to that of anti-RAD51, and the threshold for quantification of foci number is set manually. In dSTORM imaged nuclei, the number of DMC1-positive foci does not dramatically differ from the number of RAD51-positive foci. This suggests that the super-resolution techniques allowed us to detect DMC1 molecules that fell below the sensitivity limit of previous analysis using widefield microscopy, where foci that were interpreted as RAD51-only may actually be composed of both proteins. According to the speculative model presented in Chapter 4, DMC1 accumulates first, on both ends of the DSB, and RAD51 subsequently forms a longer filament, on one side of the DSBs, leading to the predominance of DSB repair foci containing a single DMC1 and a single RAD51 domain (D1R1 group) in leptotene. Comparing the high resolution to the low resolution data, it might be suggested that the initial accumulation of DMC1 at short resected ends is frequently missed at low resolution. This may be due to the limited DMC1 protein amount at the DSB-ends that likely is present in the earliest repair intermediates. From this perspective, absolute quantification of the number of detected molecules of either recombinase per focus, in nuclei imaged by dSTORM, would greatly enhance our knowledge about meiotic recombination nodules, and may provide a new perspective for understanding the mechanism of DSB repair during meiotic prophase. Direct labelling of RAD51 and DMC1 or expression of fusion proteins with a fluorescent label in meiotic cells, would be instrumental for more accurate quantification of recombinase molecules.

At damage-induced DSBs we also observed colocalisation of RAD51 and DMC1 at low resolution, indicating that both proteins are able to accumulate. At present, we do not know whether the proposed asymmetric accumulation of RAD51 at SPO11-induced DSBs also occurs at damage-induced sites. Interestingly, we observed only 10% more RAD51 foci compared to DMC1 foci at 30 minutes following irradiation, and almost equal numbers of RAD51 and DMC1 foci were observed at 60 minutes following irradiation in leptotene spermatocytes in a *Spo11*$^{YF/YF}$ background (Chapter 3). The damage at these radiation-induced foci was induced 60 minutes before the animal was killed, so that it might be expected that there is more homogeneity in the type of recombination intermediates that are present at this timepoint, compared to non-irradiated wild type leptotene spermatocytes.

Indeed, the timing of SPO11-induced DSB formation in leptotene spermatocytes may vary considerably between and within individual cells. Thus, it will be particularly interesting to apply the super-resolution analysis described in Chapter 4 to the composition of damage-induced repair foci in spermatocytes.

Homology search and partner choice

In order for meiotic homologous recombination repair to contribute to homologous chromosome recognition, at least one of the single-stranded ends of the DSB should connect with homologous DNA of the partner chromosome. This does not necessarily have to occur for all the DSBs. A certain fraction may be repaired via connection with the sister chromatid, leading to exact regeneration of the lost DNA sequence. Because of this feature, such events cannot be traced by genetic methods that measure exchange of polymorphic markers between parental chromosomes. In yeast, the frequency of intersister and interhomolog recombination intermediates can be visualised (described in Chapter 1) and it was established that there is a 10:1 ratio of interhomolog over intersister joint molecules (Kim et al, 2010; Schwacha and Kleckner, 1994). This results in a 5:1 ratio of double Holliday junctions (dHJs) formed between homologs versus sisters (Kim et al, 2010). If all templates are equally readily available, a 2:1 ratio of interhomolog versus intersister interactions would be expected, because there is one intact sister template and 2 intact templates on the homologous chromosome. In somatic cells, it would be intuitively expected that the close vicinity of sister chromatids would lead to an intrinsic bias for the formation of recombination intermediates between sister chromatids instead of between the homologs. Based on recent genetic data on yeast meiotic cells it has been proposed that the initial loading of recombinases occurs on one end of the DSB, followed by capture of the sister chromatid by the Rad51 filament (Hong et al, 2013). In this model, the presence of the cohesin Rec8 allows strand invasion in the sister chromatid, but Rad51 and Dmc1, in conjunction with additional regulators and components of the synaptonemal complex (Busygina et al, 2008; Lai et al, 2011; Lin et al, 2010; Niu et al, 2005; Sheridan and Bishop, 2006; Wan et al, 2004; Wu et al, 2010), would inhibit formation of recombination intermediates with the sister chromatid (see Table 1, Chapter 1). The engagement of one end with the sister chromatid would thus lead the other end of the DSB to more likely search for a different homologous DNA strand (i.e. the DNA of the homologous

chromosome), promoting an interhomolog bias (Hong et al, 2013). Subsequently, meiosis-specific proteins ensure that the DSB end that is associated with the sister is unlikely to form a double Holliday junction (Hong et al, 2013). Rather, capture of this second end to the interhomolog intermediate is favoured.

The data presented in Chapter 3 indicate that damage-induced DSBs in mouse meiocytes also undergo the interhomolog bias, similar to SPO11-induced DSBs, as revealed by the finding that these damage-induced DSBs are repaired with slower kinetics in a SPO11-deficient compared to a SPO11-proficient background. A genetic approach could be used to determine if mouse homologs of the genes that mediate the interhomolog bias in yeast play a similar role in regulation of partner choice in mouse meiosis as well. Double knockout of one of these genes and *Spo11*, might allow more efficient repair of damage-induced DSBs in spermatocytes compared to what can be achieved in a single *Spo11* knockout background. This would then reflect a switch to a more mitotic mode of homologous recombination, involving an intersister bias. Using this approach, the repair kinetics of damage-induced DSBs is used as readout of the interhomolog (slow repair) versus the intersister (fast repair) pathways (Figure 2). In this type of assay, we will not be able to quantitatively determine interhomolog versus intersister ratios of recombination intermediates. For this we would need an assay to determine the alleles that are involved in joint molecule formation upon induction of DSBs in meiocytes by either SPO11 or irradiation, as can be performed for yeast hotspots. Ideally, further development of the single molecule microscopy described in Chapter 4 could allow visualization of DNA strands which have been previously labelled with fluorescent nucleotides.

By detailed analysis of RAD51 and DMC1 localisation patterns, we have so far identified two predominant early repair intermediates. The so-called D1R1 intermediate may represent the initial asymmetric loading of RAD51 and DMC1, as suggested for yeast meiotic recombination, and from this intermediate the D2R1 intermediate may evolve. According to the present model, this would involve a DMC1 domain on a quiescent DSB end, and a DMC1 domain followed by an elongated RAD51 domain on the end that is resected further and invades one of the chromatids on the homologous chromosome. First it should be assessed if these two repair intermediates are also detected in a population of radiation-induced RAD51/DMC1 foci on a SPO11-deficient background. From the genetic analysis previously described, we may identify genes involved in the interhomolog bias that,

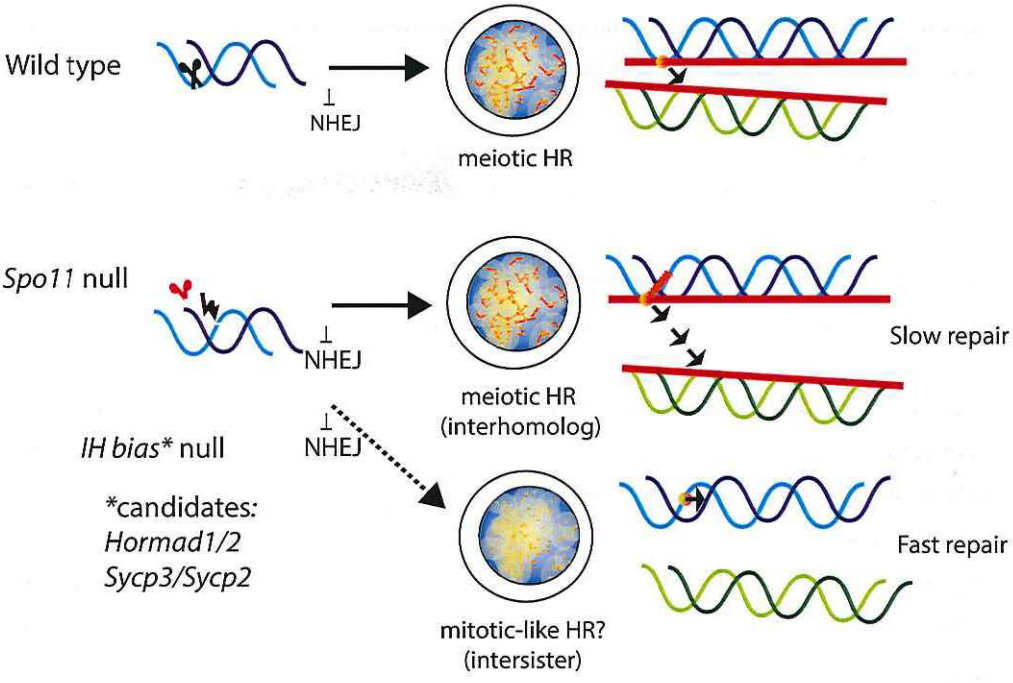

Figure 2: Analysis of damage-induced DSB repair dynamics to identify components of the interhomolog bias mechanism

In wild type meiocytes, SPO11 (indicated by scissors) will generate programmed meiotic DSBs (orange circle) that are processed on the chromosomal axes, and are subject to the interhomolog bias. Thereby their repair contributes to the establishment of homologous chromosome interactions. In *Spo11* knockout meiocytes, DSBs can be induced by exogenous damage. These DSBs are rapidly recruited to the chromosomal axes (indicated by orange zigzag line), and also subject to the interhomolog bias. This repair process occurs at a slow pace. We anticipate that removal of mediators of the interhomolog bias in a *Spo11* knockout background will allow damage-induced DSBs to be more rapidly repaired through inter-sister HR, as it occurs in mitotic cells. These mediators of interhomolog bias may be associated with absence or defects in the formation of the axial element (red line) of the SC, such as HORMAD1 and SYCP3. IH bias = interhomolog bias

if mutated, facilitate radiation-induced DSB repair on a SPO11-deficient background. In this experimental set up, we should analyse whether we may observe a change in the composition of the DMC1/RAD51 foci configuration by dSTORM imaging, to identify what type of intermediate may represent an intersister invasion. In addition, single molecule localisation of the single-stranded DNA-binding molecule RPA, components of the MRN complex, or accessory factors for loading and activity of the recombinases, combined with one of the recombinases, may provide further information that will lead to improvements of our current model. Lack or

impairment of chromosome synapsis, due to absence of any component of the synaptonemal complex, always results in failure to complete repair of meiotic DSBs. A reasonable explanation could be related to the lack of stable interchromosomal interactions, which may be necessary for proper formation of joint molecules. This hypothesis is supported by the observation of a larger distance between DMC1 clusters in the D2R1 foci in *Sycp1*$^{-/-}$ spermatocytes, as reported in Chapter 4, which may mirror a larger distance between the DNA molecules involved in HR. Alternatively, the components of the synaptonemal complex may provide a structural platform for proper assembly of the recombination machinery, or they might be involved in recombination partner choice, as has been shown for the yeast SC protein Red1. Based on this hypothesis, mutation of genes encoding such proteins may affect the configuration of recombination foci. By using the 3D-SIM dSTORM combined approach applied as described in Chapter 4, several aspects could be assessed, such as the relative amount of RAD51 compared to DMC1 and the spatial organization of the two recombinases within foci.

Fate of exogenous DSBs induced later in meiotic prophase

We did not observe major differences in the composition of RAD51/DMC1 foci on synapsed and not yet synapsed (referred to as non-synapsed) axes (described above, this chapter). Still, achievement of synapsis results in drastic changes in the molecular composition of the immediate vicinity of recombination intermediates, when axial elements become lateral elements, interacting with other SC components. In addition, it would be expected that repair of DSBs has progressed further once synapsis has been achieved, compared to the non-synapsed situation. Indeed, we observe a decrease in the number of D1R1 foci on synapsed compared to non-synapsed chromatin. Based on the observation that better achievement of synapsis correlates with faster repair, it might be suggested that early repair intermediates on synapsed axes might be relieved from the interhomolog bias, allowing faster repair via the sister chromatid. From that perspective it is interesting to study the kinetics of repair of damage-induced breaks on synapsed axes. In a previous study, Ahmed et al. (2010), showed that >80% of radiation-induced (1 Gy) γH2AX foci in early pachytene nuclei had disappeared already at 8h following damage induction (Ahmed et al, 2010). This appears to be much faster compared to what can be achieved when damage is induced at leptotene in SPO11-deficient cells, where 40%

of the damage is still present after 48 hours (Chapter 3). When we analysed accumulation of recombinases in wild type pachytene nuclei, shortly after irradiation (5 Gy), we observed hardly any increase in DMC1 foci numbers, but approximately 20 damage-induced RAD51 foci, that were relocated to the chromosomal axes (Figure 3). This finding indicates that DMC1 can no longer be loaded at newly processed DSB ends, once cells have reached pachytene, whereas this still occurs for RAD51, albeit to a much lower extent compared to the number of radiation-induced foci that we observed in leptotene nuclei (around 84) (Chapter 2). This reduced RAD51 recruitment is most likely related to the fact that part of the damage-induced DSBs in pachytene can be channelled into the non-homologous end joining (NHEJ) pathway, which is not possible in leptotene. This conclusion is based on two obser-

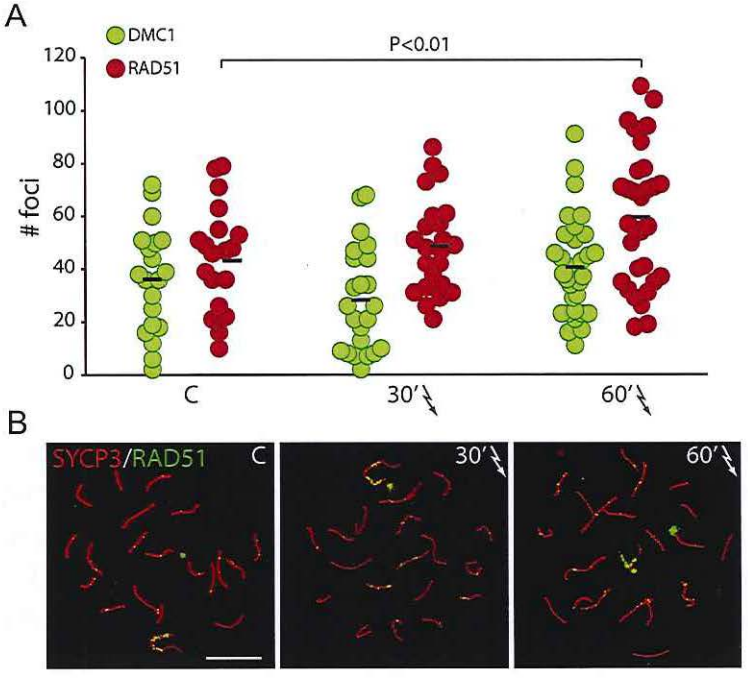

Figure 3: Recombinase recruitment to radiation-induced DSBs in wild type pachytene spermatocytes

(A) RAD51 and DMC1 foci were quantified in control pachytene spermatocyte nuclei and in pachytene spermatocyte nuclei that were spread at 30 and 60 minutes after irradiation with 5Gy. The number of DMC1 foci is not changed upon irradiation, whereas on average around 20 additional RAD51 foci are observed after 60 minutes (P<0.01). **(B)** RAD51 foci localize on the SC in the absence and presence of damage-induced DSBs. Scale bar represents 10 μm.

vations. First, a positive regulator of NHEJ, 53BP1 is expressed from midpachytene onwards (Ahmed et al, 2007), and we observed nucleus-wide accumulation of this protein upon irradiation of pachytene nuclei, but not in leptotene nuclei (Figure 4A). Second, we observed a similar level of damage-induced γH2AX signal in irradiated wild type pachytene nuclei, compared to irradiated SPO11-deficient leptotene nuclei (Figure 4B). Taking into account the limited DMC1 accumulation upon irradiation of pachytene cells, observed in widefield microscopy analysis, it would be interesting to analyse radiation-induced foci in such nuclei by dSTORM, to compare low to high resolution data. In experiments performed on wild type spermatocyte nuclei, DMC1 presence was observed by dSTORM in foci where no signal was detected in widefield images. This may indicate that the quantification of foci performed so far in widefield images may have underestimated DMC1 accumulation. Alternatively, if DMC1 is actually no longer loaded on recombination foci induced at pachytene, dSTORM imaging could be used to assess how RAD51-only configurations may differ from the patterns formed by DMC1 and RAD51 together.

Once the repair process proceeds further the recombinases should be removed, for DNA synthesis to occur. Previously, it has been shown that RAD51 removal appears impaired in *Rad54* knockout spermatocytes, leading to the formation of large linear aggregates that extend from the SC (Wesoly et al, 2006). Interestingly, DMC1 appears to be already mostly lost from recombination foci in the cells that display this aberrant RAD51 staining pattern, indicating that a factor other than RAD54 might be responsible for DMC1 removal. In budding yeast, Rdh4/Tid1 has been reported to perform a RAD54-like function in DMC1 metabolism (Holzen et al, 2006; Nimonkar et al, 2012; Shinohara et al, 2003). A mouse homolog has not yet been identified, although RAD54B has been proposed as a candidate (Tanaka et al, 2002). It would be of interest to analyse the pattern of DMC1 in *Rad54/Rad54B* double-mutants, to assess if *Rad54B* mutation has an effect on DMC1 removal, and if aggregates similar to RAD51 may also be formed.

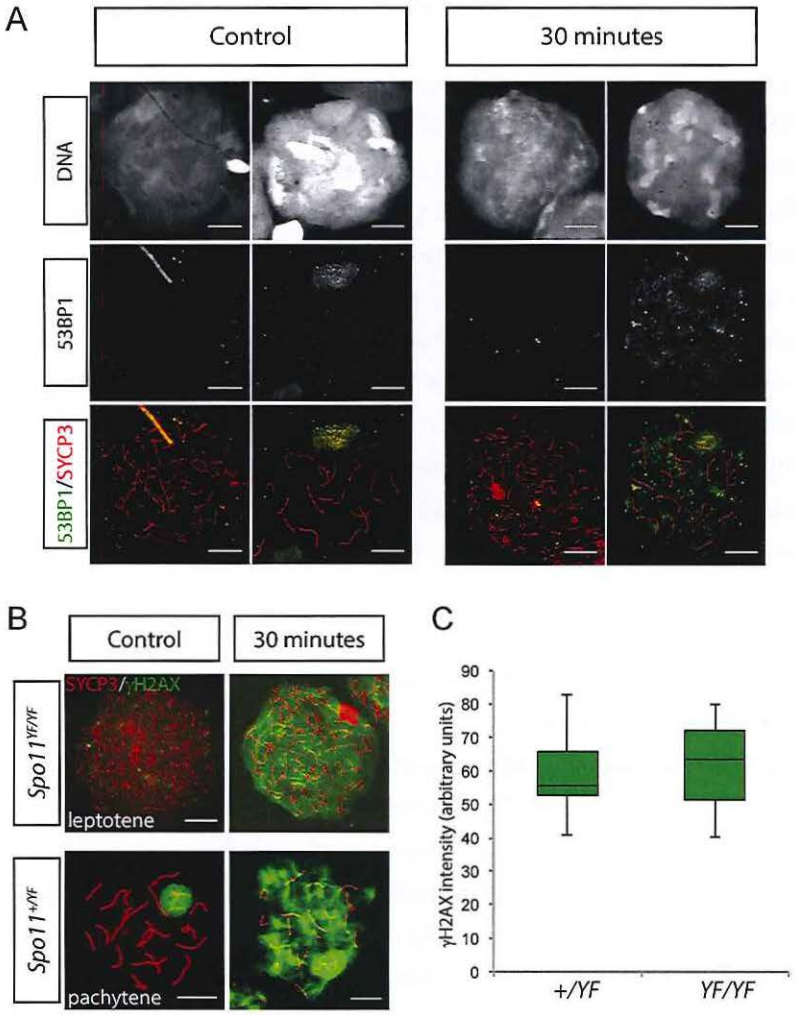

Figure 4: Different response to DNA damage in leptotene and pachytene spermatocytes
(A) Spread leptotene and pachytene nuclei of control and irradiated (5Gy; 30 minutes timepoint) mice, immunostained for SYCP3 (red) and 53BP1 (green); the DNA is shown in grayscale in the top images. 53BP1 is not detectable in leptotene nuclei, irrespective of irradiation. At pachytene, 53BP1 is highly enriched in the XY body in the absence of irradiation, but displays additional accumulation on autosomal chromatin upon irradiation. Scale bar represents 10 μm. **(B)** Spread leptotene nuclei of *Spo11*$^{YF/YF}$ mouse, and pachytene nuclei of *Spo11*$^{+/YF}$ mouse immunostained for SYCP3 (red) and γH2AX (green). Irradiation (5Gy) induces nucleus-wide γH2AX accumulation in both conditions. Scale bar represents 10 μm. **(C)** Boxplots showing quantification of γH2AX accumulation at 30 minutes following irradiation, in pachytene spermatocytes from a *Spo11*$^{+/YF}$ mouse (n=13 nuclei), and in leptotene spermatocytes from a *Spo11*$^{YF/YF}$ mouse (n=22 nuclei).

FURTHER TARGETS FOR SUPER-RESOLUTION STUDIES OF MEIOSIS

Other DNA repair proteins have been observed to form meiotic foci at later stages of DSB repair, such as MSH4/5 and MLH1/3 (de Vries et al, 1999; Edelmann et al, 1999; Hunter and Borts, 1997; Lipkin et al, 2002; Santucci-Darmanin et al, 2000). These proteins are related to the yeast MutS and MutL families, respectively, which perform nucleotide mismatch repair in somatic cells. In meiotic cells these proteins are involved in joint molecule resolution. Although the role of MSH4 in determination of dHJ fate in meiosis has not been established yet, mouse spermatocytes lacking this protein do not show any crossover event. Thus, this protein may be a candidate marker of interhomolog recombination sites. Unlike MLH1, which marks sites where crossovers have formed, MSH4 foci are observed already at an earlier meiotic stage, when RAD51 foci are also still present (Neyton et al, 2004): a colocalization study of MSH4 together with recombinases could be a useful tool for identification of intermediates that are specifically representative of interhomolog recombination. In addition, a super resolution microscopy approach could provide new insight in the actual role of MSH4 during meiosis by defining the organization of molecules within MSH4 foci.

Recently, two enzymes have been reported to contribute to crossover site designation: the SUMO-ligase RNF212 (Reynolds et al, 2013) and the ubiquitin ligase HEI10, which appear to have antagonistic functions (Qiao et al, 2014). These proteins would therefore be excellent candidates for dSTORM imaging to determine if their presence can be related to specific meiotic recombination intermediates that are in progression towards forming a crossover.

It appears rather clear that several proteins, identified to be important for meiotic recombination, would be interesting targets of super-resolution microscopy studies. Ideally, these proteins should be directly labelled to perform accurate single molecule localization analysis, which implies the generation of transgenic mouse models expressing fluorescent-tagged proteins in meiotic cells. This brings us to the ever-resurfacing drawback of studies on mammalian meiosis, the lack of in vitro models. To fully explore the genetic and molecular details of meiotic DSB repair, development of a method to efficiently induce meiotic entry followed by chromosome pairing and crossover formation in an in vitro culture system that can be genetically manipulated would allow the field to move forward at a much faster pace.

References

Agmon N, Liefshitz B, Zimmer C, Fabre E, and Kupiec M (2013). Effect of nuclear architecture on the efficiency of double-strand break repair. Nat Cell Biol *15*:694-699.

Ahmed EA, Philippens ME, Kal HB, de Rooij DG, and de Boer P (2010). Genetic probing of homologous recombination and non-homologous end joining during meiotic prophase in irradiated mouse spermatocytes. Mutat Res *688*:12-18.

Ahmed EA, van der Vaart A, Barten A, Kal HB, Chen J, Lou Z, Minter-Dykhouse K, Bartkova J, Bartek J, de Boer P, *et al.* (2007). Differences in DNA double strand breaks repair in male germ cell types: lessons learned from a differential expression of Mdc1 and 53BP1. DNA Repair (Amst) *6*:1243-1254.

Arnheim N, Calabrese P, and Tiemann-Boege I (2007). Mammalian meiotic recombination hot spots. Annu Rev Genet *41*:369-399.

Ashley T, Gaeth AP, Creemers LB, Hack AM, and de Rooij DG (2004). Correlation of meiotic events in testis sections and microspreads of mouse spermatocytes relative to the mid-pachytene checkpoint. Chromosoma *113*:126-136.

Baarends WM, Wassenaar E, van der Laan R, Hoogerbrugge JW, Sleddens-Linkels E, Hoeijmakers JH, de Boer P, and Grootegoed JA (2005). Silencing of unpaired chromatin and histone H2A ubiquitination in mammalian meiosis. Molecular and Cellular Biology *25*:1041-1053.

Baudat F, Buard J, Grey C, Fledel-Alon A, Ober C, Przeworski M, Coop G, and de Massy B (2010). PRDM9 is a major determinant of meiotic recombination hotspots in humans and mice. Science *327*:836-840.

Baudat F, Manova K, Yuen JP, Jasin M, and Keeney S (2000). Chromosome synapsis defects and sexually dimorphic meiotic progression in mice lacking spo11. Mol Cell *6*:989-998.

Bellani MA, Romanienko PJ, Cairatti DA, and Camerini-Otero RD (2005). SPO11 is required for sex-body formation, and Spo11 heterozygosity rescues the prophase arrest of Atm-/- spermatocytes. J Cell Sci *118*:3233-3245.

Busygina V, Sehorn MG, Shi IY, Tsubouchi H, Roeder GS, and Sung P (2008). Hed1 regulates Rad51-mediated recombination via a novel mechanism. Genes Dev *22*:786-795.

Cole F, Kauppi L, Lange J, Roig I, Wang R, Keeney S, and Jasin M (2012). Homeostatic control of recombination is implemented progressively in mouse meiosis. Nat Cell Biol *14*:424-430.

de Vries SS, Baart EB, Dekker M, Siezen A, de Rooij DG, de Boer P, and te Riele H (1999). Mouse MutS-like protein Msh5 is required for proper chromosome synapsis in male and female meiosis. Genes Dev *13*:523-531.

Dion V, Kalck V, Horigome C, Towbin BD, and Gasser SM (2012). Increased mobility of double-strand breaks requires Mec1, Rad9 and the homologous recombination machinery. Nat Cell Biol *14*:502-509.

Edelmann W, Cohen PE, Kneitz B, Winand N, Lia M, Heyer J, Kolodner R, Pollard JW, and Kucherlapati R (1999). Mammalian MutS homologue 5 is required for chromosome pairing in meiosis. Nat Genet *21*:123-127.

Eijpe M, Offenberg H, Jessberger R, Revenkova E, and Heyting C (2003). Meiotic cohesin REC8 marks the axial elements of rat synaptonemal complexes before cohesins SMC1beta and SMC3. J Cell Biol *160*:657-670.

Fernandez-Capetillo O, Mahadevaiah SK, Celeste A, Romanienko PJ, Camerini-Otero RD, Bonner WM, Manova K, Burgoyne P, and Nussenzweig A (2003). H2AX is required for chromatin remodeling and inactivation of sex chromosomes in male mouse meiosis. Dev Cell *4*:497-508.

Garcia V, Phelps SE, Gray S, and Neale MJ (2011). Bidirectional resection of DNA double-strand breaks by Mre11 and Exo1. Nature *479*:241-244.

Ghamari A, van de Corput MP, Thongjuea S, van Cappellen WA, van Ijcken W, van Haren J, Soler E, Eick D, Lenhard B, and Grosveld FG (2013). In vivo live imaging of RNA polymerase II transcription factories in primary cells. Genes Dev *27*:767-777.

Goedecke W, Eijpe M, Offenberg HH, van Aalderen M, and Heyting C (1999). Mre11 and Ku70 interact in somatic cells, but are differentially expressed in early meiosis. Nat Genet *23*:194-198.

Graves JA (2006). Sex chromosome specialization and degeneration in mammals. Cell *124*:901-914.

Grey C, Barthes P, Chauveau-Le Friec G, Langa F, Baudat F, and de Massy B (2011). Mouse PRDM9 DNA-binding specificity determines sites of histone H3 lysine 4 trimethylation for initiation of meiotic recombination. PLoS Biol *9*:e1001176.

Heidinger-Pauli JM, Unal E, Guacci V, and Koshland D (2008). The kleisin subunit of cohesin dictates damage-induced cohesion. Mol Cell *31*:47-56.

Holzen TM, Shah PP, Olivares HA, and Bishop DK (2006). Tid1/Rdh54 promotes dissociation of Dmc1 from nonrecombinogenic sites on meiotic chromatin. Genes Dev *20*:2593-2604.

Hong S, Sung Y, Yu M, Lee M, Kleckner N, and Kim KP (2013). The logic and mechanism of homologous recombination partner choice. Mol Cell *51*:440-453.

Hopkins J, Hwang G, Jacob J, Sapp N, Bedigian R, Oka K, Overbeek P, Murray S, and Jordan PW (2014). Meiosis-Specific Cohesin Component, Stag3 Is Essential for Maintaining Centromere Chromatid Cohesion, and Required for DNA Repair and Synapsis between Homologous Chromosomes. PLoS Genet *10*:e1004413.

Hunt PA, and Eicher EM (1991). Fertile male mice with three sex chromosomes: evidence that infertility in XYY male mice is an effect of two Y chromosomes. Chromosoma *100*:293-299.

Hunter N, and Borts RH (1997). Mlh1 is unique among mismatch repair proteins in its ability to promote crossing-over during meiosis. Genes Dev *11*:1573-1582.

Ichijima YI, M., Lou Z, Nussenzweig A, Camerini-Otero RD, Chen J, Andreassen PR, and Namekawa SH (2011). MDC1 directs chromosome-wide silencing of the sex chromosomes in male germ cells. Genes Dev *25*:959-971.

Inagaki A, Schoenmakers S, and Baarends WM (2010). DNA double strand break repair, chromosome synapsis and transcriptional silencing in meiosis. Epigenetics *5*:255-266.

Ishiguro K, Kim J, Shibuya H, Hernandez-Hernandez A, Suzuki A, Fukagawa T, Shioi G, Kiyonari H, Li XC, Schimenti J, *et al.* (2014). Meiosis-specific cohesin mediates homolog recognition in mouse spermatocytes. Genes Dev *28*:594-607.

Keeney S, Giroux CN, and Kleckner N (1997). Meiosis-specific DNA double-strand breaks are catalyzed by Spo11, a member of a widely conserved protein family. Cell *88*:375-384.

Kim KP, Weiner BM, Zhang L, Jordan A, Dekker J, and Kleckner N (2010). Sister cohesion and structural axis components mediate homolog bias of meiotic recombination. Cell *143*:924-937.

Kouznetsova A, Wang H, Bellani M, Camerini-Otero RD, Jessberger R, and

Hoog C (2009). BRCA1-mediated chromatin silencing is limited to oocytes with a small number of asynapsed chromosomes. J Cell Sci *122*:2446-2452.

Kumar R, Bourbon HM, and de Massy B (2010). Functional conservation of Mei4 for meiotic DNA double-strand break formation from yeasts to mice. Genes Dev *24*:1266-1280.

Lai YJ, Lin FM, Chuang MJ, Shen HJ, and Wang TF (2011). Genetic requirements and meiotic function of phosphorylation of the yeast axial element protein Red1. Mol Cell Biol *31*:912-923.

Lin FM, Lai YJ, Shen HJ, Cheng YH, and Wang TF (2010). Yeast axial-element protein, Red1, binds SUMO chains to promote meiotic interhomologue recombination and chromosome synapsis. EMBO J *29*:586-596.

Lipkin SM, Moens PB, Wang V, Lenzi M, Shanmugarajah D, Gilgeous A, Thomas J, Cheng J, Touchman JW, Green ED, *et al.* (2002). Meiotic arrest and aneuploidy in MLH3-deficient mice. Nat Genet *31*:385-390.

Mahadevaiah SK, Bourc'his D, de Rooij DG, Bestor TH, Turner JM, and Burgoyne PS (2008). Extensive meiotic asynapsis in mice antagonises meiotic silencing of unsynapsed chromatin and consequently disrupts meiotic sex chromosome inactivation. J Cell Biol *182*:263-276.

Mahadevaiah SK, Costa Y, and Turner JM (2009). Using RNA FISH to study gene expression during mammalian meiosis. Methods Mol Biol *558*:433-444.

Mahadevaiah SK, Turner JM, Baudat F, Rogakou EP, de Boer P, Blanco-Rodriguez J, Jasin M, Keeney S, Bonner WM, and Burgoyne PS (2001). Recombinational DNA double-strand breaks in mice precede synapsis. Nat Genet *27*:271-276.

Malki S, van der Heijden GW, O'Donnell KA, Martin SL, and Bortvin A (2014). A role for retrotransposon LINE-1 in fetal oocyte attrition in mice. Dev Cell *29*:521-533.

Mehta IS, Kulashreshtha M, Chakraborty S, Kolthur-Seetharam U, and Rao BJ (2013). Chromosome territories reposition during DNA damage-repair response. Genome Biol *14*:R135.

Milman N, Higuchi E, and Smith GR (2009). Meiotic DNA double-strand break repair requires two nucleases, MRN and Ctp1, to produce a single size class of Rec12 (Spo11)-oligonucleotide complexes. Mol Cell Biol *29*:5998-6005.

Neyton S, Lespinasse F, Moens PB, Paul R, Gaudray P, Paquis-Flucklinger V, and Santucci-Darmanin S (2004). Association between MSH4 (MutS homologue 4) and the DNA strand-exchange RAD51 and DMC1 proteins during mammalian meiosis. Mol Hum Reprod *10*:917-924.

Nimonkar AV, Dombrowski CC, Siino JS, Stasiak AZ, Stasiak A, and Kowalczykowski SC (2012). Saccharomyces cerevisiae Dmc1 and Rad51 proteins preferentially function with Tid1 and Rad54 proteins, respectively, to promote DNA strand invasion during genetic recombination. J Biol Chem *287*:28727-28737.

Niu H, Wan L, Baumgartner B, Schaefer D, Loidl J, and Hollingsworth NM (2005). Partner choice during meiosis is regulated by Hop1-promoted dimerization of Mek1. Mol Biol Cell *16*:5804-5818.

Panizza S, Mendoza MA, Berlinger M, Huang L, Nicolas A, Shirahige K, and Klein F (2011). Spo11-accessory proteins link double-strand break sites to the chromosome axis in early meiotic recombination. Cell *146*:372-383.

Pelttari J, Hoja MR, Yuan L, Liu JG, Brundell E, Moens P, Santucci-Darmanin S, Jessberger R, Barbero JL, Heyting C, *et al.* (2001). A meiotic chromosomal core consisting of cohesin complex proteins recruits DNA recombination proteins and

promotes synapsis in the absence of an axial element in mammalian meiotic cells. Mol Cell Biol *21*:5667-5677.

Qiao H, Prasada Rao HB, Yang Y, Fong JH, Cloutier JM, Deacon DC, Nagel KE, Swartz RK, Strong E, Holloway JK, *et al.* (2014). Antagonistic roles of ubiquitin ligase HEI10 and SUMO ligase RNF212 regulate meiotic recombination. Nat Genet *46*:194-199.

Revenkova E, Eijpe M, Heyting C, Hodges CA, Hunt PA, Liebe B, Scherthan H, and Jessberger R (2004). Cohesin SMC1 beta is required for meiotic chromosome dynamics, sister chromatid cohesion and DNA recombination. Nat Cell Biol *6*:555-562.

Reynolds A, Qiao H, Yang Y, Chen JK, Jackson N, Biswas K, Holloway JK, Baudat F, de Massy B, Wang J, *et al.* (2013). RNF212 is a dosage-sensitive regulator of crossing-over during mammalian meiosis. Nat Genet *45*:269-278.

Romanienko PJ, and Camerini-Otero RD (2000). The mouse spo11 gene is required for meiotic chromosome synapsis. Mol Cell *6*:975-987.

Royo H, Polikiewicz G, Mahadevaiah SK, Prosser H, Mitchell M, Bradley A, de Rooij DG, Burgoyne PS, and Turner JM (2010). Evidence that meiotic sex chromosome inactivation is essential for male fertility. Curr Biol *20*:2117-2123.

Sakaguchi K, Ishibashi T, Uchiyama Y, and Iwabata K (2009). The multi-replication protein A (RPA) system--a new perspective. FEBS J *276*:943-963.

Santucci-Darmanin S, Walpita D, Lespinasse F, Desnuelle C, Ashley T, and Paquis-Flucklinger V (2000). MSH4 acts in conjunction with MLH1 during mammalian meiosis. Faseb J *14*:1539-1547.

Schwacha A, and Kleckner N (1994). Identification of joint molecules that form frequently between homologs but rarely between sister chromatids during yeast meiosis. Cell *76*:51-63.

Shanbhag NM, Rafalska-Metcalf IU, Balane-Bolivar C, Janicki SM, and Greenberg RA (2010). ATM-dependent chromatin changes silence transcription in cis to DNA double-strand breaks. Cell *141*:970-981.

Sheridan S, and Bishop DK (2006). Red-Hed regulation: recombinase Rad51, though capable of playing the leading role, may be relegated to supporting Dmc1 in budding yeast meiosis. Genes Dev *20*:1685-1691.

Shi Q, Spriggs E, Field LL, Ko E, Barclay L, and Martin RH (2001). Single sperm typing demonstrates that reduced recombination is associated with the production of aneuploid 24,XY human sperm. Am J Med Genet *99*:34-38.

Shin YH, Choi Y, Erdin SU, Yatsenko SA, Kloc M, Yang F, Wang PJ, Meistrich ML, and Rajkovic A (2007). Hormad1 mutation disrupts synaptonemal complex formation, recombination, and chromosome segregation in mammalian meiosis. PLoS Genet *6*:e1001190.

Shin YH, McGuire MM, and Rajkovic A (2013). Mouse HORMAD1 is a meiosis i checkpoint protein that modulates DNA double- strand break repair during female meiosis. Biol Reprod *89*:29.

Shinohara M, Sakai K, Shinohara A, and Bishop DK (2003). Crossover interference in Saccharomyces cerevisiae requires a TID1/RDH54- and DMC1-dependent pathway. Genetics *163*:1273-1286.

Smagulova F, Gregoretti IV, Brick K, Khil P, Camerini-Otero RD, and Petukhova GV (2011). Genome-wide analysis reveals novel molecular features of mouse recombination hotspots. Nature *472*:375-378.

Sommermeyer V, Beneut C, Chaplais E, Serrentino ME, and Borde V (2013). Spp1, a member of the Set1 Complex, promotes meiotic DSB formation in promoters by tethering histone H3K4 methylation sites

to chromosome axes. Mol Cell *49*:43-54.

Soper SF, van der Heijden GW, Hardiman TC, Goodheart M, Martin SL, de Boer P, and Bortvin A (2008). Mouse maelstrom, a component of nuage, is essential for spermatogenesis and transposon repression in meiosis. Dev Cell *15*:285-297.

Spallanzani RG, Dalotto-Moreno T, Iraolagoitia XLR, Ziblat A, Domaica CI, Avila DE, Rossi LE, Fuertes MB, Battistone MA, Rabinovich GA, *et al.* (2013). Expansion of CD11b(+)Ly6G(+)Ly-6C(int) cells driven by medroxyprogesterone acetate in mice bearing breast tumors restrains NK cell effector functions. Cancer Immunology Immunotherapy *62*:1781-1795.

Syrjanen JL, Pellegrini L, and Davies OR (2014). A molecular model for the role of SYCP3 in meiotic chromosome organisation. Elife:e02963.

Tanaka K, Kagawa W, Kinebuchi T, Kurumizaka H, and Miyagawa K (2002). Human Rad54B is a double-stranded DNA-dependent ATPase and has biochemical properties different from its structural homolog in yeast, Tid1/Rdh54. Nucleic Acids Res *30*:1346-1353.

Tarsounas M, Morita T, Pearlman RE, and Moens PB (1999). RAD51 and DMC1 form mixed complexes associated with mouse meiotic chromosome cores and synaptonemal complexes. J Cell Biol *147*:207-220.

Turner JM (2007). Meiotic sex chromosome inactivation. Development *134*:1823-1831.

Turner JM, Mahadevaiah SK, Fernandez-Capetillo O, Nussenzweig A, Xu X, Deng CX, and Burgoyne PS (2005). Silencing of unsynapsed meiotic chromosomes in the mouse. Nat Genet *37*:41-47.

Wan L, de los Santos T, Zhang C, Shokat K, and Hollingsworth NM (2004). Mek1 kinase activity functions downstream of RED1 in the regulation of meiotic double strand break repair in budding yeast. Mol Biol Cell *15*:11-23.

Wang Y, Putnam CD, Kane MF, Zhang W, Edelmann L, Russell R, Carrion DV, Chin L, Kucherlapati R, Kolodner RD, *et al.* (2005). Mutation in Rpa1 results in defective DNA double-strand break repair, chromosomal instability and cancer in mice. Nat Genet *37*:750-755.

Wesoly J, Agarwal S, Sigurdsson S, Bussen W, Van Komen S, Qin J, van Steeg H, van Benthem J, Wassenaar E, Baarends WM, *et al.* (2006). Differential contributions of mammalian Rad54 paralogs to recombination, DNA damage repair, and meiosis. Mol Cell Biol *26*:976-989.

Wojtasz L, Cloutier JM, Baumann M, Daniel K, Varga J, Fu J, Anastassiadis K, Stewart AF, Remenyi A, Turner JM, *et al.* (2012). Meiotic DNA double-strand breaks and chromosome asynapsis in mice are monitored by distinct HORMAD2-independent and -dependent mechanisms. Genes Dev *26*:958-973.

Wu HY, Ho HC, and Burgess SM (2010). Mek1 kinase governs outcomes of meiotic recombination and the checkpoint response. Curr Biol *20*:1707-1716.

Yang F, De La Fuente R, Leu NA, Baumann C, McLaughlin KJ, and Wang PJ (2006). Mouse SYCP2 is required for synaptonemal complex assembly and chromosomal synapsis during male meiosis. J Cell Biol *173*:497-507.

Yuan L, Liu JG, Hoja MR, Wilbertz J, Nordqvist K, and Hoog C (2002). Female germ cell aneuploidy and embryo death in mice lacking the meiosis-specific protein SCP3. Science *296*:1115-1118.

Yuan L, Liu JG, Zhao J, Brundell E, Daneholt B, and Hoog C (2000). The murine SCP3 gene is required for synaptonemal complex assembly, chromosome synapsis, and male fertility. Mol Cell *5*:73-83.

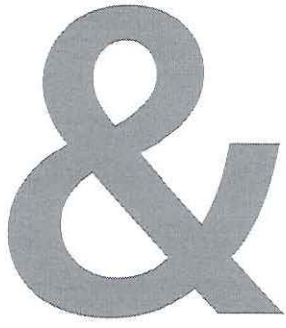

Summary

In sexually reproducing species, generation of a new organism occurs via the fusion of a maternal and a paternal gamete. Gametes are specialized cells, carrying a haploid genome. The combination of the two haploid genomes upon fertilization reconstitutes a diploid genome for the new organism. Haploidization of gametes occurs via a process named meiosis, which consists of a single DNA replication event followed by two subsequent cell divisions (meiosis I and II). During meiotic prophase I, the replicated genome undergoes homologous recombination (HR), which favours interactions between homologous chromosomes. This recombination results in genetic shuffling, thereby contributing to the generation of genetically unique haploid genomes and progeny, and also ensures a physical connection between homologs, via crossover formation, that allows proper alignment and separation of the chromosome pairs at the metaphase-to-anaphase transition. Homologous recombination in meiosis is initiated by the formation of hundreds of DNA double-strand breaks (DSBs) by the transesterase SPO11. Subsequently, a meiotic machinery is called into action, to repair these DSBs in a multi-step mechanism which is accompanied by chromosome pairing and synapsis, dynamic associations of proteins, and dynamic modifications of chromatin structure. This thesis focuses on meiotic recombination in relation to chromatin organization, in particular when homologous chromosome interactions are hampered. Chromatin in the nucleus of meiotic cells is arranged in loops via cohesins, which support and participate in the formation of a chromosomal scaffold: the synaptonemal complex. The synaptonemal complex proteins, assembled at the base of chromatin loops, form the chromosomal axes. Many meiotic events occur within this nucleo-proteinaceous framework, or are dependent on the progression of events mediated by this framework. First of all the synaptonemal complex mediates interactions between chromosomes, which result in synapsis of the homologous chromosome pairs. Lack of synapsis is associated with a transcriptional silencing response, which is named meiotic silencing of unsynapsed chromatin (MSUC). Such silencing always occurs for the largely heterologous X and Y chromosomes in male meiocytes. These sex chromosomes remain mostly unsynapsed and undergo meiotic sex chromosome inactivation (MSCI), a process that can be viewed as a specialized form of MSUC, leading to formation of the heterochromatic XY body. In **Chapter 2**, the mechanism that triggers this mei-

otic silencing process is investigated using a mouse model in which SPO11 catalytic activity is abolished, and hence, no meiotic DSBs can be induced. In meiocytes of these mice, the vast majority of chromatin remains unsynapsed, but only a limited nuclear area accumulates marks of transcriptional silencing. We show that these silenced chromosomal regions are specifically decorated with foci of proteins that are involved in DSB repair, apparently at sites of spontaneous DNA damage. This finding indicates a correlation between the presence of unrepaired DNA damage and the activation of MSUC or MSCI, similar to what has been demonstrated for silencing of chromatin in association with persistent DNA damage in mitotic cells. Thus, meiotic silencing also requires the presence of persistent DSBs, in combination with the detection of unsynapsed chromatin. To further validate this mechanistic aspect of meiotic silencing, transcriptional silencing was investigated in wild type meiotic oocytes, in which sex chromosomes are identical (two X chromosomes) and no asynapsis is expected. However, asynapsed chromosomal regions were observed relatively frequently, and they form a silenced chromatin domain in which DSB repair proteins accumulate, similar to what is found for SPO11-defective spermatocytes (and oocytes). Most interestingly, meiotic silencing in wild type oocytes can be activated even on fully synapsed chromosomes that show excessive unrepaired DSBs, indicating that persistent DNA damage alone may be sufficient to trigger transcriptional inactivation of the chromatin surrounding the damaged site.

In the absence of SPO11-induced meiotic DSBs, homologous recombination does not occur and homologous chromosome interactions are prevented. By using the mouse model lacking SPO11 catalytic activity, we investigated the fate of DSBs induced by γ-irradiation in meiotic cells (**Chapter 3**). Although not generated in a regulated manner via SPO11 and its cofactors, exogenous DSBs accumulate DNA-binding proteins involved in DNA repair, both RAD51 recombinase and its meiosis-specific counterpart DMC1. The formation of RAD51 and DMC1 foci upon irradiation only in association with the synaptonemal complex, and not at random sites in the chromatin, suggests that the randomly distributed damaged sites are first tethered to the chromosomal axes, to be able to load the recombinases. Recruitment of RAD51/DMC1 proves that repair of radiation-induced DSBs also occurs via homologous recombination (HR), akin to SPO11-dependent DSBs. HR is a repair mechanism which requires an intact homologous DNA template to

recover the missing genetic information. In meiocytes, this repair template can be found either in the sister chromatid or in the homologous chromosome. However, in SPO11-mutant meiocytes, the lack of meiotic DSBs affects homologous chromosome pairing, so that the homolog is not a readily available recombination partner as it is in SPO11-proficient meiocytes. Indeed, repair of exogenous DSBs (radiation-induced) was much less efficient in SPO11-deficient meiocytes, compared to wild type meiocytes. This observation indicates that the sister chromatid, which is available on both genetic backgrounds, is not used as a prominent recombination partner. This phenomenon has been described in yeast meiosis as interhomolog bias, and it requires several factors to favour repair of meiotic DSBs using the homologous chromosome as a recombination partner. In **Chapter 3**, we show that such a mechanism is active in mouse meiotic cells and is operational also on exogenous DSBs. Indeed, repair of a portion of radiation-induced breaks contributes to homology search in SPO11-deficient meiocytes, leading to clearly detectable occurrence of homologous chromosome associations and an increase in overall synapsis.

The exact molecular basis of the regulation of partner choice in meiotic recombination by the interhomolog bias, is still enigmatic. Studies performed in yeast and plants point to specific functions of the two recombinases that are present in meiotic cells: RAD51 and DMC1. In **Chapter 4**, we applied super-resolution microscopy (3D-SIM and dSTORM) to investigate the organization of recombinase foci and the relative accumulation patterns of RAD51 and DMC1, to obtain more insight in their possible differential functions in the process of meiotic recombination. The finding of a partitioning of recombination foci in distinct RAD51- and DMC1-specific subdomains indicates that mixed recombinase filaments are not formed. In addition, our observations indicate that the composition and the spatial organization of the RAD51/DMC1 foci undergo dynamic changes during meiotic progression, with respect to the relative amount of each recombinase and their relative position within a focus. The most represented configurations of foci consist of one DMC1 and one RAD51 subdomain (D1R1), or of two DMC1 and one RAD51 subdomain (D2R1). A possibility is that the two recombinases occupy asymmetrically the two ends of the DSB. Based on the occurrence of foci where two domains are found for DMC1, but only one domain of RAD51, we hypothesized that one end is loaded with both recombinases, whereas only DMC1 is present at the other end. Due to such differential distribution of recombinases, the two ends

may take on distinct properties, as suggested in yeast models of meiotic recombination. The results from the timecourse analysis suggest that the D2R1 configuration may evolve from the D1R1 along meiotic progression, by separation of the DMC1 domain into two clusters, when the two DSB ends diverge. These configurations may thus mirror specific substages of homologous recombination during meiosis: a recombinase loading step (D1R1) and a homology search step (D2R1). This interpretation provides a model of meiotic recombination similar to what has been proposed for budding yeast, in which meiotic DSB ends are asymmetric with respect to recombinase loading, thereby forcing only one end to branch out to perform homology search. However, further studies will be needed to translate these observations into actual mechanistic insight, and validate this hypothetical model, for mammalian species.

Chapter 5 provides a comprehensive discussion of the relationship between DSBs and meiotic processes, together with an overview of the possible directions that the study of meiotic prophase may take, also taking into account the most recent advances of microscopy technology and the high content data that this technology is able to generate.

Taken together, this thesis provides new insights about two fundamental processes of meiosis: on the one hand, the establishment of meiotic transcriptional silencing and the contribution of DSBs to elicit this mechanism; on the other hand, the meiosis-specific aspects of HR-mediated DSB repair, with respect to its role in facilitating homologous chromosome interactions and to its mechanistic regulation, promoting the interhomolog bias. Zooming in on meiosis in future experiments involving microscopic, genetic as well as biochemical approaches will undoubtedly help us to develop a clearer view on the relations between DSB repair and meiotic chromosome pairing

Samenvatting

In soorten die zich geslachtelijk voortplanten wordt het allereerste begin van een nieuw individu gevormd wanneer een mannelijke en vrouwelijk voortplantingscel, zaadcel en eicel, samensmelten bij de bevruchting. Die voortplantingscellen, gameten, zijn gespecialiseerde cellen, onder meer omdat ze een haploïd genoom bevatten. Dat wil zeggen dat van elk chromosomenpaar slechts 1 kopie in de cel aanwezig is. De fusie van twee haploïde cellen die optreedt bij de bevruchting bewerkstelligd de vorming van een organisme waarvan de cellen een diploïd genoom bevatten. Om later in de levenscyclus dan weer een cel met een haploïd genoom te vormen is het nodig dat bij het aanmaken van nieuwe zaadcellen en eicellen de meiose doorlopen wordt. Dit proces begint met een normale DNA replicatieronde, waarbij de chromosomen zich verdubbelen op dezelfde manier als wanneer een gewone celdeling (mitose) wordt voorbereid, gevolgd door twee speciale celdelingen (meiose I en meiose II). Tijdens de profase van de meiose I ontstaan interacties tussen homologe chromosomen, waarbij er paring van die homologe chromosomen optreedt en uitwisseling van grote stukken DNA door het proces van homologe recombinatie (HR). HR zorgt hiermee voor een herschikking van de genetische informatie en dit is van belang voor het vormen van gameten met een grote variatie in genetische samenstelling. Uiteindelijk is HR verder essentieel voor het verkrijgen van een daadwerkelijke verbinding tussen de homologe chromosomen, via *crossover* vorming. Deze verbinding maakt het mogelijk dat de homologe chromosoomparen zich op zodanige wijze rangschikken dat de paren op correcte wijze gescheiden kunnen worden tijdens de overgang van metafase I naar anafase I. HR in meiose wordt geïnitieerd met de vorming van enkele honderden DNA dubbelstrengsbreuken (DSBs) door het transesterase enzym SPO11. Vervolgens komt een speciaal meiotisch moleculair mechanisme op gang dat deze DSBs in een aantal stappen kan herstellen en daarbij tegelijkertijd bijdraagt aan de totstandkoming van de chromosoomparing. Al met al is dit een zeer dynamisch proces, waarbij veel verschillende eiwitten over een periode van enkele dagen interacteren met het DNA en het chromatine.

Dit proefschrift richt zich op de meiotische HR, in muizen, in relatie tot de regulatie van chromatinestructuur, met name in situaties waarbij er een probleem is ontstaan in de herkenning of de beschikbaarheid van een homoloog chromosoom.

Het chromatine in de kern van meiotische cellen is georganiseerd in lussen die aan de basis samengehouden worden met behulp van cohesine-eiwitcomplexen die bijdragen aan de vorming van een longitudinaal eiwitnetwerk, het synaptonemale complex, dat twee homologe chromosomen met elkaar verbindt. De eiwitten in dit complex vormen de chromosomale assen langs de basissen van chromatine-lussen. Veel meiotische processen spelen zich af in directe associatie met het synaptonemale complex, of zijn afhankelijk van de voortgang van gebeurtenissen die door het synaptonemale complex bewerkstelligd worden. Ten eerste wordt de directe interactie tussen de homologe chromosomen (synapsis) verzorgd door het synaptonemale complex. Wanneer synapsis niet wordt bereikt komt een mechanisme op gang dat de RNA transcriptie stillegt van chromosomen, of delen van chromosomen, die geen partner hebben gevonden. Een dergelijke uitschakeling van gentranscriptie vindt in ieder geval plaats in elke mannelijke cel die zich in de meiotische profase bevindt, en wel voor de X en Y chromosomen. Deze twee gelachtschromosomen zijn zeer verschillend van elkaar en slechts een klein deel van X en Y wordt onderling verbonden met het synaptonemale complex. Het uitschakelen van de X en Y chromosomen tijdens de mannelijke meiotische profase en de daarmee geassocieerde vorming van het zogenoemde XY lichaampje (*XY body*) in de celkern, wordt gezien als een specialisatie van een meer algemeen mechanisme dat leidt tot het stilleggen van gentranscriptie in andere gebieden zonder synapsis, in zowel mannelijke als vrouwelijke cellen in de meiotische profase. In **Hoofdstuk 2** wordt ingegaan op de processen die dit mechanisme activeren. Hierbij wordt gebruik gemaakt van een muismodel waarbij het SPO11 enzym op dusdanige wijze veranderd is dat het niet meer in staat is om DSBs te genereren. Tijdens de meiotische profase in cellen van deze muis wordt het synaptonemale complex slecht in zeer beperkte mate gevormd en wordt voor verreweg het grootste deel van de chromosomen geen synapsis verkregen. Deze blijven dus ongepaard, maar toch wordt de RNA transcriptie slechts in een gedeelte van het ongepaarde chromatine uitgeschakeld. Wij hebben aangetoond dat deze gebieden gekenmerkt worden door de aanwezigheid van eiwitten die betrokken zijn bij het herstel van DSBs. Die eiwitten markeren waarschijnlijk de plaatsen waar zich spontane DNA schade bevindt. Deze observatie geeft aan dat er een correlatie bestaat tussen de aanwezigheid van DNA schade en de activatie van het mechanisme dat de uitschakeling van genen in associatie met ongepaard chromatine bewerkstelligt. Door deze connectie vertoond dit mechanisme gelijkenis

met het uitschakelen van chromatine in gebieden met langdurig aanwezige DNA schade in mitotische cellen. Het blijkt dat niet alleen het ongepaard zijn, maar ook de aanwezigheid van DNA schade bijdraagt aan het uitschakelen van ongepaarde chromosomen of delen daarvan. Om te onderzoeken hoe algemeen deze bevinding is, hebben we ook een studie gedaan naar meiotische uitschakeling van genen in voorlopercellen van eicellen van muizen, met intact SPO11, in de profase van de eerste meiotische deling. In deze vrouwelijke cellen zijn twee X chromosomen aanwezig die normaal kunnen paren, zodat in principe geen problemen met de vorming van het synaptonemale complex worden verwacht. Toch was in een relatief groot deel van de kernen van deze voorloper-eicellen een gebied aanwezig waarin eiwitten die DSBs kunnen repareren zich opstapelden, op een manier die leek op het localisatiepatroon dat we voor deze eiwitten hadden waargenomen in mannelijke meiotische profase cellen waarbij het SPO11 enzym niet werkt. Onverwachts en zeer interessant was de observatie dat, in de zich ontwikkelende gewone eicellen, een dergelijk gebied ook wel eens gezien werd in associatie met normale vorming van het synaptonemale complex. Dit suggereert dat niet gerepareerde DNA schade op zichzelf voldoende kan zijn om het mechanisme dat de gentranscriptie uitschakelt te activeren.

Als SPO11 niet in staat is om DSBs te induceren kan er ook geen meiotische HR plaatsvinden en zijn er dus geen stabiele homologe chromosoominteracties. Door gebruik te maken van het muizenmodel waarbij SPO11 defect is, hebben we kunnen onderzoeken wat er gebeurt wanneer er onder invloed van γ-straling toch DSBs ontstaan (**Hoofdstuk 3**). Deze exogene DSBs werden niet gevormd door SPO11, maar ze zorgden toch voor een accumulatie van DNA-bindende eiwitten die betrokken zijn bij DSB herstel in meiotische cellen, zoals het recombinase RAD51 en de meiose-specifieke variant daarvan, het DMC1 eiwit. De microscopisch waarneembare plaatsen van RAD51 en DMC1 accumulatie localiseerden op het synaptonemale complex, wat suggereert dat de DSBs, die willekeurig in de kern gevormd zijn als gevolg van de straling, eerst gerelocaliseerd worden naar het synaptonemale complex, waarna de recombinases gebonden worden. De accumulatie van deze eiwitten bewijst dat de exogene DSBs op een zodanige wijze worden verwerkt dat zij, gelijk aan de SPO11-geinduceerde DSBs, meiotische HR moeten ondergaan. Het HR mechanisme vereist dat er een intacte matrijs is waarvan de missende genetische informatie kan worden gekopieerd. In cellen die zich in mei-

otische profase bevinden is er de mogelijkheid om deze informatie te kopiëren van het corresponderende DNA in de zusterchromatide, of gebruik te maken van één van de twee chromatiden van het homologe chromosoom. Echter, in cellen waarin het SPO11 enzym niet werkt is er weinig chromosoomparing en daardoor zullen de chromatiden van het homologe chromosoom over het algemeen niet direct beschikbaar zijn om als matrijs te dienen in het HR mechanisme. In een normale cel, waarbij dankzij SPO11 werking en DSB herstel de homologe chromosomen langs elkaar komen te liggen zal het homologe chromosoom mogelijk wel zodanig dichtbij zijn, dat de gewenste DNA sequentie beschikbaar is om als matrijs te dienen voor HR. Het was inderdaad zo dat de exogene DSBs op efficiëntere wijze gerepareerd werden in cellen met actief SPO11 in vergelijking met cellen met inactief SPO11. Dit resultaat geeft aan dat de zusterchromatide, die in gelijke mate beschikbaar is in beide situaties, niet de meest gebruikte partner is in het meiotische HR proces. In gist wordt een dergelijk fenomeen beschreven als interhomoloog bias. Er zijn verschillende factoren bekend die noodzakelijk zijn om ervoor te zorgen dat het HR mechanisme preferentieel uitgevoerd word met een chromatide van het homologe chromosoom in plaats van de zusterchromatide. In Hoofdstuk 3 laten we zien dat een dergelijk mechanisme ook operationeel is tijdens de meiotische profase in de muis en dat tevens de exogene DSBs die door straling zijn geïnduceerd aan deze bias worden onderworpen. Deze conclusie wordt ondersteund door de observatie dat het herstel van een deel van de exogene DSBs bijdraagt aan homologe chromosoomassociaties en een toename in de synaptonemaal complex vorming.

De precieze moleculaire basis van het mechanisme dat de partnerkeuze, in de context van meiotische HR, in de richting van het homologe chromosoom bewerkstelligt is nog niet bekend. Resultaten van experimenten die zijn uitgevoerd in gist en planten wijzen erop dat in dit proces de recombinases RAD51 en DMC1 een rol van betekenis spelen. In **Hoofdstuk 4** hebben we super-resolutie microscopie gebruikt (3D-SIM en dSTORM), om de organisatie van de structuren waarin de recombinases accumuleren precies te bepalen, om op die manier meer inzicht te krijgen in de manier waarop elk van deze recombinases wellicht op specifieke wijze bijdraagt aan meiotische HR. De waargenomen verdeling van RAD51 en DMC1 in specifieke subdomeinen van de recombinatiestructuren geeft aan dat de twee eiwitten geen gemengde recombinase-filamenten vormen. Daarnaast wijzen onze observaties erop dat de samenstelling en de precieze organisatie van RAD51- en

DMC1-bevattende structuren op dynamische wijze verandert tijdens de voortgang van de meiotische profase. Hierbij verandert namelijk de relatieve hoeveelheid van elk van de twee recombinases en hun positie ten opzichte van elkaar. Twee configuraties werden relatief vaak waargenomen, een configuratie met één DMC1 en één RAD51 subdomein (D1R1), of een combinatie bestaande uit twee DMC1 subdomeinen en één RAD51 subdomein (D2R1). Het zou kunnen dat de twee recombinases op asymmetrische wijze gebonden zijn aan de twee uiteinden van een DSB. Gebaseerd op de frequente aanwezigheid van de D2R1 configuratie kwamen we tot de hypothese dat het vaak zal voorkomen dat het ene DSB uiteinde beide recombinases accumuleert terwijl het andere uiteinde alleen DMC1 bindt. Zulke verschillen in accumulatie kunnen bijdragen aan het ontstaan van verschillen in functionele eigenschappen tussen de twee DSB uiteinden, zoals ook gesuggereerd wordt in modellen die zijn ontwikkeld voor meiotische HR in gist. De analyse van recombinatiestructuren in cellen in opeenvolgende stadia van de meiotische profase zoals beschreven in **Hoofdstuk 4** levert de suggestie dat de D2R1 configuratie mogelijk ontstaat uit de D1R1 configuratie. Dit zou kunnen worden verklaard door een vergroting van de afstand tussen de twee DSB uiteinden, waarbij het DMC1 subdomein dat in eerste instantie beide uiteinden bevat nu zichtbaar wordt als twee subdomeinen. De twee configuraties zouden dus een representatie kunnen zijn van twee opeenvolgende fases in de meiotische homologe recombinatie: een eerste fase waarin de recombinases asymmetrisch worden gebonden aan de twee DSB uiteinden (D1R1), en een tweede fase waarin het zoeken naar homologie aanvangt (D2R1). Deze interpretatie leidt tot een model voor meiotische recombinatie in de muis dat sterke overeenkomsten vertoond met datgene wat is beschreven voor gist. Ook voor gist werd voorgesteld dat de twee DSB uiteinden op asymmetrische wijze associëren met RAD51 en DMC1, waarbij het ene DSB uiteinde vrij kan bewegen in een zoektocht naar een DNA matrijs voor reparatie, terwijl het andere uiteinde minder actief is. Het is echter noodzakelijk om meer experimenten uit te voeren om onze eerste observaties in meer detail te kunnen vertalen in moleculaire gebeurtenissen tijdens de meiotische HR, zodat het huidige model voor meiotische HR in zoogdieren een breder gefundeerde basis krijgt.

Hoofdstuk 5 vormt een afsluitend hoofdstuk met een discussie over de relatie tussen DSBs en meiotische processen. Daarnaast wordt beschreven hoe het vervolgonderzoek betreffende meiotische profase zich verder zou kunnen ontwikkelen,

met name in de context van de nieuwe ontwikkelingen op het gebied van de super-resolutiemicroscopie. Alles bij elkaar genomen biedt dit proefschrift nieuwe inzichten betreffende fundamentele aspecten van meiose, met name de homologe recombinatie (HR). Enerzijds werd meer inzicht verkregen in het bewerkstelligen van transcriptionele uitschakeling en de rol van DSBs in dit proces, en anderzijds heeft het onderzoek geleid tot nieuwe ideeën betreffende meiose-specifieke aspecten van HR tijdens de meiotische profase. Dit neemt niet weg dat verder onderzoek naar de manier waarop homologe interacties tot stand komen en hoe dit gekoppeld is aan mechanistische aspecten van de voorkeur voor interhomologe interactie bij reparatie van DNA breuken nog veel verrassende waarnemingen met zich mee zal brengen, die ons een helderder inzicht zullen verschaffen.

LIST OF ABBREVIATIONS

AE	axial element
A. thaliana	*Arabidopsis thaliana*
ATM	ataxia telangiectasia mutated
ATR	ATM- and RAD3-related
BAC	bacterial artificial chromosome
bp	base pair
CE	central element
CO	crossover
CTs	chromosome territories
CTIP	CtBP-interacting protein
D-loop	displacement loop
DAPI	4',6-diamidino-2-phenylindole
DDR	DNA damage response
DISC	double-strand break -induced silencing *in cis*
DNA	deoxyribonucleic acid
DNA PKcs	DNA-dependent protein kinase catalytic subunit
dHJ	double Holliday junction
dsDNA	double-stranded DNA
DSB	DNA double-strand break
dSTORM	direct Stochastic Optical Reconstruction Microscopy
FISH	fluorescence *in situ* hybridization
GFP	green fluorescent protein
Gy	Gray
γH2AX	phosphorylated histone H2AX
HR	homologous recombination
IH	inter-homolog
IS	inter-sister
JMs	joint molecules
kb	kilobase
KDE	kernel density estimation
LE	lateral element
LINE	long interspersed nuclear element

MEA	mono-ethanolamine
MMR	mismatch repair
MRN complex	MRE11-RAD50-NBN complex
MSCI	meiotic sex chromosome inactivation
MSUC	meiotic silencing of unsynapsed chromatin
NCO	non-crossover
NHEJ	non-homologous DNA end-joining
nt	nucleotide
PAR	pseudo-autosomal region
PHD	plant homeo domain
RNA	ribonucleic acid
RNA pol II	RNA polymerase II
ROI	region of interest
ROS	reactive oxygen species
RPA	replication protein A
S. cerevisiae	*Saccharomyces cerevisiae*
SC	synaptonemal complex
SDSA	synthesis-dependent strand annealing
SET domain	Su(var)3-9/E(z)/Trx domain
3D-SIM	3dimensional-structured illumination microscopy
SMC	structural maintenance of chromosomes
SNP	single nucleotide polymorphism
ssDNA	single-stranded DNA
STAG1/2/3	stromal antigen protein 1/2/3
SUMO	small ubiquitin-like modifier
TAR	transcription-associated recombination
TF	transverse filament
TIRF	total internal reflection fluorescence

Curriculum vitae

Name Fabrizia Carofiglio
Date of birth March 15th 1986
Place of birth Bari
e-mail address f.carofiglio@erasmusmc.nl

Education

June 2010- November 2014	PhD student at the Department of Reproduction and Development, Erasmus MC, Erasmus University, Rotterdam (NL)
October 2007 - March 2010	Master in Medical Biotechnology and Molecular Medicine, University of Bari (IT) Final grade: 110/110 *cum laude*
October 2004 - July 2007	Bachelor in Health and Pharmaceutical Biotechnology, University of Bari (IT) Final grade: 110/110 *cum laude*
September 1999 - July 2004	Scientific High School, Liceo Scientifico "Arcangelo Scacchi", Bari (IT) Final grade: 100/100 *cum laude*

Research experience

Research experience

June 2010- November 2014	*Department of Reproduction and Development, Erasmus MC, Rotterdam (NL)* Zooming in on chromosomes in mouse meiosis. Prof. Dr. JA Grootegoed & Dr Ir WM Baarends
May 2009 - March 2010	*Department of Cell and Developmental Biology, University of Rome "La Sapienza", Rome (IT)* Development of an episomal vector for RNAi-mediated silencing of ENaC. Prof. F Ascenzioni & Dr M Ventura
March 2007 - July 2007	*Department of Genetics and Microbiology, University of Bari "Aldo Moro", Bari (IT)* Analysis by FISH of a case of Duchenne Muscular Dystrophy. Dr M Ventura

PhD Portfolio

Summary of PhD training and teaching

Name PhD student: Fabrizia Carofiglio Erasmus MC Department: Reproduction and Development Research School: Biomedical Sciences	PhD period: June 2010 – November 2014 Promotor(s): J. Anton Grootegoed Supervisor: Willy M. Baarends

1. PhD training	
	Year
General courses	
- Safely Working in the Laboratory	2011
Specific courses (e.g. Research school, Medical Training)	
- Cell and Developmental Biology	2011
- Genetics	2011
- Biochemistry and Biophysics	2010
- Transgenesis, gene targeting and *in vivo* imaging	2011
- Literature course	2011-2012
Seminars and workshops	
- Confocal microscopy: introductory course	2010
- MGC Symposium – Leiden	2010
- OIC Live cell and super-resolution imaging	2011
- Kleinwalsertal Winter School	2011, 2012, 2013
- Adobe Photoshop and Illustrator	2011
- International Innovative Mouse Models Workshop	2011
- PhD Workshop – Maastricht	2012
Presentations	
- Kleinwalsertal Winter School (oral presentation)	2011- 2013
- Reproduction and Development working discussion	2010-2014
(Inter)national conferences	
- Chromatin Changes in Differentiation and Malignancies – Egmond aan Zee (poster presentation)	2013
- EMBO Meiosis Meeting (poster presentation)	2011, 2013
- MGC PhD Workshop – Düsseldorf (poster presentation)	2012
- 24th MGC Symposium (oral presentation)	2014

Acknowledgements

Anybody who undertook the task of a doctorate and experienced 4 years of full-time lab-work is aware that nothing could have ever been accomplished working on their own. That's how scientific research is supposed to be, and that's what makes it exciting even when you are sleep- and sun-deprived. I really think that it is important and due at this point to acknowledge all the people who helped me making it through the last four years.

I will start with the people who gave me a chance in the first place: my promotor Prof. Dr. Anton Grootegoed, and my copromotor Dr ir Willy Baarends. The first time we spoke, I felt so nervous and inadequate that I did not even manage to start the camera on my laptop to have a decent Skype interview. And I really appreciated the way Anton suggested that I might be able to find a button somewhere to turn the video on, without making me feel like a total incompetent. It was the first of many suggestions and advice (very often asked for) that were always eye-opening, constructive, and helpful. I would like to thank you, Anton, for the great chance of discussing science with a person of such deep knowledge and critical insight, and with the ability to share it, succeeding in getting the message through. I am also grateful for the effort you put in revising my PhD thesis, because it helped me also to become a better (I hope) scientist.

Dr ir Willy Baarends, dear Willy. From the very first moment you treated me like a family person, not only the Lab-family, but your own family. I was almost shocked when you invited me for lunch at your place. It made me feel home and it cured my never lost nostalgic attitude towards my own family, back in Italy. I really think that a nice working environment can make research better, and you are definitely a pro in this! You are easy to talk to and a very good listener. You are able to set people at ease, and I will go give a speech to those students to let them know what they're missing!

I would like to thank the members of the thesis committee, Prof Dr Peter Verrijzer, Prof Dr Claire Wyman, and Prof Dr Adriaan Houtsmuller, for reading my thesis and giving me important input to improve it.

I need to spend a few more words for Adriaan, to say how much I have enjoyed collaborating with you and your group. You always ask provocative questions which give a twist to the discussion and push the limit a bit further. I am also very grateful

to you for running such a great facility as the Optical Imaging Center. Half of the work I have done would not have been possible without all the microscopes... and the people behind them! I want to thank the whole Houtsmuller group/OIC facility (I still don't know the difference): Alex, Gert-Jan, Martin, also for tolerating my visits to the office and even contributing with some payless advice for various aspects of getting a doctorate degree. Gert, you are so helpful and dedicated that I do not know how to thank you for everything you have done for me in these four years. You were always available and patient with every question or request of support (sometimes it was an actual cry for help). I have really missed having you next door... Martijn and the people in room Be346, who had to hear all discussions with my Elyra buddy, Maarten. Maarten, Chapter 4 would not exist without you and Johan. I would like to find a way to repay you for the long hours, the imaging sessions, the never-ending discussions, the last minute questions, and my excessive talking (that is actually something that would make me bankrupt, if I really had to repay everyone who suffered from it!). You both did a lot for our project and had interesting ideas and stimulating comments. Our meetings were always exciting and I really hope we can keep working together as long as possible! Maarten, good luck with the last year! Sounds scary but you can do it! And Johan, I will miss your fun facts and your enthusiasm for every little detail and every little step forward! That's a driving force and I hope you keep it that way! Last, but not least, in the microscopy crew, B-J! The first person I met that shared my microscopy nerdosity, and my first ski lesson in Kleinwalsertal... I didn't do that well, did I? Thank you for all the nice conversations and the pep talks: they really helped a lot! Now I look forward to your defense! I am sure you will do great anywhere you decide to go. Good luck with your next step!

Another community that I could not survive without is the one from my home country: the Italian support system, the one that welcomed me as soon as I arrived in Rottedam, handing me a Netherlands-101 support guide: Elisa, Francesca, and Isa. With Isa I can start thanking the thesis-support group, aka paranymphs ad honorem: Isa, Simone, Jessica and Thomas. Isa, I can't thank you enough for all the information and directions in the procedure to "apply for a doctorate degree at the Erasmus University". You are always so kind and willing to help! The preparation to the defense would have been a nightmare without you. Luckily, we managed to squeeze in some nice talks, between the choice of the printer for the thesis and the calculation of the number of copies! Thank you for being there. Simone, I promise

you won't have to see my face so often after this is done! Thank you for your help and for the best housewarming party ever! Although that might have been Flavia's merit... Jessica, I owe you so much for all the help with the thesis procedure and layout. You were always ready to answer all my questions (and there were many!). Thank you for hosting the first Italian game in the last world cup, and not kicking me out when I showed the devil in me! Thomas, I was really tempted to ask you to be my paranymph... just to lengthen your list! And to ensure my party would be nice! I think it is enough if you are there, the soul of every party! Thank you for having always a pun ready! Beastie is fine, but won't make focaccia: are you sure you want to hang out with Luca and Beastie?

Now it's time for the actual paranymphs: Hegias and Alice. Two of my best friends. Hegias, I have known you for two years and it looks like a lifetime. I can read your mind and I totally know what you are going to say. Maybe because I would say the same! I was very lucky that day Joost hired you and decided you would sit next to me in the office, and in the lab. Probably our efficiency at work was slightly affected... The only flaw of our friendship is that once we start talking there is no way we can stop. Thank you for being there for me, accepting all my moments (hours maybe) of crap, my freaking out, and my mood swings. Mi è difficile spiegare in una lingua che non mi appartiene quanto ti sono grata di essermi stato vicino, spassionatamente, parlandomi sempre a cuore aperto e senza giudicare mai. Ti voglio bene. Alice, I have known you for most of my life and still don't get enough of you. For being my little sister you are always shockingly sage and clear thinker. Sometimes looking through your eyes is way better! Thank you for the unconditioned love that only a sister can give, and for spicing that up with sharp comments that will make me do better. Grazie perché.. appena l'ho scritto mi è venuto in mente Ramazzotti ed è meglio di no. Andrò in terapia per fermare le citazioni musicali. Però, passerotto non andare via

The lab 902. Sure it was super cool that so many PhD students started basically at the same time and could share the good and the bad of being in a new place, on a new job, with new people. It is now extra sad because roads will be inevitably splitting soon. We put together an awesome group to hang out and support each other in these years, and I am really afraid I will never have such a great time again. I want to say thank you to each of you. To Federica, who was forced to hear my infinite talking about work, about tiredness, about food, about the thesis, and was so unfor-

tunate to have her desk just behind me, so that only the "mouse house" would give her a safe way out! You are such a caring, thoughtful, kind person to everyone, that many times I am afraid not everyone really deserves you. Your genuine interest in how people feel and your being so unselfish make you special, and I am really happy we spent together the last four years. Grazie. Un grazie anche al Bizzaro perché è un po' anche per lui se sei finita in queste lande pianeggianti. Tra un po' facciamo dottore anche lui e non so se la casa reggerà i festeggiamenti! Agnese, I knew you would get the PhD position with Joost, just as I know you will get anywhere you want to go. You are made for it. I am just happy that your first step was in this lab, because that gave me four years of a phenocopy of my sister, and it is more than I could wish for. You are bright and sparkling, and you give a twist to the lab. I can really feel it when you are not around. Sei trascinante – e non lo so come si dice in inglese – come il diavoletto della Tazmania (ho Cristina d'Avena in testa). Pensa solo che, quando parlo con i miei, mi chiedono: perché parli come Agnese? Wherever I am, you have a place to visit! Da Sandra a Raimondo, la coppia che scoppia. Friedo, I will explain it to you. Or maybe I will just show you a youtube video. I guess we got to be a bit more than colleagues, right? If not, please don't tell me, I might cry... Thank you for being always the devil's advocate and trying to push people out of their comfort zone. I grew a lot talking with you. There is no limit to what you can learn from people. And that is why you are still in time to bake a nice focaccia! In the end, I did climb a bit, before my panic attack! Aristea, the ninja goat! I am a bit jealous you are such a natural talent, but that is mainly because I am totally the opposite! When you came to the lab, you started questioning yourself on being too rough with people. After overhearing a conversation with your brother, I know it is a Greek thing. Or a Crete thing. Or a Magaraki thing. Anyway, you don't hate us. I think you are brilliant, and your motivation and decisiveness are of reference to me. You always talk straight and never hide your opinion, which makes you a great friend. Thank you for being this way with me too. And let's arrange that sailing trip around Greek islands! Cheryl, it is time for changes and I can see that things are turning out the way you wish them to be. I hope this is just the start! Thank you for the small chats in the hallways, for listening and for confiding in me. The doctors: Ruben, Bas, Annegien. In Italy we say that it is always nice to have a physician in the family. So glad I had three!! Ruben, thank you for your constant jokes! But you may want to reconsider calling the attention of every girl with a whistle... I am sure

you have other weapons in your armory! Bas, thank you for showing up always with a smile that can set the whole lab in a good mood! Annegien, thank you for being so joyful and enthusiastic, even when asked to translate medical stuff... Andrea, thank you for enriching the team of the Southern countries! Suerte with your PhD! Cristina, thank you for your advice, in science and in daily life (I still remember your instructions for the BSN, the bank account and everything else, four years ago!). Catherine, bring the baby! I want to see her! Good luck with your new (life-long) job! Eskeww, even if you are no longer in the lab, you will always be part of it for me. Thank you for being so open when I first got to Rotterdam, for your housing advice, for sparing your kitchen to make risotto, for being so sweet. And, of course, for putting up with my grumpy days... Joost, thank you for being in my grote commissie, but mostly for being in the Monday morning meetings with nice questions and useful suggestions. It was always nice to see your smiling face on the way in and on the way out. Maureen, thank you for all the nice talks through the door! Joke, thank you for your tips and tricks about the life of a last-year-PhD student! Godfried, dear Willibrord! Thank you for being so involved in my work issues and for always providing food for thought (not only scientific thought).

Now the cornerstones of the lab: Marja, Esther, Eveline, Jos and Evelyne. Without you, much less would be accomplished. For sure much less music! Evelyne, you are such a great person to work with. You are professional, dedicated, active, and always helpful. I am really grateful for everything you have done in these years to ease my tasks and to teach me skills I did not have. You are thoughtful and kind. Thank you for being a nice person, besides being an amazing colleague.

Benno, you are no longer in the department of Reproduction and Development, but I still want to thank you for everything you did setting up interviews, moving, housing arrangements, and more. Your humour was unique! I miss it. Together with your impressive organizational skills and qualities as secretary!

Even if everybody knows I spent most of my days in a dark room behind a microscope, I still got the chance to meet amazing people all around The Building, including some other bits of the renowned Italian community. On the 10th floor, the lab 1030 with Widia, Jessica, and Kerstin. The recently moved Sjaak's group with Maria and Ileana! The stem cell people, Mehrnaz, Tracy, Chris (I am kind of jealous of your life in Scotland from how you portray it!), and Nesrin. Nesrin, you are so much fun, your laugh is contagious! I wish you good luck with the hard times

coming, and I hope to applaud your success very soon! Fanny, either I only met exceptional French, or the cliché about French people is completely wrong! Thank you for being always nice and caring! And, yes, we should meet more often!

Few floors down, on the 7th, I want to thank Maaike, Martì, Johan, Erik (lost somewhere in Australia); the harem of DNA repair, Cristine, Barbara, Franzie, Yasemine, Mariangela, thank you for Easter Monday and the great gatherings! The other part of the Italian crew: Sara, Chiara, and Andrea. Thank you guys for the dinners and drinks, and for the trash songs on youtube that night... On the 6th, Nathalie!! Thank you for the nice talks in the lab, for the knitting discussions, and for ALOT more! (stupid autocorrect almost got me again!) Elisa, Enrico, and Michael. Michael, I will keep that proposition for my party and claim that nobody can put Fabrizia in a corner! Thank you for your support and for having always something to share. With you, every day is a learning experience. What about the unicorns, then?

In four years the Erasmus MC got to be sort of home to me, but it could never replace family. Family that was always right behind me, ready to catch me if I fell, and to push me forward when I was stumbling. My mother, who is the first one to believe in me no matter what, and to whom I say I love her too rarely. Grazie mamma, per non avermi mai lasciata sola, per aver sempre creduto in me, molto più di quanto faccia io stessa. Grazie per essere presente, talvolta pressante, cosicché io non senta di essere così lontana da casa. Alice, questa volta come membro della famiglia, grazie per esserti arrabbiata immancabilmente ogni anno quando ho mancato il tuo compleanno, e tutte le volte che le mie ferie erano troppo corte. Grazie a mio padre che pianifica sempre il mio prossimo passo. Zia Mina e zio Tonio, la mia famiglia "putativa", quella che ingerisce meno nelle mie scelte, ma che comunque le segue e le consiglia per aiutarmi e sostenermi. Grazie di essere il muro di rinforzo, quello che non mi lascerà mai crollare. Grazie a mia nonna, che pensa che io sia sempre la più brava.

In the extended family, there are two more people who are extremely important to me. My lifelong best friend, met 25 years ago on a kindergarten day and never lost. Claudia, we may not talk much, and may not meet more than twice per year, but everytime we get together is as if we never missed one second. I will always be there for you. Luca, I know how hard these months have been for you, and that I have been an electrified wire. Thank you for never letting go, for being always supportive and understanding. You are my rock. Thank you for holding me.